THE UNIVERSITY OF EDINBURGH

EDINBURGH
UNIVERSITY
LIBRARY

Shelf Mark ROBERTSON LIBRARY

BRITTON, PH.D. 2007

30150 023698019

'Modelling the recovery of the atmosphere from fossil fuel perturbation and quantifying its associated uncertainty'

Clare Britton

Submitted for the degree of Doctor of Philosophy
at the University of Edinburgh, 2006

EX BIBL UNIV EDINBURGH

Abstract

This thesis addresses the response of the atmosphere to past and possible future anthropogenic CO_2 emissions on timescales of up to a million years. Although rate and magnitude of emissions are important, natural controls of the response are the buffering of CO_2 by deep marine sediments and weathering flux of alkalinity from land. Increased CO_2 and temperature on land will indirectly increase weathering through the stimulation of plant growth. However, past studies on the long-term fate of fossil fuel CO_2 have neglected this. This thesis examines the effect of this biologically enhanced weathering on the concentration of CO_2 in the atmosphere over 10^4-10^6 years. The uncertainty which exists in all models due to things such as parameter uncertainty and measurement error is often ignored due to the complexity of biogeochemical and climate models. This thesis sets out to not only look at the response of CO_2 in the atmosphere, but to also assess the uncertainty in this result.

Deep marine sediments and weathering were added to an efficient global carbon cycle model. The effect of enhanced weathering on atmospheric CO_2 response to fossil fuel CO_2 release was investigated for a range of emissions scenarios. 11 parameters in the ocean and sediment system were allowed to vary and the model was calibrated with atmospheric CO_2 data using a Bayesian methodology. This model was then used to assess the uncertainty in atmospheric CO_2 response with and without biotic feedbacks on carbonate and silicate weathering.

The enhancement of weathering due to increases in CO_2 and temperature is found to significantly accelerate the drawdown of CO_2 on timescales of 10^4-10^5 years, although it will still take $>10^6$ years for the CO_2 concentration to stabilise. Enhanced weathering has most effect when all sediments in the ocean are dissolved. Timescale of response in the atmosphere depends on the weathering formulation used. Silicate weathering is required to

return CO_2 to pre-industrial concentrations. Calibrating with data improved the model response as mean peak CO_2 concentrations were ~235ppmv lower than results from previous studies. Uncertainty in CO_2 response due to parameter uncertainty is >500ppmv in some cases, this uncertainty peaks on the millennial timescale and decreases thereafter. The range of uncertainty in CO_2 response for a single emissions scenario encompasses the range of uncertainty due to varying emissions from 300 to 5000GtC in other studies. The time for the atmosphere to return to current concentrations of CO_2 is also greatly uncertain, with the earliest possibility (which is however highly unlikely) occurring at ~ year 10,000 but most likely occurrence at ~year 100,000.

Acknowledgements

I would like to thank all my PhD supervisors for providing support ideas and feedback, thanks for reading my work! My thanks to Tim Lenton for giving me the chance to do a PhD, allowing me to use his model in my research, helping me to pull it all together and also to publish my first paper. Thanks to David Cameron, for helping me to grapple with statistical uncertainty, stepping in after supervisory migration, providing endless technical and statistical support via skype and a regular trip to 'the vets' to chill out over lunch! I am also grateful for Marcel van Oijen's time in discussing Bayesian matters - even over coffee - and for reading my work. Matt Williams also needs to be thanked for showing an interest in my work and dealing with the administration required by the University.

Thanks to my friends at CEH Edinburgh and the University of Edinburgh, especially for the distractions at lunch and coffee. Also for being patient when I asked questions, shouted at my computer in public and talked about my PhD! My special thanks to Zana for listening, agreeing, laughing, dancing and lots more (including an endless supply of blank CD's from her desk!). I probably would have managed the PhD without you, but it would have been a lot less fun!

My thanks to Simon for believing in me when I didn't, listening to me, cooking for me, making me laugh and moving with me to Scotland. Also, I thank my Mum and Dad for being supportive all these years and always showing an interest in what I do.

Table of Contents

List of Figures

List of Tables

1 Introduction

1.1 *The global carbon cycle*

Carbon is one of the most fundamental elements in the earth system and through atmospheric CO_2 and the greenhouse effect (Arrhenius 1896) the carbon cycle is intimately linked with the climate of the planet. Carbon is cycled through a variety of reservoirs (Figure 1-1), organic and non-organic, through the hydrosphere, biosphere, atmosphere and lithosphere. The timescales which operate in the carbon cycle vary widely; vegetation for example will affect the carbon cycle on a seasonal and yearly basis (Keeling and Whorf 2005), whereas the operation of the silicate weathering cycle can cause changes on the million year timescale (Holland 1978). As well as the many processes and feedbacks that exist within the carbon cycle, humans are interfering with the natural cycling of carbon, by burning fossil fuels and deforestation. Fossil fuel burning releases carbon which was originally stored in the crustal part of the lithosphere, as CO_2 into the atmosphere. The release of such carbon would have naturally taken millions of years, but instead has been released over the past ~200 years. Humans are having an impact on the Earth system, through changes in the carbon cycle and CO_2, which are affecting the climate (IPCC 2001). These effects and their magnitude are the focus of much current global research and debate (Stainforth et al. 2005, Barnett et al. 2006, IPCC 2001). Much of the current work focuses on the impact of anthropogenic input in the next 50-100 years, which is a timescale relevant to human life. However, the planet has been in existence for 4.5 billion years, so it is also important to look at the long term consequences of anthropogenic change. This thesis addresses the questions: What will be the long-term impact of releasing such large quantities of CO_2 into the earth's atmosphere? How will the Earth system react to the human perturbation on long timescales?

Figure 1-1: *Current state of the carbon cycle. Background/pre-industrial fluxes in black. Human perturbations are in red. (a) Overview. (b) Ocean system. (c) Land system. From (Sabine et al. 2004)*

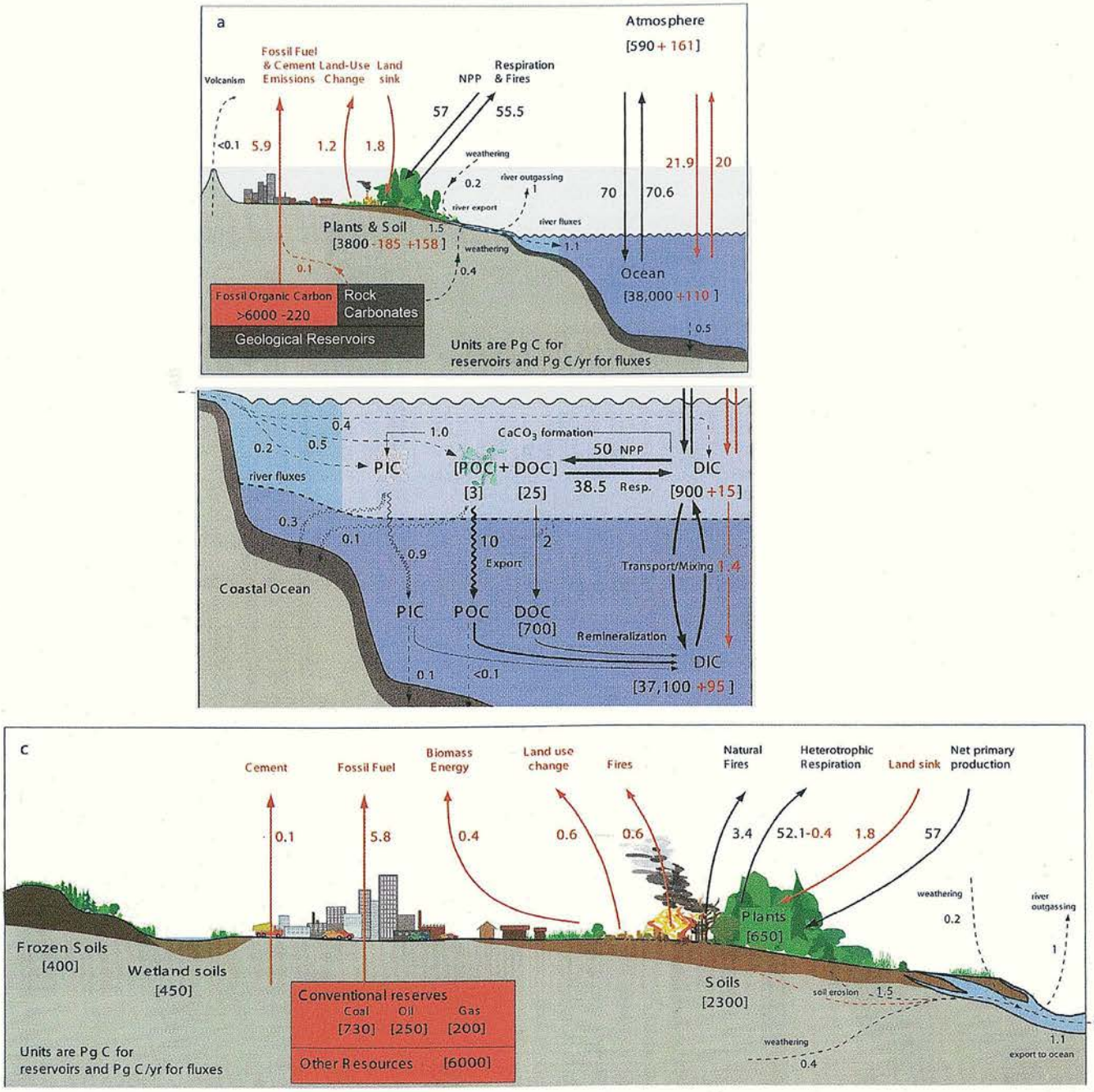

1.1.1.1 Reservoirs and turnover

The lithosphere contains the largest carbon reservoir, which is estimated to be between 66-100 million GtC (Holland 1978). Greater than 60 million GtC of the lithosphere is estimated to be sedimentary carbonates (e.g. limestones), 15 million GtC is thought to be organic carbon stores (kerogens), and 4000-5000 GtC stored as fossil fuels (coal, gas etc). The next

largest reservoir is the ocean, which stores ~38,000GtC. After this is the terrestrial biosphere at ~3150GtC, then finally the atmosphere which holds only ~750GtC at the present time (Sabine et al. 2004). There is therefore a large disparity between the sizes of the reservoirs, as well as the timescales on which they operate (Table 1-1).

Reservoir	**Turnover Rates (magnitude of fluxes, GtC/yr)**	**Reservoir Size (GtC)**
Atmosphere	10^{1}-10^{2}	750
Lithosphere	10^{-1}-10^{1}	60-100 million
Oceans	10^{1}-10^{2}	38,000
Terrestrial Biosphere	10^{-1}-10^{-2}	3150

Table 1-1: *Range of magnitude of turnover rates by reservoir (Bolin et al. 1978) and reservoir size (references within section 1.1.1.1).*

1.1.1.2 Terrestrial Biosphere

The terrestrial biosphere consists of plants (650GtC) and the soil that supports them (2300GtC), also wetlands (450GtC) and permafrost soils (400GtC) (Sabine et al. 2004). The fluxes of carbon between the terrestrial biosphere and the atmosphere are due to photosynthesis (sink of CO_2), autotrophic and microbial respiration, fires, and changes in land-use (sources of CO_2). Due to the seasonal behaviour of plants, the CO_2 concentrations in the atmosphere are seen to oscillate (Figure 1-2), which reflects the change in sign of the net exchange between atmosphere and terrestrial biosphere throughout the year. There are also geographical differences, as the distribution of land is unequal across the planet's surface, more land surface being present in the Northern hemisphere. However, it is on the scale of decades to centuries that the terrestrial biosphere can affect the CO_2 concentration in the atmosphere. The net effect of the terrestrial biosphere has so far been as a sink, defined by net primary productivity (NPP-the balance of photosynthesis in and plant respiration out) minus the sources from decomposition, land-use change and fires (Prentice et al. 2001). However, it is not assured that the terrestrial biosphere will remain a sink; several studies have shown that it may become a source in future (Cox et al. 2000, Lenton 2000, Lenton &

Huntingford 2003). Linking the terrestrial biosphere to the lithosphere and the ocean is the weathering of rocks on land, which is a long-term process. Although the carbon that is liberated from the rocks comes from the lithosphere, and the products of the weathering are passed via rivers to the ocean, the terrestrial biosphere has a direct effect on the level of weathering (Schwartzman and Volk, 1989, Berner 1997, Berner and Kothavala 2001). The occurrence of soils greatly increases the level of rock weathering, due to the water and other chemicals that it holds which aid the dissolution of both carbonate and silicate minerals.

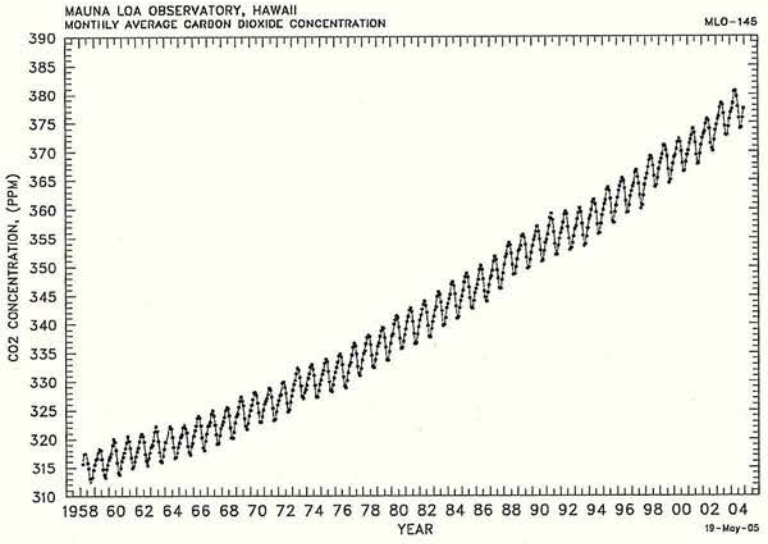

Figure 1-2: *Measurements of CO_2 from Mauna Loa Hawaii, 1958-2004. (Keeling and Whorf 2005).*

1.1.1.3 Ocean

The ocean is the largest carbon store on the surface of the planet that interacts on a timescale of less than 10^6 years (Holland 1978). It exchanges CO_2 with the atmosphere, and as with the terrestrial biosphere, the sign of that exchange is dependent on geography. The reasons behind the geographical distribution are threefold; (1) the solubility of CO_2 as a function of temperature, (2) the biological activity and export within the ocean and (3) the physical constraints on circulation, such as temperature and salinity. CO_2 is more soluble in cold water, therefore it is the deeper ocean waters that hold more CO_2, and when they reach the surface cause a net outflux of CO_2 to the atmosphere. This occurs in the tropics at sites of cold upwelling water, whereas at the temperate and high latitudes, warmer water arrives that is then cooled, and takes on CO_2. This water then sinks, to become the intermediate and deep waters of the ocean, rich in CO_2. When the $CO_{2(gaseous)}$ is dissolved in the ocean it dissociates

into H_2CO_3 (carbonic acid), CO_3^{2-} (carbonate) and HCO_3^- (bicarbonate ions), as well as part of it remaining as $CO_{2(aqueous)}$, these four species make up the dissolved inorganic carbon pool (*DIC*) of the ocean. The quantity of each species is dependent upon the concentration of *DIC*, and also the acid-titrating capacity of seawater, alkalinity (in this thesis alkalinity will refer to carbonate alkalinity only, i.e. the charge needed to balance only the negatively charged **carbon** based ions within the ocean, rather than **all** of them, which would include elements such as Bromine and Chlorine).

The circulation of ocean water is very important, surface circulation is dependent on wind movements, but deep circulation is based on temperature and salinity, colder saltier water being denser, sinks below warmer fresher water masses. This circulation also interacts with the other two main carbon systems within the ocean, both dependent on biology, the soft-tissue and carbonate pumps.

1.1.1.3.1 Soft-tissue pump

Organic carbon is used by organisms in the ocean to build the soft parts of their bodies, when they are dead the carbon sinks through the water column, and is re-mineralized into *DIC*. The only way for this carbon to return to the surface ocean and be exchanged with the atmosphere, is through the circulation of the ocean water, it is therefore locked up in the ocean from decades to centuries.

1.1.1.3.2 Carbonate pump

The carbonate pump is based on the creation, sinking, and final deposition or dissolution of $CaCO_3$ tests (skeletons) which are made by organisms in the ocean. The creation of $CaCO_3$ tests decreases the *DIC* and alkalinity within the ocean, this is then either returned through the dissolution of the test, or locked away from the ocean in the sediments. Whether a test is dissolved in the water column or remains to land on the seafloor in general depends on the carbonate ion saturation state of the surrounding water. The saturation state depends on the temperature and pressure at that point in the ocean, and the concentration of carbonate ions in the ocean water. When the $CaCO_3$ test passes into an area of undersaturation it begins to dissolve. However, a fraction of $CaCO_3$ tests also dissolve in saturated areas. Several reasons for this have been proposed, including digestion inside zooplankton (Milliman et al. 1999), acidic micro-environments in 'marine snow' aggregates (Jansen et al. 2002) and the shallower susceptibility of the aragonite polymorph to dissolution (Chung et al. 2003, Feely

et al. 2004). At this point however there is much uncertainty as to the importance of each of these mechanisms in dissolution within saturated areas.

1.1.1.3.3 Sediment Deposition

Where areas of oversaturation meet with the seafloor, carbonate sediments are deposited. Due to the pressure (and temperature) dependencies of $CaCO_3$, the ocean is oversaturated at shallower levels. This means that sediments with the highest proportions of $CaCO_3$ are deposited at shallower depths in the ocean. There is a depth band within the ocean where dissolution of $CaCO_3$ in the sediment occurs, but where there is still net deposition, this is called the lysocline. Deeper within the lysocline, the more dissolution occurs. Finally a depth is reached within the ocean beyond which no $CaCO_3$ exists in the sediments, this is the carbonate compensation depth. Characteristics such as the depth where the lysocline begins and to what depth it reaches (i.e. the carbonate compensation depth) vary with ocean basin.

As well as $CaCO_3$ being deposited, a small fraction of organic carbon is also buried within the sediments. Much of this organic carbon is then metabolized by bacteria and benthic organisms, releasing CO_2. This release of CO_2 into sediment pore-waters can also cause dissolution of $CaCO_3$, even in sediments beneath saturated ocean waters.

1.1.1.3.4 Closing the sedimentation cycle

Net sedimentation builds up year on year, and the material finally undergoes diagenesis, becoming limestone. Sediments which survive to become limestone represent the removal of alkalinity and *DIC* from the ocean system. To balance this loss, the rivers pass alkalinity and *DIC* which has been unlocked from the weathering of carbonate and silicate minerals to the surface ocean. The magnitude of the flux of alkalinity to the surface ocean is intimately linked to the depth of the lysocline. This means that an increase in the alkalinity flux on land deepens the lysocline within the ocean, encouraging the deposition of more sediments, which brings the usage of alkalinity in sediment deposition in line with that delivered from the continents (Sigman and Boyle 2000). As well as the production of deep sea carbonates, biogenic precipitation and burial of $CaCO_3$ also occurs in coral reefs, and shallow carbonate banks. A range of estimates exist for the level of river alkalinity which is removed by deep sea sedimentation, it is suggested that deep sea sedimentation uses up to 50% of the total river alkalinity flux, (Archer 1996, Milliman et al. 1999, Milliman and Droxler 1996), leaving the rest for use by the shallow carbonate system.

1.1.1.4 Lithosphere

The lithosphere provides the final link between the ocean sediments and the atmosphere, through the rock carbon cycle. It has already been mentioned that the terrestrial biosphere has a great effect on the weathering that occurs on land, weathering rates are also affected by temperature and precipitation (Berner et al.1983, White and Blum, 1995). The weathering of carbonate and silicate minerals uses CO_2 from the atmosphere, and releases Calcium (Ca^{2+}), Magnesium (Mg^{2+}) and bicarbonate ions (HCO_3^-) and therefore alkalinity, which enters the ocean carbon cycle via stream flow and affects its chemistry. However the way in which the carbonate and silicate weathering cycles interact with the global carbon cycle are different, each case is outlined below.

1.1.1.4.1 Carbonate Weathering Cycle

The weathering of carbonate minerals requires water and CO_2 derived from the atmosphere (Equation 1-1a), the dissolved products (and therefore alkalinity) from this weathering are then transported along the rivers (Equation 1-1b) and reach the ocean. Deposition of $CaCO_3$ within the ocean locks up carbon and alkalinity, and CO_2 (which was used in weathering the minerals) is ultimately released back into the atmosphere (Equation 1-1c). The $CaCO_3$ which has been deposited within the shallow sediments is later uplifted, becoming vulnerable to weathering (on the order of tens of thousands of years) and the cycle begins again.

$$\underbrace{CaCO_3 + CO_2 + H_2O}_{(a)\,Weathering} \rightarrow \underbrace{Ca^{2+} + 2HCO_3^-}_{(b)\,Transport} \rightarrow \underbrace{CaCO_3 + CO_2 + H_2O}_{(c)\,Sedimentation} \qquad \textbf{Equation 1-1}$$

1.1.1.4.2 Silicate Weathering Cycle

The weathering of silicates requires 2 units of CO_2 from the atmosphere (rather than the one required for carbonate weathering) (Equation 1-2a). Again the dissolved products are transported along rivers (Equation 1-2b). However at the sedimentation stage, one unit of CO_2 (which was originally used in the weathering of the silicates) is released to the atmosphere due to the creation of $CaCO_3$, however the other unit of CO_2 is preserved in the sediments themselves (Equation 1-2c). Eventually the deep sea sediments storing this CO_2 are subducted into the mantle, where they become decarbonised, to form calcium silicate

rocks. The CO_2 released from this is eventually outgassed from volcanoes back to the atmosphere – the whole cycle taking hundreds of millions of years.

$$\underbrace{CaSiO_3 + 2CO_2 + 2H_2O \rightarrow Ca^{2+}}_{(a)Weathering} + \underbrace{2HCO_3^- + 2H^+ + SiO_3^{2+}}_{(b)Transport} \rightarrow \underbrace{CaCO_3 + SiO_2 \cdot H_2O + H_2O + CO_2}_{(c)Sedimentation}$$

Equation 1-2

1.1.1.5 Atmosphere

Carbon that enters the atmosphere (such as that from fossil fuel burning) can only be removed through exchange with the terrestrial biosphere, ocean and lithosphere. The carbon content of the atmosphere varies seasonally due to plant growth, and geographically due to the distribution of land masses, and the circulation patterns of the ocean. However, on timescales longer than a year it can be thought of as well mixed. CO_2 has a direct effect on the temperature of the planet, through the greenhouse effect, and therefore influences climate.

1.1.2 Past changes in the carbon cycle

Although the current high CO_2 concentration in the atmosphere is still of great concern, for much of the past 500 million years the CO_2 concentration in the atmosphere has been higher than it is today (Figure 1-3). Atmospheric CO_2 has varied quite dramatically (from ~180ppmv to possibly 6000ppmv), and this is due to a wide range of factors which interact with the long term (10^6+ year timescale) carbon cycle, where the uptake of CO_2 through silicate weathering is balanced by volcanic outgassing and metamorphic processes (Berner and Kothavala 1994, Bergman et al 2004). During the more recent past (up to 650,000 years ago), CO_2 concentrations have been oscillating between ~180-280ppmv (Figure 1-4) (Siegenthaler et al. 2005). The variations seen are due to glacial cycles, superimposed over the long term CO_2 concentration (Siegenthaler et al. 2005). During this period of time the CO_2 concentration is also closely linked to the Antarctic temperature (Monnin et al. 2001). On a smaller scale, within the last 10,000 years (all within the current interglacial) CO_2 concentrations continue to vary (Figure 1-5). However, such changes seen in the CO_2 concentration of the past thousand years are dwarfed by the effects of man since the industrial revolution (Figure 1-6) (Etheridge et al. 1998, Keeling and Whorf 2005). The

concentration of CO_2 at the present day (382ppmv) (www.cmdl.noaa.gov/ccgg/trends/) is higher than that seen in at least the past 700,000 years (Petit et al. 1999, Indermuhle et al. 2000, Kawamura et al. 2003).

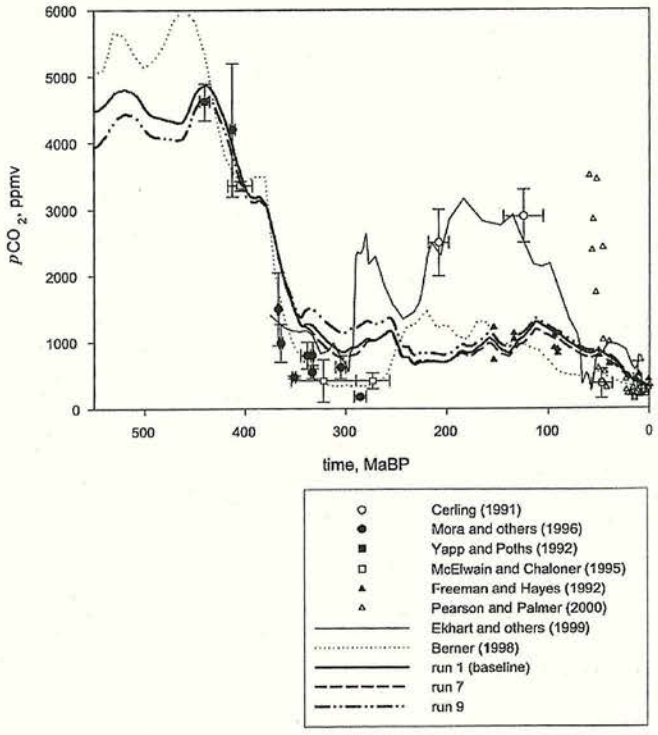

Figure 1-3: *Phanerozoic predictions of CO_2 from COPSE model (run 1,7,9) (Bergman et al. 2004) and GEOCARB III (Berner 1998) and a compilation of proxies and models.*

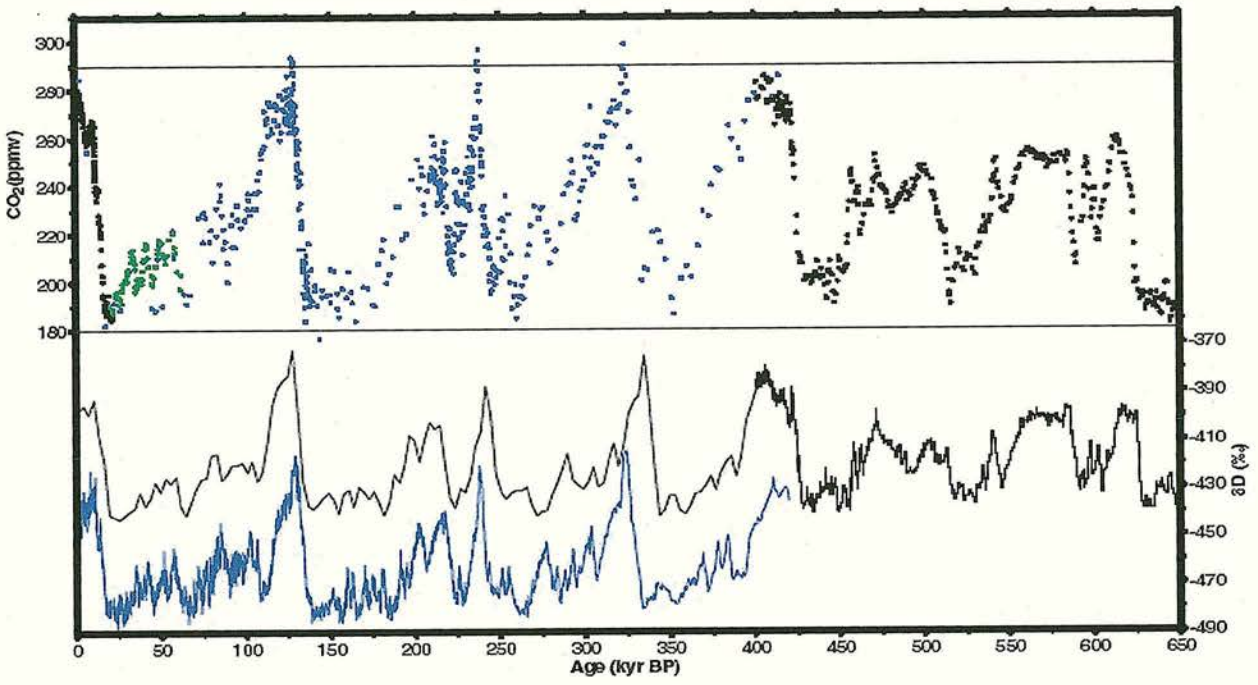

Figure 1-4: *CO_2 in the atmosphere for the last 6 glacial cycles (Siegenthaler et al. 2005, from a composite of three ice-cores). δD values, a proxy for temperature is also shown.*

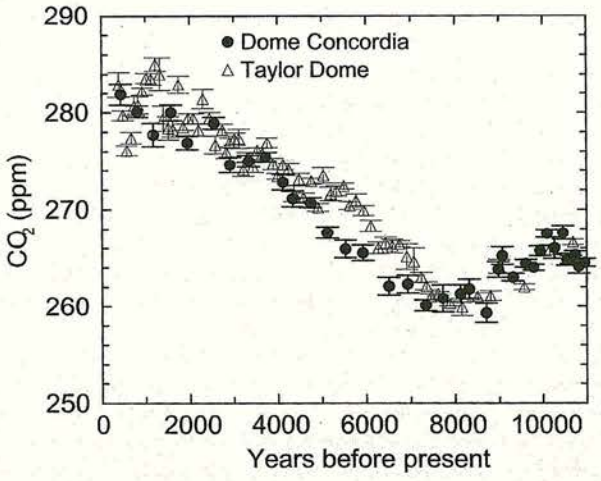

Figure 1-5: *Holocene CO_2 variations from ice-cores in Taylor Dome (Indermuhle et al. 1999) and Dome Concordia (Fluckiger et al. 2002).*

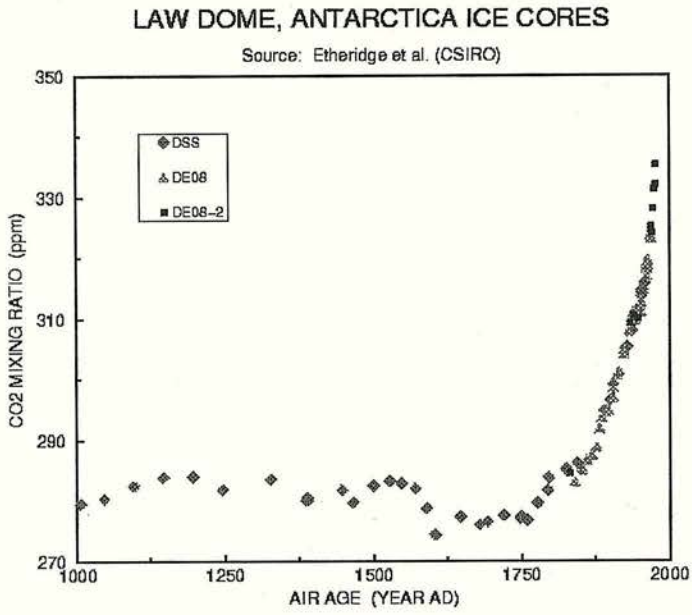

Figure 1-6: *CO_2 concentrations in the atmosphere from 1000A.D. to 2000A.D. (Etheridge et al. 1998).*

1.1.3 Present

The pre-industrial concentration of CO_2 hovered around 280ppmv (Etheridge et al. 1998), and it is currently ~380ppmv (http://cdiac.ornl.gov/) after we have emitted ~400GtC in the past ~200 years (Marland et al. 2006, Houghton and Hackler 2002). It is obvious that the burning of fossil fuels and land-use change has had an effect on the level of CO_2 in the atmosphere to date. In terms of gathering data on various components of the global carbon cycle and how they are changing, the increase in CO_2 in the atmosphere is probably the most robust. The increase of CO_2 in the atmosphere does not however match that of the total emissions, this is due to the existence of negative feedbacks within the system (see section 1.1.4) which mean that as CO_2 has increased, the ocean and terrestrial biosphere have become carbon sinks (Sabine et al. 2004). Estimates of terrestrial biosphere atmosphere exchange for the 1990's are -1.2 +/- 0.8 GtC/yr, and for the ocean atmosphere exchange -1.9 +/- 0.7 GtC/yr (Le Quere et al. 2003). There exist however, large uncertainties in the estimates of these exchange fluxes and in the past few decades alone, the thinking regarding the nature of the land sink has changed dramatically. The initial conclusion was that the

increased land sink was mainly due to fertilisation of the biosphere by CO_2, it is recognized now that the sink is due to a complex interaction of many fluxes and feedbacks, and the effect of fertilisation may not be as strong as previously thought (Sabine et al. 2004). One of the greatest challenges in looking at carbon cycle of the present and the future is in determining which of the effects currently seen is due to human influence in the past 200 years, or the natural processes of the global carbon cycle.

Although there is still much debate about how much our emissions and energy consumption will affect the climate of the planet in the next 200 years, it is generally accepted that anthropogenic emissions are having an impact on global temperature. IPCC (2001) reported a global trend of increasing maximum temperature from 1950 to 1993 of 0.1^0C per decade.

1.1.4 Future feedbacks and their timescales

The response of the land-atmosphere exchange flux is very important, and it may well become a source of carbon in the years to come (Cox et al. 2000, Lenton et al 2000, Lenton and Huntingford 2003). However, the land carbon cycle affects the atmosphere on a timescale of decades to centuries (Gruber et al. 2004). The ocean sink too is very important, as it has taken an estimated 30% of total industrial emissions out of the atmosphere, so far (Le Quere and Metzl 2004, Sabine et al 2004). Climate feedbacks on the ocean system, and therefore the ocean sink, include changes to the chemistry, temperature, salinity, biological productivity, and calcification of organic tests (Le Quere and Metzl 2004). The maximum residence time of ocean water masses (~1000 years) sets the timescale for these feedbacks to affect CO_2 in the atmosphere, through the circulation, and overturning of water masses. Sarmiento et al. (1992), states that the uptake of CO_2 by the ocean in the next tens to hundreds of years will be limited by the transport of anthropogenic carbon to the ocean interior. Lenton (2000) modelled the millennial response of the terrestrial biosphere, ocean and atmosphere to fossil fuel emissions, and found that by the year 3,000 the exchange between these three components will be approaching equilibrium.

The only components of the carbon cycle that can impact the system on timescales of 10^4 years or more are the sediment and weathering cycles. While equilibration of anthropogenic CO_2 between the ocean and the atmosphere will occur in under a millennium, neutralization of this fossil fuel by dissolution of seafloor sediments will occur on the timescale of 10^5 years (Archer 2005). Sediments will be replenished, and finally reach equilibrium, due to the

continuing input of carbon and alkalinity from weathering of rocks on land. Archer et al. (1998) estimate that this final equilibrium leaves ~7-8% of the fossil fuel CO_2 in the atmosphere to be neutralized by the silicate rock cycle, which operates on scales of 10^6 years (Holland 1978, Berner 1999).

The time that the sediment system and therefore the atmosphere takes to recover from fossil fuel release, is intimately linked to the alkalinity flux to the ocean, derived from the weathering of rocks on land. Weathering fluxes are coupled to the carbon-climate system themselves, dependent on factors such as temperature, CO_2 and plant cover meaning that they have not remained constant during past earth history (Raymo 1991, Berner et al. 1983). Studies of past climate using models such as GEOCARB III (Berner and Kothavala 2001) and COPSE (Bergman et al. 2004) have demonstrated the feedback between weathering and CO_2 during times of global change.

The emission of fossil fuels has increased the CO_2 and temperature of the planet, and will continue to do so for many years to come. These increases in temperature and CO_2 will have been affecting the level of weathering on land in comparison to that of the pre-industrial. Walker & Kasting (1992) explicitly included the possible effects of temperature and CO_2 on weathering in a model to look at the future responses to anthropogenic perturbation and Sundquist (1991) also looked at the effects of increased CO_2 on weathering. This covers the direct effects of temperature and CO_2 on weathering, but what about more indirect effects? Temperature and CO_2 have effects on plant growth, and plants and the soil which supports them also encourage weathering, what effect will this feedback have on the system? Experimental studies such as (Berner et al. 1998, Williams et al. 2003) have demonstrated the possibility of this indirect biological enhancement of weathering. Caldeira (2006) has developed preliminary parameterizations of the possible effects, and the impact of forest cover, due to their greater absorption of solar radiation, but it has not been incorporated into a model looking beyond the next 200 years. What will the effect be of enhanced weathering due to the direct and indirect effects of temperature and CO_2, on sediment neutralization and atmospheric CO_2 response, on timescales of greater than 10^3 years?

1.2 *Modelling the global carbon cycle*

1.2.1 Existing models of the carbon cycle and climate interactions

Since the 1980's (Broecker 1981, Berner et al. 1983, Sellers et al. 1986), there has been a growth in the number of scientists that have been trying to represent aspects of the carbon cycle, and its response to different climatic regimes in computer models. The interaction of the carbon cycle and climate can be complex, and computing power is limited (despite continual advances) therefore many models concentrate on specific aspects of the carbon cycle, such as the land (Sellers et al. 1986, Haxeltine & Prentice 1996 (BIOME3), Friend & White 2000 (HYBRID), Cox et al. 2001 (TRIFFID)), the ocean (Knox and McElroy 1984, Siegnethaler & Joos 1992 (HILDA), Maier-Reimer et al. 1993) or the lithosphere (Berner et al. 1983 (BLAG), Berner 1994, Berner & Kothavala 2001 (GEOCARB II&III)). However as time passed it was recognised that to fully understand the interactions of carbon cycle and climate, some models would have to couple the action of the land and the ocean together, this is however very difficult with the more complex models that exist.

Models which include a carbon cycle component vary widely in complexity. At the high end dynamic global vegetation models DGVM's (BIOME3, HYBRID, TRIFFID, Krinner et al. 2005) model vegetation and carbon on land. Ocean general circulation models (OGCM's) incorporate the physical processes of the ocean by resolving the fluid dynamics of the ocean into a network of smaller boxes, but not necessarily the carbon cycle (Maier-Reimer et al. 1993). The interactions of the carbon cycle have been added to the physical framework of the ocean models in several cases (Sarmiento et al. 1992, Cox et al. 2000 (HadOCC)). General circulation models also exist for the atmosphere, and are often attached to the ocean GCM's to make AOGCM's (Manabe et al. 2004, Johns et al. 1997, Voss and Mikolajewicz 2001). Again these represent the physical processes and carbon cycle elements have to be added explicitly. At the lower end of complexity are a range of 'box models' which are used for biogeochemical modelling, where each reservoir is represented by a box, and fluxes pass between them (Knox and McElroy 1984, Lenton 2000, Stephens and Keeling (2000)). These models do not have the complex resolution and physics which is incorporated in general circulation models. However, extra complexity within box models has been achieved by including extra boxes for some reservoirs (Siegenthaler and Joos 1992), and diffusion in the ocean reservoirs (Harvey and Huang 1995, Joos et al. 1996, Raper et al. 2000).

At the start of this century, models that couple the land and ocean carbon cycles to climate began to appear (Cox et al. 2000, Lenton et al. 2000), however, when complex models were used in this way it meant that resolution sometimes had to be reduced (Cox et al. 2000). To combat the problems of integrating the global carbon cycle and climate on centennial and millennial timescales, a new generation of models began to be developed, Earth System Models of Intermediate Complexity (EMICs). These are a halfway house between the models of highest and lowest complexity, that aim to capture some of the complexity of the climate system, but still allow millennial integrations. To do this an approximation of the climate system has to be made, which is not as complex as GCM's, such as a statistical-dynamical atmosphere model (Ganopolski et al. 2001), or an energy moisture balance model (Schmittner and Stocker 1999, Weaver et al. 2001, Marsh et al. 2004, Lenton et al. 2006). These EMICs have been used to look at millennial scale climate change, and some have been coupled to the carbon cycle, (Schmittner and Stocker 1999, Lenton et al. 2006). However, on timescales of greater than a million years, or where a large ensemble is being run, EMIC's are too computationally demanding, therefore more 'simple' models, (Berner & Kothavala 2001, Walker & Kasting 1992, Lenton 2000) or models that are not fully coupled (Archer 1996, 2005, Archer et al. 1998) have to be used.

1.2.2 Models which investigate the fate of fossil fuel CO_2 on timescales of 10^3 years or more

Fewer models exist of the climate and carbon cycle which work dynamically on timescales of over 10^4 years, they have been used to address various questions, such as atmospheric CO_2 over Phanerozoic time (Berner 1994, Berner & Kothavala 2001, Bergman et al. 2004) and the effect of various mechanisms on glacial-interglacial CO_2 variations (Ridgwell 2001). Sunquist (1991) used a model to assess the response of atmospheric CO_2 and carbonate sedimentation to global perturbations in chemical weathering and decarbonation reactions, however it was not applied to the fate of fossil fuel CO_2. This means that an even smaller number of models exist which have been used to address the long term fate of fossil fuel CO_2; important studies in this area are Walker & Kasting 1992, Archer 1996, 2005, Archer et al. 1998.

Walker & Kasting (1992) looked at the effect of fuel and forest conservation on future concentrations of atmospheric CO_2. Their model coupled ocean reservoirs with a sediment system, to an atmosphere and land biota, and the weathering flux to the ocean was dependent

on temperature and CO_2. They included experiments out to 10^6 years, looking at the sensitivity of the system to the dissolution of sediments, and two weathering functions. They concluded that due to the circulation times in the ocean, the dissolution of carbonates has no effect on the system in the first few hundred years after the start of emissions. Beyond year 2400 however, the dissolution was beginning to decrease the CO_2 in the atmosphere in comparison to a system without sediment dissolution. They also concluded that weathering sensitivity was important, but again only after year 2200, although the weathering levels increased immediately, the chemicals released are still subject to the timescales of ocean circulation. The long term response is a slow recovery of the system, as it is replenished by alkalinity from weathering on land. They calculated a timescale of ~350,000 years to totally neutralize the fossil fuel releases.

Archer (1991, 1996) developed a model of $CaCO_3$ diagenesis and the ocean lysocline, which has been used in studies (Archer et al. 1998, Archer 2005) to look at the effect of fossil fuel release on the dissolution of deep sea sediments, and the response of the atmosphere on timescales up to year 100,000. Archer et al. (1998) concluded that $CaCO_3$ dissolution plays only a minor role in the fate of fossil fuel in the coming millennium. The effects that occurred were in 5 phases. 1) 70-80% of the CO_2 released would be in the ocean on timescales of hundreds of years. 2) the initial dissolution spike after CO_2 dissolves in the ocean accounts for 10% of the total $CaCO_3$ dissolution due to fossil fuel release. 3) Dissolution continues until the lysocline reaches a local equilibrium at around year 10,000. 4) The replenishment of alkalinity occurs in the next 8,000 years. At which point 7-8% of the CO_2 release is left in the atmosphere and the system is at steady-state. 5) The silicate rock cycle (not modelled) would be expected to remove the rest of the CO_2 release on timescales on thousands of years.

Archer (2005) took the work further, examining the effects of air-sea equilibrium, ocean temperature feedback, $CaCO_3$ compensation and silicate weathering on the residual anthropogenic CO_2 in the atmosphere. The study concluded that with a 'best-guess' case (i.e. when all the possible feedbacks were included) for a range of emissions scenarios 17-33% of the CO_2 release will still be in the atmosphere 1,000 years from now. This will be 10-15% by year 10,000 and 7% at year 100,000.

1.2.3 Models which include weathering feedbacks

Walker & Kasting (1992) did couple their weathering function to temperature and CO_2, and concluded that the CO_2 in the atmosphere was sensitive to the level of weathering, when forced with anthropogenic emissions into the future. However, their weathering formulation was linearly dependent on the concentration of CO_2 in the atmosphere, this means that the level of weathering increases dramatically with increasing CO_2. Also the indirect enhancement of weathering due to the fertilisation of the biosphere etc, was not included. The work represented a first look at the inclusion of such a feedback whilst assessing the response of CO_2 to fossil fuel perturbation.

The GEOCARB model versions (Berner 1994, Berner & Kothavala 2001) included a more sophisticated weathering function, which included the effects of temperature and CO_2, runoff and CO_2 fertilisation of plants. As the model was used to look at the CO_2 concentrations millions of years in the past, general plant types were also included. Different formulations for carbonate and silicate weathering were used, unlike earlier model versions. Berner & Kothavala (1994) also found that the CO_2 concentrations in the past atmosphere were especially sensitive to the effects of CO_2 fertilisation and temperature on acceleration of chemical weathering, and also the role of different plant groups to accelerating weathering.

The COPSE model (Bergman et al. 2004) combined carbon, oxygen, phosphorous and sulphur cycles to look at their evolution over Phanerozoic time. One of the model predictions was the concentration of CO_2 in the atmosphere, and the system had a weathering function, based in part on the work of Berner & Kothavala (GEOCARB II). Differences to this earlier model weathering system was the way in which the biological effects on weathering were incorporated, being dependent on the actual land productivity, rather than forcing functions as in GEOCARB II. The silicate weathering system was seen to affect the CO_2 history of the atmosphere on the 10^6 year timescales being addressed in this study. This was through its dependency on the CO_2 concentration, and connections to the carbon cycle.

1.3 *Modelling the uncertainty in the global carbon cycle*

1.3.1 Uncertainty in modelling

Modelling represents the only way of assessing the 'big-picture' of the earth system, by integrating all the available knowledge that we have from experimental work and data, on processes and values, into one coherent representation of the system. However, as with data collection, there is always an uncertainty associated with your model output. Modelling of the future climate system has become a very important topic over the past few decades, due to the gradual realisation that emitting such large quantities of CO_2 has global environmental consequences. Therefore the general public and politicians increasingly want to quantify the effect (scientifically and economically) that our past and future emissions may have (Weaver & Zwiers 2000). The idea that science is not 'certain' is a difficult one for the public and politicians to grasp; if a scientist is not certain, then he or she might be wrong. However, as politicians realise that they are going to have to make decisions based on the work of scientists, then the notion of uncertainty begins to be embraced. What is needed is a quantification of the probability of a particular event occurring. Calculating that there is a 1 in 5 chance that your house will be washed away in 10 years is much more useful than saying it *might* happen.

Uncertainty in model systems comes from several sources (Zaehle et al. 2005, Goldstein & Rougier *in press*). This can be from the measurement error on the data that your model is based on also model imperfection, as models are only ever *representations* of the real world. There is also uncertainty in the model response due to uncertainty in the parameters (important values within the model equations which remain constant throughout the model run). Also there may well be uncertainty associated with the responses that you actually want the model to represent, due to natural variability, i.e. we may not know precisely the initial state of the system we are trying to model

All of these areas introduce uncertainty into a model, but it is easier to look at the effects of some more than others. Model imperfection is the most difficult to address within the confines of one model, however, some attempts have been made, by comparing the output of several different models that all have the same initial conditions (Palmer & Raisanen 2000, Tebaldi et al. 2005, Furrer et al. 2006). Quantifying uncertainties in natural variability within a model (rather than model imperfection) has also been attempted in several studies, by changing the initial conditions of the model (Kharin & Zweirs 2000, Meehl & Tebaldi 2004).

Attempts have also been made to look at the model output uncertainty due to parameter uncertainty (Zaehle et al. 2005, Challenor et al. 2006, Barnett et al. 2006), although some recent attempts are being made to incorporate all elements of uncertainty into one theoretical framework (Goldstein & Rougier *in press*).

It is worth at this stage making a distinction between what we mean by quantifying model parameter uncertainty and other uses of varying parameters in models. Model parameters are often used to 'tune' or optimise the response of the model, to observational data. The system of tuning a model in this way, especially if a number of parameters is used could generate the right results for the wrong reason (Williams et al. 2001), and is open to bias. This approach also assumes that the observational data targets have no errors which is unlikely to be true. It is however a useful tool for setting up a reasonable model state. In another commonly used technique, the sensitivity study, the parameters within the model system are varied to assess the effect of parameters on model response. This is however, different to quantifying the uncertainty in model response. Also, unless more than one parameter is varied at one time, then important interactions between the parameters could be missed.

1.3.2 Bayes' Theorem and addressing uncertainty in model systems

In order to quantify the uncertainty due to model parameters we need to appeal to the mathematics of probabilities. What we need to calculate is the probability of a set of model parameters being correct given the observational data that we have of the climate system.
The mathematical equation for this is known as Bayes theorem (Equation 1-3). In essence we make an initial assessment about plausible parameter settings (the prior) which is updated using Bayes theorem and observational data to improve our initial assessment and quantify the uncertainty given the data (the posterior). This is known as 'Bayesian Calibration'.

posterior = prior x likelihood **Equation 1-3**

The 'likelihood' is then the likelihood of the data (expressed as a probability distribution) given the parameters. In theory, calculating the posterior when you have a prior and likelihood is fairly straightforward, however, in practice this is not the case. A multivariate probability distribution of the parameters (the prior) cannot be incorporated into the model.

Also the model has to be used to translate the effect of the parameters into model response, for comparison to real world data. Therefore the prior has to be sampled, and an ensemble of runs with differing parameter sets are generated and used.

To apply Bayes Theorem to a model a technique called 'accept-reject' (Chib & Greenberg 1995) can be used. This technique contains five steps (1) Defining the prior, (2) Sampling the prior, (3) Running the model, (4) Calculating the likelihoods, (5) A rejection step. This system calibrates the parameters of the model, using the data chosen. The resulting posterior parameter distribution can then be used to run the model in a predictive mode, to assess the uncertainty in model response and values.

Running an ensemble of the model system, and applying the accept-reject technique requires large amounts of computing power, especially with models of great complexity. Therefore in many studies the methodology is based on what is possible in terms of available computing power, and the accept-reject system is not used.

1.3.3 Current state of ensemble modelling studies based on parameter uncertainty, what remains to be addressed?

The number of ensemble and uncertainty studies involving the climate system and its interactions with the carbon cycle has grown in recent years, but is still limited by the complexity of the models involved and the computing power available. Studies are often limited to using 2 or 3 parameter settings, the minimum, maximum and most likely value (chosen by experts) (Hallgren & Pitman 2000, Murphy et al. 2004, Stainforth et al 2005, Barnett et al. 2006). Other studies have handled the high number of runs that are required with all permutations of their chosen parameters, by using a preliminary experiment to determine the most important parameters (Zaehle et al. 2005) or by constructing an emulator, a statistical representation of model behaviour which is more efficient (Challenor et al. 2006).

Many ensembles are low in number, examples are 53 (Murphy et al. 2004, Barnett et al. 2006), 400 (Zaehle et al. 2005), 2,017 (Stainforth et al. 2005). Wigley & Raper (2001) have a respectable 109,375 members in their ensemble, and a reasonable probability based sampling of parameter values, however this still represents only a choice of 25 different values for 1 parameter, and 5 different values for 3 more. Wigley & Raper (2001) do

however adopt a Bayesian methodology for their study. Few studies seem to assess the validity of their model response to selected parameter sets in a rigorous way, Challoner et al. (2006) for example, only exclude the runs that crash. Many ensemble studies are often concentrated on the uncertainty in response in the next 100 years (Stainforth et al. 2005, Barnett et al. 2006), and do not involve fully coupled models. However, what is the uncertainty in the response beyond this time? Also, can uncertainty studies be conducted more rigorously if they are not limited by computing power?

1.4 *Focus of the study*

1.4.1 Main Themes

The main theme of this thesis is the long term effect of fossil fuel CO_2 release on the CO_2 concentration of the atmosphere. Past studies (Walker & Kasting 1992, Archer 2005) have shown that the atmosphere will take on the order of several hundred thousand years to recover. They also indicate that the controls on the long term response of this system are increases in ocean uptake through the dissolution of deep sea sediments, and the replenishment of the alkalinity pool in the ocean by the weathering of rocks on land. The level of weathering on land is directly and indirectly dependent on temperature and CO_2. This has been known and used in studies of past climate and global change, however a system which incorporates the indirect effects of increasing temperature and CO_2 on the future CO_2 concentrations of the atmosphere has not been modelled. This study aims then to address this, by asking; what will the effect of enhanced weathering be on the response of CO_2 in the atmosphere, especially on timescales of 10^4-10^6 years?

Due to the complexity of the Earth's systems, models always contain uncertainty in the way they are constructed, the parameters and data that they are based on and ultimately in their results. Many studies have attempted to acknowledge a level of uncertainty in their models, it has therefore been recognized that model results should be presented with an acknowledgement of the uncertainty they represent. Although more studies are attempting to quantify the uncertainty in their model predictions, most are restricted by the time that their model takes to run. Therefore most studies have low numbers in their ensemble and have been used to look at the next 100 years, also many have rather subjective selection systems.

This study aims to address the uncertainty in its model predictions in as comprehensive a way as possible, with an accept-reject system and trying to address issues such as a suitable sample size for uncertainty studies. The uncertainty which is addressed is mainly that of the parameters in the model, but the Bayesian system we are using dictates that we include the uncertainty associated with the data for the calibration process. Therefore the measurement error and natural variability associated with the data used (in this case atmospheric CO_2) has been taken into consideration in a small part of the study. Likewise the introduction of weathering schemes in later parts of the study will provide a preliminary assessment of structural uncertainty in weathering for the climate system. By excluding model structural effects we are making an assumption that given the correct set of parameters and initial state the model will make a perfect prediction. This is of course unlikely to be true but it allows us to make an initial attempt at quantifying uncertainty that future studies which relax this assumption can build upon. Due to the long term outlook of the Earth system being investigated here, it will also be possible to look at the uncertainty on timescales which may not have been attempted before. The study therefore poses the question, what will the uncertainty be in the long term response of CO_2 in the atmosphere to anthropogenic perturbation?

1.4.2 Key Questions

In summary this thesis aims to address two main questions; what will the long-term impact be of releasing such large quantities of CO_2 into the earth's atmosphere and how will the earth system react to the human perturbation on the timescale of 10^4-10^6 years? Two themes have been identified as being important in answering these questions, the nature of a weathering feedback and uncertainty in Earth system models. Below are the three key sub-questions addressed by the chapters in this thesis:

1. *What effect will enhanced carbonate and or silicate weathering have on the concentration of CO_2 in the atmosphere on timescales of 10^3-10^6 years?*
2. *What effect does parameter uncertainty have on the CO_2 response of the atmosphere and how does this change with time?*
3. *What effect does parameter uncertainty have on the CO_2 response of the atmosphere when a weathering feedback is included, especially on timescales of one hundred thousand years or more?*

1.4.3 How the key questions are to be addressed

The questions will be addressed by the addition of a sediment model (Chapter Two) to a pre-existing earth system model. The chosen base model has a fully coupled land, atmosphere and ocean, but is efficient enough to be run for millions of years, and in ensembles of several thousand. It is important when constructing the sediment system that the model does not lose any of is efficiency, whilst representing the system appropriately. The addition of the sediments allows the investigation of enhanced weathering functions on the model system (Chapter Three), by inclusion of three variable weathering modes. The model will then be run into the future with a variety of emissions scenarios that are used in studies of millennial climate change and beyond.

Chapters Four and Five will investigate the uncertainty in the model response for the model system with sediments and fixed weathering, then with variable weathering. The methodology will be set up in Chapter Four, and used again in Chapter Five, including an assessment of a suitable sample size for the study.

The combination of this work means that a relatively unstudied feedback on future atmospheric concentrations of CO_2 will be investigated and a first investigation into the uncertainty associated with such a feedback will also be made. Quantifying uncertainty on long timescales will also be attempted.

1.5 *Model used in this study*

The model described in Lenton (2000) provides an excellent base for this study (Figure 1-7). It is a 7-box global carbon cycle model with atmosphere, 4-box ocean, vegetation and soil reservoirs, coupled to an energy balance approximation of climate. The processes the model captures are photosynthesis, plant respiration, litter fall/mortality, soil respiration and CO_2 exchange between the atmosphere and surface ocean. Total carbon dioxide, nitrate and alkalinity are circulated through the 4 ocean boxes. Importantly this base model has already been used to provide an insight into the millennial response of the atmosphere to fossil fuel CO_2 (Lenton 2000), and can handle emissions to the atmosphere from fossil fuel emissions, and land-use change. The model also has the ability to permanently decrease a proportion of the vegetation which is lost to land-use change.

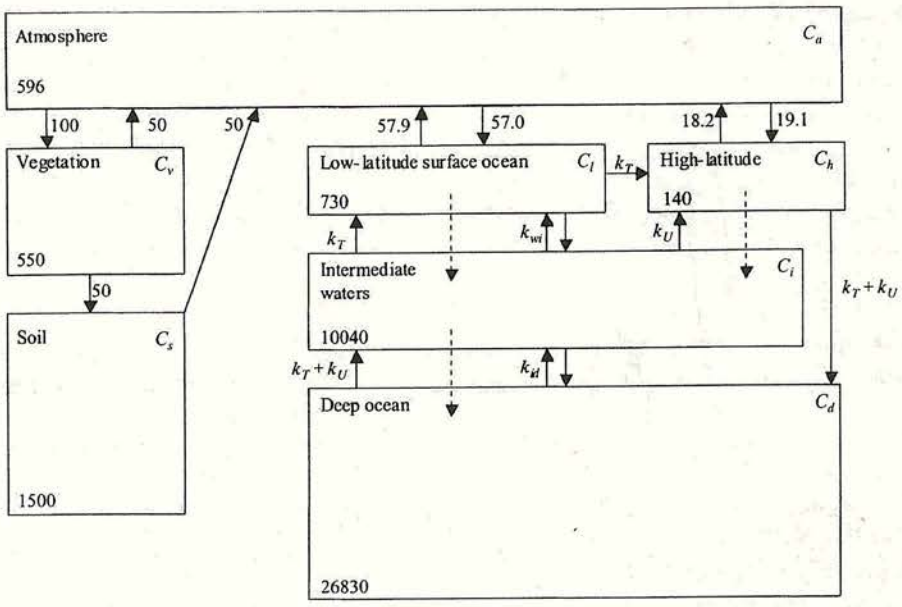

Figure 1-7: *Lenton 2000 model outline. Reservoir sizes in GtC, fluxes in GtC/yr, ocean circulation fluxes (k) detailed in Lenton 2000.*

1.6 Chapter Outline

1. ***Introduction***

   Introduction to thesis topic and structure, sets out key questions to be addressed, and how they are to be addressed.

2. ***Sediment Model Description***

   This technical document describes the addition of a sediment system to the Lenton (2000) base model and compares it to previous studies, some text is from publication Lenton and Britton (2006).

3. ***'Enhanced carbonate and silicate weathering accelerates recovery from fossil fuel CO_2 perturbations'***

   This chapter describes the addition of carbonate and silicate weathering feedbacks to the model version described in Chapter Two. The model is then used to look at the effect of these added feedbacks on the recovery of the atmosphere from fossil fuel emissions (as published in Lenton and Britton (2006) Appendix A). Text is mainly from the Lenton and Britton (2006) publication, with amendments to fit into this thesis. Question 1 is addressed in this chapter.

4. ***'Uncertainty in atmospheric CO_2 recovery from fossil fuel perturbation due to the ocean-sediment system'***

   This is a paper in preparation (co-authors Tim Lenton, David Cameron, Marcel van Oijen, Matt Williams) which outlines a methodology for quantifying uncertainty in model response with an efficient carbon cycle model on timescales of 10^4-10^6 years. The method is used to look at the uncertainty in the response of the model described in Chapter Two to fossil fuel emissions, due to the uncertainty in parameters in the ocean and sediment systems (fixed weathering only). Question 2 is addressed in this chapter.

5. ***'Assessing uncertainty in weathering feedbacks on anthropogenic CO_2 concentrations: The role of the ocean-sediment system.'***

   A paper in preparation (co-authors Tim Lenton, David Cameron, Marcel van Oijen, Matt Williams), which continues the work outlined in Chapter Four by applying the same method to the model when variable carbonate and or silicate weathering feedbacks are applied (as added in Chapter Three). Questions two and three are addressed in this chapter.

6. ***Summary and conclusions***

   This chapter summarises the key findings of earlier chapters, discusses the limitations of the work, and its wider implications. The answers to questions posed in Chapter One are given as the conclusions for this thesis.

1.7 *References*

Archer, D., Modelling the calcite lysocline, *Journal of Geophysical Research, 96*, 17037-17050, 1991.

Archer, D, A data-driven model of the global calcite lysocline, *Glob. Biogeochem. Cycl.* 10, 511-526, 1996.

Archer, D. Fate of fossil fuel CO_2 in geologic time, *Journal of Geophysical Research (Oceans)*, doi:10.1029/2004JC002625, 2005.

Archer, D., H. Kheshgi, and E. Maier-Reimer, Dynamics of fossil fuel CO2 neutralization by marine CaCO3, *Glob. Biogeochem. Cycl. 12*, 259-276, 1998.

Arrhenius, S. On the influence of carbonic acid in the air upon the temperature of the ground. *The London, Edinburgh and Dublin Philosophical Magazine and Journal of Sciences 41*, 237-276, 1896.

Bolin, B., E. T. Degens, P. Duvigneaud and S. Kempe, *(eds.) SCOPE 13 - The Global Carbon Cycle The Global Biogeochemical Carbon Cycle.*

Barnett, David N., Simon J. Brown, James M. Murphy, David M. H. Sexton, Mark J. Webb. Quantifying uncertainty in changes in extreme event frequency in response to doubled CO_2 using a large ensemble of GCM simulations. *Clim. Change, 26,* 489–511, 2006.

Barnola, J.-M., D. Raynaud, C. Lorius, and N.I. Barkov.. Historical CO_2 record from the Vostok ice core. *In Trends: A Compendium of Data on Global Change. Carbon Dioxide Information Analysis Center, Oak Ridge National Laboratory, U.S. Department of Energy, Oak Ridge, Tenn., U.S.A.,* 2003.

Bergman, N. M., T. M. Lenton, and A. J. Watson, COPSE: a new model of biogeochemical cycling over Phanerozoic time, *American Journal of Science, 304*, 397-437, 2004.

Berner, R. A. Geocarb II: A revised model of atmospheric CO_2 over Phanerozoic time, *American Journal of Science, 294*, 56-91, 1994.

Berner, R. A. The Rise of Plants and Their Effect on Weathering and Atmospheric CO_2, *Science, 276*, 544-546, 1997.

Berner, R.A., A New Look at the Long-term Carbon Cycle, *GSA today, v. 9, no. 11,* November 1999.

Berner, R. A. and M. F. Cochran, Plant-induced weathering of Hawaiian basalts, *Journal of Sedimentary Research, 68*, 723-726, 1998.

Berner, R. A. and Z. Kothavala, Geocarb III: A revised model of atmospheric CO2 over Phanerozoic time, *American Journal of Science, 301*, 182-204, 2001.

Berner, R. A. A. C. Lasaga, and R. M. Garrels, The carbonate-silicate geochemical cycle and its effect on atmospheric carbon dioxide over the past 100 million years, *American Journal of Science, 283*, 641-683, 1983.

Berthelot, M., P. Friedlingstein, P. Ciais, P. Monfray, J-L. Dufresne, H. Le Treut, L. Fairhead, Global response of the terrestrial biosphere to CO_2 and climate change using a coupled climate-carbon cycle model, *Glob. Biogeochem. Cycl.,10,* 2002.

Broecker, W.S., Glacial to interglacial changes in ocean and atmosphere of the carbon cycle, *In Climatic Variations and Variability: Facts and Theories,* 1981.

Caldeira, K. Forests, climate, and silicate rock weathering, *Journal of Geochemical Exploration 88,* 419–422, 2006.

Challoner, P.G., in: Avoiding dangerous climate change *(eds. Joachim Schellnhuber, Wolfgang Cramer, Nebojsa Nakicenovic, Tom Wigley, Gary Yohe), Cambridge University Press,* 2006.

Chib, S. and E. Greenberg, Understanding the Metropolis–Hastings algorithm, *American Statistician 49,* 327–335, 1995.

Chung, S-N., et al., Calcium carbonate budget in the Atlantic column inorganic carbon chemistry, *Glob. Biogeochem. Cycl.,17,* 2003.

Cox, P.M., Description of the "TRIFFID" Dynamic Global Vegetation Model. *Hadley Centre Technical Note 24*, 2001.

Cox, P. M., R. A. Betts, C. D. Jones, S. A. Spall, and I. J. Totterdell, Acceleration of global warming due to carbon-cycle feedbacks in a coupled climate model, *Nature, 408*, 184-187, 2000.

Delmas, R.J., J.-M. Ascencio, and M. Legrand, Polar ice evidence that atmospheric CO_2 20,000 yr BP was 50% of present. *Nature* 284, 155-57, 1980.

Dufresne, J-L., P. Friedlingstein, M. Berthelot, L. Bopp, P. Ciais, L. Fairhead, H. Le Treut, P Monfray, Effects of climate change due to CO_2 increase on land and ocean carbon uptake, *Geophysical Research Letters, 29,* 2002.

Etheridge D.M., L.P. Steele, R.L. Langenfelds, R.J. Francey, J.-M. Barnola and V.I. Morgan. Historical CO_2 records from the Law Dome DE08, DE08-2, and DSS ice cores. *In Trends: A Compendium of Data on Global Change. Carbon Dioxide Information Analysis Center, Oak Ridge National Laboratory, U.S. Department of Energy, Oak Ridge, Tenn., U.S.A.*, 1998.

Feely, R.A., et al., Impact of Anthropogenic CO_2 on the $CaCO_3$ system in the oceans, *Science 305*, 362-366, 2004.

Fluckiger, J., E. Monnin, B. Stauffer, J. Schwandler, T.F.Stocker, J. Chapellaz, J. Raynaud, J-M. Barnola, High resolution Holocene N2O ice core record asnd its relationship with CH_4 and CO_2. *Glob. Biogeochem. Cycl., 16*, 2002.

Friedlingstein, P., L. Bopp, P. Ciais, J-L. Dufresne, L. Fairhead, H. Le Treut, P. Monfray, J. Orr, Positive feedback between climate change and the carbon cycle?, *Tellus, 55,* 692-700, 2001.

Friend, A.D., A. White, Evaluation and analysis of a dynamic terrestrial ecosystem model under preindustrial conditions at the global scale *Glob. Biogeochem. Cycl., 14 (4),* 1173-1190 2000.

Furrer R., S. Sain, D. Nychka, G. Meehl, Multivariate Bayesian analysis of atmosphere-ocean general circulation models, *Environ Ecol Stat (in press),* 2006.

Ganopolski, A., V. Petoukhov, S. Rahmstorf, V. Brovkin, M. Claussen, A. Eliseev, & C. Kubatzki, 'CLIMBER-2: A climate system model of intermediate complexity. Part II: Model sensitivity', *Climate Dynamics 17,* 735–751, 2001.

Goldstein, M. & J.C. Rougier, Bayes Linear Calibrated Prediction for Complex Systems, *Journal of the American Statistical Association, forthcoming,* 2006.

Gruber, N., et al., The Vulnerability of the Carbon Cycle in the 21st Century: An assessment of Carbon-Climate-Human Interactions, *in: The global carbon cycle, (eds. C.B. Field & M.R. Raupach) Island Press,* 2004.

Hallgren, W. S., & A. J. Pitman, The uncertainty in simulations by a global biome model (BIOME3) to alternative parameter values, *Global Change Biol., 6,* 483– 495, 2000.

Hasselmann K., S. Hasselmann, R. Giering, V. Ocana, H. Storch, Sensitivity study of optimal CO_2 emissions path using a simplified structural integrated assessment model (SIAM), *Clim. Change 37,* 345–386, 1997.

Harvey, L. D. D. & Z. Huang, 'Evaluation of the potential impact of methane clathrate destabilization on future global warming', J. *Geophys. Res. 100,* 2905–2926, 1995.

Haxeltine, A., I.C. Prentice. BIOME3: an equilibrium terrestrial biosphere model based on ecophysiological constraints, resource availability and competition among plant functional types. *Glob. Biogeochem. Cycl., 10(4),* 693–709, 1996.

Holland, H.D., The chemistry of the atmosphere and oceans. *New York Wiley interscience 351p,* 1978.

Houghton R.A., & J.L. Hackler, Carbon flux to the atmosphere from land-use changes. Trends: a compendium of data on global change. *Tech. rep., Carbon Dioxide Information Analysis Center, Oak Ridge National Laboratory, Oak Ridge, Tenn., USA,* 2002.

Huybrechts, P., J.D. Wolde, The dynamic response of the Greenland and Antarctic ice sheets to multiple-century climatic warming. *J Clim 12,* 2169–2188, 1999.

Indermuhle, A., T.F. Stocker, F. Joos, H. Fischer, H. Smith, B. Wahlen, D. Deck, J. Mastroianni, J. Tschumi, T. Blunier, R. Meyer, B. Stauffer, Holocene carbon cycle dynamics baed on CO_2 trapped in ice at Taylor Dome Antarctica, *Nature, 398,* 121-126, 1999.

Indermuhle, A., E. Monnin, B. Stauffer, T.F. Stocker, M. Wahlen, Atmospheric CO_2 concentration from 60 to 20 kyr BP from the Taylor Dome ice core, Antarctica, *Geophysical Research Letters, 27,* 735-738.

IPCC, 2001: Climate Change 2001: Synthesis Report. *A Contribution of Working Groups I, II, and III to the Third Assessment Report of the Integovernmental Panel on Climate Change [Watson, R.T. and the Core Writing Team (eds.)]. Cambridge University Press, Cambridge, United Kingdom, and New York, NY, USA, 398 pp.*

Jansen, H., R.E. Zeebe, and D.A. Wolf-Gladrow, Modelling the dissolution of settling $CaCO_3$ in the ocean, *Glob. Biogeochem. Cycl., 16,* 2002.

Johns, T. C., R. E. Carnell, J.F. Crossley, J.M. Gregory, J.F.B. Mitchell, C.A. Senior, S.B. Tett, & R.A. Wood, 'The Second Hadley Centre coupled ocean-atmosphere GCM: Model description, spin-up and validation', *Climate Dynamics 13,* 103–134, 1997.

Joos, F., M. Bruno, R. Fink, U. Siegenthaler, T.F. Stocker, C. LeQuere, & J.L. Sarmiento, 'An efficient and accurate representation of complex oceanic and biospheric models of anthropogenic carbon uptake', *Tellus 48B,* 397–417, 1996.

Kawamura, K., T. Nakazawa, S. Aoki, S. Sugawara, T. Fujii, O. Watanabe, Atmospheric CO_2 variations over the last three glacial-interglacial climatic cycles deduced from the Dome Fuji deep ice core, Antarctica, using a wet extraction technique, *Tellus, 55(B),* 126-137, 2003.

Keeling, C.D. & T.P. Whorf, Atmospheric CO_2 records from sites in the SIO air sampling network. *In Trends: A Compendium of Data on Global Change. Carbon Dioxide Information Analysis Center, Oak Ridge National Laboratory, U.S. Department of Energy, Oak Ridge, Tenn., U.S.A.,* 2005.

Kharin V., F. Zwiers, Changes in the extremes in an ensemble of transient climate simulations with a coupled atmosphere ocean GCM, *J Climate, 13,* 3760–3788, 2000.

Krinner G., N. Viovy, de Noblet-Ducoudre et al., A dynamic global vegetation model for studies of the coupled atmosphere-biosphere system, *Glob. Biogeochem. Cycl., 19 (1),* 2005. Art. No. GB1015

Knox, F., & M. B. McElroy, Changes in atmospheric CO_2: Influence of the marine biota at high latitude, *J. Geophys. Res., 89,* 4629–4637, 1984.

Le Quere, C., O. Aumont, L. Bopp, P. Bousquet, P. Ciais, R. Francey, M. Heimann, D. Keeling, R.F. Keeling, H. Khesghi, P. Peylin, S.C. Piper, I.C. Prentice, & P.J. Rayner, Two decades of ocean CO_2 sink and variability, *Tellus, 55(B),* 649-656, 2003.

Le Quere, C., Metzl, N., Natural Processes Regulating the Uptake of CO_2, *in: The global carbon cycle, (eds. C.B. Field & M.R. Raupach) Island Press,* 2004.

Lenton, T. M. Land and ocean carbon cycle feedback effects on global warming in a simple Earth system model, *Tellus, 52B,* 1159-1188, 2000.

Lenton, T. M. Climate Change to the end of the Millennium, *Clim. Change, 76,* 7-29, 2006.

Lenton, T. M. & M. G. R. Cannell, Mitigating the Rate and Extent of Global Warming, *Clim. Change, 52,* 255-262, 2002.

Lenton T.M., & C. Huntingford, Global terrestrial carbon storage and uncertainties in its temperature sensitivity examined with a simple model. *Glob Change Biol, 9,* 1333–1352, 2003.

Lenton T.M., & C. Britton, Enhanced carbonate and silicate weathering accelerates recovery from fossil fuel CO_2 perturbations, *Glob. Biogeochem. Cycl., 20 (3),* 2006.

Lenton, T. M. M. S. Williamson, N. R. Edwards, R. Marsh, A. R. Price, A. J. Ridgwell, J. G. Shepherd, S. J. Cox, and theGENIEteam, Millennial timescale carbon cycle and climate change in an efficient Earth system model, *Climate Dynamics*, doi: 10.1007/s00382-00006-00109-00389, 2006.

Maier-Reimer, E., U. Mikolajewicz, K. Hasselman, Mean circulation of the Hamburg LSG OGCM and its sensitivity to the thermohaline surface forcing. *Journal of Physical Oceanography, 23,* 731-757.

Manabe, S., R. T. Wetherald, P.C.D Milly, T.L. Delworth, & R.J. Stouffer, 'Century-scale change in water availability: CO_2-quadrupling experiment', *Clim. Change 64,* 59–76, 2004.

Marland G, T.A. Boden, R.J. Andres, Global, regional, and national fossil fuel CO_2 emissions. *Trends: a compendium of data on global change. Tech. rep., Carbon Dioxide Information Analysis Center, Oak Ridge National Laboratory, Oak Ridge, Tenn., USA,* 2003.

Marland G, T.A. Boden, R.J. Andres, Global, regional, and national fossil fuel CO_2 emissions. *Trends: a compendium of data on global change., Carbon Dioxide Information Analysis Center, Oak Ridge National Laboratory, Oak Ridge, Tenn., USA,* 2006.

Marsh, R. J., A. Yool, T. M. Lenton, M. Y. Gulamali, N. R. Edwards, J. G. Shepherd, M. Krznaric, S. Newhouse, & S.J. Cox, 'Bistability of the thermohaline circulation

identified through comprehensive 2-parameter sweeps of an efficient climate model', *Climate Dynamics, 23,* 761–777, 2004.

Meehl G., C. Tebaldi, More intense, more frequent, and longer lasting heat waves in the 21st century, *Science 305,* 994–997, 2004.

Milliman ,J.D., A.W. Droxler, Neritic and pelagic carbonate sedimentation in the marine environment: Ignorance is not bliss, *Geologische Rundschau 85,* 496-504, 1996.

Milliman, J.D. et al., Biologically mediated dissolution of calcium carbonate above the chemical lysocline? *Deep-sea research I, 46,* 1653-1669, 1999.

Monnin,E, A.L. Indermuhle, A. Daalenbach, J. Fluckiger, B. Stauffer, T.F. Stocker, D. Raynaud, J. Barnola, Atmospheric CO_2 concentrations over the last glacial termination, *Science 291*, 1862-1865, 2001.

Murphy, J., D. Sexton, D. Barnett, G. Jones, M. Webb, M. Collins, D Stainforth, quantification of modelling uncertainties in a large ensemble of climate change simulations. *Nature 430,* 768–772, 2004.

Neftel, A., H. Oeschger, J. Schwander, B. Stauffer, and R. Zumbrunn, Ice core measurements give atmospheric CO_2 content during the past 40,000 yr. *Nature* 295:220-23, 1982.

Palmer, T., J. Raisanen, Quantifying the risk of extreme seasonal precipitation events in a changing climate, *Nature, 415,* 512–514, 2002.

Petit, J.R., J. Jouzel, D. Raynaud, N.I. Barkov, J-M. Barnola, I. Basile, M. Bender, J. Chapellaz, M. Davis, G. Delagyue, M. Delmotte, V.M. Kotylakov, M. Legrand, V.Y. Lipenkov, C. Lriuos, L. Pepin, C. Ritz, E. Saltzman, M. Stievenard, Climate and atmospheric history of the past 420,000 years from the Vostok ice core, Antarctica. *Nature, 399,* 429-436, 1999.

Prentice, I.C., W. Cramer, S.P. Harrison et al., A global biome model based on plant physiology and dominance, soil properties and climate, *Journal of Biogeography, 19(2),* 117-134, 1992.

Rahmstorf S., A. Ganopolski, Long term global warming scenarios computed with an efficient coupled climate model, *Clim Change 43,* 353–367, 1999.

Raymo, M.E., Geochemical evidence supporting TC Chamberlin's theory of glaciation, *Geology 19,* 344–347, 1991.

Raper, S. C. B., J. M. Gregory & T. J. Osborn, 'Use of an upwelling-diffusion energy balance climate model to simulate and diagnose A/OGCM results', *Climate Dynamics 17,* 601–613, 2000.

Ridgwell, A. J. *Glacial-interglacial perturbations in the global carbon cycle*, 134 pp. University of East Anglia, Norwich, 2001.

Sabine et.al, Current Status and Past Trends of the Global carbon cycle, *in: The global carbon cycle, (eds. C.B. Field & M.R. Raupach) Island Press,* 2004.

Sarmiento J.L, Biogeochemical ocean models in: *Climate System Modelling (ed. K.E. Trenbarth) Cambridge University Press,* Cambridge, 511-549, 1992.

Sarmiento, J.L., J.C. Orr, U. Siegenthaler, A perturbation simulation of CO_2 uptake in an ocean general circulation model, *Journal of Geophysical Research 97(C3),* 3621-3645.

Schmittner, A. & T. F. Stocker, 'The stability of the thermohaline circulation in global warming experiments', *Journal of Climate* 12, 1117–1133, 1999.

Sellers, P.J., Y. Mintz, Y.D. Sud, et al., A simple biosphere model (SIB) for use within general-circulation models, *Journal of the Atmospheric Sciences, 43(6),*505-531, 1986.

Siegenthaler, U., F. Joos, Use of a simple for studying oceanic tracer distributions of the global carbon cycle, *Tellus, 44B,* 186-207, 1992.

Siegenthaler U., E. Monnin, K. Kawamura, R. Spahni, J. Schwander, B. Stauffer, T.F. Stocker, J.-M. Barnola, H. Fischer, High resolution CO_2 records over the last 1000 years from the EPICA Dronning Maud Land ice core. *Tellus 57B*, 51-57, 2005.

Sigman, D, M., E.A. Boyle, Glacial-interglacial variations in atmospheric carbon dioxide. *Nature, 407,* 2000.

Schwartzman, D. W. and T. Volk, Biotic enhancement of weathering and the habitability of Earth, *Nature, 340,* 457-460, 1989.

Stainforth, D., T. Aina, C. Christensen, M. Collins, N. Faull, D. Frame, J. Kettleborough, S. Knight, A. Martin, J. Murphy, C. Piani, D. Sexton, L. Smith, R. Spicer, A. Thorpe, M. Allen Uncertainty in predictions of the climate response to rising levels of greenhouse gases. *Nature 433,* 403–406, 2005.

Stephens, B.B. and R.F. Keeling, The influence of Antarctic sea ice on glacial-interglacial CO_2 variations, *Nature, 404, 171-174,* 2000.

Sundquist, E.T., Steady- and non-steady-state carbonate-silicate controls on atmospheric CO_2 *Quaternary Science Review,* **Vol. 10, Pages 283-296**, 1991

Tebaldi C., R. Smith, D. Nychka, L. Mearns, Quantifying uncertainty in projections of regional climate change: a Bayesian approach to the analysis of multi-model ensembles. *J Climate, 18,* 1524–1540, 2005.

Volk, T., & M. I. Hoffert, Ocean carbon pumps: Analysis of relative strengths and efficiencies in ocean-driven atmospheric CO_2 changes, *Geophys. Monogr., 32,* 99-110, 1985.

Voss, R. and Mikolajewicz, U., 'Long-term climate changes due to increased CO_2 concentration in the coupled atmosphere-ocean general circulation model ECHAM3/LSG', *Clim. Dynamics, 17,* 45–60, 2001.

Walker, J. C. G. and J. F. Kasting, Effects of fuel and forest conservation on future levels of atmospheric carbon dioxide, *Palaeogeography, Palaeoclimatology, Palaeoecology (Global and Planetary Change Section), 97,* 151-189, 1992.

Weaver, A.J., F.W. Zwiers, Uncertainty in climate change. *Nature, 407,* 571-572, 2000.

Weaver, A. J., M. Eby, E. C. Wiebe, C. M. Bitz, P. B. Duffy, T. L. Ewen, A.F. Fanning, M. M. Holland, A. McFadyen, H. D. Matthews, K. J. Meissner, O. Saenko, A. Schmittner, H. Wang, & M. Yoshimori, 'TheUVic earth system climate model: Model description, climatology, and applications to past, present and future climates', *Atmosphere-Ocean, 39*, 2001.

White, A. F., and A. E. Blum, Effects of climate on chemical weathering in watersheds, *Geochim. cosmochim. Acta, 59,* 1729-1747, 1995.

Wigley, T. M. L. & Raper, S. L. Interpretation of high projections for global mean warming. *Science 293*, 451–454, 2001.

Williams, E. L. L. M. Walter, T. C. W. Ku, G. W. Kling, and D. R. Zak, Effects of CO2 and nutrient availability on mineral weathering in controlled tree growth experiments, *Glob. Biogeochem. Cycl. 17*, 1041, 2003.

Williams, E. L. L. M. Walter, T. C. W. Ku, G. W. Kling, and D. R. Zak, Effects of CO_2 and nutrient availability on mineral weathering in controlled tree growth experiments, *Glob. Biogeochem. Cycl. 17*, 1041, 2003.

Williams, M., B.J. Bond, Ryan M.G. et al., Evaluating different soil and plant hydraulic constraints on tree function using a model and sap flow data from ponderosa pine. *Plant, Cell and Environment, 24,* 679-690, 2001.

Zaehle, S., S. Sitch, B. Smith, and F. Hatterman, Effects of parameter uncertainties on the modeling of terrestrial biosphere dynamics, *Glob. Biogeochem. Cycl., 19,* 2005, GB3020, doi:10.1029/2004GB002395.

2 Sediment Model Description

2.1 *Introduction*

This Chapter outlines the addition of an ocean-sediment system to the base model detailed in Lenton (2000). All parameters and settings are as described in Lenton (2000) unless stated otherwise. Firstly there is a brief description of how the ocean-sediment part of the Earth system works and how this has been incorporated into previous models. This is followed by a detailed description of the sediment model, spinning up the model to steady-state, and applying historical and future emissions. The section finishes by comparing the model response to fossil fuel CO_2 emissions with the previous model version (Lenton 2000), and an ocean-sediment model (Archer et al. 1998). Both of these models have been used to look at the response in the atmosphere to burning fossil fuels, beyond the year 2100.

2.1.1 Pelagic sediments and the ocean carbon cycle

Pelagic sediments are an important part of the ocean carbon cycle (Figure 2-1) as they provide a feedback with the ocean chemistry. As the ocean exchanges CO_2 with the atmosphere, changes to the sediment system can affect the concentration of CO_2 in the atmosphere and vice-versa. Through the greenhouse effect CO_2 has an impact on the climate of the planet, making sediments a very important part of the carbon-climate system.

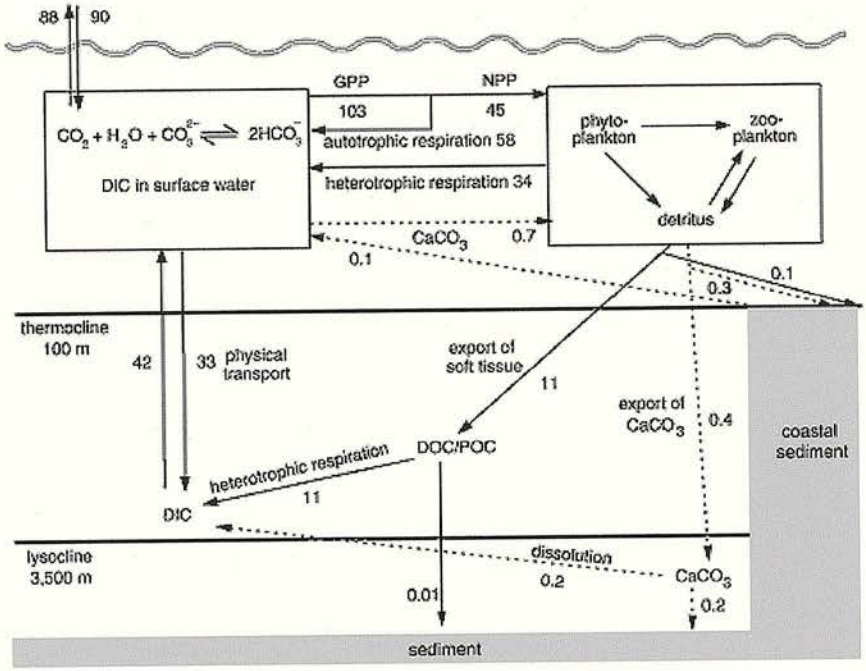

Figure 2-1: *Overview of the ocean carbon cycle, reservoirs in GtC and fluxes in GtC/yr. (From IPCC (Houghton et al. 2001).*

The chemical operation of the ocean depends on the relative concentrations of dissolved inorganic carbon (*DIC*), and alkalinity (*ALK*) (in this case, carbonate alkalinity, described in Chapter 1, section 1.1.1.3). *DIC* represents the sum of carbonate chemicals produced when CO_2 dissolves in seawater, free carbon dioxide ($CO_{2(aqueous)}$ as opposed to the gaseous form, which has not dissolved), carbonic acid (H_2CO_3), bicarbonate (HCO_3^-), and carbonate (CO_3^{2-}). The distribution of *DIC* and *ALK* is controlled by three pumps (Volk and Hoffert 1985), the 'solubility pump', soft-tissue pump' and the '$CaCO_3$ pump' (Figure 2-2). The solubility pump arises from the physical properties of carbon dioxide gas, which is more soluble at lower temperatures, the result being that when the surface ocean equilibrates with the atmosphere there is a net uptake of CO_2 into the ocean in colder areas, and an outgassing of CO_2 in warmer areas. The 'soft-tissue pump' describes the uptake of *DIC* (and increase in *ALK* due to nitrate usage) when plankton produce the soft-tissue organic carbon of their bodies, which then sinks, slowly decaying (re-mineralising), which releases the *DIC* (and decreasing the *ALK*) back into the ocean. Finally there is the '$CaCO_3$ pump', where plankton build their skeletons (tests) out of $CaCO_3$ from the *DIC* pool (this in turn decreases *ALK* due to the use of Ca^{2+}), after the death of the plankton, these particles also sink through the

ocean. Dissolution of these particles will occur if the seawater is undersaturated with respect to calcite. Due to the depth dependence of solubility, undersaturated water is found at depth in the ocean, meaning that dissolution of the $CaCO_3$ particles occurs if they sink past the calcite saturation horizon. After this point dissolution can occur, but slowly, therefore the depth where dissolution becomes more marked is termed the 'lysocline', and beyond this depth dissolution continues (within the lysocline transition zone) to a depth where all $CaCO_3$ is dissolved (the carbonate compensation depth – CCD). When the $CaCO_3$ dissolves it is returned as *DIC* and *ALK* to the ocean, however, some particles do reach the ocean floor before they can dissolve. In this situation they can be dissolved at the ocean-sediment interface, or they may remain to become sediments, locking up the *DIC* and *ALK* that they have essentially removed from the surface ocean. $CaCO_3$ is also precipitated in the shallow seas to make carbonate reefs.

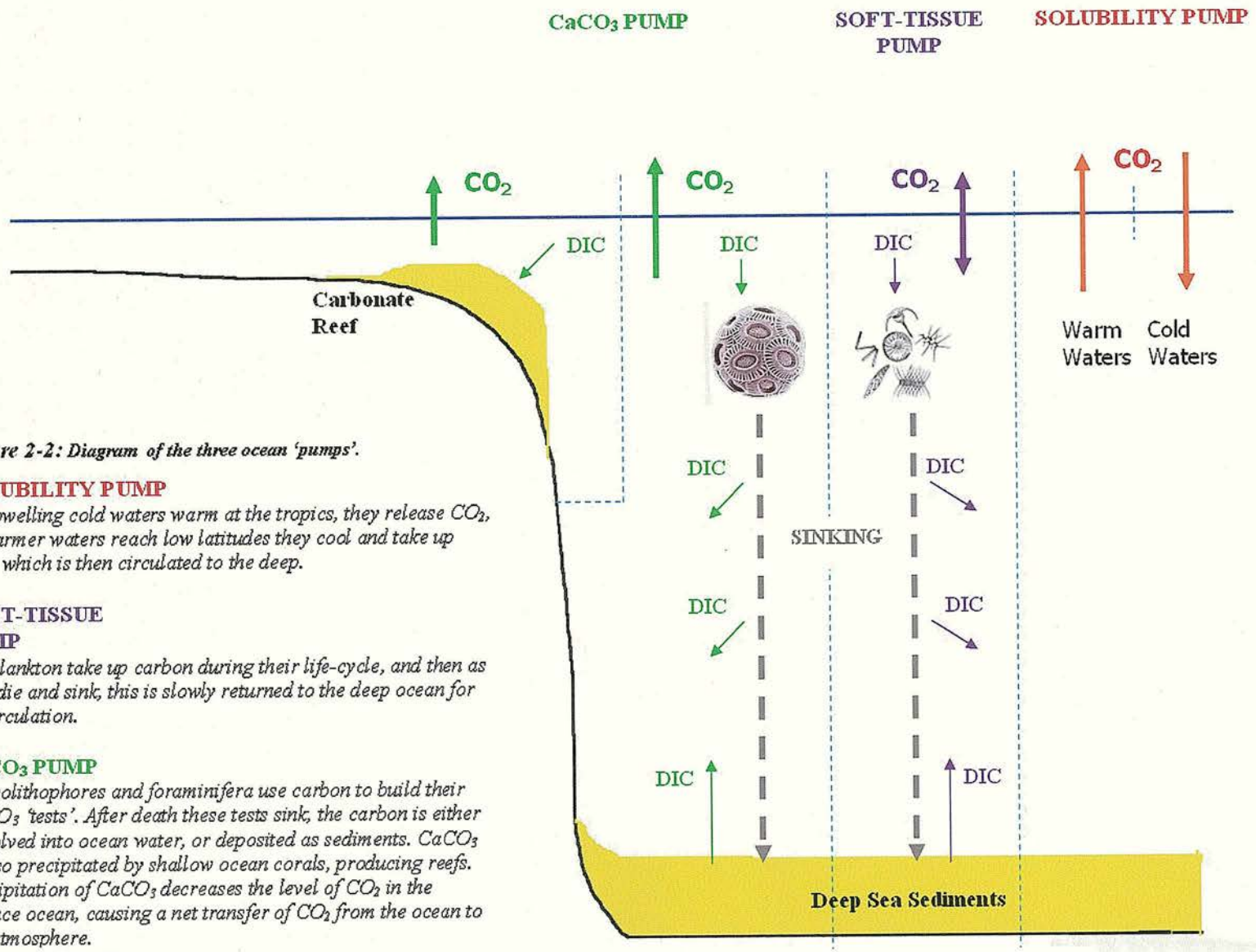

***Figure 2-2:** Diagram of the three ocean 'pumps'.*

SOLUBILITY PUMP

As upwelling cold waters warm at the tropics, they release CO_2, as warmer waters reach low latitudes they cool and take up CO_2, which is then circulated to the deep.

SOFT-TISSUE PUMP

Zooplankton take up carbon during their life-cycle, and then as they die and sink, this is slowly returned to the deep ocean for re-circulation.

$CaCO_3$ PUMP

Coccolithophores and foraminifera use carbon to build their $CaCO_3$ 'tests'. After death these tests sink, the carbon is either dissolved into ocean water, or deposited as sediments. $CaCO_3$ is also precipitated by shallow ocean corals, producing reefs. Precipitation of $CaCO_3$ decreases the level of CO_2 in the surface ocean, causing a net transfer of CO_2 from the ocean to the atmosphere.

2.1.2 Important constituents of the ocean-sediment system

In order to model the ocean-sediment carbon cycle system effectively, the three pumps described above all need to be represented. This covers the 'in-transit' re-mineralization of organic carbon, and dissolution of $CaCO_3$. However the 'in-situ' fate of the organic carbon and $CaCO_3$, i.e. whether it is re-mineralised or dissolved or deposited at the sediment surface also needs to be included. 'In-situ' dissolution of $CaCO_3$ depends on a number of factors which are connected to the sediment itself, such as its porosity, the amount of $CaCO_3$, bioturbation (sediment displacement by organisms), and organic carbon respiration. There is also a flux of non $CaCO_3$ material (i.e. biogenic opal, dust) to the seafloor, which also undergoes lithification into sediment, and must be modelled.

2.1.3 Existing sediment models

The explicit modelling of pelagic sediments began with formulas to describe the apparent solubility product of calcite in the ocean with respect to temperature and depth, and the relationship between saturation state and 'in-situ' calcium carbonate dissolution (Ingle 1975, Keir 1980). This lead to a number basic sediment models (Broecker & Peng 1982, Keir 1988, Archer 1991, Munhoven and Francois 1992), which became the basis for other approaches (Opdyke and Walker 1992, Caldeira and Rampino 1993, Sigman 1998; Archer 1996, Archer et al. 1998, Heinze 1999, Ridgwell 2001; Munhoven & Francois 1996). The approach of each model is tailored to the type of study, the timescales involved, and the computational availability. In terms of the in-situ dissolution system there are three distinct methods, the least complex being to compute the fractional seafloor above the calcite lysocline (Caldeira & Rampino 1993). Next in the range of complexity involves calculating the dissolution flux from a sediment box or layer, the depth of which represents the depth within the sediment which dissolution can affect (generally taken to be about 10cm, due to the bioturbation of the sediment), the area represents the surface area of seafloor at that water depth. In most cases this gives complete coverage of the seafloor (except for Opdyke & Walker (1992); who used boxes at 15 discrete ocean depths, and then extrapolated between them). Most of the researchers with models of this level of complexity (e.g. Keir 1988, Munhoven and Francois 1996) also resolve their oceans into boxes, so there are sediment levels at various depths for each basin. Models of the next level of complexity also have a sediment box for a specific depth, but this then contains a set of discretized layers (e.g. 0.5cm - 2cm), and the model predicts the steady-state concentration, dissolution and burial of

$CaCO_3$. These models also tend to be much more spatially resolved than an ocean basin based system.

Although the method of calculation of the rate of dissolution that occurs varies amongst the models, the basic principle of dissolution being proportional to the bottom water saturation, and the same rate equation of dissolution are used throughout (Keir 1980). The least complex models either have equations to calculate the dissolution directly, e.g. working 'online' (e.g. Keir 1988, Munhoven and Francois 1996), or have used more complicated 'offline' sediment models to produce parameterisations for multiple variables, which they then use in the model (Sigman 1998). The more complex models (Archer 1991, Archer 1996, Archer et al. 1998, Ridgwell 2001) include the effect of the porosity, active bioturbation and respiration of organic carbon within the 10cm sediment layer (the parameterisations used by Sigman (1998) also include the effects of organic carbon respiration).

The dissolution of calcium carbonate can exceed its deposition, and in the real ocean the carbonate sediments that are below can be eroded. This has meant that the more complex models have also included the dissolution of sediments that are below this initial 10cm sediment layer. In the case of (Archer 1996, Archer et al. 1998), the erosion of carbonate from below the initial layer is allowed to continue until the initial layer is completely filled with non-$CaCO_3$ material. In other models that are derived from Archer's earlier work (Heinze 1999, Ridgwell 2001) the sediment system actually has an aspect of 'memory' in that a series of sedimentary 'stacks' or sub-layers are created below the initial 10cm sediment layer, these can be filled and emptied as appropriate to the dissolution or accumulation of the 10cm layer above, which must always stay a constant volume.

The sediment stacks can also be filled in different ways, Heinze (1999) used an 'open-bottomed' stacking system, where each of the layers below the initial layer is always full, and any extra material is lost or gained from below the lowest stack, which means that the system is not conservative. Whereas the solution given in Ridgwell (2001) was to have an 'open-topped' stacking system, where a new 'sub-layer' or stack would be created at the base of the initial layer if the one below was overfilled, and the sub-layer does not need to be full. Now the system is conservative, and less computationally demanding. However, this method does still require a lot of computing power, and to counteract this the dissolution at the sediment water interface is obtained by referencing a 'look-up' table of values with variables such as the undersaturation, fraction of $CaCO_3$ and organic carbon. This model is one of the few to

explicitly include the aragonite lysocline within the ocean (calcium carbonate can exist as two polymorphs, calcite and aragonite which have different dissolution kinetics, aragonite makes up ~5 % of the $CaCO_3$ export production (Ridgwell 2001)).

Treatment of the carbon export fluxes also differ in sediment models, most however relate the organic carbon export to the nutrient concentration of the surface ocean (phosphate or nitrate) (Keir 1988, Munhoven and Francois 1994, Sigman 1998, Caldeira & Rampino 1993) using the Redfield ratios (C:N:P, 106:16:1 (Redfield et al. 1963)), but more complex systems which involve nutrient tracers calculate the limit of organic carbon export as a function of latitude and temperature, as well as nutrient concentration (Archer 1996).

The calculation of inorganic carbon is usually set as a ratio to organic carbon export, for the models discussed here this has taken a range of values (e.g. 0.25 (Caldeira & Rampino 1993) - 0.46 (Sigman 1998)), to incorporate things such as high and low latitude differences, and different suggestions from data. In the case of the more complex models (Ridgwell 2001) the ratio remains an optimizable parameter. The decay of the organic and inorganic carbon as it passes through the water column is also of differing complexity in the models, the simplest being a straight division of re-mineralization or dissolution between intermediate and deep boxes (Sigman 1998), and the more involved including a fraction of the carbon being resistant to decay, and landing on the seafloor, the rest surviving being dependent upon depth, the parameterisation of which comes from various data based studies (Ridgwell 2001). However some models now also include the effect of aggregation and disaggregation of a range of particle sizes on the transport of organic carbon.

2.2 *Sediment Model Description*

The base model (Lenton 2000) was chosen for this study due to its fully coupled land, atmosphere and ocean carbon cycles, whilst still being computationally efficient. Retaining this efficiency was important for two reasons, firstly to allow the investigation of the long term (>1Myr) effects of adding anthropogenic CO_2 to the atmosphere, and secondly to allow multiple runs of the model for uncertainty studies. The sediment system used in this study was therefore designed and implemented with this efficiency in mind. More complex representations of the sediment interaction with the ocean already exist, however these are not currently appropriate for the task being attempted here.

2.2.1 Model Structure

The original model structure (see Chapter One and Lenton (2000)) has been extended by adding 10 sediment levels, variable nutrients and *ALK* in the ocean boxes, and a riverine alkalinity and carbon flux to the warm surface ocean (Figure 2-3). To allow the calculation of organic and inorganic biogenic carbon export, re-mineralization and dissolution through the water column and landing on the seafloor, the ocean has been subdivided into a set of 'depth zones', (Figure 2-3). The depth zones correspond to a vertical range of 500m which means two for the intermediate ocean box, and eight for the deep. The surface ocean (0-100m) is not included within a depth zone, as the re-mineralization and dissolution in the water column begins after this depth. To have 10 depth zones the deepest ocean floor has been set at 5100m, so any volume of water beyond this is included in the 10th depth zone, the real ocean does reach considerably deeper than this, however the current lysocline is within the set 5100m. Corresponding to each depth zone is a sediment box, which simulates the area of ocean floor beneath it, and sediment to a depth of 10cm, these will be described in more detail later. The fractional area of seafloor beneath each depth zone (and therefore also the fractional surface area of each sediment box) was calculated from summed 100m resolution bathymetry data from the National Geophysical Data Center (Boulder Colorado, USA). The TerrainBase Global DTM version 1.0 database contains a matrix of land topography and ocean bathymetry for the entire world, gridded at 5 minute intervals. For ease of data-handling, this matrix was first averaged down to one gridded at 30 minute intervals. The appropriate values for this study are shown in Table 2-1.

Layer i	Depth interval (m)	Fraction of seabed A_i (%)	Area of seafloor (10^{12} m^2)	Volume of layer V_i (10^{12} m^3)
1	100-600	5.056	17.39	0.4347
2	600-1100	2.095	7.20	0.1801
3	1100-1600	2.294	7.89	0.1972
4	1600-2100	2.662	9.15	0.2288
5	2100-2600	3.584	12.33	0.3081
6	2600-3100	6.488	22.31	0.5578
7	3100-3600	10.630	36.56	0.9139
8	3600-4100	14.832	51.01	1.2752
9	4100-4600	17.345	59.65	1.4913
10	4600-5100	35.014	120.41	3.0103

Table 2-1: *Depth zone information*

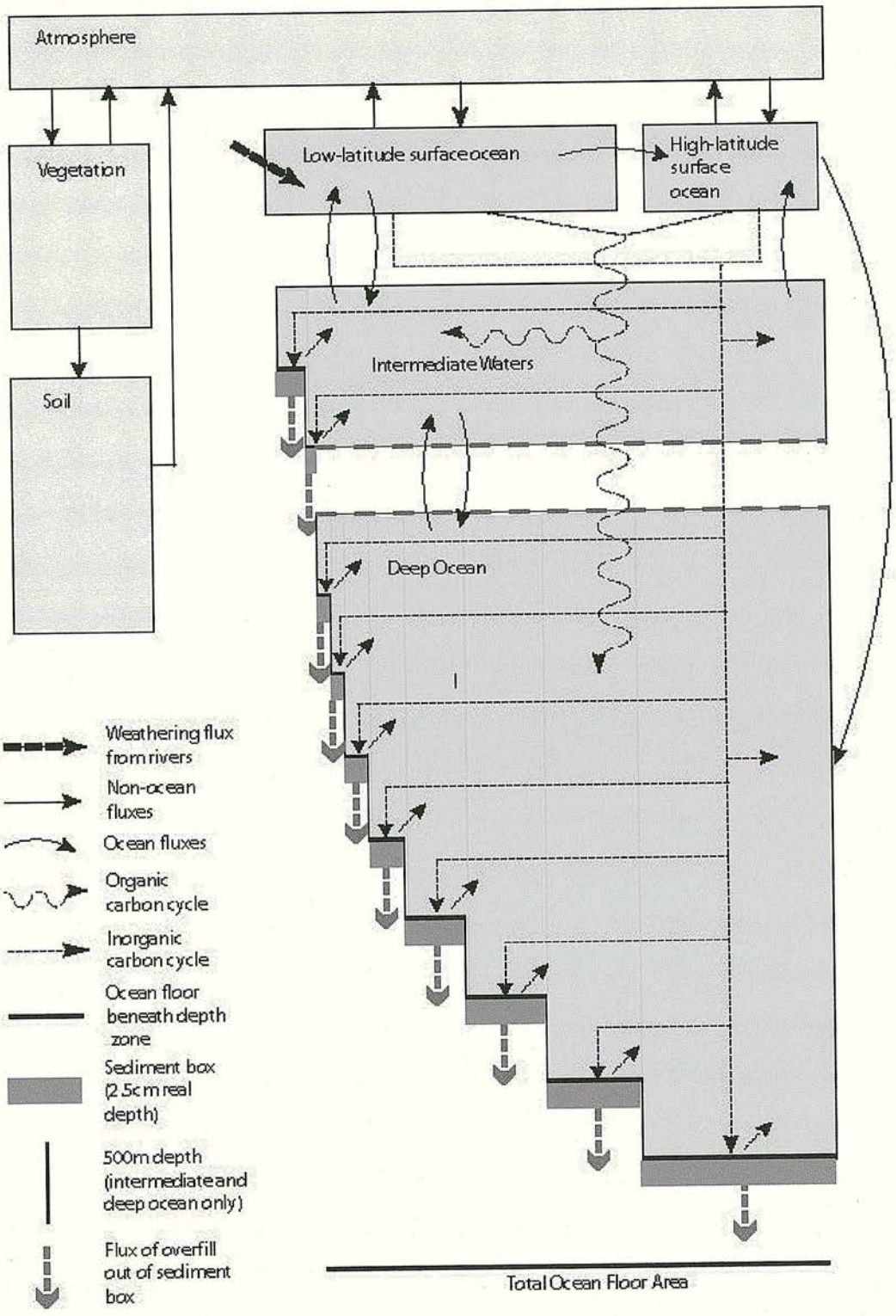

Figure 2-3: *Additions to the ocean part of the original model, including the depth zone structure.*

2.2.1.1 Detrital Flux

Ocean sediments are modelled as partly calcium carbonate and partly detrital material, such as biogenic opal and dust. The detrital flux in this model is considered to consist of only opal (to allow easier calculation of the volumes), and its distribution over the seafloor is strictly dependent on the fraction of seafloor of any depth level, as the opal does not decay in the water column. F_D^i (mol/yr), the flux of detritus to the sediments for a specific depth zone (i), where A_i is the fractional area of seafloor for sediment beneath depth zone (i) is given below:

$$F_D^i = F_D A_i \qquad \textbf{Equation 2-1}$$

The total flux of detritus $F_D = 6\text{x}10^{12}$mol/yr (Archer et al. 1998), and is constant throughout all runs of the model. To interact with the sediment box system, the fluxes are converted into volumes of detritus per layer V_D^i using a conversion factor ($K_{VD} = 4.16781\times10^{-5}$, m^3/mol), obtained from the molar volume of Opal (H_4SiO_4).

2.2.1.2 Productivity

Nitrate is the proximate limiting nutrient on timescales of thousands of years (Lenton and Watson 2000, Tyrell 1999). The ocean system used here is based on Knox and McElroy (1984), which uses a generic nutrient labelled as 'nitrate' (F_N) to fuel ocean productivity. As productivity is limited by nutrients in the warm surface ocean, the nitrate is totally consumed in the warm surface ocean. However, parts of the high latitude ocean (e.g. the Southern ocean) are high-nutrient low-chlorophyll (HNLC) regions, where productivity is limited by iron and/or light rather than nutrients. Therefore the parameter α is used to limit the fraction of nutrient usage in the high latitude ocean box.

2.2.1.3 Organic Carbon Cycle

The organic carbon export flux F_{OrgC} is proportional to productivity (F_N) using a Redfield ratio of $R_{C/N} = 7$ (Knox & McElroy 1984), given by:

$$F_{OrgC} = F_N R_{C/N} \qquad \textbf{Equation 2-2}$$

Organic carbon is re-mineralised as it sinks through the water column, however some will land on the seafloor before this has happened, and some will reach the deepest parts of the ocean. In this model all of the organic carbon is re-mineralised; any which reaches the sediment water interface is re-mineralised without having any effect on the sediments due to respiration and the re-mineralization is resolved into the intermediate and deep boxes. The amount of organic carbon which lands on the seafloor below any depth zone is dependent upon the fraction of seafloor for that depth zone (A_i), and $F_{OrgC}(z)$, the amount of organic carbon that is still left to sink at depth (z), given by:

$$F_{OrgC}(z) = F_{OrgC}\left(0.05 + 0.95\left(\frac{100 + (z - z_0)}{100}\right)^{-0.950}\right) \qquad \textbf{Equation 2-3}$$

This equation comes from Ridgwell (2001), and represents a fraction of organic carbon that settles through the water column unaltered (0.05) while the rest is degraded according to a simple power law. The resistant fraction which lands on the seafloor, the non-resistant fraction which lands on the seafloor and the organic carbon which is re-mineralised within the water column can then be calculated for each depth zone. In reality this is only calculated for the first two depth zones, which are summed to represent the re-mineralization within the intermediate ocean box. The deep box re-mineralization is then equal to the remaining organic carbon flux, as there is 100% re-mineralization in this model. The return of nitrate to each of the ocean boxes is then calculated using the ratio $R_{C/N}$.

2.2.1.4 Inorganic Carbon Cycle

2.2.1.4.1 Export Flux

The calcite export flux in this model (F_{CaCO_3}) is linked proportionally to the organic carbon export flux, a system which has been used in other sediment models (Caldeira & Rampino 1993, Munhoven and Francois 1996, Sigman 1998).

$$F_{CaCO_3} = F_N R_{(C/N)} R_{(CaCO_3/OrgC)} \qquad \textbf{Equation 2-4}$$

Where $R_{(CaCO_3/OrgC)}$ is the ratio of inorganic to organic carbon export, set at 0.25 (Knox and McElroy 1984).

2.2.1.4.2 *In-transit dissolution*

In-transit dissolution of inorganic carbon, that which takes place in the water column, is dependent on a decay scheme and the distribution of seafloor with depth. This is similar to the system used for organic carbon export, however it is necessary to keep track of the activity in each layer, rather than resolving it into the intermediate and deep ocean boxes. The settling flux of calcite with depth, ($F_{CaCO_3}(z)$) is taken from (Ridgwell 2001), and is valid where ($z > z_0$).

$$F_{CaCO_3}(z) = F_{CaCO_3}\left(0.4 + 0.6e^{\left(\frac{-(z-z_0)}{500}\right)}\right) \qquad \textbf{Equation 2-5}$$

The contribution of *DIC* to each depth zone (i) due to in-transit dissolution is given by:

$$F_{Tdiss(DIC)}(i) = 0.6F_{CaCO_3}(1-e)e^{-(i-1)}\prod_{k=1}^{(i-1)}(1-A_k) \qquad \textbf{Equation 2-6}$$

The contribution is then summed for intermediate and deep layers.

2.2.1.4.3 *Flux of carbon available for in-situ dissolution*

Carbon which does not dissolve in-transit and reaches the seafloor, will either become sediment, or be dissolved in-situ at the ocean sediment interface. $F_{CaCO_3}(i)$ is the amount of $CaCO_3$ that reaches the ocean-sediment interface at the bottom of depth zone (i):

$$F_{CaCO_3}(i) = F_{CaCO_3}A_i\prod_{k=1}^{(i-1)}(1-A_k) \qquad \textbf{Equation 2-7}$$

This $CaCO_3$ is then available for in-situ dissolution, or lithification into a sedimentary rock. In the model system, $F_{CaCO_3}(i)$ is converted to a volume ($V_{CaCO_3}(i)$), using the molar volume of $CaCO_3$ ($K_{VCaCO_3} = 3.70692 \times 10^{-5}$, m^3/mol).

2.2.1.4.4 *In-situ dissolution*

The volume of in-situ dissolution at the ocean-sediment interface is given by:

$$V_{Sdiss}(i) = V_{CaCO_3} \chi (1-\Omega)^{\varepsilon}$$ **Equation 2-8**

This makes the in-situ dissolution dependent upon the saturation state of the water above the sediment box (Ω), and the volume of $CaCO_3$ within the sediment (Keir 1980, Sigman 1998, Archer et al. 1998, Ridgwell 2001). A Dissolution exponent of ($\varepsilon = 4.5$) was used initially (Keir 1980, Berelson et al. 1994, Archer et al. 1998, Ridgwell 2001) and a dissolution constant of ($\chi = 20$) (Ridgwell pers.comm.). Dissolution exponent values vary widely within the literature (Ridgwell 2001, Keir 1980, Morse 1978, to quote but a few), however the effect of uncertainty in the initial value of this parameter on CO_2 response will be addressed in Chapters Four and Five. The volume of in-situ dissolution releases *DIC* back into the ocean, described by:

$$F_{Sdiss(DIC)}(i) = \frac{V_{Sdiss(DIC)}(i)}{K_{VCaCO_3}}$$ **Equation 2-9**

The saturation state of ocean water (Ω) is dependent upon the ratio of the total ion concentration product ($[Ca^{2+}] \bullet [CO_3^{2-}]$, the in-situ value) to the apparent solubility product of calcite (*ksp*) (Keir 1980), given by:

$$\Omega = \frac{[Ca^{2+}] \bullet [CO_3^{2-}]}{ksp}$$ **Equation 2-10**

The apparent solubility product (*ksp*) is a function of the temperature (*T* (degrees Kelvin)& *Tc* (degrees Celsius), pressure (*P*), and salinity (*sal*) of the water (Ingle 1975) and is calculated for each of the depth levels within the model as given below:

$$ksp = \exp(corr) \times 10^{cal}$$ **Equation 2-11**

$$corr = (-(-48.8 + 0.53Tc) + ((5 \times 10^4 (-11.8 + 0.369Tc))P)\frac{P}{RT}$$ **Equation 2-12**

$$cal = -171.9065 - 0.077993T + \frac{2839.319}{T} + 71.595(\log T) + \left(-0.77712 + 0.0028426T + \frac{178.34}{T}\right) sal^{0.5} - 0.07711 sal + 0.0041249 sal^{1.5}$$ **Equation 2-13**

R is the molar gas constant, and pressure and temperature was taken to be that for the mid-depth for each of the depth zones (Table 2-2), (NODC (Levitus) World Ocean Atlas 1998, http://www.cdc.noaa.gov/cdc/data.nodc.woa98.html).

Layer	*Temp(°K)*	*Pressure (atm)*
1	273.15	35
2	278.0275	85
3	276.431	135
4	275.664	185
5	275.2366	235
6	274.9537	285
7	274.7467	335
8	274.5696	385
9	274.4655	435
10	274.4535	485

Table 2-2: *Temperature and pressure by depth zone*

The calcuim ion concentration (Ca^{2+}) is not thought to vary by more than 1.5% in the whole ocean, therefore its value remains constant in the model, dependent upon salinity, calculated as below (Millero 1979):

$$Ca^{2+} = sal(2.937 \times 10^{-4})$$ **Equation 2-14**

The carbonate ion concentration (CO_3^{2-}) is derived using the same carbonate equilibrium calculations that are used in the surface ocean (Lenton 2000, Park 1969) however, the temperature, *ALK* and *DIC* values that are used in each depth zone correspond to the ocean box in which the depth zone is situated. Basically these variables are not resolved to depth zone level. Average temperature for the intermediate and deep ocean boxes is 280°K and 275°K respectively.

EX BIBL UNIV EDINBURGH

2.2.1.4.5 Sediment Box System

The sediment boxes represent the surface area of seafloor underneath each depth zone, and the 10cm depth within the sediment that dissolution is thought to reach (with the aid of bioturbation). There are therefore 10 sediment boxes in total (Figures 2-3). All sediments contain a certain amount of porosity (where there is no sediment) this can fill with pore waters. The existence of such pore waters can aid the dissolution of the sediment. However this level of complexity is beyond the scope of the sediment boxes here. The porosity does however affect the volume of sedimentary material within the 10cm layer, as it represents space which is occupied by neither $CaCO_3$ or detrital material. Sediment box contents are worked out using a mass balance approach, where the volume of the sediment box remains constant at all times. Sediment boxes have therefore been 'collapsed' to represent the actual amount of sediment that is within the 10cm depth. This is done by calculating the average porosity over a 10cm sediment depth, and then re-calculating a depth that would consist only of sediment. The equation for porosity is given below (Ridgwell 2001), where z represents the depth within the sediment:

$$\phi_{(z)} = 0.69 + 0.26(1+z)^{-1.2} \qquad \textbf{Equation 2-15}$$

Porosity for 1cm intervals and the overall average for 10cm are shown in Table 2-3.

Depth (z)	*Porosity*
0	0.95
1	0.803172
2	0.759571
3	0.739261
4	0.727689
5	0.720283
6	0.715168
7	0.711442
8	0.708616
9	0.706405
10	0.704632
Average	0.749658

Table 2-3: *Porosity at 1cm depth intervals and average over 10cm.*

Re-calculating the sediment depth with porosity gives a 'compacted' depth of 2.5cm for each sediment box. Total volume of the box for each sediment depth (V_i) is calculated using a depth of 2.5cm, and the area of seafloor that it represents, see Table 2-1 for the final values.

The sediment boxes are viewed by the fractional volumes of detritus and calcium carbonate material that they contain, therefore against depth, the fractional volume of calcium carbonate should be different, and the general level of the lysocline can be identified. Figure 2-4 shows the sediment box and the fluxes which interact with it; in any one timestep there will be a deposit of detritus, and either a net addition or removal of calcium carbonate, this means that the 10cm sediment box will in most cases either become over- or under-filled.

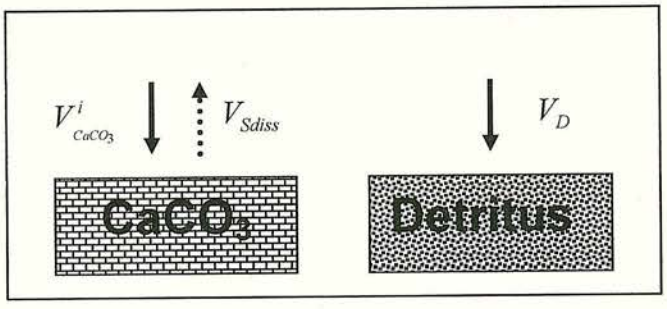

Figure 2-4: *Sediment box fluxes*

To maintain the constant volume (V_i) of the sediment box material is either permanently gained or removed from below, however, this material is not accounted for within the model. The net gain/loss of a sediment layer over time, can however be calculated for a model run to gauge the effect of dissolution. The volume balance of the sediment box is achieved by calculating intermediate steps of the total change of volume to the layer (Δ) and the total amount of $CaCO_3$ and detritus separately ($\Sigma V^i_{CaCO_3}, \Sigma V^i_D$), see below:

$$\Delta = V^i_{CaCO_3} - V^i_{SdissCaCO_3} + V^i_D \qquad \textbf{Equation 2-16}$$

$$\Sigma V^i_{CaCO_3} = V^i_{CaCO_3(t-1)} + V^i_{CaCO_3} \qquad \textbf{Equation 2-17}$$

$$\Sigma V^i_D = V^i_{D(t-1)} + V^i_D \qquad \textbf{Equation 2-18}$$

Material which is removed or added to the sediment layer at time t is added with the proportions of $CaCO_3$ and detritus at time t-1, therefore the $CaCO_3$ levels within the sediment will never reach zero. However, the depth zone in which the carbonate compensation depth is situated (this is the depth beyond which the sediments have no $CaCO_3$ component) can be seen in the model environment. It is indicated by a large decrease in $CaCO_3$ proportion between one sediment box and the next, the lower one containing virtually no $CaCO_3$.

2.2.1.5 River Alkalinity Flux

The deposited *DIC* and *ALK* in both neritic and pelagic sediments, is balanced by the carbon and alkalinity transported by rivers to the ocean. This carbon and alkalinity is derived from the action of weathering rocks on land. Fluxes F^W_{ALK} and F^W_{DIC} are therefore added to the warm surface ocean box in the model, $F^W_{ALK} = 2\times10^{13}$ mol/yr, and $F^W_{DIC} = 1\times10^{13}$ mol/yr. The *DIC* flux is set to half that of *ALK*, as this is the ratio of removal of these components from the deposition of sediments. The *ALK* flux is derived by removing the neritic depositional component of the *ALK* flux (~1×10^{13} mol yr^{-1}, Milliman 1993), from the total *ALK* flux (~3.0×10^{13} mol yr^{-1} Amiotte-Suchet et al. 2003).

2.2.1.6 State Equations

Equations of state for the four ocean boxes are included in Appendix B, for the *DIC*, *ALK* and *N* cycles. The *DIC* pool is affected by the creation of organic and inorganic carbon in the surface ocean, the re-mineralization or dissolution of this carbon, and the input of carbon from the river flux. The *ALK* in the ocean boxes also relates to these processes, however the ratio of alkalinity to nitrate, or $CaCO_3$ ($R_{(ALK/NIT)} = 1, R_{(ALK/CaCO_3)} = -2$) also has to be included to account for the fact that nitrate (NO_3^-) is used in the production of organic matter, and Ca^{2+} is used in the production of $CaCO_3$. Nitrate is used in the production of organic carbon matter, and its value is related proportionally to the amount of $CaCO_3$ that is produced. However, all the organic carbon is re-mineralised in this model, so all the nitrate is returned, therefore at present, the nitrate in concentration in each box remains at a constant value.

2.3 *Model Setup*

Parameters that are either new or modified from that used in Lenton (2000) are listed in Table 2-4. Explanations of new parameters have been detailed in earlier text and parameters that have been modified are discussed in the appropriate section below.

Table 2-4: *Parameters altered from [Lenton, 2000] and new parameters*

Parameter	Description	Value	Reference / Notes
k_T	Thermohaline overturning	2.5×10^7 (m^3s^{-1})	[*Knox and McElroy*, 1984]
k_U	High-latitude overturning	2.7×10^7 (m^3s^{-1})	[*Knox and McElroy*, 1984]
K_M	Half-saturation point for CO_2 fertilisation	180 ppmv	Tuned to give 1800-1990 CO_2 change
k_{MM}	Photosynthesis normalising constant	1.717	Normalises for pre-industrial conditions
ε	Dissolution exponent	4.5	[*Berelson et al.*, 1994]
χ	Dissolution constant	20 % day^{-1}	[*Berelson et al.*, 1994]
F_D	Detrital flux	6×10^{12} mol/yr	[*Treguer et al.*, 1995]
$F^w_{Alk,0}$	Pre-industrial alkalinity input flux*	2×10^{13} mol Alk/yr	[*Amiotte-Suchet et al.*, 2003; *Milliman*, 1993]
$F^w_{DIC,0}$	Pre-industrial carbon input flux*	1×10^{13} mol C/yr	[*Amiotte-Suchet et al.*, 2003; *Milliman*, 1993]

*Having subtracted neritic deposition flux from the river flux.

2.3.1 Steady-State

The model was spun up initially with no $CaCO_3$ in the sediments and river alkalinity and carbon fluxes as detailed in Table 2-4. The ocean circulation fluxes K_T and K_U were 2.5×10^7 (m^3s^{-1}) and 2.7×10^7 (m^3s^{-1}), as in the original ocean box model of (Knox and McElroy 1984). Steady-state initial fractions of $CaCO_3$ in each sediment level are given in Table 2-5, they are found to give a model CCD somewhat below 3600m as indicated by a drop to a low weight fraction of $CaCO_3$ in sediment layer 8 (3600-4100m). In the real ocean the CCD varies with ocean basin, being at ~5 km in the Atlantic and at ~3.5 km in the Pacific, meaning there is no single 'global' value but the model mean state is closer to the Pacific (the largest ocean basin). The model has a net sediment deposition of ~0.121GtC/yr, which is within estimates of net pelagic sediment deposition (Broecker 1974). The concentration of CO_2 in the

atmosphere is 287ppmv. This concentration of CO_2 is ~9ppmv higher than the often quoted concentration of 278ppmv CO_2 at the pre-industrial (Enting et al. 1994), and is ~7ppmv higher than that used in the Lenton (2000) model. However, in comparison to other ocean-sediment system models that interact with the atmosphere (Archer et al. 1998), the concentration of CO_2 in the model here is quite close to the concentration of pre-industrial CO_2.

Sediment Level	*% $CaCO_3$*
1	0.876
2	0.839
3	0.820
4	0.810
5	0.803
6	0.796
7	0.785
8	0.056
9	0.003
10	0.001

Table 2-5: *% $CaCO_3$ by sediment level, at steady-state*

2.3.2 Historical forcing and tuning model response

The same historical emissions scenario is used in this study as in Lenton (2000), which incorporates fossil fuel burning and land-use change (Table 2-6) (Marland et al. 1998, Houghton & Hackler 1998) until year 1990. The lower values used for parameters K_T and K_U, which control the level of thermohaline circulation and the mixing of waters in the high-latitude surface ocean and the deep, weakened the ocean-atmosphere sink. Tuning of the parameter (K_M) (Table 2-4), which is the half-saturation constant for CO_2 fertilisation, improved the fit of the atmospheric CO_2 concentration to historical data. The effect of increasing K_M to 180ppmv was to increase the strength of the land-atmosphere sink.

Year	*Fossil Fuel*	*Land-use*	*Total*
1800	0	0.35	0.35
1850	0.05	0.35	0.4
1947	1.2	0.8	2.0
1980	5.2	1.5	6.7
1990	6.0	1.4	7.4

Table 2-6: *Estimated historical CO_2 emissions (Marland et al. 1998, Houghton & Hackler 1998)*

2.3.3 Future global change

To look at the response of the atmosphere to anthropogenic perturbation, emissions beyond the year 1990 are applied to the model (Table 2-7). Emissions scenarios were chosen for comparison with previous studies Lenton (2000) and Archer et al. (1998). The 'L' scenarios in which there are land-use change (LUC) emissions, default set-up is for the LUC carbon to be removed from vegetation and for a fraction ($k_t = 0.27$) of it to tend to permanently reduce steady-state vegetation carbon ($C_{v(s)}$) (Lenton 2000). This represents the reduction in biomass associated with replacing forest with cropland or pasture. This permanent LUC can be removed from the model without affecting total emissions, by treating LUC emissions as fossil fuel emissions and assuming no permanent reduction in vegetation carbon.

Table 2-7: *Long-term CO_2 emissions scenarios used in this study and descriptions of the fossil fuel emissions trajectories.*

Label	Total LUC* emission (GtC)	Total fossil emission (GtC)	1990-2100	Beyond 2100	Reference, label therein
L1	212	2660	IS92a	Linear decline to zero in 2200	[*Lenton*, 2000], 1
L2	212	1134	IS92c	Linear decline to zero in 2200	[*Lenton*, 2000], 2
L3	212	4107	IS92e	Linear decline to zero in 2200	[*Lenton*, 2000], 3
L4	212	4000	IS92a	Linear decline to zero in 2332	[*Lenton*, 2000], 4
L5	212	4000	1990 concentration	Linear decline to zero in 2926	[*Lenton*, 2000], 5
L6	212	4000	IS92e	Linear decline to zero in 2194	[*Lenton*, 2000], 6
L7	212	9213	IS92a	+0.16 GtC/yr/yr to 2150 then linear decline to zero in 2599	[*Lenton*, 2006]
L8	212	15000	IS92a	+0.16 GtC/yr/yr to 2250 then linear decline to zero in 2634	[*Lenton*, 2006]
A23	0	4546	BAU A	Constant 22.5 GtC/yr until 2300 and zero thereafter	[*Archer et al.*, 1998], A23

*In scenarios L1 to L8 the land-use change (LUC) scenario is identical and based on IS92a (Lenton 2000).

2.4 *Comparison to other studies*

This section compares the model with additional sediment system to the base model (Lenton 2000), and the sediment model of Archer et al. (1998), which also addressed the fate of atmospheric CO_2 to anthropogenic perturbation.

2.4.1 Comparison to Lenton (2000) version

The new model system (with sediments) was first contrasted with the base model (Lenton 2000) (no sediments) (Figure 2-5). In 1990, atmospheric CO_2 is 364ppmv, 11ppmv higher than in the original model and observations. However, as CO_2 started 9ppmv above observations the CO_2 change is well captured. During the 1990s the ocean carbon sink is

~1.2 GtC yr^{-1}, somewhat below the observationally constrained estimate of 2.1±0.7 GtC yr^{-1} (Le Quéré et al. 2003). This is largely compensated for by a strong land carbon sink of ~2.7 GtC yr^{-1} compared to estimates of 1.6–4.8 GtC yr^{-1} (House et al. 2003). Heading into the future, for a given emissions scenario, CO_2 typically peaks at a 10-20% higher concentration in the new model, due largely to the weaker ocean carbon sink. Toward the end of the millennium, however, CO_2 in the new model drops below that in the old model, as a consequence of dissolution of ocean carbonate sediments. By year 3000, CO_2 has fallen below that in the original model. By year 4500, CO_2 is still falling gradually and is much lower than that in the original model, in which it has stabilised.

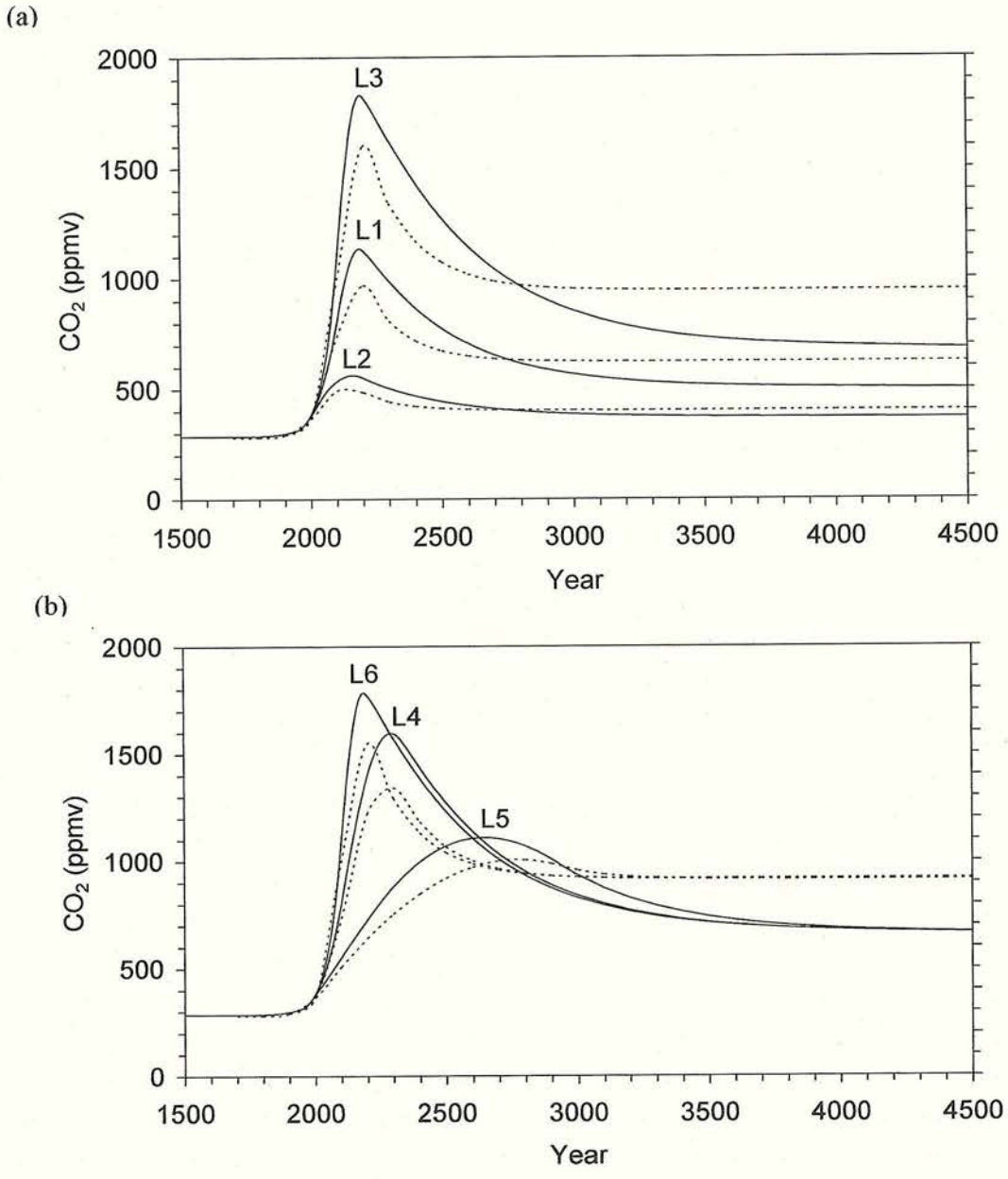

Figure 2-5: *Comparing the multi millennial timescale CO_2 response of the extended model with carbonate sediments and fixed weathering fluxes (solid lines) with the original model (dashed lines) (Lenton 2000) under different emissions scenarios (Table 2-7): (a) Burning different amounts of fossil fuel in the same time period (scenarios L1–L3). (b) Burning the same amount of fossil fuel (4000 GtC) in different time periods (scenarios L4–L6). For a given emissions scenario, peak atmospheric CO_2 is always higher and final atmospheric CO_2 is always lower in the extended model.*

2.4.2 Comparison to Archer et al. (1998)

Next the model is compared with that of Archer et al. (1998) (Figure 2-6). When driven with the same total emissions, atmospheric CO_2 peaks 130ppmv lower in this model, having started ~30ppmv lower. However, by year 10,000 the two models have reached similar atmospheric CO_2, sediment dissolution being close to complete and the total amount of dissolution being set by the total amount of fossil fuel emitted. Carbonate sediments dissolve much faster in the model here than in Archer et al. (1998), thus maintaining a large ocean carbon sink on the millennial timescale (Figure 2-6(b)) and drawing down atmospheric CO_2 more rapidly. Although at the time of peak CO_2 (year 2300), the land has become a large carbon source, uptake of carbon by the land surface since pre-industrial time exceeds loss giving a net gain of 250GtC, whilst 970GtC have entered the ocean. Net land uptake can thus account for the reduction in peak atmospheric CO_2 relative to Archer's model of ~210GtC, suggesting that the ocean sinks are of similar strength in the two models. In both Archer's model and the one here, carbonate sediments are not totally dissolved under this emissions scenario. Complete stabilisation of the system takes over 100kyr, but the system is close to steady state after 60kyr, with atmospheric CO_2 at about 475ppmv, which is ~200ppmv above the pre-industrial. This corresponds to a remaining airborne fraction (of added CO_2) of 9.3% in close agreement with Archer et al. (1998). The fate of this remaining anthropogenic CO_2 depends on the response of carbonate and silicate weathering processes.

(a)

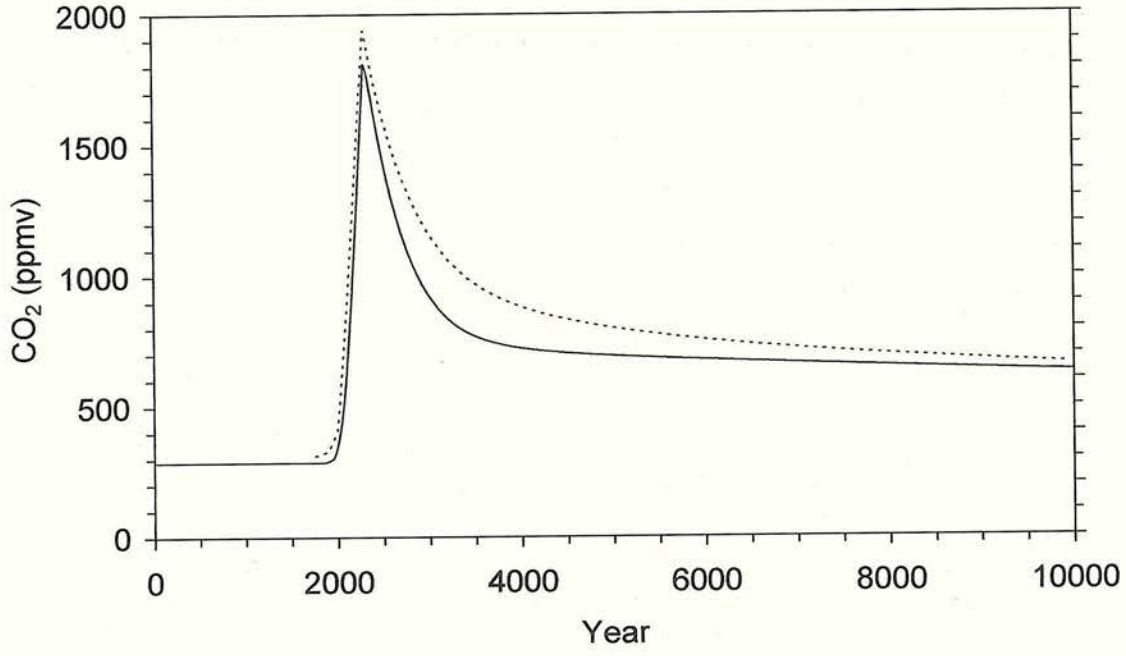

(b)

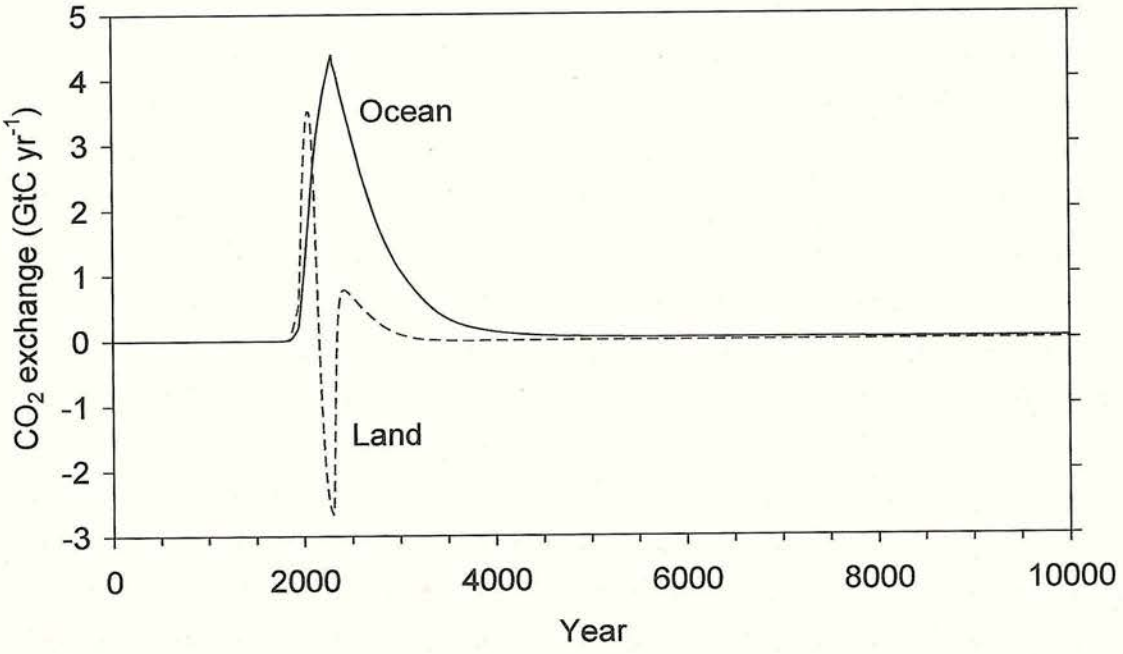

Figure 2-6: *(a) Atmospheric CO_2 responses to year 10,000 for emissions scenario A23 (Table 2-7) of the extended model with fixed weathering fluxes (solid line) and the model of Archer et al. (1998) also with fixed weathering fluxes (dotted line). (b) CO_2 exchange in the extended model with fixed weathering fluxes from atmosphere to ocean (solid line) and from atmosphere to land (dashed line). Positive values indicate a carbon sink, negative values a carbon source.*

Carbonate sediments dissolve more rapidly in this model than in previous studies (Archer et al. 1998). The most likely reason for this is due to the very simple treatment of bioturbation within the sediment layer. Bioturbation moves sediment vertically and horizontally within the sediment column, to a depth of around 10cm. This allows $CaCO_3$ to be exhumed to the sediment surface where it may be subject to dissolution. Therefore at the time of dissolution $CaCO_3$ further down the 10cm layer may be protected by non-$CaCO_3$ material, but it will subsequently be exhumed and dissolved at a later time. In this model, treating the 10cm layer as 'well-mixed' may well have allowed a higher rate of dissolution during the major phase of sediment 'burn-down'. Archer's approach to bioturbation (and others) is to model the 10cm sediment layer as a series of discretized 'sub-layers' with bioturbational movement of material between layers dependent on a 'biodiffusion coefficient'. This is most likely why Archer's dissolution rates (and others) are significantly lower. However, adding sub-layers within the sediment layer of this model would have demanded more computing power, causing issues later in the study. The effect of the increased dissolution rate is a large drawdown of CO_2 on the millennial timescale, relative to a version of the model without sediments. In the transient response, dissolution can exceed weathering as a source of alkalinity by a factor of ~20. This response should be treated with caution given the simplicity of the sediment model system (as described above). Despite this caveat, after ~10kyr the responses of the model and that of Archer et al. (1998) are almost identical for the same total amount of CO_2 released, because a simple titration has occurred.

2.5 References

Amiotte-Suchet, P., J.-L. Probst, and W. Ludwig, Worldwide distribution of continental rock lithology: Implications for the atmospheric/soil CO_2 uptake by continental weathering and alkalinity river transport to the oceans, *Glob. Biogeochem. Cycl. 17*, 1038, 2003.

Archer, D., Modelling the calcite lysocline, *Journal of Geophysical Research, 96*, 17037-17050, 1991.

Archer D, A data-driven model of the global calcite lysocline, *Glob. Biogeochem. Cycl.* 10, 511-526, 1996.

Archer, D. H. Kheshgi, and E. Maier-Reimer, Dynamics of fossil fuel CO2 neutralization by marine CaCO3, *Glob. Biogeochem. Cycl., 12*, 259-276, 1998.

Berelson, W. M. D. E. Hammond, J. McManus, and T. E. Kilgore, Dissolution kinetics of calcium carbonate in equatorial Pacific sediments, *Glob. Biogeochem. Cycl. 8*, 219-235, 1994.

Broecker, W.S., *Chemical Oceanography, Harcourt Brace Jovanovich, Inc.*, NY, 1974.

Broecker, W.S. & T.H. Peng, *Tracers in the sea, Palisades, New York, Lamont-Doherty Geological Observatory,* 1982.

Caldeira, K., M.R. Rampino, Aftermath of the End-Cretaceous Extinction-Possible biogeochemical stabilization of the carbon-cycle and climate, *Palaeoceanography, 8(4),* 515-525, 1993.

Enting, I. G., T. M. L. Wigley, and M. Heimann, Future Emissions and Concentrations of Carbon Dioxide: Key Ocean/Atmosphere/Land Analyses, *CSIRO Division of Atmospheric Research Technical Paper No. 31, Commonwealth Scientific and Industrial Research Organisation, Aspendale, Australia,* 1994.

Heinze, C., E. Maier-Reimer, A.M.E. Winguth, D. Archer, A global oceanic sediment model for long-term climate studies, *Glob. Biogeochem. Cycl., 13,* 221-250, 1999.

Houghton, J.T., J.L. Hackler, Continental scale estimates of the biotic carbon flux from land cover change: 1850 to 1980 (1995). *In: Trends: A Compendium of Data on Global Change. Carbon Dioxide Information Analysis Center, Oak Ridge National Laboratory, U.S. Department of Energy, Oak Ridge, Tenn., U.S.A.,* 1998.

Houghton, J.T., Y. Ding, D.J. Griggs, M. Noguer, P.J. van der Linden and D. Xiaosu (Eds.), *Climate Change 2001: The Scientific Basis, Cambridge University Press,* 2001.

House, J. I. I. C. Prentice, N. Ramankutty, R. A. Houghton, and M. Heimann, Reconciling apparent inconsistencies in estimates of terrestrial CO2 sources and sinks, *Tellus B, 53B,* 345-363, 2003.

Ingle, S.E., Solubility of Calcite in the ocean, *Marine Chemistry, 3,* 301-319, 1975.

Keir, R.S., The dissolution kinetics of biogenic calcium carbonates in seawater, *Geochimica and Cosmochimica Acta, 44,* 241-252, 1980.

Keir, R.S., On the late Pleistocene ocean geochemistry and circulation, *Paleoceanography, 3(4),* 413-445, 1988.

Knox, F., & M. B. McElroy, Changes in atmospheric CO_2: Influence of the marine biota at high latitude, *J. Geophys. Res., 89,* 4629–4637, 1984.

Le Quéré, C. O. Aumont, L. Bopp, P. Bousquet, P. Ciais, R. Francey, M. Heimann, C. D. Keeling, R. F. Keeling, H. Kheshgi, P. Peylin, S. C. Piper, I. C. Prentice, and P. J. Rayner, Two decades of ocean CO2 sink and variability, *Tellus B, 55B,* 649-656, 2003.

Lenton, T. M. Land and ocean carbon cycle feedback effects on global warming in a simple Earth system model, *Tellus, 52B,* 1159-1188, 2000.

Marland, G., T.A. Boden, R.J. Andres, A.L. Brenkert, C.A. Johnston, Global, regional, and national fossil fuel CO_2 emissions. *In: Trends: A Compendium of Data on Global*

Change. Carbon Dioxide Information Analysis Center, Oak Ridge National Laboratory, U.S. Department of Energy, Oak Ridge, Tenn., U.S.A., 1998.

Millero, F.J., Thermodynamics of the carbonate system in seawater, *Geochemica Et Cosmochimica Acta, 43(10),* 1651-1661 1979

Milliman, J. D. Production and accumulation of calcium carbonate in the ocean: Budget of a nonsteady state, *Glob. Biogeochem. Cycl. 7,* 927-957, 1993.

Morse, J. W., Dissolution kinetics of calcium carbonate in sea water: VI. The near equilibrium dissolution kinetics of calcium carbonate rich deep sea sediments, *Am. J. Sci., 278,* 344-353, 1978.

Munhoven, G., L.M. Francois, Glacial-interglacial changes in continental weathering: Possible implications for atmospheric CO_2, *In: Carbon cycling in the glacial ocean: Constraints on the ocean's role in global change, (eds.) Zahn, R., Pedersen, T.F., Kaminski, M.A., Labeyrie, L., Springer-Verlag, Berlin,* 1994.

Munhoven, G. & L.M. Francois, Glacial-interglacial variability of atmospheric CO_2 due to changing continental silicate rock weathering: A model study, *Journal of Geophysical Research, 101,* 21423-21437, 1996.

Opdyke, B.N., J.C.G. Walker, Return of the coral reef hypothesis: Basin to shelf partitioning of $CaCO_3$ and its effect on atmospheric CO_2, *Geology, 20,* 733-736, 1992.

Park, P.K., Oceanic CO_2 system: an evaluation of ten methods of investigation. *Limnology and Oceanography,* 14, 179-186, 1969.

Redfield, A. C., B. H. Ketchum, and F. A. Richards, The influence of organisms in the composition of sea water, *In: Hill, N. M. (eds), The Sea, pp, 26-77, Wiley-Interscience, New York,* 1963.

Ridgwell, A. J. *Glacial-interglacial perturbations in the global carbon cycle*, 134 pp. University of East Anglia, Norwich, 2001.

Sarmiento, J.L., J.R. Toggweiler, A new model for the role of the oceans in determining atmospheric CO_2, *Nature, 308,* 621-624, 1984.

Siegenthaler, U., T.H. Wenk, Rapid atmospheric CO_2 variations and ocean circulation, *Nature, 308,* 624-626, 1984.

Sigman, D.M., D.C. McCorkle, W.R. Martin, The calcite lysocline as a constraint on glacial/interglacial low-latitude production changes, *Glob. Biogeochem. Cycl., 12(3),* 409-427, 1998.

Treguer, P. D. M. Nelson, A. J. Van Bennekom, D. J. DeMaster, A. Leynaert, and B. Queguiner, The silica balance in the world ocean: A reestimate, *Science, 268,* 375-379, 1995.

Volk, T., & M. I. Hoffert, Ocean carbon pumps: Analysis of relative strengths and efficiencies in ocean-driven atmospheric CO_2 changes, *Geophys. Monogr., 32,* 99-110, 1985.

3 'Enhanced carbonate and silicate weathering accelerates recovery from fossil fuel CO_2 perturbations'

3.1 *Abstract*

Increasing atmospheric CO_2 and surface temperatures should increase carbonate and silicate weathering rates, directly via warming, and indirectly via the CO_2 fertilisation effect enhancing plant productivity. Enhanced weathering should in turn increase alkalinity input to the ocean and accelerate long-term CO_2 uptake. We added silicate and carbonate weathering, to an existing global carbon cycle and surface temperature model which has carbonate sediments, and subjected it to a range of long-term fossil fuel emissions scenarios, spanning 1100–15000GtC in total. Emissions of ≥7350GtC dissolve all carbonate sediments, and enhanced carbonate and silicate weathering accelerate subsequent CO_2 removal from the atmosphere by up to a factor of 4. For 1100–4000GtC emissions, enhanced weathering accelerates CO_2 removal by a factor of 1.5–2.5. However, it takes >1Myr for silicate weathering to stabilise atmospheric CO_2. If land-use tends to suppress vegetation and weathering rates on this timescale, then CO_2 will stabilise above pre-industrial concentrations.

3.1 Introduction

Humans are adding CO_2 to the atmosphere through fossil fuel burning and land-use change. Fossil fuel burning dominates current annual CO_2 emissions and is likely to dominate total future CO_2 emissions. The global carbon cycle will respond to the added CO_2 over a range of timescales (Archer et al. 1998, Archer et al. 1997, Walker and Kasting 1992). At present the land and ocean are both acting as carbon sinks and buffering the rate of CO_2 rise. Over the coming centuries the land may become a carbon source (Cox et al. 2000, Lenton 2000) whilst the ocean is likely to remain a robust carbon sink (Bala et al. 2005, Joos et al. 1999, Lenton et al. 2006). On the millennial timescale, emissions are likely to have ceased due to reserves running out, if not to a conscious policy. The added carbon will have been initially apportioned between the ocean, land and atmosphere, with the ocean being the main sink (Lenton and Cannell 2002). The fraction of added CO_2 that enters the ocean on this timescale depends inversely and non-linearly on the amount of CO_2 emitted (Lenton 2006, Lenton and Cannell, 2002). Model estimates of ocean uptake range from ~80–90% (Archer et al. 1997, Kasting and Schultz 1996) for minimal emissions of ~1000GtC to as little as ~30% if ~15,000GtC of exotic plus conventional fossil fuel are emitted (Lenton 2006, Lenton et al. 2006).

In the coming centuries, the acidification of ocean waters by CO_2 will begin to dissolve marine carbonate sediments causing the carbonate compensation depth (CCD) to shoal toward the ocean surface. Over an estimated ~5-6kyr, this process of dissolution will add alkalinity to the ocean and thus increase its capacity to store CO_2, removing a further 9-15% of added CO_2 from the atmosphere (Archer et al. 1998, Archer et al. 1997). Carbonate weathering on land will replenish ocean alkalinity thus allowing carbonate sediments to be re-deposited and removing an estimated further 3-8% of added CO_2 on a timescale of ~8kyr (Archer et al. 1998). This will still leave ~10% of the added CO_2 in the atmosphere, to be removed by the weathering of silicate rocks and subsequent deposition of carbonates in the ocean, over hundreds of thousands of years (Archer et al. 1998, Walker and Kasting 1992). Thus, what was rock-bound organic carbon (fossil fuel) will gradually return to the Earth's crust as carbonates, lowering atmospheric O_2 very slightly.

Although two studies (Sundquist 1991, Walker and Kasting 1992) both looked at the long-term response of the atmosphere with variable weathering levels fluxes, only Walker and Kasting (1992) were looking specifically at the fate of fossil fuel CO_2. All other existing

studies of the long-term response to fossil fuel burning have assumed fixed weathering fluxes (Archer et al. 1998, Archer et al. 1997, Ridgwell and Edwards, in press). However, it is well known that the rate of weathering reactions increase with temperature, precipitation and with CO_2 concentration in soil (Berner et al. 1983, Walker et al. 1981, White and Blum 1995). Furthermore, the process of weathering is actively amplified by plants and their associated fungal mycorrhizae, as well as by lichens, and various free living soil organisms (Berner 1997, Berner and Cochran 1998, Lovelock and Watson 1982, Schwartzman and Volk 1989). These factors have been included in models of the long-term carbon cycle and CO_2 on geologic timescales (Bergman et al. 2004, Berner 1997, Berner and Kothavala 2001). In a pioneering study, Walker and Kasting (1992) included the rock cycle and carbonate and silicate weathering in long-term projections of future global change. They assumed an abiotic CO_2-dependence of both types of weathering, which encapsulates the effects of temperature and associated changes in precipitation and runoff (Walker et al. 1981). On multi-millennial timescales, enhanced carbonate weathering was found to have a greater drawdown effect on atmospheric CO_2 than the dissolution of carbonate sediments (Walker and Kasting 1992).

We postulate a further biologically-amplified increase in the rate of weathering of carbonate and silicate minerals, induced by CO_2–fertilisation of plant growth and global warming increasing rates of soil respiration and producing higher soil pCO_2. In support of this, tree growth experiments under elevated CO_2 suggest that in nutrient replete conditions, carbonate weathering is increased (Williams et al. 2003). Biological amplification of weathering will increase the flux of alkalinity to the oceans, and thus accelerate the replenishment of the ocean with alkalinity and removal of residual added CO_2 from the atmosphere. Enhanced carbonate weathering should be important on a 10^3-10^4yr timescale, whilst enhanced silicate weathering should be important over 10^3-10^6yr timescales.

We pose the question: What effect will these mechanisms have on the concentration of CO_2 in the atmosphere on timescales of 10^3-10^6 years? To address this we extended a simple box model of the global carbon cycle and surface temperature, which contains a sediment system (see Chapter Two), to include carbonate weathering and silicate weathering. The resulting model is distinguished from that of Walker and Kasting (1992) in that it includes one deep ocean box instead of three, but has more sophisticated representations of carbonate sediments and land biota, and a direct dependence of carbonate and silicate weathering on plant productivity. We place more emphasis on longer timescales than Walker and Kasting

(1992), separating out the impacts of carbonate and silicate weathering, considering a wider range of total CO_2 emissions, and quantifying the size of CO_2 release required to dissolve all carbonate sediments.

3.2 Model Description

3.1.1 Base Model

We started with a 7-box global carbon cycle model, with marine carbonate sediments at 10 different depth intervals, which is coupled to an energy-balance model approximation of global temperature (Lenton (2000) & Chapter Two). This version of the carbon cycle model comprises reservoirs in the atmosphere, vegetation, soil, high-latitude surface water, low-latitude surface water, intermediate waters, deep-ocean and 10 sediment layers. Processes captured are photosynthesis, plant respiration, litter fall/mortality, soil respiration, CO_2 exchange between the atmosphere and surface ocean, circulation and mixing between various ocean boxes, export production and re-mineralization. Nitrate and alkalinity also circulates through the ocean boxes. The ocean model is based on that of Knox and McElroy (1984) and here we use their circulation fluxes. To this we added carbonate and silicate weathering processes and their controls, together with net input fluxes of alkalinity and carbon. All parameters are as in Chapter Two, unless stated otherwise. The energy-balance model has an equilibrium climate sensitivity of 2.8°C for doubling CO_2, whilst quadrupling CO_2 gives 6.3°C warming at equilibrium.

3.1.2 Addition of weathering

The net deposition of $CaCO_3$ in sediments and removal out of the system is balanced by a flux of alkalinity (F^w_{Alk}) and dissolved inorganic carbon (F^w_{DIC}) from weathering of carbonate and silicate rocks on land (Chapter Two). These weathering fluxes are fixed in the version of the model described in Chapter Two, and the results presented there are used in this chapter as a baseline from which to examine the effects of variable weathering. Now that the effects of carbonate and silicate weathering are to be handled separately, (rather than contributing to a generic weathering flux) the alkalinity flux must be apportioned accordingly. The fraction of the input flux of alkalinity due to carbonate weathering is f_{Ca} = 0.75 (1.5×10^{13} mol yr^{-1}) and the remainder due to silicate weathering is f_{Si} = 0.25 (5×10^{12} mol yr^{-1}) (Bergman et al. 2004, Walker and Kasting, 1992).

The carbon input flux is set at half the alkalinity flux, $F^{w}_{DIC,0} = 1\times10^{13}$ mol yr^{-1}, in order to balance the proportions in which carbon and alkalinity are removed from the system (under marine sediments). In effect this means that the input flux of volcanic/metamorphic CO_2 which is removed by silicate weathering and subsequent carbonate deposition, is added directly to rivers, rather than going via the atmosphere. This represents the smaller fraction (25%) of the river carbon flux, the remainder (75%) coming from carbonate weathering.

Three formulations were used to separate the effects of variable carbonate and silicate weathering. In the first, the greater fraction (75%) of the river fluxes of alkalinity and carbon derived from carbonate weathering become a function of environmental variables, but silicate weathering remains fixed. We take the temperature response of carbonate weathering from the GEOCARB II model (Berner 1994) and include plant productivity (P) in a manner similar to the COPSE model (Bergman et al. 2004):

$$F^{w}_{Alk} = F^{w}_{Alk,0}\left(f_{Si} + f_{Ca}\left(P/P_0\right)\left(1+0.087\left(T-T_0\right)\right)\right) \qquad \textbf{Equation 3-1}$$

$$F^{w}_{DIC} = F^{w}_{DIC,0}\left(f_{Si} + f_{Ca}\left(P/P_0\right)\left(1+0.087\left(T-T_0\right)\right)\right) \qquad \textbf{Equation 3-2}$$

Where T_0 is the initial (pre-industrial) temperature (288.15K) and P_0 is the initial gross primary productivity, already calculated in the model as a function of CO_2 and T (Lenton, 2000). It is assumed that carbonates saturate the soil or ground water in contact with them so rapidly that changes in runoff do not result in appreciable dilution (Berner 1994). Hence the temperature term does not include the effect of changes in runoff. Changes in CO_2 have their dominant impact via their effect on plant productivity, represented by Michaelis-Menten kinetics (a hyperbolic response) and plant productivity responds to temperature following a cubic function (Lenton 2000).

In the second formulation, carbonate weathering is fixed and the smaller fraction (25%) of the river flux of alkalinity due to silicate weathering becomes a function of environmental variables. The whole river carbon flux must remain fixed because the fraction (25%) that counterbalances silicate weathering is derived from volcanic and metamorphic processes that are assumed constant on the timescales considered here. Once again the temperature

response is taken from GEOCARB II and plant productivity introduced as a simple multiplier:

$$F_{Alk}^{w} = F_{Alk,0}^{w}\left(f_{Si}(P/P_0)(1+0.038(T-T_0))^{0.65}e^{0.09(T-T_0)} + f_{Ca}\right) \quad \textbf{Equation 3-3}$$

$$F_{\mathrm{DIC}}^{w} = F_{\mathrm{DIC},0}^{w} \quad \textbf{Equation 3-4}$$

Changes in temperature have a direct effect on silicate weathering (the exponential term) and an indirect effect via changes in runoff (Berner 1994).

In the third formulation, both carbonate and silicate weathering are a function of environmental variables, making the river flux of alkalinity:

$$F_{Alk}^{w} = F_{Alk,0}^{w}(P/P_0)\left(f_{Si}(1+0.038(T-T_0))^{0.65}e^{0.09(T-T_0)} + f_{Ca}(1+0.087(T-T_0))\right)$$

Equation 3-5

In this case, the river flux of carbon is given by Equation 3-2.

3.1.3 Land-Use Change

In the real world land-use change (LUC) affects the amount of carbon stored in the biosphere, which affects the global carbon balance. The model used here allows the option of permanently removing from the biosphere a fraction of the vegetation lost due to land-use (see Chapter 2). Allowing the (partial) permanent destruction of vegetation should lower productivity, decreasing the weathering flux and the speed at which CO_2 is removed from the atmosphere. In the long term the permanent destruction of parts of the biosphere will mean that the level of weathering in the model should stabilise at a level which is lower than that of the present day. This in turn should raise the final equilibrium concentration of CO_2 in the atmosphere in comparison to a system which does not permanently remove a portion of vegetation from the biosphere.

3.3 Methods

The new set of model versions was subjected to a range of long-term CO_2 emissions scenarios (see Chapter Two, Table 2-7). These were chosen for comparison with earlier

studies and to explore the effect of a wide range of plausible total CO_2 emissions. For each scenario the model was run with fixed weathering fluxes, with variable carbonate weathering, with variable silicate weathering, and with variable carbonate and silicate weathering. The default setting is for a fraction of the land-use change (LUC) to be permanently removed from the biosphere. This option has been switched off in some experiments.

3.4 Results

Our results contrast the effects of fixed weathering, variable carbonate weathering, variable silicate weathering, or variable carbonate and silicate weathering with or without land-use change, on the long-term response of atmospheric CO_2. Results for all the different emissions scenarios are summarised in Table 3-1. The effect of variable weathering on the future trajectory of atmospheric CO_2 is felt on 10^3-10^6 year timescales, there being only a minor effect on the atmospheric CO_2 peak that occurs on centennial timescales. Allowing carbonate weathering alone to vary accelerates the drawdown of CO_2 on 10^3-10^4 year timescales, lowers the final steady state modestly, but still leaves it well above the pre-industrial concentration and does not alter the ~10^5 year timescale of response. Allowing only silicate weathering to vary has a similar effect to carbonate weathering on 10^3-10^4 year timescales, but on 10^5-10^6 year timescales it causes ongoing drawdown of CO_2, which, in the absence of permanent land-use change (e.g. scenario A23), is eventually returned to pre-industrial concentration. Allowing carbonate and silicate weathering to vary together further accelerates CO_2 drawdown on 10^3-10^4 year timescales, but gives similar results to silicate weathering alone on 10^5-10^6 year timescales.

Table 3-1: *The effects of variable carbonate (Ca) and silicate (Si) weathering fluxes and permanent land-use change (LUC) on long-term atmospheric CO_2 for different emissions scenarios. The LUC switch does not alter total CO_2 emissions for a given scenario.*

Scenario	Permanent LUC?	Variable weathering?	Atmospheric CO_2 (ppmv) in year				
			Peak	3000	10,000	100,000	1,000,000
L1	Yes	Fixed	1136	567	465	400	396
	Yes	Ca	1131	556	442	384	384
	Yes	Si	1131	555	441	361	323
	Yes	Ca & Si	1125	545	423	361	324
	No	Ca & Si	1100	534	409	345	291
L2	Yes	Fixed	562	386	355	338	335
	Yes	Ca	561	384	351	332	331
	Yes	Si	561	384	351	328	321
	Yes	Ca & Si	559	381	347	327	322
	No	Ca & Si	545	378	339	312	289
L3	Yes	Fixed	1830	855	615	466	461
	Yes	Ca	1822	829	560	442	442
	Yes	Si	1822	824	557	397	325
	Yes	Ca & Si	1814	799	516	396	326
	No	Ca & Si	1796	776	494	369	292
L4	Yes	Fixed	1596	839	602	461	455
	Yes	Ca	1585	814	548	437	437
	Yes	Si	1583	810	545	394	325
	Yes	Ca & Si	1572	787	508	394	325
	No	Ca & Si	1552	765	488	367	292
L5	Yes	Fixed	1110	933	602	460	455
	Yes	Ca	1093	909	549	437	437
	Yes	Si	1092	907	546	394	325
	Yes	Ca & Si	1075	883	510	393	325
	No	Ca & Si	1054	862	490	367	292
L6	Yes	Fixed	1785	829	603	461	456
	Yes	Ca	1777	804	549	438	438
	Yes	Si	1777	800	546	395	325
	Yes	Ca & Si	1769	776	509	394	325
	No	Ca & Si	1751	754	488	367	292

'Enhanced carbonate and silicate weathering accelerates recovery from fossil fuel CO_2 perturbations'

L7	Yes	Fixed	3619	2753	1892	764	750
	Yes	Ca	3590	2695	1521	665	665
	Yes	Si	3575	2658	1413	528	329
	Yes	Ca & Si	3547	2600	1154	512	331
	No	Ca & Si	3559	2578	1057	476	297
L8	Yes	Fixed	6235	5303	4160	1342	1208
	Yes	Ca	6209	5257	3730	1004	1002
	Yes	Si	6182	5195	3284	670	334
	Yes	Ca & Si	6155	5149	2869	665	338
	No	Ca & Si	6201	5166	2676	627	302
A23	No	Fixed	1810	923	630	474	469
	No	Ca	1797	889	563	437	434
	No	Si	1796	884	560	385	292
	No	Ca & Si	1783	852	508	373	292

The acceleration of CO_2 drawdown due to variable weathering is greatest in scenarios where sufficient fossil fuel is emitted to dissolve all carbonate sediments in the ocean, which corresponds to $\geq$ 7350GtC. In such cases, the buffering effect of the sediments is removed, and the further drawdown of atmospheric CO_2 relies on weathering and the consequent increase in ocean alkalinity, until the sediments start to recover. To illustrate this, Figure 3-1 shows the results of emitting a total of 15,000GtC from 'exotic' and 'conventional' fossil fuel reserves. Allowing carbonate weathering alone to vary accelerates the recovery of atmospheric CO_2 by more than a factor of 2 over much of the range of CO_2 drawdown. For example, instead of reaching 2000ppmv after 61,000 years it is reached in 28,000 years. Allowing silicate weathering alone to vary accelerates the drawdown of CO_2 by a factor of 3 over much of the range, for example, 2000ppmv is reached in 20,000 years. Allowing both carbonate and silicate weathering to vary accelerates the recovery by roughly a factor of 4 over much of the range, 2000ppmv being reached in 15,000 years. Variable silicate weathering also allows an ongoing drawdown of CO_2 over the 10^5-10^6 year timescale. The temperature changes seen under this emission scenario are huge (Figure 3-1(b)). Without variable silicate weathering, temperature remains indefinitely 5.6°C (variable carbonate weathering) or 6.6°C (fixed weathering) above pre-industrial. Although temperature continues to decrease on the 10^5 year timescale in both the variable silicate only and the variable carbonate and silicate systems, a divergence of the two temperature trends can be

seen at about year 500,000 (Figure 3-1). This is due to the response of the sediment levels at this point and is discussed later on.

(a)

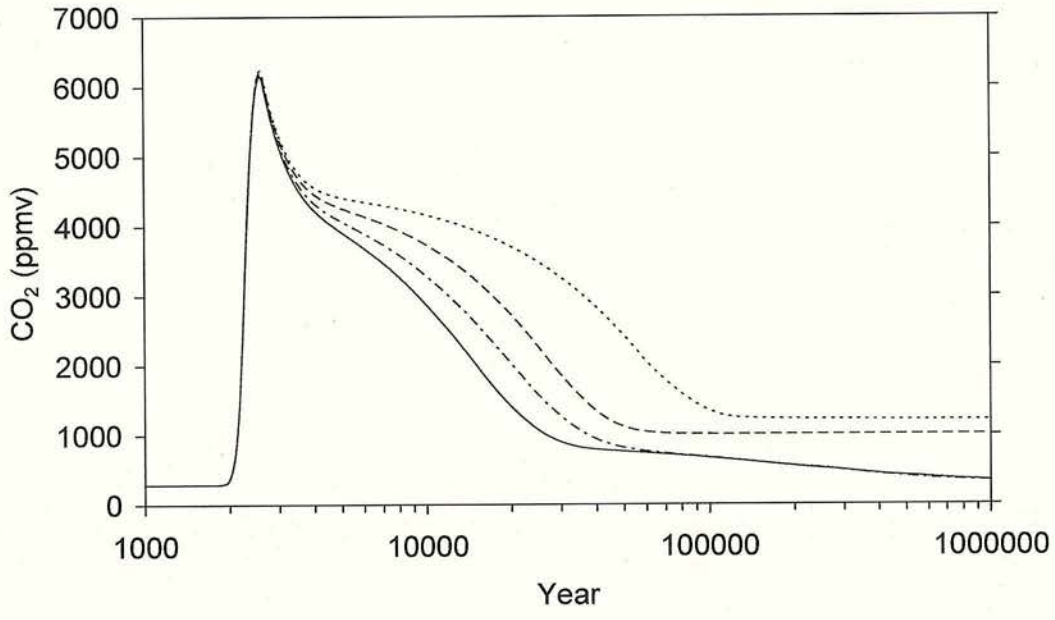

(b)

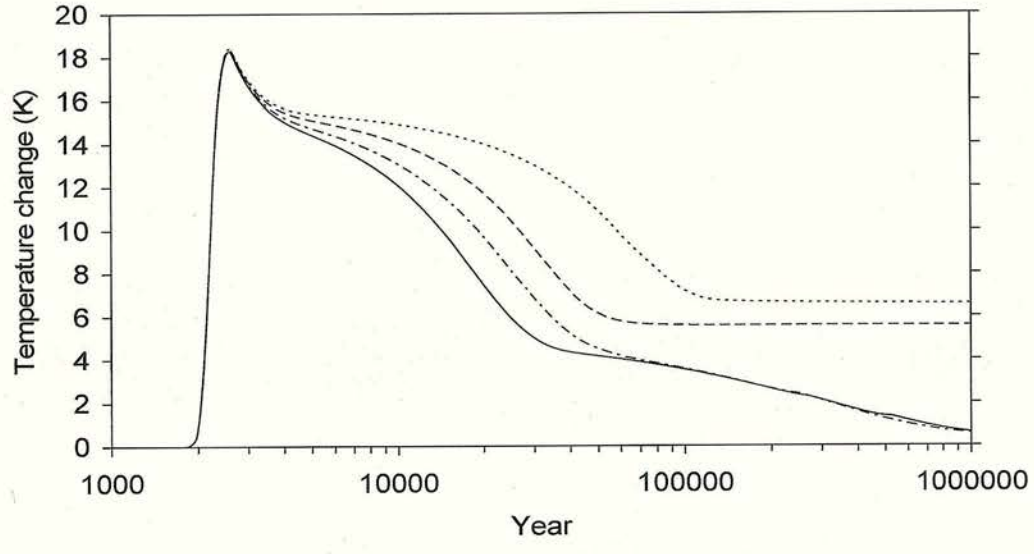

Figure 3-1: *The long-term response of (a) atmospheric CO_2 and (b) global temperature to scenario L8, 15,000GtC emissions of 'exotic' and conventional fossil fuel reserves, for different model variants: fixed weathering (dotted line), variable carbonate weathering (dashed line), variable silicate weathering (dot-dash line) and variable carbonate and silicate weathering (solid line).*

Figure 3-2 shows the relative effects of temperature and productivity on the level of weathering, for all three weathering cases (scenario L8, where 15,000GtC is emitted). In all three cases the initial increase in weathering is due to the large increases in temperature and productivity and continues occurs for between 400 and 600 years (depending on the weathering setup). After this time the excessive warming which has occurred suppresses productivity and causes a dip in the level of weathering. This is most marked in the case of the carbonate only weathering and least in the case of the silicate only weathering; this is due to the differing dependencies of each weathering case on productivity (see equations 3-1 & 3-3). The drop in the level of weathering continues until the temperature drops low enough for the productivity to recover. The weathering level then recovers beyond original levels and peaks, followed by a long slow decline in weathering level to the year 1 million. The time taken to reach this peak weathering level is dependent upon the type of weathering involved, silicate only weathering peaks the quickest as the influence of the recovering productivity is relatively small. In the silicate and carbonate weathering case the productivity has a greater relative influence, delaying the peak until ~yr 6500, but by this time the temperature has become the dominant control. In the case of the carbonate only weathering the temperature decrease over time is shallower but also the productivity continues to have a relatively large effect on the weathering level, causing a weathering peak much later than that of the other two weathering cases, at ~yr 20,000. At year 1 million the level of weathering has stabilised above its original value CO_2 in the atmosphere has stabilised above the original 280ppmv. In the case of the silicate only and the silicate and carbonate only weathering the level of weathering continues to decline at year 1 million as the CO_2 in the atmosphere has not yet stabilised. However the level of weathering for silicate only and the carbonate and silicate weathering system has converged due to the continued decrease in productivity to the year 1 million.

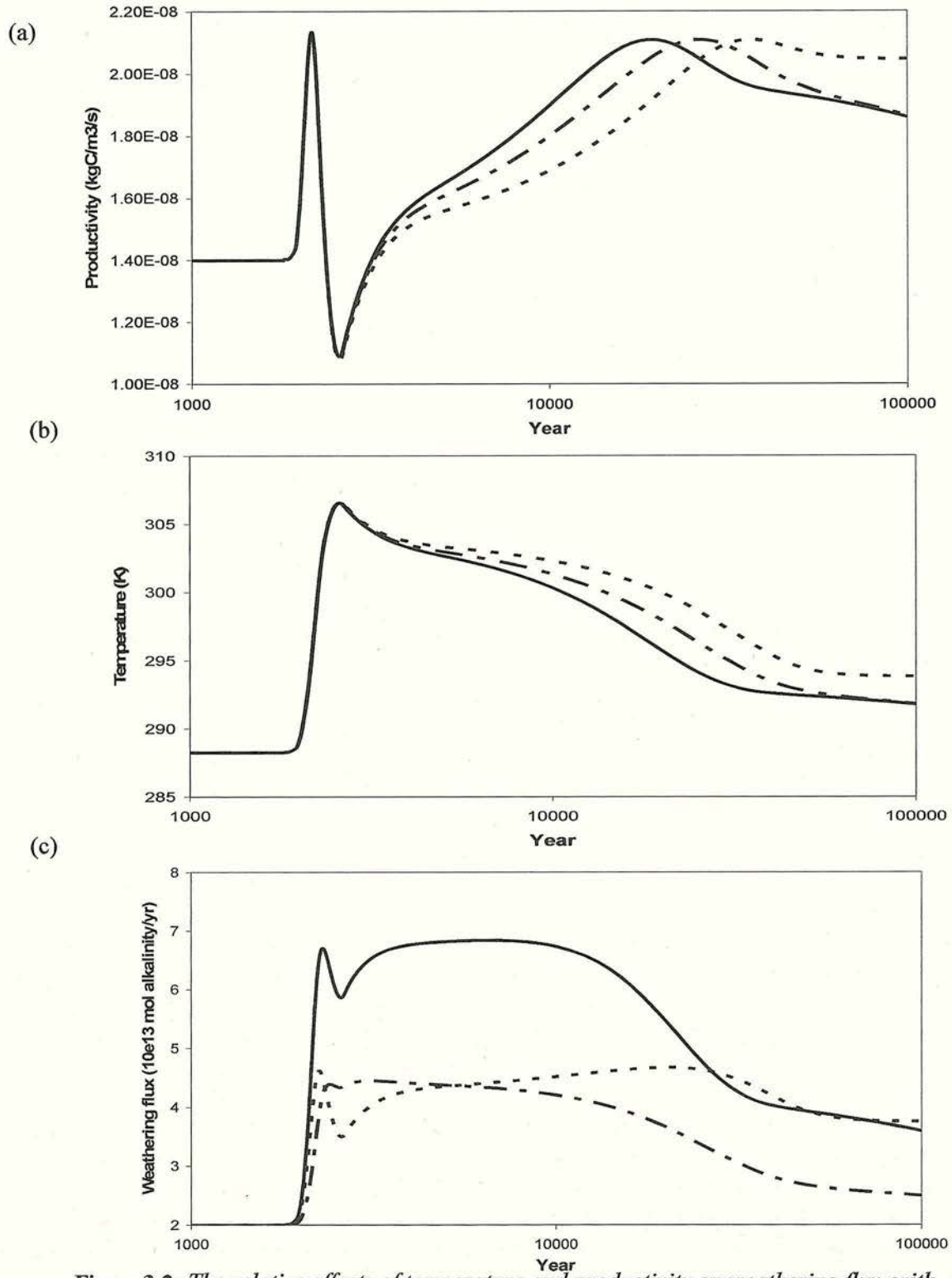

Figure 3-2: *The relative effects of temperature and productivity on weathering flux, with scenario L8, 15,000GtC emissions of 'exotic' and conventional fossil fuel reserves, for different model variants: variable carbonate weathering (dashed line), variable silicate weathering (dot-dash line) and variable carbonate and silicate weathering (solid line). (a) Productivity, (b) Temperature, (c) Weathering flux.*

With variable carbonate and silicate weathering, the input flux of alkalinity is more than tripled for thousands of years (Figure 3-3 (a)). All carbonate sediments dissolve within the millennium by year 2800 (Figure 3-3 (b)). The top layer of sediments begins to recover 14,000 years later and takes a further 11,000 years for its $CaCO_3$ content to exceed 80%. Each subsequent sediment layer with depth recovers in turn and takes progressively longer to do so. As the sediments recover they remove alkalinity from the ocean and thus buffer and slow the fall of CO_2. The bottom sediment layer starts to recover 28,000 years after the fossil fuel perturbation is complete and reaches a peak carbonate content of 65% after 75,000 years. This represents an over-compensation by the system and over the following hundreds of thousands of years, as the ocean continues to receive an enhanced alkalinity input from weathering, the CCD shoals. However, during this time temporary periods of sediment stability are established, marked by slowing/stability of total net sedimentation which continue until the CCD reaches the next sediment layer that has overshot its original level. This slows the decrease of temperature and CO_2 in the atmosphere at those times, thus accounting for the divergence between the temperature levels seen at ~year 500,000 between variable silicate weathering alone and that with both variable carbonate and silicate weathering (Figure 3-1). These periods of temporary stability can be seen at other times, but are more difficult to discern on the plots presented here. After 1Myr, the CCD has yet to return to its original depth and CO_2 is still at 338ppmv, 52ppmv above its pre-industrial concentration, and falling at

$\sim 5 \times 10^{-5}$ ppmv yr^{-1}.

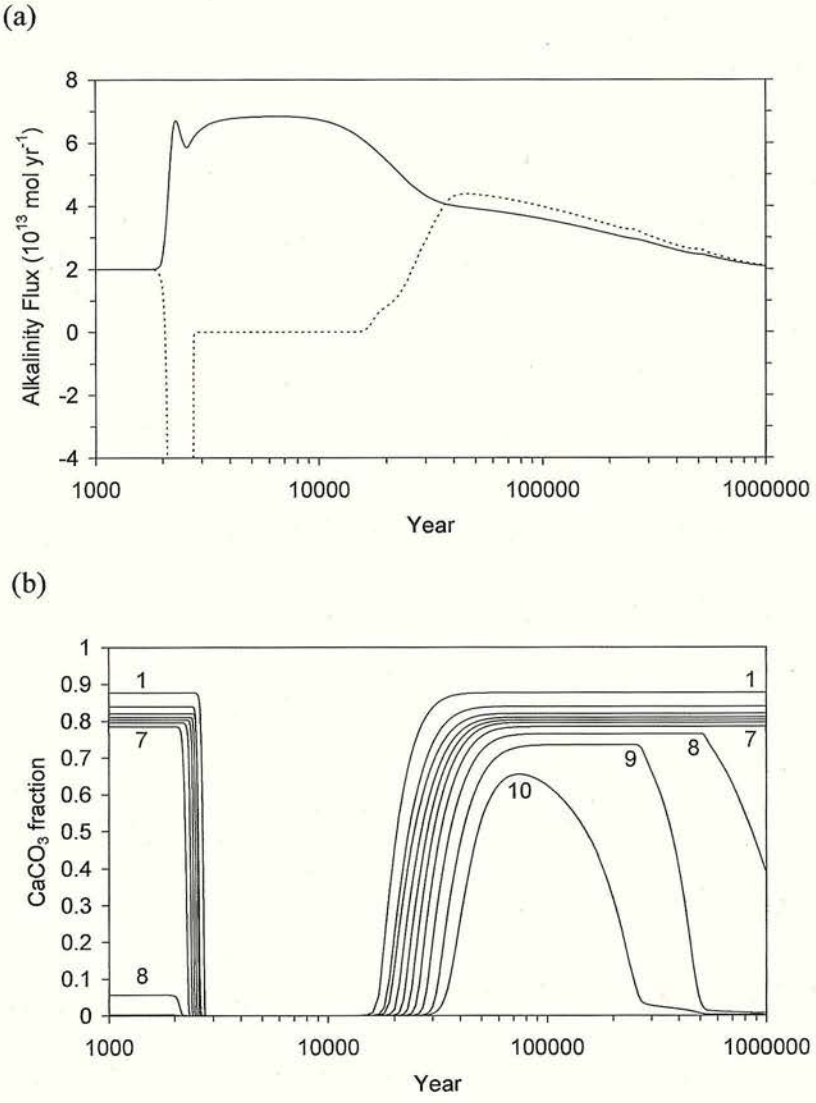

Figure 3-3: *The long-term responses of weathering and sediments to scenario L8, 15,000GtC emissions, in the model with variable carbonate and silicate weathering. (a) Alkalinity fluxes from weathering (solid line) and net sediment deposition or dissolution (dashed line). (b) Calcium carbonate fraction in the 10 sediment layers (number labels increase with depth). A negative value for the dashed line in (a) indicates net sediment dissolution (i.e. addition of alkalinity to the ocean). When the weathering and sedimentation fluxes are equal the system is in steady-state.*

Atmospheric CO_2 eventually stabilises after ~8 Myr at 320ppmv, still 34ppmv above pre-industrial. CO_2 fails to return to the pre-industrial concentration because it is assumed that a fraction (k_t = 0.27 (Lenton 2000)) of land-use change tends to permanently reduce vegetation

carbon. This in turn tends to reduce the global terrestrial gross primary productivity (P), which is assumed to affect weathering. In order to compensate for this and return P and hence silicate weathering flux to its original value, to match the fixed volcanic CO_2 flux, CO_2 and temperature must stabilise above pre-industrial levels.

In response to emitting 4,000GtC of conventional fossil fuel reserves to the atmosphere initially following business-as-usual (scenario L4), although the CO_2 perturbation is much smaller and not all carbonate sediments are dissolved, weathering still greatly accelerates the recovery to a given CO_2 concentration and temperature (Figure 3-4). To return to a global temperature of 2.0°C above pre-industrial, corresponding to 475ppmv, takes until year 37,000 with fixed weathering, year 19,000 with variable carbonate weathering, year 18,000 with variable silicate weathering, and year 13,000 with variable carbonate and silicate weathering. Silicate weathering has a similar impact to carbonate weathering on 10^3-10^4 year timescales (Figure 3-4), despite supplying only 25% of the initial alkalinity input flux, because it is the excess input flux of alkalinity relative to carbon that contributes to CO_2 drawdown. This is very similar in both cases because when silicate weathering is amplified there is no change in the corresponding carbon flux, whereas when carbonate weathering is amplified both carbon and alkalinity fluxes are increased, the latter more than the former.

(a)

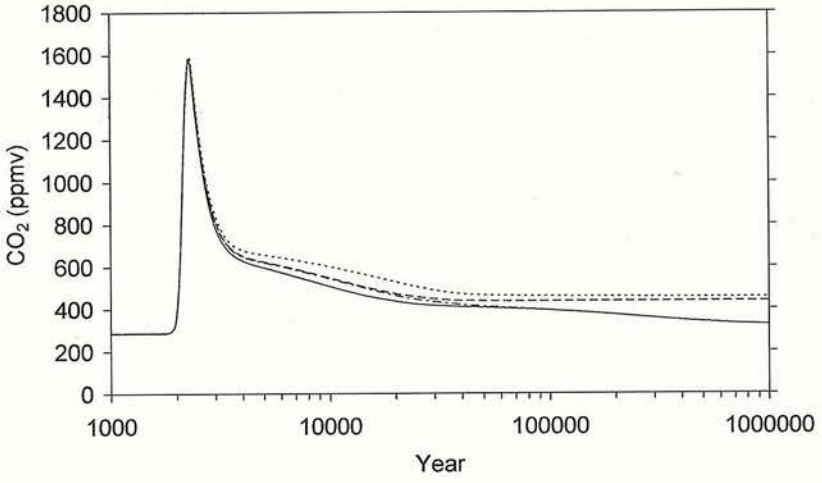

(b)

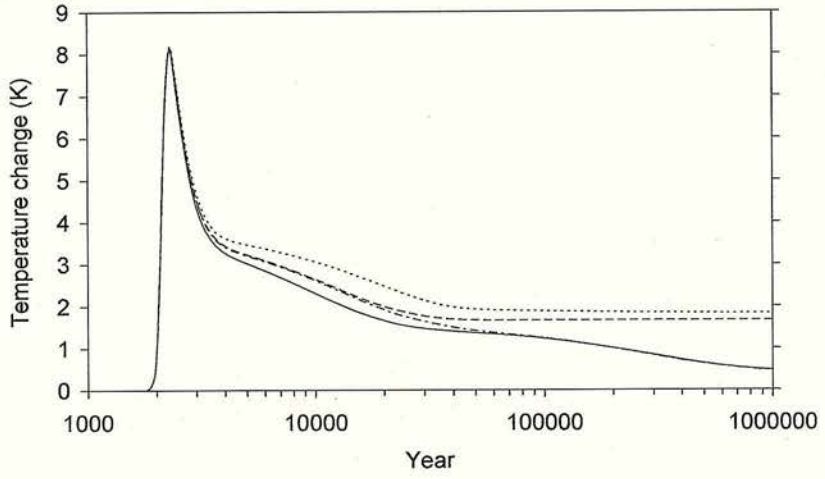

Figure 3-4: *The long-term response of (a) atmospheric CO_2 and (b) global temperature to scenario L4, 4,000GtC emissions of all conventional fossil fuel reserves, for different model variants: fixed weathering (dotted line), variable carbonate weathering (dashed line), variable silicate weathering (dot-dash line) and variable carbonate and silicate weathering (solid line).*

With variable carbonate and silicate weathering, the input flux of alkalinity nearly triples on the centennial timescale and is double pre-industrial in year 3000 (Figure 3-5 (a)). Carbonate sediments below 1600m are completely dissolved by year 3000 (Figure 3-5 (b)) and those in the range 600-1600m experience ongoing dissolution, losing around half their carbonate by year 4000. The sediment system then begins to recover. At around 30,000 years after fossil fuel perturbation, alkalinity input from weathering and alkalinity removal in carbonate

dissolution are temporarily in balance (Figure 3-5 (a)) and hence CO_2 is stabilised. However, deposition continues to increase, with a maximum depth for the CCD being reached after 70,000 years. The system overshoots in that carbonate deposition and corresponding alkalinity removal exceeds alkalinity input, causing ongoing dissolution. This process is incomplete after 1 Myr when CO_2 is at 325ppmv, 39ppmv above its initial pre-industrial concentration and falling at ~10^{-5} ppmv yr^{-1}. CO_2 eventually stabilises at 320ppmv, as before, because this is determined by the land-use change scenario which is the same for the different fossil fuel scenarios.

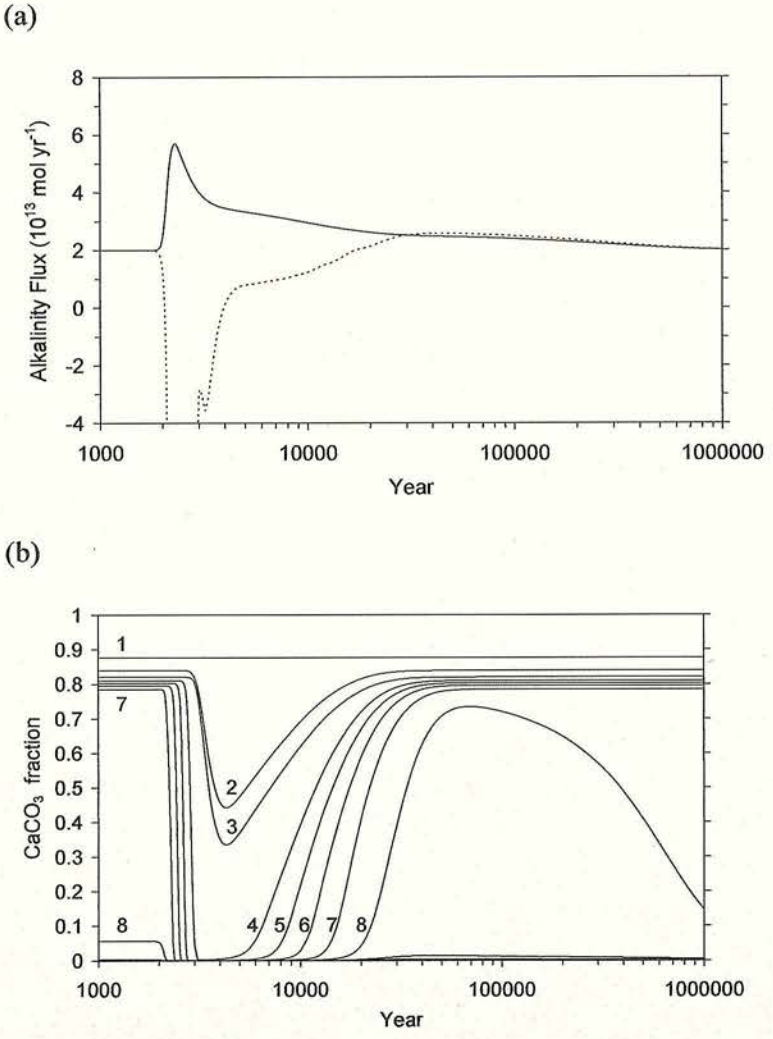

Figure 3-5: *The long-term responses of weathering and sediments to scenario L4, 4,000GtC emissions, in the model with variable carbonate and silicate weathering. (a) Alkalinity fluxes from weathering (solid line) and net sediment deposition or dissolution (dashed line). (b) Calcium carbonate fraction in the 10 sediment layers (number labels increase with depth).*

In response to a minimum emissions scenario (L2) totalling ~1,100GtC, weathering still markedly accelerates the recovery to a given CO_2 concentration (Table 3-1) and temperature. 350ppmv is reached around year 14,000 with fixed weathering, year 11,000 with variable carbonate or silicate weathering, and year 9,000 with variable carbonate and silicate weathering. The effect of variable carbonate weathering on final CO_2 after 1Myr is small, lowering it from 335ppmv to 331ppmv, whilst variable silicate weathering reduces it further to 321ppmv, only 1ppmv above its final steady state, with a rate of decline of $\sim 10^{-6}$ ppmv yr^{-1}. When land-use change is assumed not to cause a permanent reduction in vegetation carbon, atmospheric CO_2 does eventually return to its pre-industrial concentration, being 25ppmv above it after 100kyr and only 2ppmv above it after 1Myr.

The fraction of cumulative CO_2 emissions remaining in the atmosphere on different timescales is summarised in Table 3-2 for all the emissions scenarios, in the model with variable carbonate and silicate weathering and no permanent land use. This emphasises that the lifetime of the remaining added CO_2 increases with time (Kasting and Schultz, 1996) and it will take more than a million years for all of it to be removed (Walker and Kasting, 1992).

Table 3-2: *The fraction of cumulative CO2 emissions remaining in the atmosphere at different times for all emissions scenarios. The model used is with variable Ca and Si weathering and no permanent land-use change, hence the airborne fraction eventually reaches zero.*

Scenario	Airborne fraction (%) in year											
	2000	2100	2300	2500	3000	5000	10k	30k	100k	300k	500k	1M
L1	46.3	55.8	48.9	32.8	18.3	12.4	8.99	5.66	4.30	2.10	1.06	0.25
L2	45.9	44.3	31.6	22.8	14.2	10.5	8.22	5.31	3.87	1.97	1.07	0.32
L3	46.6	63.5	63.4	44.8	24.0	14.9	10.2	5.70	4.01	2.25	1.10	0.24
L4	46.3	55.8	64.5	46.3	24.1	14. 9	10.2	5.71	4.02	2.23	1.10	0.24
L5	46.0	45.7	48.6	46.1	29.1	15.1	10.3	5.72	4.03	2.24	1.10	0.24
L6	46.6	63.5	62.3	43.8	23.5	14.9	10.1	5.70	4.02	2.24	1.10	0.24
L7	46.3	55.8	80.3	76.3	51.7	30.7	17.4	6.22	4.26	2.08	1.18	0.21
L8	46.3	55.8	87.4	86.3	68.3	49.9	33.4	7.33	4.76	2.10	1.04	0.20
A23	47.6	52.1	70.2	51.9	26.5	15.4	10.4	5.71	4.02	2.27	1.11	0.23

3.5 Discussion

We have not used the same emissions scenarios as Walker and Kasting (1992). However, comparing their 'profligate' scenario (Figs. 27 and 29 of Walker and Kasting (1992)), which emits 4200GtC in a peaked fashion, to similar scenarios (L3, L4, L6, A23) in our model, it is clear that for the same emissions, peak CO_2 would be lower in our model, suggesting a stronger ocean sink. CO_2 recovers faster in our model over the first few thousand years, for all formulations of weathering, indicating a much greater impact of sediment dissolution. Walker and Kasting (1992) find that carbonate weathering significantly enhances CO_2 drawdown on the millennial timescale, because it depends linearly on CO_2 in their standard model, and hence peaks at ~8 times the present rate. In contrast, variable carbonate and silicate weathering become more important for CO_2 drawdown after year 3000 in our model. However, beyond year 20,000 the two models converge, and both take over a million years for atmospheric CO_2 to recover to pre-industrial concentrations.

We find that the contribution of enhanced weathering to carbon cycle recovery is somewhat dependent on whether all sediments dissolve and corresponding buffering capacity is lost in the ocean. The amount of fossil fuel CO_2 required to dissolve all carbonate sediments in our model is 7350GtC, whereas Archer (2005) calculates ~5000GtC. The difference is due to the calculated initial inventory of $CaCO_3$, which is in turn a function of assumed sediment depth, detrital flux and calculated CCD. Emitted CO_2 in excess of that required to dissolve all carbonate sediments tends to remain in the atmosphere until weathering can provide the alkalinity to neutralise it. Enhancement of weathering can accelerate the recovery of CO_2 in this regime by a factor of 4. However, even when all sediments are not dissolved, recovery can be accelerated by more than a factor of 2.

Archer (2005) calculates that ~7% of added CO_2 remains in the atmosphere longer than 100kyr. With variable carbonate and silicate weathering and no permanent land use, we estimate ~4–5% (Table 3-2) depending on the total emissions. This lower value is to be expected given the modelled enhancement of weathering. The lingering fossil CO_2 has potentially important consequences for the glacial-interglacial cycles that characterised the Quaternary. Archer and Ganopolski (2005) have recently calculated that a fossil fuel perturbation of 5000GtC is sufficient to prevent glacial inception for at least the next 500,000 years.

Our results support the suggestion that artificially accelerating carbonate weathering by reacting CO_2-rich power plant gases with seawater and then reacting the resulting carbonic acid solution with carbonate rocks would be an effective way of sequestering CO_2 (Caldeira and Rau 2000). They also show interesting interactions between the negative feedbacks in the carbon cycle involving carbonate compensation and silicate weathering. The interaction is antagonistic and slows the recovery of atmospheric CO_2 when, after 20-50kyr, sediments are re-establishing. Indeed, CO_2 is temporarily stabilised when alkalinity removal from the ocean due to carbonate deposition temporarily matches alkalinity input. The system then overshoots and over 10^5-10^6yr, the interaction between carbonate dissolution and silicate weathering is synergistic, with a slight, gradual dissolution of sediments contributing to CO_2 uptake.

This complicates the traditional interpretation of the response time of the silicate weathering feedback. Other studies (Archer 2005, Archer and Ganopolski 2005) have assumed a ~400kyr response time based on the work of Sundquist (1991). We find that after ~100kyr, once sediments begin their final adjustment phase, the half-life for the decay of added CO_2 is ~200kyr regardless of the amount of CO_2 added (Table 3-1), or whether land-use change is assumed to permanently reduce vegetation carbon or not. Ongoing sediment dissolution must be contributing to reducing this response time.

It is notable that in the presence of land-use change, CO_2 never recovers to pre-industrial concentrations in our simulations even when they are run out to equilibrium. This is because it is assumed that a fraction (k_t = 0.27 (Lenton 2000)) of land-use change tends to permanently reduce vegetation carbon, which in turn tends to reduce the global terrestrial gross primary productivity (P), which in turn affects weathering. To achieve a long-term steady state, the silicate weathering flux must return to its initial value and match the fixed volcanic CO_2 flux. This can only be achieved by stabilising CO_2 and temperature above their pre-industrial concentrations. The assumption that there is a permanent element to land-use change may be flawed, as it presumes either that humans will still be around and using the land a million years hence, or that if we are not, natural ecosystems will have failed to recover to their pre-industrial and pre-agricultural state. However, some vegetation-climate systems such as the Amazon rainforest are thought to be bi-stable (Betts 1999) and if the forest either dies back (Cox et al. 2004) or is deforested, they may remain in an alternative steady state with lower carbon storage. If that state tends to have smaller weathering fluxes, then the long-term steady state for CO_2 will accordingly be shifted upwards.

Natural mechanisms that have caused glacial drawdown of CO_2 by ~80-100ppmv could in principle over-ride the longer-term control by silicate weathering. However, drawdown of CO_2 appears to follow glacial inception, and Archer and Ganopolski (2005) have pointed out that a ~5000GtC fossil fuel perturbation could prevent glaciation for at least the next 500,000 years. Our results agree with this and suggest that if humans choose to exploit 'exotic' fossil fuel reserves and emit ~15,000GtC, then glaciation could be prevented for over a million years. Furthermore, if there is a permanent change in vegetation cover that tends to reduce silicate weathering rates, then it may cause atmospheric CO_2 to remain at concentrations that prevent glaciation indefinitely.

3.6 Conclusions

Increasing atmospheric CO_2 and global temperatures are expected to increase carbonate and silicate weathering rates, via the direct effects of warming, and indirectly, via the CO_2 fertilisation effect on plants and warming enhancing soil respiration. This enhanced weathering should in turn increase alkalinity input to the ocean and long-term CO_2 uptake. Our model experiments suggest that amplified carbonate and silicate weathering will greatly accelerate CO_2 removal from the atmosphere 10^4-10^5 yrs after the fossil fuel perturbation. The acceleration of CO_2 drawdown is greatest for emissions of $\geq$ 7350GtC, which cause the dissolution of all carbonate sediments. However, it still takes $>10^6$ yr for silicate weathering to stabilise CO_2. The final steady state CO_2 could be above the pre-industrial ~280ppmv if the effects of land-use change persist on a million year timescale and tend to reduce global productivity and weathering rates relative to pre-industrial and pre-agricultural conditions (e.g. by having transformed areas of forest to pasture or cropland). This in turn could prevent glaciation indefinitely.

3.7 References

Amiotte-Suchet, P. J.-L. Probst, and W. Ludwig, Worldwide distribution of continental rock lithology: Implications for the atmospheric/soil CO2 uptake by continental weathering and alkalinity river transport to the oceans, *Glob. Biogeochem. Cycl. 17*, 1038, 2003.

Archer, D. Fate of fossil fuel CO2 in geologic time, *Journal of Geophysical Research (Oceans)*, doi:10.1029/2004JC002625, 2005.

Archer, D. and A. Ganopolski, A movable trigger: Fossil fuel CO2 and the onset of the next glaciation, *Geochemistry Geophysics Geosystems*, *6*, doi:10.1029/2004GC000891, 2005.

Archer, D. H. Kheshgi, and E. Maier-Reimer, Dynamics of fossil fuel CO2 neutralization by marine CaCO3, *Glob. Biogeochem. Cycl. 12*, 259-276, 1998.

Archer, D. H. S. Kheshgi, and E. Maier-Reimer, Multiple timescales for neutralization of fossil fuel CO2, *Geophys. Res. Lett. 24*, 405-408, 1997.

Bala, G. K. Caldeira, A. Mirin, M. Wickett, and C. Delire, Multicentury Changes to the Global Climate and Carbon Cycle: Results from a Coupled Climate and Carbon Cycle Model, *Journal of Climate*, *18*, 4531-4544, 2005.

Berelson, W. M. D. E. Hammond, J. McManus, and T. E. Kilgore, Dissolution kinetics of calcium carbonate in equatorial Pacific sediments, *Glob. Biogeochem. Cycl. 8*, 219-235, 1994.

Bergman, N. M. T. M. Lenton, and A. J. Watson, COPSE: a new model of biogeochemical cycling over Phanerozoic time, *American Journal of Science*, *304*, 397-437, 2004.

Berner, R. A. Geocarb II: A revised model of atmospheric CO2 over Phanerozoic time, *American Journal of Science*, *294*, 56-91, 1994.

Berner, R. A. The Rise of Plants and Their Effect on Weathering and Atmospheric CO_2, *Science, 276*, 544-546, 1997.

Berner, R. A. and M. F. Cochran, Plant-induced weathering of Hawaiian basalts, *Journal of Sedimentary Research, 68*, 723-726, 1998.

Berner, R. A. and Z. Kothavala, Geocarb III: A revised model of atmospheric CO2 over Phanerozoic time, *American Journal of Science, 301*, 182-204, 2001.

Berner, R. A. A. C. Lasaga, and R. M. Garrels, The carbonate-silicate geochemical cycle and its effect on atmospheric carbon dioxide over the past 100 million years, *American Journal of Science, 283*, 641-683, 1983.

Betts, R. A. Self-beneficial effects of vegetation on climate in an Ocean- Atmosphere General Circulation Model, *Geophys. Res. Lett. 26*, 1457-1460, 1999.

Caldeira, K. and G. H. Rao, Accelerating carbonate dissolution to sequester carbon dioxide in the ocean: Geochemical implications, *Geophys. Res. Lett. 27*, 225-228, 2000.

Cox, P. M. R. A. Betts, M. Collins, P. P. Harris, C. Huntingford, and C. D. Jones, Amazonian forest dieback under climate-carbon cycle projections for the 21st century, *Theoretical and Applied Climatology, 78*, 137-156, 2004.

Cox, P. M. R. A. Betts, C. D. Jones, S. A. Spall, and I. J. Totterdell, Acceleration of global warming due to carbon-cycle feedbacks in a coupled climate model, *Nature, 408*, 184-187, 2000.

House, J. I. I. C. Prentice, N. Ramankutty, R. A. Houghton, and M. Heimann, Reconciling apparent inconsistencies in estimates of terrestrial CO2 sources and sinks, *Tellus B, 53B*, 345-363, 2003.

Ingle, S. E. Solubility of calcite in the ocean, *Mar. Chem. 3*, 301-309, 1975.

Joos, F. G.-K. Plattner, T. F. Stocker, O. Marchal, and A. Schmittner, Global Warming and Marine Carbon Cycle Feedbacks on Future Atmospheric CO2, *Science, 284*, 464-467, 1999.

Kasting, J. F. and P. A. Schultz, Reservoir time-scales for anthropogenic CO2 in the atmosphere: commentary, *Tellus B*, *48B*, 703-706, 1996.

Knox, F. and M. B. McElroy, Changes in Atmospheric CO2: Influence of the Marine Biota at High Latitude, *Journal of Geophysical Research*, *89*, 4629-4637, 1984.

Le Quéré, C. O. Aumont, L. Bopp, P. Bousquet, P. Ciais, R. Francey, M. Heimann, C. D. Keeling, R. F. Keeling, H. Kheshgi, P. Peylin, S. C. Piper, I. C. Prentice, and P. J. Rayner, Two decades of ocean CO2 sink and variability, *Tellus B*, *55B*, 649-656, 2003.

Lenton, T. M. Land and ocean carbon cycle feedback effects on global warming in a simple Earth system model, *Tellus*, *52B*, 1159-1188, 2000.

Lenton, T. M. Climate Change to the end of the Millennium, *Clim. Change*, *76*, in press, 2006.

Lenton, T. M. and M. G. R. Cannell, Mitigating the Rate and Extent of Global Warming, *Clim. Change*, *52*, 255-262, 2002.

Lenton, T. M. M. S. Williamson, N. R. Edwards, R. Marsh, A. R. Price, A. J. Ridgwell, J. G. Shepherd, S. J. Cox, and theGENIEteam, Millennial timescale carbon cycle and climate change in an efficient Earth system model, *Climate Dynamics*, doi: 10.1007/s00382-00006-00109-00389, 2006.

Lewis, E. and D. Wallace, Program developed for CO2 system calculations, Carbon Dioxide Information Analysis Centre, Oak Ridge, 1998.

Lovelock, J. E. and A. J. Watson, The regulation of carbon dioxide and climate: Gaia or geochemistry? *Planetary and Space Science*, *30*, 795-802, 1982.

Millero, F. J. The thermodynamics of the carbonate system in seawater, *Geochim. cosmochim. Acta*, *43*, 1651-1661, 1979.

Milliman, J. D. Production and accumulation of calcium carbonate in the ocean: Budget of a nonsteady state, *Glob. Biogeochem. Cycl. 7*, 927-957, 1993.

Ridgwell, A. J. *Glacial-interglacial perturbations in the global carbon cycle*, 134 pp. University of East Anglia, Norwich, 2001.

Ridgwell, A. J. and U. Edwards, Geological Carbon Sinks, in *Greenhouse Gas Sinks*, edited by D. Reay, N. Hewitt, J. Grace, and K. Smith, CABI publishing, in press.

Schwartzman, D. W. and T. Volk, Biotic enhancement of weathering and the habitability of Earth, *Nature*, *340*, 457-460, 1989.

Sundquist, E. T. Steady- and non-steady-state carbonate-silicate controls on atmospheric CO2, *Quaternary Science Reviews*, *10*, 283-296, 1991.

Treguer, P. D. M. Nelson, A. J. Van Bennekom, D. J. DeMaster, A. Leynaert, and B. Queguiner, The silica balance in the world ocean: A reestimate, *Science*, *268*, 375-379, 1995.

Walker, J. C. G. P. B. Hays, and J. F. Kasting, A negative feedback mechanism for the long-term stabilisation of Earth's surface temperature, *Journal of Geophysical Research*, *86*, 9776-9782, 1981.

Walker, J. C. G. and J. F. Kasting, Effects of fuel and forest conservation on future levels of atmospheric carbon dioxide, *Palaeogeography, Palaeoclimatology, Palaeoecology (Global and Planetary Change Section)*, *97*, 151-189, 1992.

White, A. F. and A. E. Blum, Effects of climate on chemical weathering in watersheds, *Geochim. cosmochim. Acta*, *59*, 1729-1747, 1995.

Williams, E. L. L. M. Walter, T. C. W. Ku, G. W. Kling, and D. R. Zak, Effects of CO2 and nutrient availability on mineral weathering in controlled tree growth experiments, *Glob. Biogeochem. Cycl. 17*, 1041, 2003.

4 'Uncertainty in atmospheric CO_2 recovery from fossil fuel perturbation due to the ocean-sediment system'

4.1 *Abstract*

The response of atmospheric CO_2 to a given fossil fuel perturbation depends on uncertain parameters in the Earth system. Here we focus on 10^3–10^5 year time scales of CO_2 recovery over which the ocean, marine sediments, and weathering flux of alkalinity control the response. A Bayesian ensemble method is used to quantify uncertainties in the response of the ocean-sediment component of a simple Earth system model. 11 parameters are allowed to vary within ranges informed by the literature. Latin hypercube sampling and a likelihood based accept-reject system are used to calibrate the model parameters, producing a subset of the ensemble that gives likely responses for pre-industrial atmospheric CO_2, and anthropogenic rise in CO_2. From an initial ensemble of 14400 members, 637 remain. These were run into the future with an extended 'business-as-usual' emissions scenario emitting 4000 GtC of fossil fuel after 1990. The most probable peak value for CO_2 is 1363ppmv, with a range of 1156-1609ppmv that encompasses earlier studies with the same model. Uncertainty in atmospheric CO_2 varies with time and is greatest sometime around the year 2450. The airborne fraction of added CO_2 in year 3000 ranges over 14–31% due to parameter uncertainty, comparable with the range due to varying total emissions over 300–5000 GtC in a different model. Atmospheric CO_2 eventually stabilises above the pre-industrial concentration because weathering is assumed constant over time. The timescale for CO_2 to approach this (quasi)equilibrium varies widely from year 13,000 to 57,000. After stabilisation, the remaining airborne fraction is 7–9.5% and the final CO_2 concentration tends to be linearly related to the pre-industrial concentration, with a similar range of uncertainty.

4.2 *Introduction*

The response of atmospheric CO_2 to fossil fuel burning and land-use change will be a key determinant of future climate change. Numerous studies have considered the fate of added CO_2 over a range of timescales (Archer 1998, Cox et al. 2000, Lenton 2000, Friedlingstein et al. 2001, Berthelot et al. 2002, Archer 2005). Present knowledge can be summarised thus:

On the multi-centennial timescale, the rate of CO_2 emissions, as well as the total CO_2 emitted, have a first order effect on the rate of CO_2 rise and peak concentrations of CO_2, with the response of ocean and land CO_2 exchange providing a second order control (Lenton and Cannell 2002). If the land becomes a carbon source this can greatly amplify peak CO_2, as can a warming-induced reduction in the ocean carbon (Walker & Kasting 1992, Cox et al. 2000, Lenton 2000, Dufresne et al. 2002). On the millennial timescale, atmospheric CO_2 approaches a quasi-equilibrium determined by the total amount of CO_2 emitted and the cumulative ocean uptake of CO_2, with any net gain or loss of carbon by the land surface making a secondary contribution (Lenton 2000, Lenton et al. 2006). The dissolution of ocean carbonate sediments may have begun to influence CO_2 on the millennial timescale, and will be responsible for an ongoing drawdown of CO_2 over the order of $\sim 10^4$ years (Archer et al. 1998, Archer 2005). The weathering of carbonate and silicate rocks on land will gradually replenish the ocean with alkalinity over a similar timescale, eventually allowing the carbonate sediments to recover (Walker & Kasting 1992, Archer 2005, Lenton & Britton 2006). Over the order of 10^5-10^6 years, enhanced silicate weathering and corresponding carbonate deposition will remove the remaining anthropogenic CO_2 from the atmosphere. As the sediments recover, they may overshoot the original carbonate compensation depth (CCD) and then go into net dissolution making for interesting dynamics of atmospheric CO_2 (Lenton and Britton 2006 – see Chapter Three).

Here we focus on 10^3-10^5 year timescales over which processes in the oceans, carbonate sediments, and the flux of alkalinity from weathering exert the key controls on the recovery of atmospheric CO_2 (Archer 2005). We use a simple Earth system model (Lenton and Britton 2006 – see Chapter Two) to make a first attempt at comprehensive analysis of uncertainty in the long-term response of CO_2 due to ocean and sediment processes. We treat the river flux of alkalinity as one of the fixed parameters that we vary at the outset. Hence any acceleration of CO_2 drawdown by enhanced weathering, and the final removal of added CO_2 by silicate weathering over 10^5-10^6 years are ignored here. The model is based on a box representation of the carbon cycle including ocean sediments, coupled to an energy-balance formula for surface temperature. This is an appropriate tool for the 10^5 year timescales we address, being fast enough to allow us to conduct a thorough and statistically sound uncertainty analysis.

The amount of CO_2 emitted will determine the absolute value of atmospheric CO_2 at any given time, but here we concentrate instead on the influence of uncertain ocean and sediment parameters, for a single given emissions scenario of CO_2. We select an extended 'business-

as-usual' scenario of CO_2 emissions that releases 4000 GtC of fossil fuel after 1990, 224 GtC from historical (fossil fuel plus land use change) emissions prior to 1990, and 213 Pg C from future land-use change, giving 4437 GtC emissions in total (Lenton 2006). This scenario has been used in previous studies (Lenton 2000, Lenton et al. 2006) and similar scenarios have been used in other models.

There is currently a great deal of interest in uncertainty analysis of climate models, and in particular, constraining the climate sensitivity to a doubling of pre-industrial CO_2 (Houghton et al. 2001). We do not address this problem here, because our model is not appropriate for the task. The climate sensitivity of our model is 2.8°C, which is close to the ~3°C that is emerging as the most probable value from other studies (Houghton et al. 2001). We do consider the effects of temperature change on CO_2 exchange by the land and ocean in a fully interactive fashion.

Uncertainty in modelling comes from three areas: firstly, measurement error in the data on which the model is based; secondly, model imperfection – i.e. even with perfect parameters any model would not be a perfect representation of the real world – as it is just that, a representation; thirdly, model uncertainty – which is addressed here. This is the uncertainty in the model response which comes from the uncertainty in its parameters. Ensemble modelling – running the model multiple times whilst varying the parameter values - can be used to address the uncertainty in the parameters, by calibrating the parameters and model response with respect to data. However, even with the simplest climate or biogeochemical model computer power and availability limits the ability to explore parameter space. Even if it is possible to conduct the necessary runs, criteria for valuing or selecting runs from the ensemble that are 'reasonable' in terms of the system under consideration is still necessary.

Ensemble studies that have been conducted on climate and biogeochemical models in the past (Murphy et al. 2004, Stainforth et al 2005, Zaehle et al. 2005, Barnett et al. 2006), had to base their methodology on what is possible in terms of computing power – which is not ideal. This means that in many cases the number of ensemble members is small (Murphy et al. 2004, Barnett et al. 2006), the sampling of the parameters only changes between minimum, maximum and mean values (Hallegran & Pitman 2000, Stainforth et al 2005), and the selection process of 'reasonable' ensemble members can be subjective (Challoner et al. 2006). Due to having a relatively fast model, we have been able to apply a rigorous methodology for our ensemble study, including an attempt to define a suitable sample size

for the ensemble, and a careful selection system. Such an ensemble analysis on the timescale of up to 10^5 years has, to our knowledge, not been attempted before.

The aim of our study is to quantify a probability distribution for our model parameters, (and therefore our model's output) using information from data and taking into account measurement errors. In essence we are trying to calibrate our model with data. Bayes' theorem, which defines a relationship between conditional probabilities (Equation 4-1) provides us with a means of quantifying the distribution that we want, which is known as the 'posterior'. The 'prior' is an n-dimensional joint probability distribution for the parameters, and allows the inclusion of any existing information on the parameters. The 'likelihood', which can be calculated easily, is the likelihood of getting the data from the model output given the parameter value that has been used in that run of the model. This involves constructing another conditional probability distribution based on the data and its measurement error.

$$Posterior = Prior \times Likelihood \qquad \textbf{Equation 4-1}$$

The application of Bayes' theorem to our model study requires a numerical approach and we use 'accept-reject' (Chib & Greenberg 1995), which consists of five steps. (1) Defining the prior, (2) Sampling the prior, (3) Running the model, (4) Calculating the likelihoods, (5) A rejection step. The posterior parameter distribution that this approach produces is then used to run our model into the future, whilst applying an emissions scenario. This provides us with a posterior results distribution, allowing us to look at the uncertainty in our results due to parameter uncertainty.

We aim to answer the question; how does parameter uncertainty in the ocean and sediment system affect the CO_2 response of the atmosphere and how does this change with time? The relatively efficient nature of the model used here allows us to use a well constructed methodology, including an accept-reject technique and we will also try to address issues such as suitable sample size.

4.3 *Methods*

4.3.1 Model setup

We use the 7-box global carbon cycle model with a coupled 10-layer sediment system and energy-balance approximation of global temperature, which is described in Chapter Two (also in Lenton & Britton (2006)). All parameters, except those that are varied in this study (see next section) are the same as in Chapter Two/Lenton and Britton (2006). The high and low latitude surface ocean box temperatures are allowed to vary, depending on the global average surface temperature, as described in Lenton (2000). The enhanced carbonate and silicate weathering system is not switched on for this study, meaning that the alkalinity flux from the land remains constant with time, the carbon flux from the land is half of the alkalinity flux, at all times (see Chapter Two/Lenton and Britton (2006) fixed weathering case). The processes that are captured within the model are, photosynthesis, plant respiration, litter fall/mortality, soil respiration, CO_2 exchange between the atmosphere and surface ocean, circulation of carbonate chemistry and nutrients between the ocean boxes, and the production and decay of organic carbon and $CaCO_3$ particulate matter in the ocean. The equilibrium climate sensitivity of the energy balance model is 2.8°C for a doubling of CO_2, and 6.3°C for a quadrupling of CO_2 (Lenton 2006).

4.3.2 CO_2 emissions scenario

When forcing the model with historical or future CO_2 emissions we used a single scenario, taken from previous work (Lenton 2000 scenario 4). In the historical interval (defined here as up to 1990) the fossil fuel data of Marland et al. (1998) is used. Beyond 1990 anthropogenic fossil fuel emissions follow IS92a (Leggett et al. 1992) until year 2100, then undergo a linear decline using up 4000GtC. Additional emissions (year 1800 onwards) come from a land-use change scenario (Houghton & Hackler 1998), taking the total emissions level to 4437GtC. The runs were stopped at the year 200,000.

4.3.3 Defining the prior

The emphasis of the study is on the uncertainty in future atmospheric CO_2 on timescales of up to 10^5 years, with respect to the buffering effects of the ocean sediments. Therefore, the 11 parameters we chose to vary in this study (Table 4-1) are connected to the biogeochemistry and physics of the ocean and the sediments. The joint probability

distribution function for the prior was made by first constructing probability density functions for the 11 individual parameters – this was achieved with reference to literature on the means and most likely/most used values for each parameter (see Table 4-1). Literature also provided suitable maximum, minimum and mean values for each parameter, so that each probability density function could be recalculated as a truncated distribution, which therefore provided limits for the sampling stage (Table 4-1). A distribution was chosen for each of the parameters – this was a normal distribution in most cases, except in the case of the dissolution constant, where a log normal distribution was used. This distribution allowed the selection of parameter values that spanned the large range of values seen in data, but gave a greater probability to the selection of lower values that were often used in previous modelling studies. We did not include any correlations between the parameters.

Table 4-1: ***Information and references for the parameters varied in the study.***

Parameter Description	*Mean Value*	*Standard Deviation*	*Minimum*	*Maximum*	*References and notes*	*Lenton and Britton (2006) value*
Nutrient uptake in the Southern Ocean (.)	0.5	0.3	0.0	1.0	Knox & McElroy (1984)	0.01
Piston velocity – determines the exchange of CO_2 between the ocean and atmosphere ($m\ yr^{-1}$)	0.18	0.07	0.02	0.34	Wanninkhof (1992)	0.2
High-latitude overturning ($m^3 s^{-1}$)	4.5×10^{7}	1.25×10^{7}	1.5×10^{7}	7.5×10^{7}	Knox & McElroy (1984), Lenton (2000)	2.7×10^{7}
Thermohaline overturning ($m^3 s^{-1}$)	4.5×10^{7}	1.25×10^{7}	1.5×10^{7}	7.5×10^{7}	As High-latitude overturning	2.5×10^{7}
Intermediate-deep exchange ($m^3 s^{-1}$)	2.4×10^{8}	0.5×10^{8}	0.8×10^{8}	4.0×10^{8}	As High-latitude overturning	2.0×10^{8}
Warm-intermediate exchange ($m^3 s^{-1}$)	1.5×10^{7}	0.25×10^{7}	0.5×10^{7}	2.5×10^{7}	As High-latitude overturning	1.25×10^{7}
Salinity (ppt)	34.5	0.4	33	36	Knox and McElroy (1984), Boyle (2002)	34.7
Flux of alkalinity to the ocean (mol/yr)	3.00×10^{13}	1.10×10^{13}	0.47×10^{13}	5.22×10^{13}	Amiotte-Suchet (2003), Jones et al. (2002), Gaillardet (1999), Munhoven (2002), Walker & Opdyke (1995), Archer et al. (1998), Milliman (1993), Milliman & Droxler (1996), Vescei (2004)	2×10^{13}
Flux of detritus to the seafloor (mol/yr)	18.3×10^{12}	7.5×10^{12}	0.6×10^{12}	36.0e12	Archer et al. (1998)	6×10^{12}
Exponent in the dissolution of carbonate equation (.)	2.75	1.2	0.5	5	Ridgwell (2001), Keir (1980), Morse (1978), Archer (1996), Archer et al. (1998), Sigman et al. (1998), Archer & Maier-Reimer (1994), Archer (1991)	4.5
Constant in the dissolution of carbonate equation (% per day) [Logged distribution]	1.7	2	-5	3	As dissolution exponent	1.3

4.3.4 Sampling the prior

4.3.4.1 Method

A latin hypercube (McKay et al. 1979) was used to sample the prior, by splitting each of the 11 parameter ranges into *n* segments (*n*=sample size). Segment sizes are of equal probability, and a value from each segment is randomly selected. Combinations of parameter segments are then selected at random, but with the stipulation that each segment can only be sampled once. A latin hypercube ensures effective sampling of the whole distribution, but is not entirely random.

Our Bayesian methodology dictates that we treat the parameters as distributions, with associated probabilities. Therefore we use the latin hypercube to sample the prior, which takes into account the probabilities of each parameter value. This is a different method of sampling to choosing high and low values for each parameter, and then combining them with the other parameters to give a total sample size of $n=2^x$ where x is the number of parameters. This system dictates that each parameter value chosen is just as likely as another, which is the same as giving the parameter a uniform distribution.

4.3.4.2 Selecting a suitable sample size

A key question in designing this study was the selection of a suitable initial sample size for the ensemble. There are no hard and fast rules about the required size for an ensemble study, obviously as with all statistical procedures the larger the sample size the better, however sample sizes of infinity are not possible. There will also come a point when the inclusion of more data makes no appreciable difference to the result. Ensemble modelling sample sizes are often guided by their demand on computing facilities, as our model is relatively fast, we were able to conduct large ensembles. However we still had to define and validate the size of our ensemble in some way.

We selected five initial sample sizes, where n = 600, 2400, 9600, 14400, and 19200. 10 latin hypercubes were created for each sample size, the one with the lowest correlation between parameters was used in the study in an attempt to avoid bias in the sampling. We made two comparisons on the posterior for each of the five sample sizes. The first was on the posterior parameter distribution, and the second was on posterior results. The posterior results in this

case are the response of the CO_2 in atmosphere when the posterior parameter distribution is used to run the model into the future, with the application of the aforementioned emissions scenario. The choice of sample size from these comparisons is discussed in the results section.

4.3.5 Likelihood and rejection steps

The model was run using parameter sets from the sampled prior, firstly to steady state, and then from steady state forced with historical emissions. This provided output to use in the likelihood and rejection stages. The data used to inform the model in our study is the pre-industrial concentration of CO_2 in the atmosphere, and the rise in CO_2 between the pre-industrial and year 1990 (when historical emissions have been applied). Therefore we are representing the equilibrium state of the model, and its response to perturbation by anthropogenic CO_2. A probability distribution was estimated for each of the data points, with reference to literature (http://cdiac.esd.ornl.gov/). Pre-industrial CO_2 was assigned a mean of 280ppm, the rise in CO_2 between year 1800 and 1990 a mean of 74ppm, and the standard deviation of both distributions was 8ppm.

The likelihood of getting either of the data points given the model output is found using the probability distribution for that data point, which is then normalised by the maximum likelihood for that data point. However, we are informing our model with two pieces of data; we therefore calculated the likelihood as follows:

$$\log(Combined(L)) = [\log(L_1) + \log(L_2)] - [\log(Max(L_1)) + \log(Max(L_2))]$$

Equation 4-2

Where: L_n = The likelihood of data, given model output, from distribution n.

$Max(L_n)$ = Maximum likelihood from distribution n.

The rejection step compares the log likelihood (L) to a randomly generated number that is also logged (R). Where L>R the parameter sets that generated the output are accepted otherwise they are rejected.

Using this approach we obtained 2 different posterior parameter distributions. The first is when the likelihood was calculated with reference to only the pre-industrial CO_2

concentration (posterior 1, 2215 members). The second was with reference to both the pre-industrial CO_2 concentration, and the rise in CO_2 between year 1800 and 1990 (posterior 2, 637 members). The posterior 1 parameter distribution can yield information about the equilibrium response of the model and posterior 2 for the combined affect of the equilibrium and transient responses. Posterior 1 for parameters and results was also used in selecting a suitable sample size for the study. Apart from its use in selecting a suitable sample size, or examining the effects of the equilibrium accept-reject on the posterior 1 parameter distribution, posterior 1 is not looked at in this chapter.

4.3.6 Computing considerations

Although the model used in this study is relatively efficient, the task of running up to 19200 runs for 200,000 years each is still computationally demanding. In order to run the ensemble the code was ported onto a networked cluster of processors which could run different versions of the model simultaneously. It is important to point out that this is not parallelisation, merely using a cluster to run the model multiple times simultaneously. Extra code was written to allocate different parameter sets to each model version, to store the variables from the steady-state runs and organise them for re-use in the historical emissions runs. Results from both sections of the experiment were then used in the likelihood and rejection steps and the appropriate variables and parameters were set up for use in the future projection part of the study. When the final results from these runs were produced the data had to be extracted from all the parent directories and then analysed. Data matrices were handled using python scripts due to the large and multidimensional nature of the data sets.

4.4 *Results*

4.4.1 Sample Size Selection

We define a suitable sample size as being one where the inclusion of more members made no appreciable difference to the results, or their general character. A sample size of 14400 was chosen based on a comparison of the posterior parameter distributions and the posterior results from five initial sample sizes. We used information from both posterior 1 and posterior 2 to reach this decision.

Sample sizes below 14400 were eliminated based on the parameter distribution for posterior 1 and 2. The cumulative posterior 1 parameter distributions for the five sample sizes show that as the sample size increases, the distribution is converging towards a final specific distribution (Figure 4-1 (a & b) one parameter only). Sample sizes n=600, 2400, 9600, can be seen to be homing in on the final distribution, but inadequately sample the parameter space. The n=14400 and 19200 sample sizes have much more similar distributions. Cumulative posterior 2 parameter distributions for n=14400 and n=19200 are also very similar (Figure 4-1 (c & d), one parameter only).

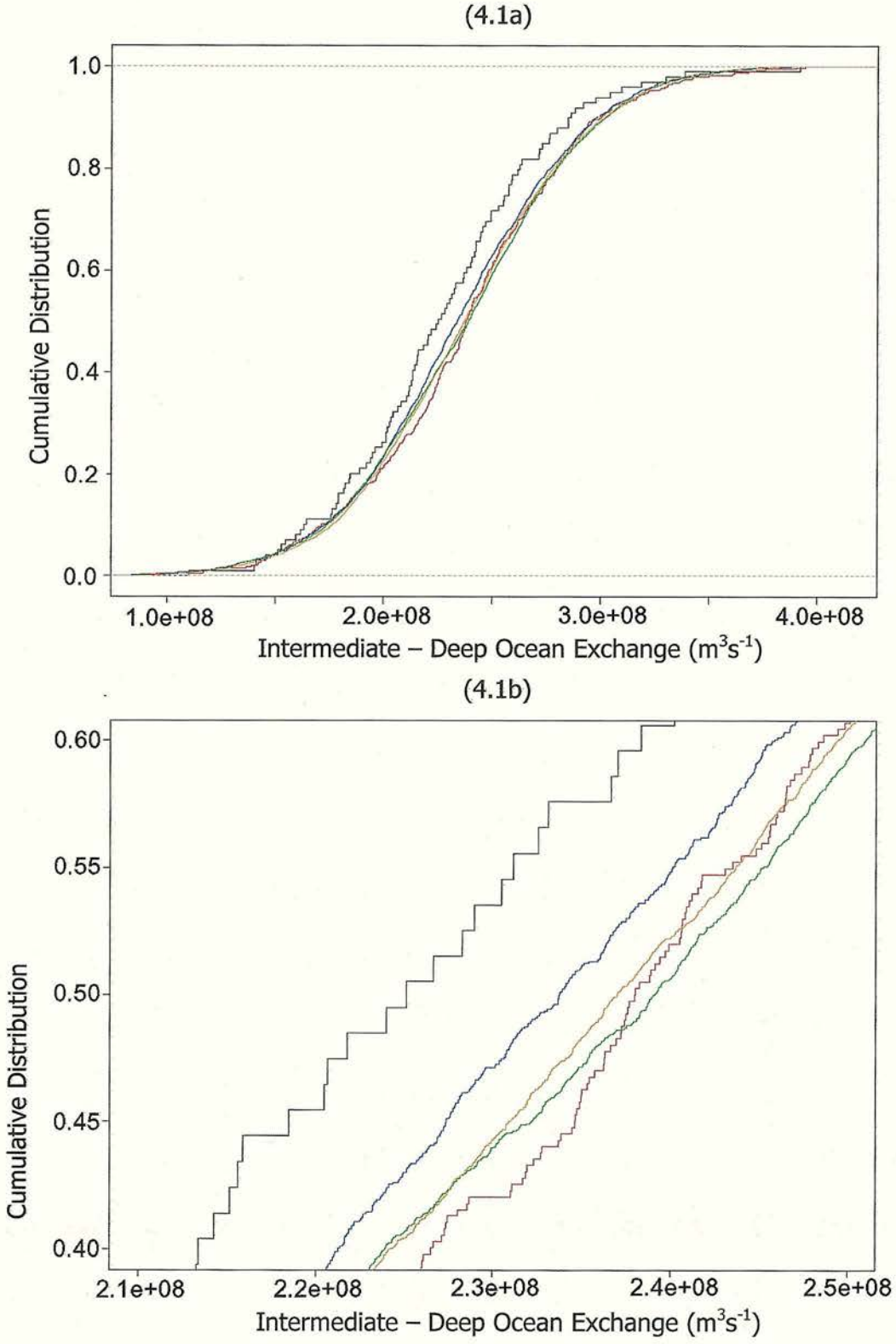

Figure 4-1(a,b): *Cumulative distribution curves for posterior 1, intermediate-deep ocean exchange parameter. Sample size n=600 (black), 2400 (red), 9600 (black), 14400 (green), 19200 (orange). (a) Whole curve (b) Enlarged section.*

(4.1c)

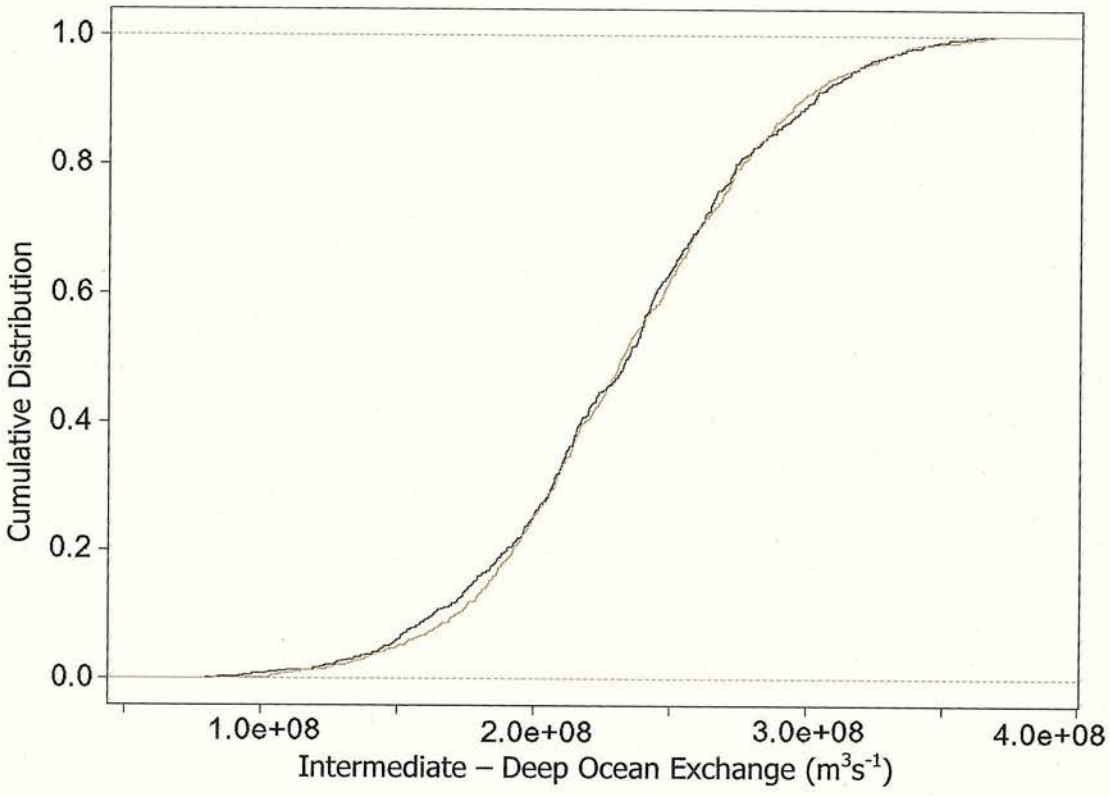

(4.1d)

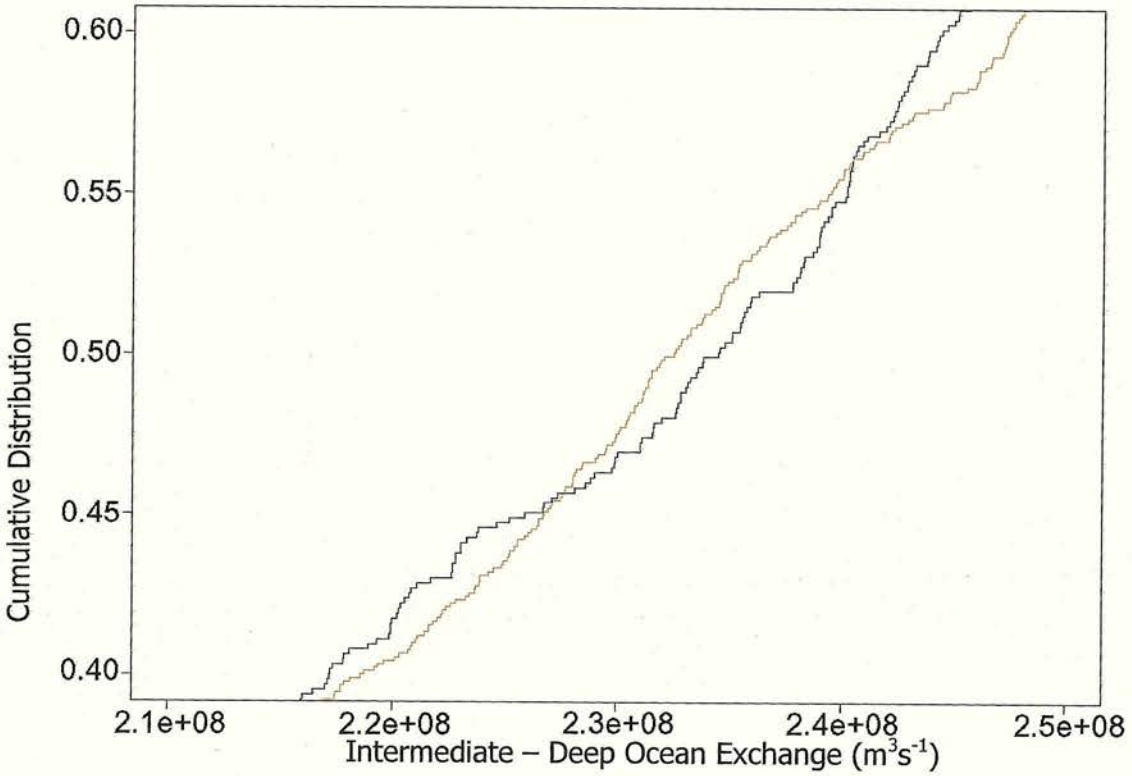

Figure 4-1(c,d): *Cumulative distribution curves for posterior 2, intermediate-deep ocean exchange parameter. Sample size n=14400 (black), 19200 (orange). (a) Whole curve (b) Enlarged section.*

The posterior 2 distribution of peak CO_2 from sample size 14400 does not greatly differ from that of sample size 19200 (Figure 4-2(a)). The mean and variances for the 2 sample sizes vary by only 0.35 and 0.16 % respectively. The distributions can also be seen to be very similar in character, by eye. The difference between the distributions is smaller than the uncertainty we see in each result, which is one measure of whether the sample size is suitable. A comparison of all five sample sizes for posterior 1 peak CO_2 distribution has also been included (Figure 4-2(a)), to illustrate the differences between distributions that can be seen when the sample size is too low.

Figure 4-2: *Peak CO_2 in the atmosphere. (a) Posterior 2, sample sizes n=14400 and 19200. (b) Posterior 1, sample sizes n=600, 2400, 9600, 14400, 19200.*

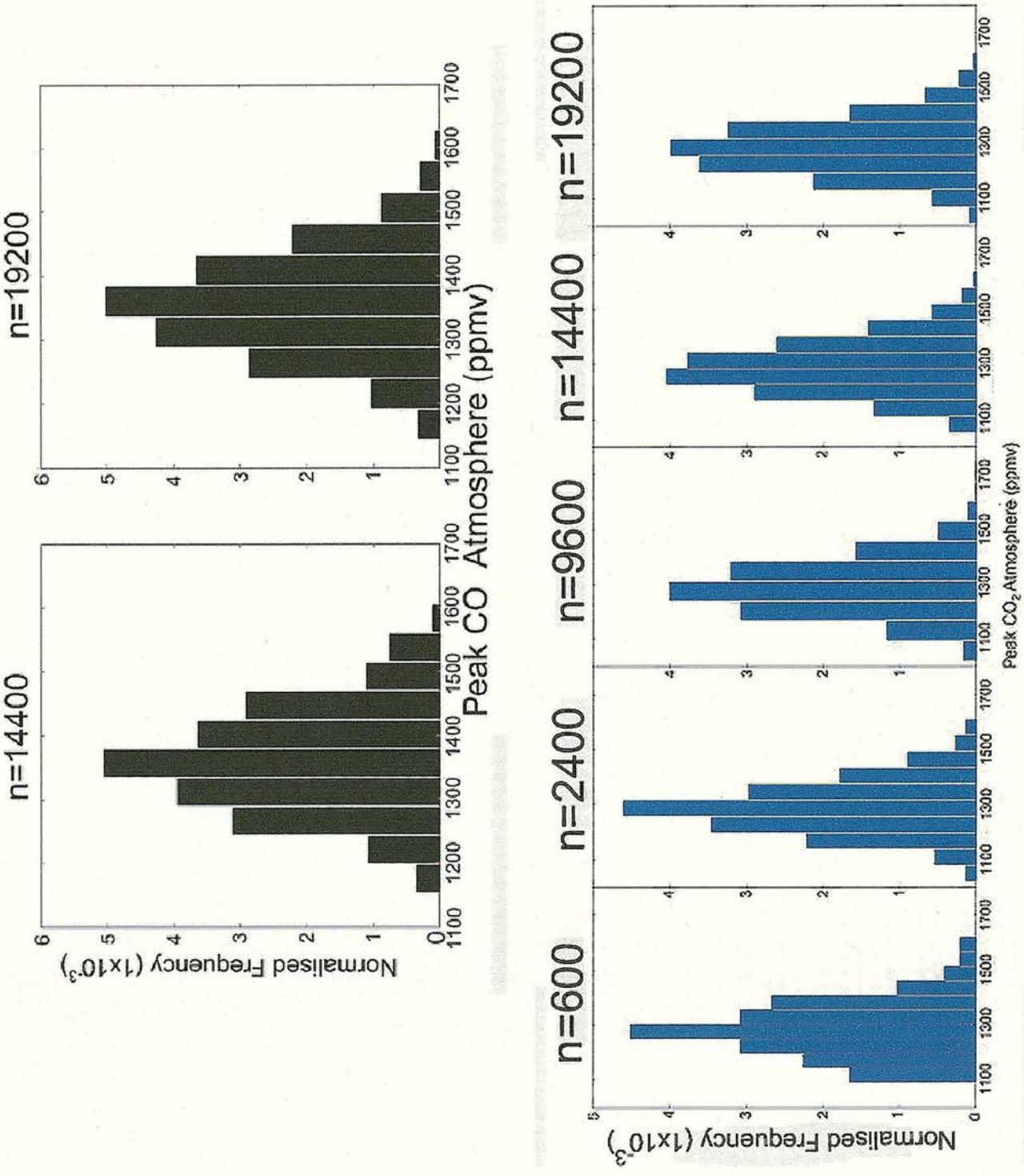

4.4.2 Parameter Calibration

There is a decrease in ensemble members between the prior and posterior 1 and 2, indicating that many of the parameter combinations did not provide a likely response with reference to data. The calibration of the parameters can also be seen in their prior, posterior 1 and posterior 2 distributions (Figure 4-3, selected parameters). The change is not large for many of the parameters (Table 4-2), but the effect of the calibration can still be seen. The effect of calibrating with only the pre-industrial (equilibrium situation), also produces distinctly different results to calibrating with both the pre-industrial and the rise in historical CO_2 (Figure 4-3(b)). Four parameters show very clear effects from the calibration (Figure 4-3), the nutrient utilisation parameter (α) and the river alkalinity flux have posteriors that appear to improve on the prior (Figure 4-3(a & b)). The dissolution parameters however appear not to have been improved by the calibration process (Figure 4-3(c & d)). These parameters are discussed in more detail below.

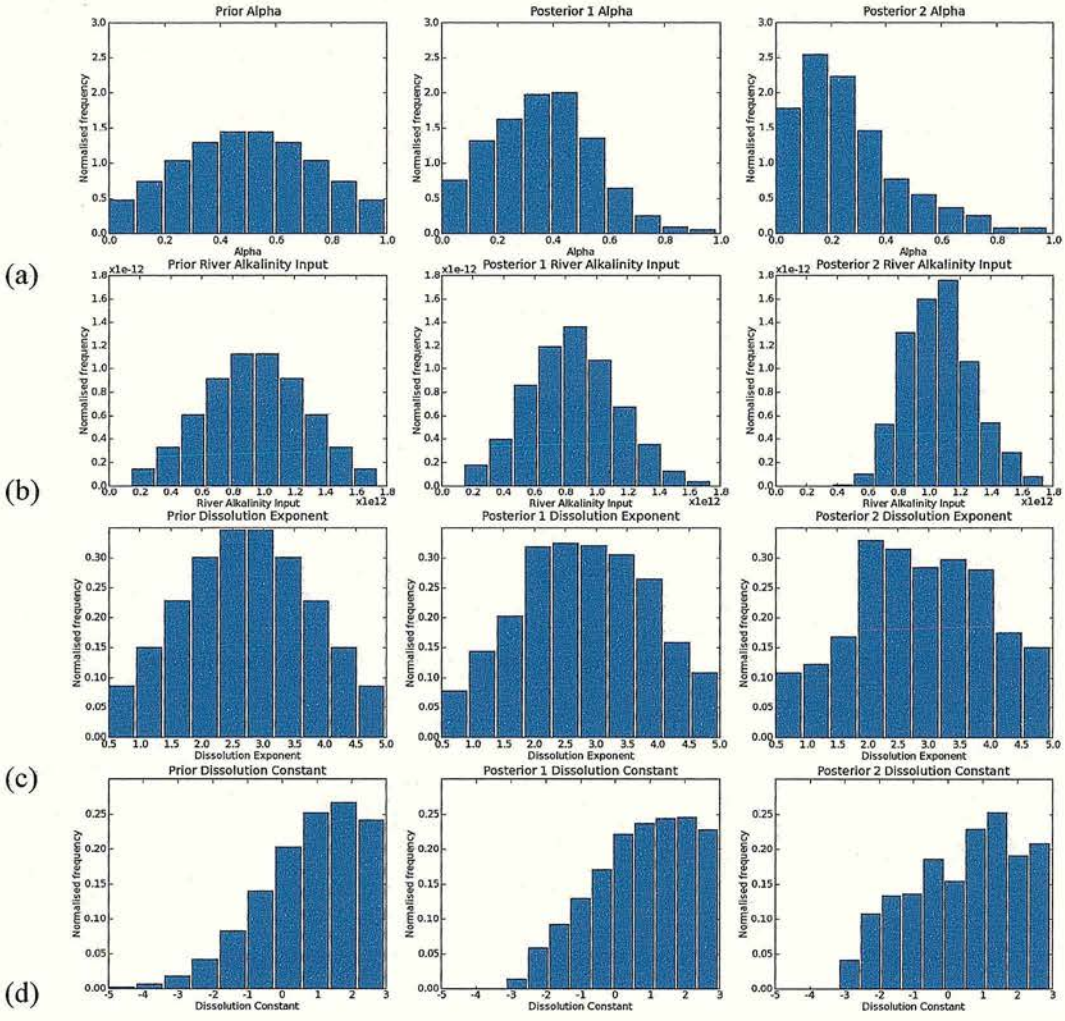

Figure 4-3: Prior, Posterior 1, and Posterior 2 parameter distributions. (a) Nutrient utilisation parameter (α). (b) Flux of alkalinity from the rivers. (c) Dissolution exponent (d) Dissolution constant (logged). For units see Table 4-1.

Table 4-2: *Brief description of the difference between the prior and posterior 1, posterior 1 and posterior 2 for parameters not included in Figure 4-3.*

Parameter	*Difference between prior and posterior 1*	*Difference between posterior 1 and posterior 2*
Piston Velocity	Very slight negative skew	Some negative skew still, definite peak in range 0.15-0.75 (m yr^{-1}).
High Latitude Overturning	Slight positive skew	More defined positive skew
Thermohaline overturning	Very little difference	Definite negative skew
Intermediate – Deep Exchange	Very slight positive skew	More positive skew
Warm-Intermediate Exchange	Decrease in range of values, symmetrically.	Further decrease in range symmetrically.
Salinity	Some symmetrical decrease in range	Tightening of distribution, and symmetrical decrease in range.
Detrital Flux	Little difference	Tightening of distribution, with definite peak at ~1.5×10^{13}-1.8×10^{13} (mol yr^{-1}).

4.4.2.1 Nutrient Utilisation Parameter

Parts of the high-latitude oceans, especially the Southern Ocean, are high-nutrient low-chlorophyll (HNLC) regions, where productivity is limited by the micro-nutrient iron and/or light. Within the model, a macro-nutrient (nitrate) utilisation parameter (alpha, α), determines the fraction of up-welled nitrate that leaves the high-latitude oceans in a sinking flux of organic material. Knox and McElroy (1984) demonstrated the sensitivity of CO_2 in the atmosphere to nutrient utilisation in the high latitudes in a 5-box model, adopting α = 0.01 for the pre-industrial state. We allowed α to vary between 0 and 1, i.e. high-latitude nutrient utilisation could be from 0 to 100%, covering all possibilities for an interglacial or glacial ocean.

Using pre-industrial CO_2 as a selection criterion (Figure 4-3, posterior 1), skews the posterior distribution to lower values. However, values in the range 0.9-1, although a lot less likely, are still acceptable. With both pre-industrial and the anthropogenic rise in CO_2 as selection criteria (Figure 4-3, posterior 2), a negative skew in the distribution is more pronounced, although values in the range 0.8-1 are still possible. Most likely values are found in the range 0.1-0.2, which is still an order of magnitude higher than the 0.01 used previously by Knox and McElroy (1984), Lenton (2000) and Lenton and Britton (2006).

4.4.2.2 River Alkalinity Input

The river alkalinity input derives from rock weathering and here represents the flux which counterbalances the removal of alkalinity by the deposition of sediments in the deep ocean. The output of alkalinity through the building of reefs and shallow carbonates in the shelf seas is assumed constant and the corresponding alkalinity input neglected. Changes in the magnitude of the river alkalinity input flux result in a different carbonate compensation depth at steady-state. We assume that the weathering-sedimentation system is close to steady state in the pre-industrial world. The range of river alkalinity flux ($0.47x10^3$-$5.22\ x10^{13}$ mol/yr) was chosen to span literature values (see Table 4-1).

The pre-industrial CO_2 constraint (Figure 4-3, posterior 1), slightly skews the distribution to lower values, and tightens it up a little. However, adding the anthropogenic rise in CO_2 as a selection criterion (posterior 2), shifts the distribution in the opposite direction and makes it a lot tighter. It was suspected that the alkalinity input is setting the steady-state concentration of alkalinity in the ocean, and that this in turn is affecting the CO_2 uptake but this is not the case - plotting river alkalinity flux against the steady-state alkalinity within the ocean shows no correlation. This suggests that the magnitude of the alkalinity flux itself plays a direct role in the transient decadal to centennial timescale response of the ocean carbon sink, rather than and indirect role through its effect on the equilibrium state of the ocean.

4.4.2.3 Dissolution Parameters

The dissolution constant and exponent govern the level of dissolution in the model, for a given change in chemistry (Chapter Two), given by:

$$Dissolution = CaCO_3 \times \chi(1-\Omega)^{\varepsilon} \qquad \textbf{Equation 4-3}$$

Where: χ=dissolution constant, Ω=saturation state of water, ε=dissolution exponent

Increases in either of these values will then result in higher dissolution. A literature search revealed that the values chosen by other modellers, and those from experimental studies, vary widely, therefore the range we specified for the prior was quite large. In the case of the dissolution constant we assigned a log normal distribution for the prior (unlike the normal distributions chosen for all other parameters). This allowed the inclusion of a large range of values, but a larger concentration of the sampling in an area of values that were often used in other studies.

The posterior 1 distribution for the dissolution exponent has a wider distribution, and is much less peaked, the four most central ranges having very similar normalised frequencies (Figure 4-3(c)). Posterior 2 has an even wider distribution, it is very difficult to tell what the overall trend is of this distribution. In other studies a dissolution exponent of 4.5 has been used (Keir 1980, Archer 1996). The posterior 2 distribution does show 4.5 to be more likely than it is defined in the prior, but it is not the most likely value in the study.

The dissolution constant posterior 1 distribution eliminates the possibility of some of the lower part of the range assigned in the prior. However, the rest of the distribution has widened rather than tightened. Posterior 2 has an unusual distribution, it could be tending towards a uniform distribution, but we cannot say that with any certainty. The range remains the same between posterior 1 and posterior 2. A value of 20% per day has been used in previous work (Lenton and Britton 2006, Berelson et al. 1994). This value does not seem to correspond with any well defined peak in the distribution.

The failure to constrain the dissolution parameters may suggest that (in the context of this study and data used) these parameters are not having a large effect on the model response. However, what is more likely is that the data points chosen were not informative for the parameters; this could be due to the choice of data point or the length of time over which the calibration is made. The data has however had some effect, otherwise the experiment would have returned the same prior. Although we have done our best to ensure that the sample size is large enough, it is also possible that if the posterior was sampled more (i.e. a larger number of ensemble members survived the accept-reject stage) then it would be easier to see what the posterior distributions were tending towards. In terms of the equilibrium response of the model, net preservation has to balance the river alkalinity flux. Plotting the posterior parameter values of river alkalinity against the dissolution exponent or dissolution constant

'Uncertainty in atmospheric CO_2 recovery from fossil fuel perturbation due to the ocean-sediment system'
shows no correlation. Perhaps the river alkalinity is the dominant control on the equilibrium system.

4.4.3 Comparison to historical data

Comparing model output to the rise in CO_2 between the pre-industrial and year 1990 effectively constrains the historical ocean uptake of CO_2 and the net ocean-atmosphere CO_2 exchange flux within the model, because parameters controlling land uptake of CO_2 are kept fixed. There is some variation in historical land uptake of CO_2 and net land-atmosphere CO_2 exchange flux because the ocean sink and consequently atmospheric CO_2 are permitted to vary somewhat. Figure 4-4 shows the rise in atmospheric CO_2, land-atmosphere CO_2 exchange and net ocean-atmosphere CO_2 exchange over years 1800-2000.

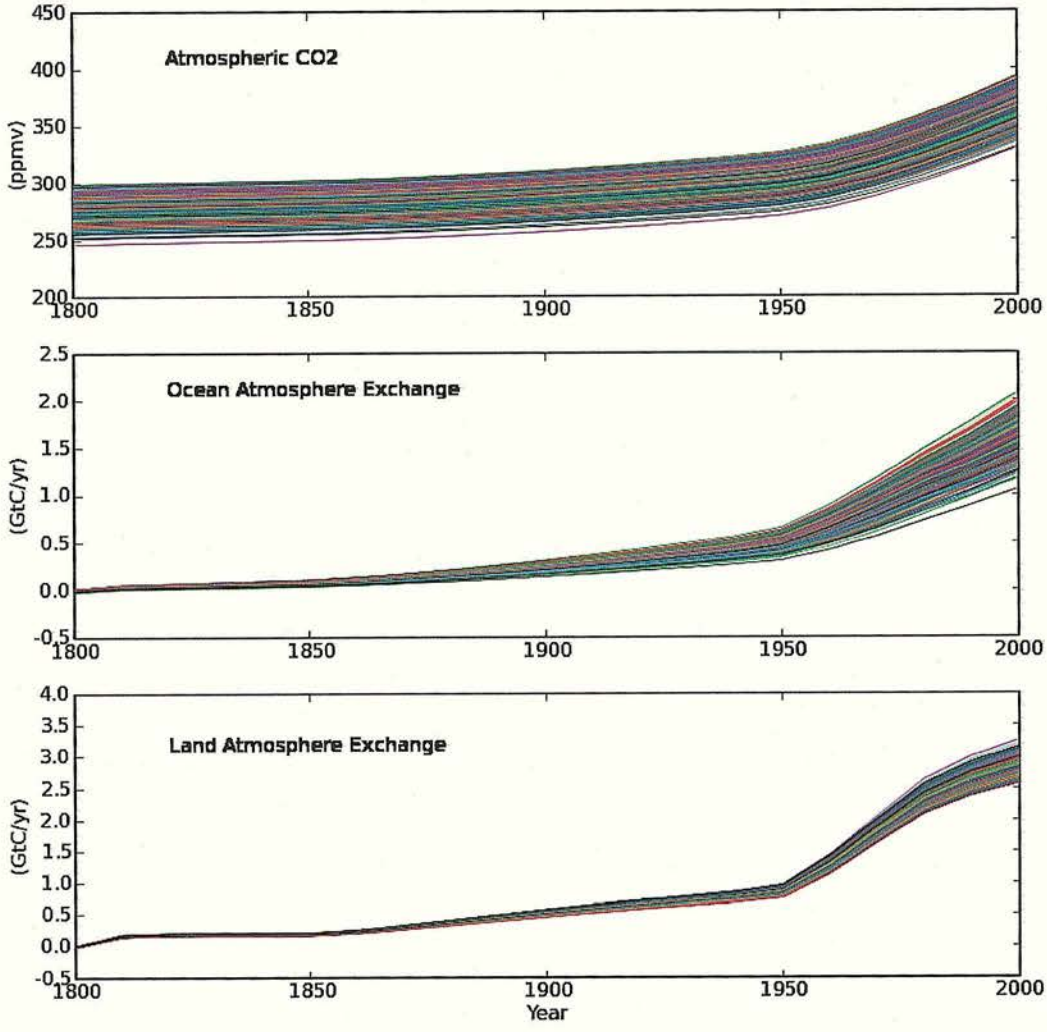

Figure 4-4: *Atmospheric CO_2, Land-Atmosphere Exchange and Ocean-Atmosphere exchange for posterior 2.*

In year 1990 the model has a mean ocean carbon sink of ~1.4 GtC yr^{-1} with a range of ~0.9-1.8 GtC yr^{-1}. This is somewhat below the observationally constrained estimates of 1.8 ± 0.8 GtC yr^{-1} for the 1980s (House et al. 2003) and 1.9 ± 0.7 GtC yr^{-1} for the 1990s (Le Quere et al. 2003). The upper end of the model ensemble roughly corresponds with the mid point of the observational estimates. This is because the model land carbon sink is rather strong at 2.2-2.8 GtC yr^{-1} for the 1980s and 2.4-3.1GtC yr^{-1} 1990s. The model tends to generate a strong land carbon sink and our fixed parameter choices for the land (from previous work)

are maintaining this. Thus our future projections start with a pessimistic view of the strength of the ocean carbon sink and an optimistic view of the strength of the land carbon sink.

4.4.4 Future Projections

The uncertainty in the response of the model, due to parameter choice, varies considerably with time (Figures 4-5 & 4-6). An initially quite well constrained system (probably due to our selection process), widens in its uncertainty as it approaches peak CO_2, this broad uncertainty continues during the initial drawdown of CO_2, until year 2450. Beyond this point as time progresses, the uncertainty decreases. After the year 10,000 the CO_2 concentration in each of the members of the ensemble reaches a plateau, however the range of times over which this occurs is in the order of $\sim 10^4$ years. Finally, the uncertainty in atmospheric CO_2 at year 100,000 is similar to but slightly larger than that of the range of equilibrium starting positions (Figure 4-6). A breakdown of the results by timescale and other factors is now presented.

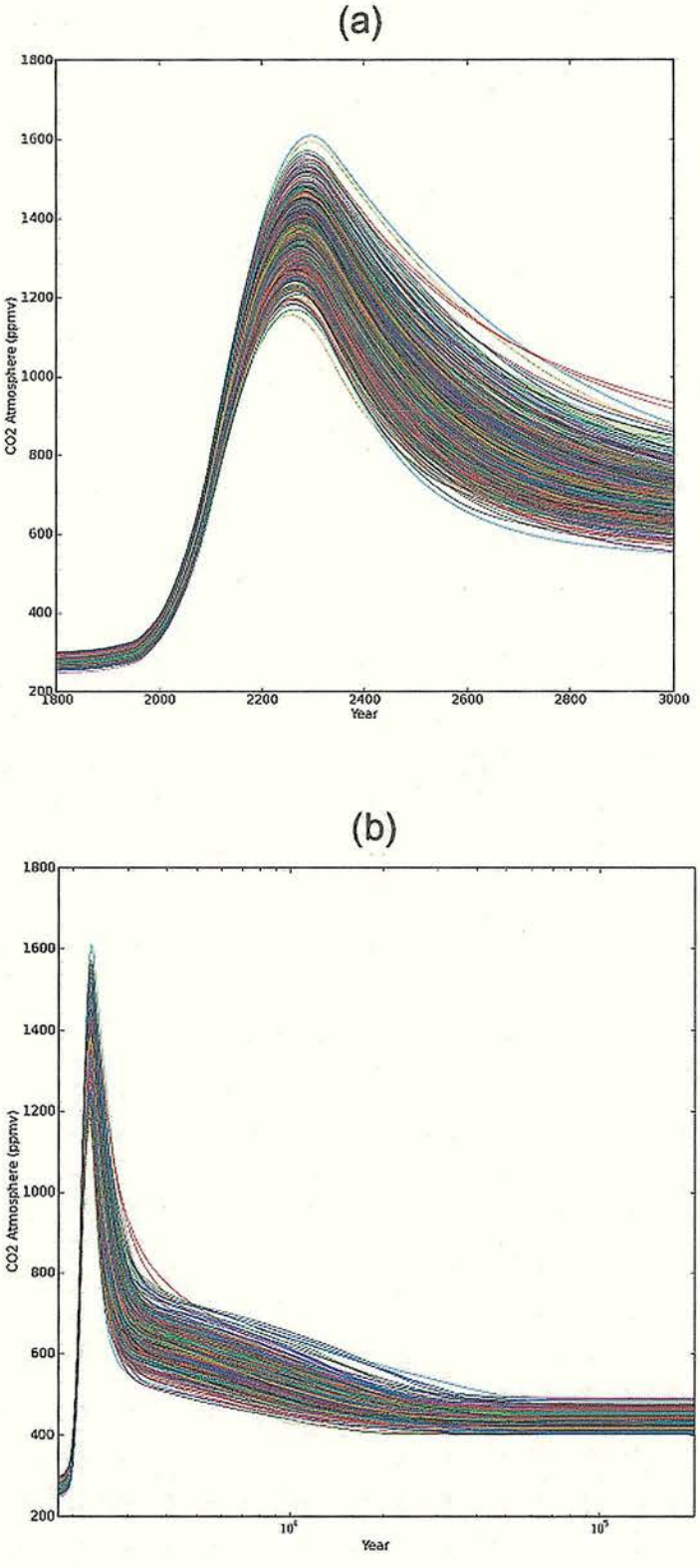

Figure 4-5: *CO_2 concentrations in the atmosphere with time, posterior 2, (a) year 1800 to 3000 (b) year 1800 to 200,000, log timescale.*

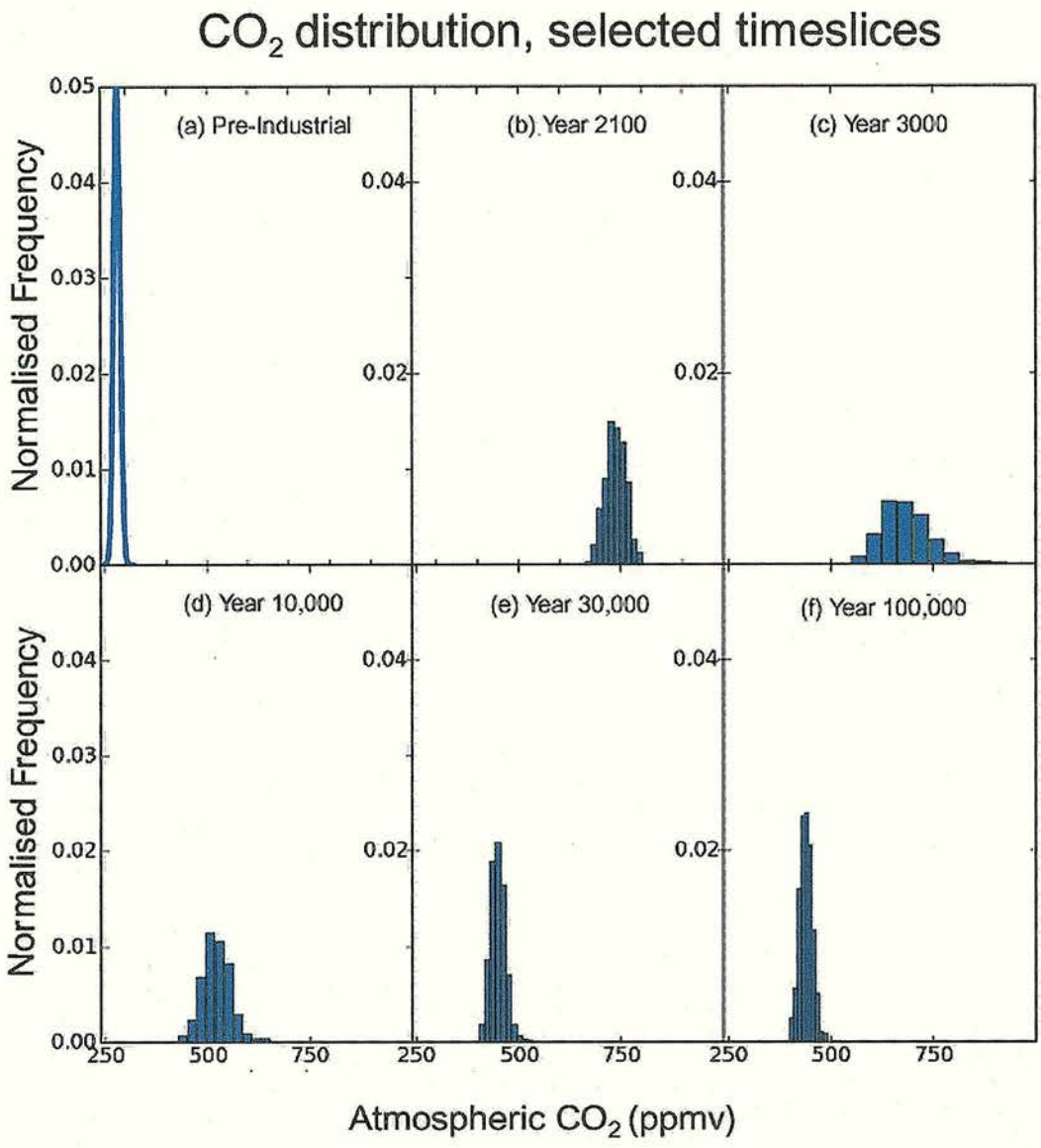

Figure 4-6: *(a) Probability distribution curve for the pre-industrial CO_2 data used in the accept-reject scheme. (b-f) Posterior 2, CO_2 concentrations at selected timeslices, (year 2100, 3000, 10000, 30000, 100000).*

4.4.4.1 Century timescale

Many climate studies focus on the effects of the anthropogenic emissions in the next 50-100 years, as this is a timescale to which humans can relate. The present model is not intended as a predictive tool for the next century, but the results that it gives for this time period still

merit attention. The uncertainty in the concentration of atmospheric CO_2 (due only to ocean and sediment parameters) increases from ~60ppmv in 1990 to ~140ppmv in year 2100, primarily because of variation in ocean uptake. The ocean carbon sink in year 2100 varies by a factor of ~2 from ~3.1-6.2 GtC yr^{-1}. It has been calibrated to a certain degree by the comparison-to-data stage, but while the flux in year 2100 is positively correlated with that in 1990 (not shown), there is also considerable scatter. The variation in the ocean sink is primarily due to the ocean circulation parameters k_T and k_U, which control the strength of the solubility pump. The land carbon sink has peaked and is declining by 2100 with a range of ~1.4-2.7 GtC yr^{-1} due primarily to the variation in atmospheric CO_2 and corresponding global warming. The land-atmosphere sink is therefore responding to the variation in the ocean sink.

4.4.4.2 Peak CO_2

Beyond the year 2100, atmospheric CO_2 across the ensemble diverges much more widely, with the peak CO_2 concentration ranging by ~450ppmv over 1155-1609 ppmv. The timing of the peak also varies and is correlated with the peak concentrations. Lower peaks occur earlier, higher peaks later, as the sinks finally outweigh the sources. These dynamics are controlled by the ocean carbon sink, with the lowest peak CO_2 corresponding to the strongest ocean sink ~7.6 GtC yr^{-1} and the highest peak CO_2 to the weakest ocean sink, ~3.6 GtC yr^{-1}. Cross plots of initial parameter values versus peak CO_2 indicate that the thermohaline and overturning fluxes (K_T and K_U) are negatively correlated with peak CO_2 in the atmosphere (Figure 4-7), because these parameters control the strength of the solubility pump. The land is a carbon source at the time of peak CO_2 of 0.4-0.56GtC yr^{-1}, thus contributing to the peak.

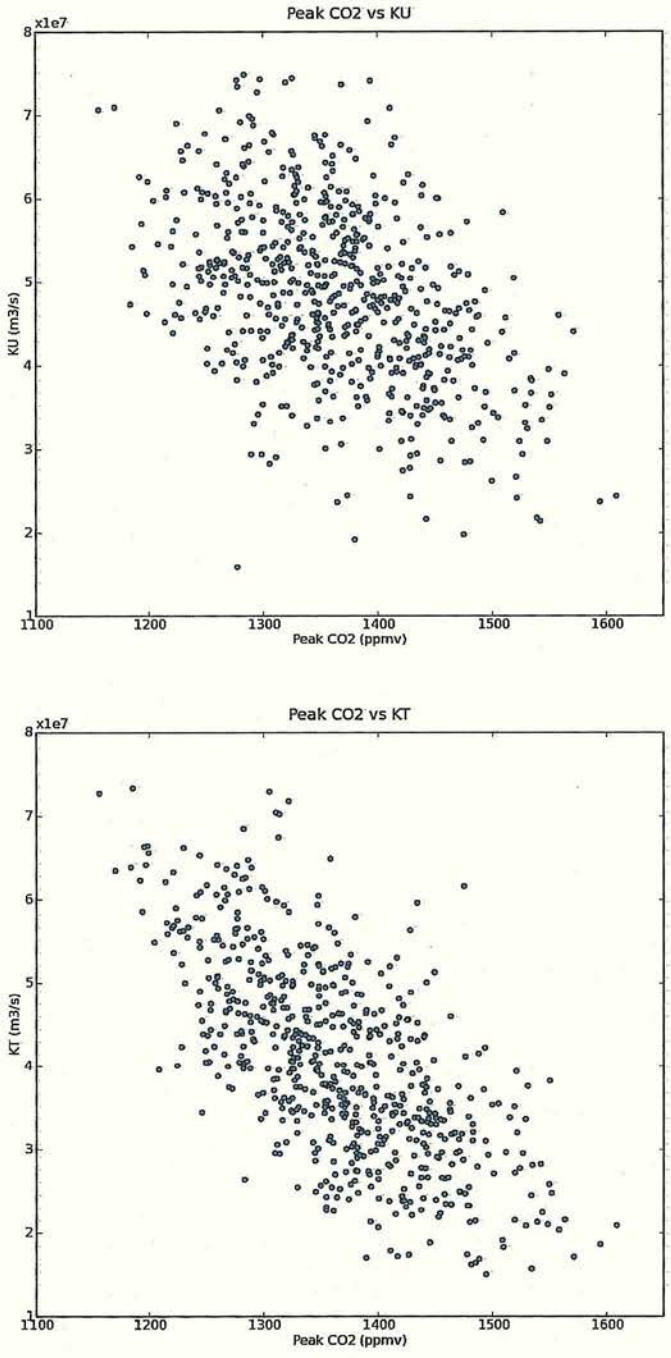

Figure 4-7*: Scatter plot of parameters KU and KT against Peak CO_2.*

4.4.4.3 Millennial timescale

After the peak in CO_2, the range in atmospheric CO_2 continues to diverge, with a maximum range occurring around year 2450. Atmospheric CO_2 has a range of ~550-930ppmv in year 3000, which is somewhat smaller in absolute terms than the range in the peak, but greater in relative terms. The range of possible CO_2 values at year 3000 is slightly skewed to lower values and the airborne fraction of added CO_2 (Figure 4-8) ranges over 14-31% in year 3000. Atmospheric CO_2 is still declining in all ensemble members at year 3000, due to dissolution of carbonate sediments driving an ongoing ocean carbon sink that ranges from ~0.1-1.0 GtC yr^{-1}. Land-atmosphere CO_2 exchange is close to equilibrium on the millennial timescale ranging from -0.1-0.1 GtC yr^{-1}. After year 3000, atmospheric CO_2 and the absolute range in its uncertainty continue to decrease over time.

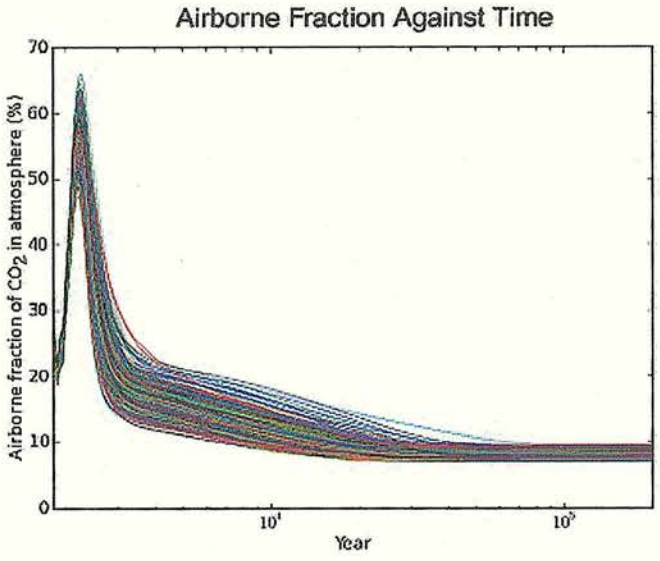

Figure 4-8: *Airborne fraction of emissions with time (the difference between pre-industrial CO_2 and current CO_2 as a fraction of total emissions) for posterior 2. The time is on a logged axis.*

4.4.4.4 Longer timescales

Beyond the millennial timescale, the continuing drawdown of atmospheric CO_2 is due to the dissolution of carbonate sediments, the replenishment of the ocean with alkalinity, and the eventual recovery of the sediments. All ensemble members eventually reach a stable atmospheric CO_2 on the 10^5 year timescale, because we have excluded the effect of variable

silicate weathering. By year 10,000, atmospheric CO_2 is a mean of 523ppmv corresponding to an airborne fraction of 8.5-18%, in year 30,000, CO_2 is as mean of 441ppmv and airborne fraction 7.1-12.6%, and in year 100,000 CO_2 is a mean of 441ppmv (90ppmv range) and airborne fraction 7-9.6% (Figures 4-5 & 4-6). Thus, over 10^4-10^5 years, both the absolute and relative uncertainty in CO_2 decrease along with the actual concentration. Much of the response can be seen by the year 30,000, but there is some change over the next 70,000 years, in particular the skew to lower values (seen in all three time-slices), is somewhat reduced (Figure 4-6). The distribution in uncertainty of atmospheric CO_2 at year 100,000 has a similar range to the one set for the pre-industrial for the accept-reject stage (80ppm), but it is much less tight.

4.4.4.5 Time to approach stabilisation

The time taken for CO_2 to stabilise clearly varies considerably across the ensemble (Figures 4-5 & 4-7). We used a value of 0.001ppm yr^{-1} variation in atmospheric CO_2 to define a 'quasi-equilibrium' concentration of atmospheric CO_2, this was decided in reference to the maximum change of 0.002ppm yr^{-1} that is seen in the Holocene prior to year 1800. It is not a true equilibrium as the CO_2 in the atmosphere was still varying (if only slightly) in many of the runs. However, given that we have neglected long term processes such as silicate weathering it is a reasonable criterion. The uncertainty in the time taken to reach 'quasi-equilibrium' is year 13,000-57,000 (Figure 4-9) with a mean value of ~year 28,000, there is also a distinct skew to lower values.

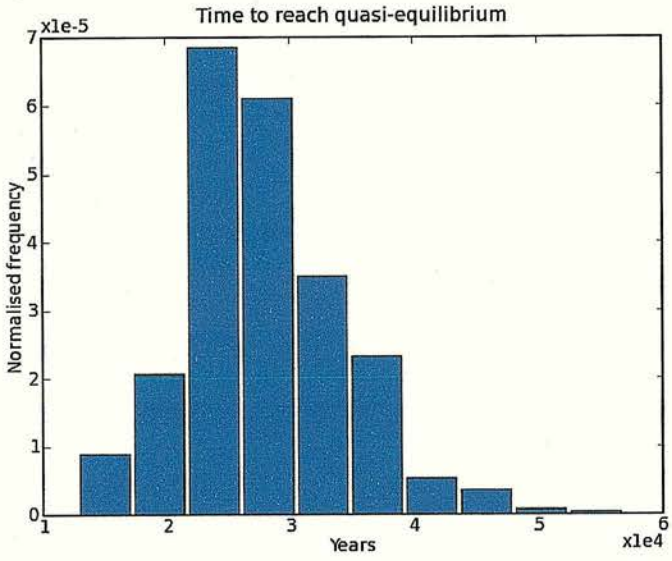

Figure 4-9: *Histogram of time to reach quasi-equilibrium for posterior 2.*

Comparing the initial parameter values against the time to quasi-equilibrium (not shown) indicates weak negative correlations with the thermohaline circulation parameter K_T, and the river alkalinity flux. The parameter (K_{id}) controlling the ocean exchange flux between the intermediate and the deep also seems to be positively correlated, although this is very weakly. An increased river alkalinity flux would help the buffering of CO_2 in the atmosphere, by the ocean and sediments, and the thermohaline circulation could help to move this alkalinity more effectively, meaning the system can reach stabilisation in a shorter space of time. Why the intermediate to deep flux would be positively correlated with time to stabilisation is less obvious. A positive link is visible between the peak CO_2 reached in the atmosphere and the time that it takes to reach quasi-equilibrium, however, it is not highly correlated and therefore other factors are affecting the system.

4.4.4.6 CO_2 Offset

Atmospheric CO_2 does not return to the pre-industrial concentration because the silicate weathering cycle is ignored in this version of the model. The final concentration of CO_2 in the atmosphere in year 200,000 is positively correlated with that in year 1800 (Figure 4-10), with a positive offset that increases with increasing initial CO_2 concentration. The distribution of the CO_2 offset is skewed to the lower values, and ranges over 146-199ppmv. Its normalised frequencies are also an order of magnitude higher than for all the other data presented so far. The most likely offset in CO_2 seems to be in the range 155 to 160ppmv.

There may be some negative correlation between the river alkalinity flux and the CO_2 offset seen in the course of each run.

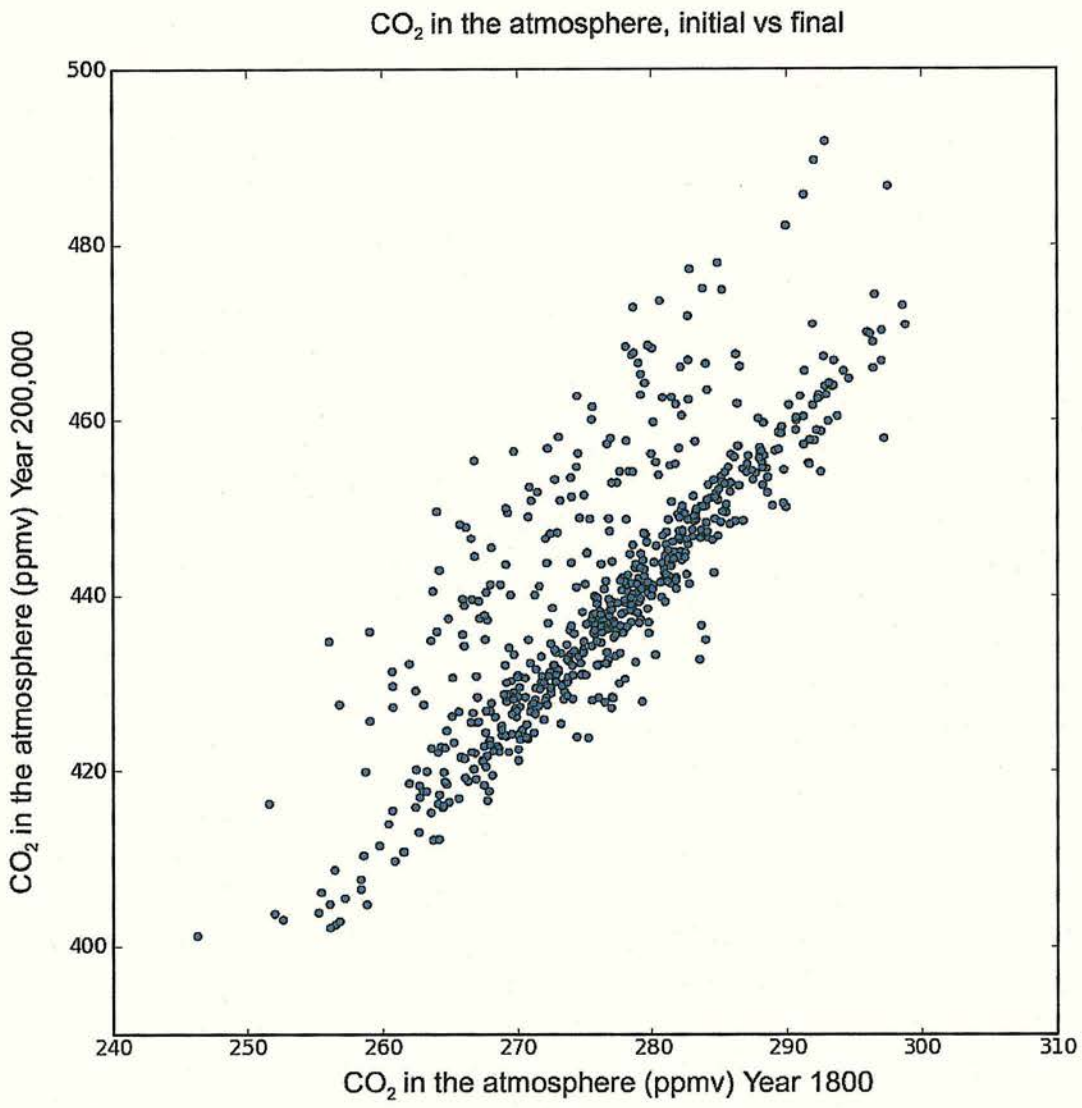

Figure 4-10: *Initial CO_2 concentrations in the atmosphere plotted against the concentration at quasi-equilibrium*

4.5 *Discussion and Conclusions*

This is the first study of this nature using this model, and we therefore limited the data used to calibrate the parameters, and the parameters varied, in order to demonstrate and clarify the

method. We see this study as the first in a series of studies where the elements that are varied increase stepwise. The land-atmosphere and ocean-atmosphere exchange fluxes are well studied, and could have provided another set of calibration data. A comparison to the historical record shows that our model still has a weaker ocean sink, and stronger ocean sink than observations would suggest. The ocean sink will have been constrained by the rise in CO_2 between year 1800 and 1990 criterion, but through the atmosphere the land-atmosphere exchange is still affecting the system. The parameters within the land system have not been varied here, so no improvements in this area could be made. Future studies should allow the land parameters to vary, and perhaps use land-atmosphere fluxes as a data constraint.

A sample size of 14400 was deemed suitable for this study, and it yielded 2215 members after comparison to one data constraint, and 637 after comparison to two data constraints. The posterior results from sample size 14400 and 19200 were very similar, as were the cumulative distribution curves for the posterior parameter distribution. However, it is difficult to know where to draw the line regarding the similarity of distributions.

Although the posterior parameter distributions (both posterior 1 and 2) differ from the prior distributions, the difference is not large in many of the parameters. In those cases calibration due to data has been minimal. This is still a useful exercise in terms of understanding the model behaviour. However, it may be that if different data were included to calibrate the model, then more of an effect may be seen in the other parameters. There were distinct differences seen in the nutrient utilisation parameter (α), and the river alkalinity flux. A smaller difference was seen in the dissolution exponent and constant, where the distributions appeared to be less well defined after the calibration process. This may be due to the data chosen for calibration or (less likely) the sample size chosen for the study. In future work it would be useful perhaps to include a data point for calibration which captures the strength of the dissolution response of the sediments to the chemical changes within the ocean brought about by increased CO_2 in the atmosphere.

Pre-industrial atmospheric CO_2 and the anthropogenic rise in CO_2 are particularly sensitive to the effectiveness of biological nutrient uptake in the high-latitudes (α), which determines the strength of the biological carbon pump. The 'most likely' posterior value for α that emerges is much higher than that used in past studies (Knox and McElroy 1984, Lenton 2000, Lenton and Britton 2006). Pre-industrial CO_2 and the anthropogenic rise in CO_2 are also sensitive to the river flux of alkalinity, possibly due to the transient effects on the ocean

sink, from higher values of this flux. The 'most likely' posterior value is greatly above the mid-point of the prior range suggested by literature values.

The most likely peak CO_2 from this study, 1363ppmv, is much lower than in existing work with the same model (Lenton and Britton 2006), 1596ppmv, which is close to the upper limit of the range in this study. This indicates that we have improved the strength of the ocean sink with our parameter calibration. However mean peak CO_2 from this study still remains above that from a previous version of the model (1229ppmv) without sediments (Lenton 2000) and during the historical interval our current ocean-sink is weaker than observations. Therefore it would be preferable to improve the strength of the ocean-sink further in future studies. Peak CO_2 is clearly sensitive to certain parameters, as strengthening the thermohaline circulation (K_T) or the mixing between the high-latitude surface ocean and the deep ocean (K_U) strengthens the ocean carbon sink and lowers peak CO_2. (K_T) is acting via strengthening the solubility pump, (K_U) by strengthening the biological pump.

Although the uncertainty in CO_2 grows somewhat over this century, much the largest variation occurs beyond the century timescale, reaching a maximum around the year 2450. It is on this timescale that increases in CO_2 and temperature will have an effect on the stabilisation of ice-sheets, such as in Greenland (Alley et al. 2005). Modelling predictions (Alley et al. 2005) suggest that if the atmosphere stabilises at 1000ppmv then the Greenland ice-sheet will largely have melted by the year 5,000, but that even with stabilisation at 550ppmv the ice-sheet will still melt, but at a slower rate. The melting of such ice-sheets causes sea-level rise, therefore reducing uncertainty on this timescale would be highly beneficial to future predictions of climate change, however that is not the focus of this study. The variation in atmospheric CO_2 from this study in 2100 is smaller than for the following 20,000 years. We are therefore more able to accurately predict the long term response of the Earth system to anthropogenic perturbations, than peak atmospheric CO_2 or its initial drawdown later this millennium.

Archer (2005) has also modelled the decay of the airborne fraction over timescales of 10^3-10^5 years. At year 3000, for our total emissions, we estimate that Archer's model would give an airborne fraction of ~32%, at the upper end of our range of 14-31%. Our lower values arise because of the tendency for more aggressive dissolution of carbonate sediments in our model on the millennial timescale (Chapter Two, also Lenton and Britton 2006) whilst they dissolve more slowly in Archer's model. Archer (2005) considers four different emissions

scenarios, totalling 300-5000 GtC, which spans the range from known historical emissions to total known conventional fossil fuel reserves. The corresponding range in airborne fraction at year 3000 is 14-34%, similar to what we have found, merely due to parameter variation, with one emissions scenario. Thus the uncertainty in millennial timescale airborne fraction due to ocean-sediment parameter uncertainty is comparable with that due to uncertainty in total emissions.

With interactive sediments but in the absence of silicate weathering, Archer (2005) has shown that the airborne fraction of CO_2 continues to decline beyond year 10,000 (although this is misrepresented in his Table 1 – as the values given for year 10,000 and year 100,000 are the same, indicating equilibrium has been reached by year 10,000). For 5000 GtC emitted Archer (2005) predicts an airborne fraction of 17.5% at year 10,000, again at the upper end of our range here. By year 100,000 our airborne fraction has dropped to 7-9.5%, giving a more optimistic long-term prognosis than Archer (2005). However, we see a large range in the time taken for CO_2 to reach 'quasi–equilibrium' from year 13,000 to 57,000. This includes values that are both much shorter and much longer than the ~35kyr suggested by Archer (2005). Hence the recovery from anthropogenic CO_2 perturbation could be either much faster or slower than previously predicted. The concentration of CO_2 at stabilisation also ranges over 91ppmv, which is greater than the range originally chosen for the pre-industrial CO_2 concentration likelihood curve. CO_2 in the atmosphere does not return to pre-industrial concentrations, as this model version does not include variable silicate weathering. Allowing weathering fluxes (carbonate and silicate) to vary within the model will tend to speed the recovery (Chapter Three, also Lenton and Britton 2006), and draw CO_2 to much lower concentrations. Including that interaction will be the subject of the next chapter.

The long lifetime of anthropogenic CO_2 is well known to carbon cycle modellers, although it is still not fully appreciated by policy makers. Previous studies have shown how the airborne fraction of added CO_2 varies over time and how it depends somewhat on total CO_2 emissions (Walker and Kasting 1992, Archer et al. 1998, Archer 2005, Lenton and Britton 2006). Here we have demonstrated its sensitivity to uncertainties in ocean and sediment parameters. Although the pre-industrial CO_2 concentration and the anthropogenic rise in CO_2 constrain the model parameters somewhat, there is still a sizeable spread in the ensemble when projecting into the future with a fixed emissions scenario.

4.6 *References*

Alley, R.B. et al., Ice-sheet and sea-level changes, *Science (310),* 5747: 456-460, 2005.

Amiotte-Suchet, P., J.-L. Probst, and W. Ludwig, Worldwide distribution of continental rock lithology: Implications for the atmospheric/soil CO_2 uptake by continental weathering and alkalinity river transport to the oceans, *Glob. Biogeochem. Cycl. 17*, 1038, 2003.

Archer, D., Modelling the calcite lysocline, *Journal of Geophysical Research, 96*, 17037-17050, 1991.

Archer D, A data-driven model of the global calcite lysocline, *Glob. Biogeochem. Cycl.* 10, 511-526, 1996.

Archer, D. Fate of fossil fuel CO2 in geologic time, *Journal of Geophysical Research (Oceans)*, doi:10.1029/2004JC002625, 2005.

Archer, D. E. & E. Maier-Reimer, Effect of deep-sea sedimentary calcite preservation on atmospheric CO_2 concentration, *Nature, 367,* 260-264, 1994.

Archer, D., H. Kheshgi, & E. Maier-Reimer, Dynamics of fossil fuel CO2 neutralization by marine CaCO3, *Glob. Biogeochem. Cycl. 12*, 259-276, 1998.

Barnett, David N., Simon J. Brown, James M. Murphy, David M. H. Sexton, Mark J. Webb. Quantifying uncertainty in changes in extreme event frequency in response to doubled CO_2 using a large ensemble of GCM simulations. *Clim. Change, 26,* 489–511, 2006.

Berelson, W. M. D. E. Hammond, J. McManus, and T. E. Kilgore, Dissolution kinetics of calcium carbonate in equatorial Pacific sediments, *Glob. Biogeochem. Cycl. 8*, 219-235, 1994.

Berthelot, M., P. Friedlingstein, P. Ciais, P. Monfray, J-L. Dufresne, H. Le Treut, L. Fairhead, Global response of the terrestrial biosphere to CO_2 and climate change using a coupled climate-carbon cycle model, *Glob. Biogeochem. Cycl.,10,* 2002.

Boyle, E.A, Oceanic salt switch. *Science*, **298**: 1724–1725, 2002.

Challoner, P.G., in: Avoiding dangerous climate change *(eds. Joachim Schellnhuber, Wolfgang Cramer, Nebojsa Nakicenovic, Tom Wigley, Gary Yohe), Cambridge University Press,* 2006.

Cox, P. M. R. A. Betts, C. D. Jones, S. A. Spall, and I. J. Totterdell, Acceleration of global warming due to carbon-cycle feedbacks in a coupled climate model, *Nature, 408,* 184-187, 2000.

Chib, S. and E. Greenberg, Understanding the Metropolis–Hastings algorithm, *American Statistician 49,* 327–335, 1995.

Dufresne, J-L., P. Friedlingstein, M. Berthelot, L. Bopp, P. Ciais, L. Fairhead, H. Le Treut, P Monfray, Effects of climate change due to CO_2 increase on land and ocean carbon uptake, *Geophysical Research Letters, 29,* 2002.

Friedlingstein, P., L. Bopp, P. Ciais, J-L. Dufresne, L. Fairhead, H. Le Treut, P. Monfray, J. Orr, Positive feedback between climate change and the carbon cycle?, *Tellus, 55,* 692-700, 2001.

Gaillardet, J., B. Dupre, P. Louvat, C.J. Allegre, Global silicate weathering and CO_2 consumption rates deduced from the chemistry of large rivers, *Chem. Geol., 159(3),* 1999.

Hallgren, W. S., & A. J. Pitman, The uncertainty in simulations by a global biome model (BIOME3) to alternative parameter values, *Global Change Biol., 6,* 483– 495, 2000.

Houghton, J.T., Y. Ding, D.J. Griggs, M. Noguer, P.J. van der Linden and D. Xiaosu (Eds.), *Climate Change 2001: The Scientific Basis, Cambridge University Press,* 2001.

Houghton R.A., & J.L. Hackler, Carbon flux to the atmosphere from land-use changes. Trends: a compendium of data on global change. *Tech. rep., Carbon Dioxide*

Information Analysis Center, Oak Ridge National Laboratory, Oak Ridge, Tenn., USA, 2002.

House, J. I. I. C. Prentice, N. Ramankutty, R. A. Houghton, and M. Heimann, Reconciling apparent inconsistencies in estimates of terrestrial CO2 sources and sinks, *Tellus B, 53B*, 345-363, 2003.

Keir, R.S., The dissolution kinetics of biogenic calcium carbonates in seawater, *Geochimica and Cosmochimica Acta, 44,* 241-252, 1980.

Knox, F., & M. B. McElroy, Changes in atmospheric CO_2: Influence of the marine biota at high latitude, *J. Geophys. Res., 89,* 4629–4637, 1984.

Le Quéré, C. O. Aumont, L. Bopp, P. Bousquet, P. Ciais, R. Francey, M. Heimann, C. D. Keeling, R. F. Keeling, H. Kheshgi, P. Peylin, S. C. Piper, I. C. Prentice, and P. J. Rayner, Two decades of ocean CO2 sink and variability, *Tellus B, 55B,* 649-656, 2003.

Leggett, J.A., W.J. Pepper, and R.J. Swart, 1992: Emissions scenarios for the IPCC: an update, *In: Climate Change, The Supplementary Report to the IPCC Scientific assessment. [Houghton, J.T., B.A. Callander and S.K. Varney (eds.)]. Cambridge University Press, Cambridge,* pp. 69-95, 1992.

Lenton, T. M. Land and ocean carbon cycle feedback effects on global warming in a simple Earth system model, *Tellus, 52B,* 1159-1188, 2000.

Lenton, T. M. Climate Change to the end of the Millennium, *Clim. Change, 76,* 7-29, 2006.

Lenton, T. M. & M. G. R. Cannell, Mitigating the Rate and Extent of Global Warming, *Clim. Change, 52,* 255-262, 2002.

Lenton T.M., & C. Britton, Enhanced carbonate and silicate weathering accelerates recovery from fossil fuel CO_2 perturbations, *Glob. Biogeochem. Cycl., 20 (3),* 2006.

Lenton, T. M. M. S. Williamson, N. R. Edwards, R. Marsh, A. R. Price, A. J. Ridgwell, J. G. Shepherd, S. J. Cox, and theGENIEteam, Millennial timescale carbon cycle and climate change in an efficient Earth system model, *Climate Dynamics*, doi: 10.1007/s00382-00006-00109-00389, 2006.

Marland, G., T.A. Boden, R.J. Andres, A.L. Brenkert, C.A. Johnston, Global, regional, and national fossil fuel CO_2 emissions. *In: Trends: A Compendium of Data on Global Change. Carbon Dioxide Information Analysis Center, Oak Ridge National Laboratory, U.S. Department of Energy, Oak Ridge, Tenn., U.S.A.*, 1998.

M. D. McKay, R. J. Beckman, and W. J. Conover, A comparison of three methods for selecting values of input variables in the analysis of output from a computer code, *Technometrics, 21(2),* 239-245, 1979.

Milliman, J. D. Production and accumulation of calcium carbonate in the ocean: Budget of a nonsteady state, *Glob. Biogeochem. Cycl. 7*, 927-957, 1993.

Milliman, J.D., & A.W. Droxler, Neritic and pelagic carbonate sedimentation in the marine environment: Ignorance is not bliss. *Geol. Rundsh., 85,* 496-504, 1996.

Morse, J. W., Dissolution kinetics of calcium carbonate in sea water: VI. The near equilibrium dissolution kinetics of calcium carbonate rich deep sea sediments, *Am. J. Sci., 278,* 344-353, 1978.

Munhoven G. Glacial-interglacial changes of continental weathering: Estimates of the related CO_2 and HCO_3^- flux variations and their uncertainties. *Glob Planet Change, DOI: 10.1016/S0921-8181(02)00068-1,* 2002.

Murphy J., D. Sexton, D. Barnett, G. Jones, M. Webb, M. Collins, D Stainforth, quantification of modelling uncertainties in a large ensemble of climate change simulations. *Nature 430,* 768–772, 2004.

Ridgwell, A. J. *Glacial-interglacial perturbations in the global carbon cycle*, 134 pp. University of East Anglia, Norwich, 2001.

Sigman, D.M., D.C. McCorkle, W.R. Martin, The calcite lysocline as a constraint on glacial/interglacial low-latitude production changes, *Glob. Biogeochem. Cycl., 12(3),* 409-427, 1998.

Stainforth, D., T. Aina, C. Christensen, M. Collins, N. Faull, D. Frame, J. Kettleborough, S. Knight, A. Martin, J. Murphy, C. Piani, D. Sexton, L. Smith, R. Spicer, A. Thorpe, M. Allen Uncertainty in predictions of the climate response to rising levels of greenhouse gases. *Nature 433,* 403–406, 2005.

Vecsei, A., A new estimate of global reefal carbonate production including the fore-reefs. *Global Planet Change 43*, 1–18, 2004.

Walker, J. C. G. and J. F. Kasting, Effects of fuel and forest conservation on future levels of atmospheric carbon dioxide, *Palaeogeography, Palaeoclimatology, Palaeoecology (Global and Planetary Change Section)*, *97*, 151-189, 1992.

Wanninkhof, R., Relationship between gas exchange and wind speed over the ocean., *J. Geophys. Res.*, 97, pp. 7373-7381, 1992.

Zaehle, S., S. Sitch, B. Smith, and F. Hatterman, Effects of parameter uncertainties on the modeling of terrestrial biosphere dynamics, *Glob. Biogeochem. Cycl., 19,* 2005, GB3020, doi:10.1029/2004GB002395.

5 'Assessing uncertainty in weathering feedbacks on anthropogenic CO_2 concentrations: The role of the ocean-sediment system.'

5.1 *Abstract*

Enhanced weathering of rocks on land due to increases in temperature and CO_2 from anthropogenic forcing will accelerate the recovery of atmospheric CO_2 on timescales of 10^3-10^6 years. However, the temperature and CO_2 response of the earth system is dependent on parameters within the ocean and sediment system that are uncertain. This chapter assesses the uncertainty in the 10^3-10^6 year response of atmospheric CO_2 when including carbonate and or silicate weathering processes. Variable weathering is permitted after year 1800 but all other aspects of the study are the same as in Chapter Four and the same emissions scenario, which emits 4000GtC after 1990 is also used again. An initial ensemble size of 14400 runs was reduced to 664, 656 and 624 runs depending on the model variant chosen.

Calibration of the model with atmospheric CO_2 data was very effective, lowering the most likely peak CO_2 concentration by ~230ppmv in all three weathering cases. Previous model peak CO_2 estimates from these model versions, in a non-ensemble study, are shown to be highly unlikely. The lowest mean peak CO_2 estimate is 1335ppmv, and the lowest possible value 1047ppmv. Similar mean peak CO_2 between model variants did not guarantee a similar range in uncertainty, and the greatest uncertainty in peak CO_2 was found with the most complex of the three feedbacks. However, the possibility of peak CO_2 being between 1300 and 1400ppmv was ~45% in all three variable weathering cases. The general trend of uncertainty in all three models follows the same pattern of peak and decline. However it requires the action of silicate weathering to bring the range of uncertainty in CO_2 concentration to below that of the initial starting conditions for the experiment. The final mean concentration of CO_2 in the atmosphere with the most realistic setup of the model (variable carbonate and silicate weathering) is ~311ppmv, which is higher than the pre-industrial. This is due to the permanent destruction of parts of the biosphere caused by the land-use change setup of the model.

The study demonstrates that the effect of ocean and sediment parameter uncertainty on the response of CO_2 in the atmosphere is important. If the model and calibration technique is assumed to be correct then the results suggest that for the emissions scenario chosen here, there is a 45% chance that even with the effect of variable carbonate and silicate weathering the atmosphere will reach between 1300 and 1400ppmv and an 18% chance that it will take the atmosphere to beyond the year 100,000 to recover to even current concentrations of CO_2.

5.2 *Introduction*

A calibration and uncertainty analysis on the model described in Chapter Three, which includes the ability to vary the weathering of carbonate and silicate minerals on land is attempted here by allowing the ocean and sediment parameters (as described in Chapter Four) to vary, this time within three different model versions (see Chapter Three). We are then addressing the question; what effect does parameter uncertainty have on the CO_2 response of the atmosphere when a weathering feedback is included, especially on timescales of one hundred thousand years or more?

To address this question the level of either carbonate, silicate or combined carbonate and silicate weathering are allowed to vary according to changes in temperature and CO_2 (as outlined by equations in (Chapter Three). In the ensemble work in Chapter Four the prior distribution for the 11 parameters was sampled, and this sample was used firstly to run the model to steady-state and then secondly from steady-state with historical emissions applied. The same two stages are undertaken here, however the weathering is only allowed to vary during the second stage (model forced with historical emissions). We are assessing the impact of the ocean and sediment parameter uncertainty when the weathering feedbacks are switched on, allowing the river alkalinity flux to vary. We are not attempting to vary any of the parameters that are within the weathering equations (see Chapter Three) such as those on land (see Lenton 2000), which will affect the level of weathering indirectly. It is not therefore an uncertainty analysis on the weathering feedback, but the effect of the ocean and sediment system parameter uncertainty on the feedback.

Although the steady-state runs for this chapter and Chapter Four are the same, the switching on of the weathering feedback beyond the year 1800 may affect the final calibration of the ocean and sediment parameters. We would expect to see a change in the number of members of the ensemble that survive the accept-reject process in this study, merely due to the random

element of the selection process (see Chapter Four), however, the total number may also be affected by the inclusion of the weathering feedback.

The timescale of importance in Chapter Four was that of 10^4-10^5 years due to the weathering being fixed. This chapter will cover this timescale again with the inclusion of the carbonate only weathering feedback, and the uncertainty of its response can be directly compared to that of the fixed weathering. Chapter Three demonstrated that the addition of carbonate weathering decreases the time taken to reach stabilisation in the atmosphere, and the uncertainty in timescale to stabilisation with fixed weathering alone was considerable. What uncertainty will be associated with the stabilisation of the atmosphere when carbonate only weathering is included? The timescale of 10^5-10^6 years is also important in this study, with the inclusion of silicate weathering. What effect will this have on the uncertainty of the response of CO_2 in the atmosphere? Although the parameters that are varied in this study are the same as that for Chapter Four, we are providing a more complete set of uncertainty results for our model system. We are providing results for the most realistic version of the Earth system that we have developed. By changing the model setup we are also investigating the structural uncertainty within our model, but this is only a minor consideration here.

5.3 *Methods*

Methods should be assumed to be identical to that in Chapter Four unless stated below.

During the calibration process the weathering feedback is switched on for the runs from year 1800-1990 forced with historical emissions, but the steady-state runs are exactly as in Chapter Four. The weathering feedback operates by allowing the river alkalinity flux (previously a parameter with constant value) to become a variable (beyond year 1800), the value of which is calculated by scaling the river alkalinity parameter, linked to increases in temperature and CO_2. Although this neglects the interaction of the weathering feedback when the model is brought to equilibrium, the alkalinity flux (which basically represents the level of weathering) is one of the 11 parameters that were included in the uncertainty work in Chapter Four. Therefore the weathering will be scaled up from a range of baselines. The weathering feedback continues to be included beyond year 1990, to the end of the runs. Due to the inclusion of silicate weathering, some model runs were run out to the year 2 million, i.e. from year 0 A.D. to year 2 million A.D. and emissions began at year 1800 A.D. The computational challenges were similar to that described in Chapter Four, however the longer

runtimes obviously increased the computational time needed for the runs and the amount of data which was extracted and analysed.

As the steady-state runs were the same as that used in Chapter Four the initial sample size is also 14400 for this study. The selection of an appropriate sample size was discussed at length in Chapter Four, so is not covered here. This means that all the results presented here are for posterior 2 (as referred to in Chapter Four), when the observational data for both the pre-industrial and the anthropogenic rise in CO_2 are used in the accept-reject process. After the accept-reject process, from the initial 14400 runs 664 remained for the variable carbonate weathering, 656 for the variable silicate weathering, and 624 for the combined variable carbonate and silicate weathering (for reference, 637 runs remained from the initial 14400 in the fixed weathering case).

5.4 *Results*

5.4.1 Abbreviations

To minimise confusion between weathering modes in the results section, the abbreviations F, VC, VS and VCS are used in the tables within this chapter. These refer to fixed weathering, variable carbonate, variable silicate & variable carbonate and silicate respectively. Also, during this chapter some values are not new data, but are included for comparison, these are detailed in grey.

5.4.2 Parameter Calibration

The posterior parameter distributions for the variable carbonate, variable silicate and variable carbonate and silicate are very similar to that for the fixed weathering case (see Chapter Four for most relevant plots for fixed weathering). In most cases the variation can probably be attributed to the random element of the accept-reject process. The reason behind this similarity is due to the short space of time (190 years) that the weathering feedback affects the system for calibration.

5.4.3 Future Projections

As with the fixed weathering case in Chapter Four, the uncertainty in model response, changes with time (Figure 5-1). The initially well constrained system increases in uncertainty and peaks (in all three variable weathering cases) before the year 2500. After this the

uncertainty declines to the end of the runs. This decline appears to occur in phases, which are similar for the fixed weathering and the variable carbonate systems and are similar for the two systems which allow variable silicate.

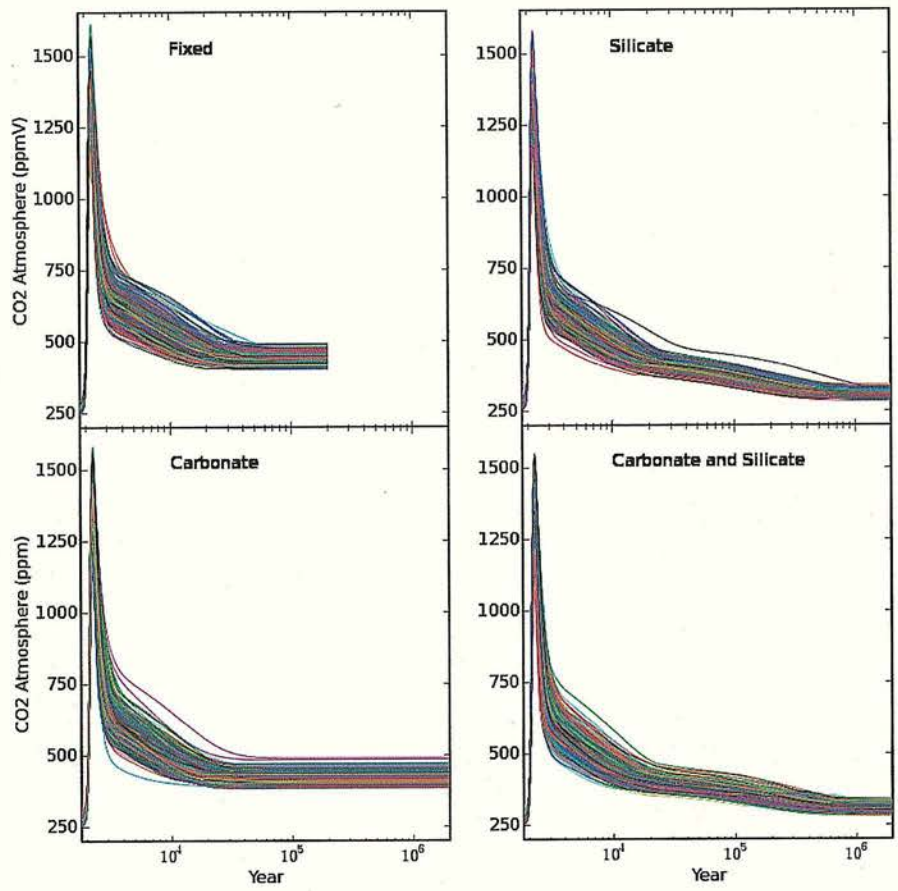

Figure 5-1: *CO_2 response against time for all four model variants.*

5.4.3.1 Peak CO_2

The inclusion of both variable carbonate and silicate weathering mechanisms decreases the peak CO_2 seen in the atmosphere (Table 5-1), this is as would be expected. This increase in complexity also appears to increase the uncertainty in the range of values. The overall

chance of peak CO_2 being somewhere between 1300 and 1400ppmv is however very similar between model variants, and is around 45%.

Peak CO_2 in the atmosphere					
Model Variant	Minimum (ppmv)	Maximum (ppmv)	Mean (ppmv)	Range (ppmv)	Results between 1300 and 1400ppmv (% of total ensemble)
Fixed Weathering (F)	1156	1609	1363	453	---
Variable Carbonate Weathering Only (VC)	1131	1580	1349	449	44.3
Variable Silicate Weathering Only (VS)	1141	1579	1348	438	45.6
Variable Carbonate AND Silicate Weathering (VSC)	1047	1547	1335	500	46.2

Table 5-1: *Peak CO_2 in the atmosphere for all four model variants*

5.4.3.2 Selected Timeslices

The effects of the variable weathering systems on the CO_2 concentration with time are summarised below (Table 5-2) actual values are in Table 5-3.

Table 5-2: *(on following page): Comments on CO_2 behaviour with time, for all three variable weathering cases and in comparison to the fixed weathering case detailed in Chapter Four.*

Timescale		Observations
Year 3,000		Peak in CO_2 and also peak in uncertainty has been passed at this point, therefore CO_2 is decreasing. Mean concentration of CO_2 at this time decreases as the effect of weathering increased as expected, and VS weathering alone has more impact than VC. Considerable overlap in range of uncertainty (in all four cases), which means that although peak CO_2 varies with weathering set-up chosen, the percentage of ensembles which have reached between 600 and 700ppmv by year 3,000 is still similar at 65.2%(VC), 66.8%(VS), 67.2%(VCS).
Year 10,000		CO_2 concentrations continue to drop. VS weathering mean CO_2 concentration is similar to VC, but its range of uncertainty is similar to VCS. Carbonate weathering is still affecting the system at this point. With VCS, the atmosphere has returned to concentrations similar to the present day (~380ppmv), but this is less than 1% of the ensemble.
Year 100,000	VC	CO_2 concentrations have stabilised (as defined in Chapter Four, section 4.4.4.5) (Figure 5-1) for VC weathering (and also F weathering). Mean CO_2 concentration is similar for F and VC weathering. Stabilisation is above pre-industrial, for reasons discussed in Chapter Three, this offset (between pre-Industrial and stabilisation concentrations) is between 122-193ppmv (Figure 5-3). There is a positive correlation between the pre-industrial concentration and that at stabilisation, but there is some spread. Range of final values is larger than that defined for the pre-industrial in the experiment. Stabilisation ranges from ~year 12,000 to 38,000 (Figure 5-4), with the most probable intervals being year 20,000 to year 22,500. 79% of the ensemble stabilises between the years 16,000 to 26,000. This compares with only 43% in the F weathering case. The addition of VC weathering greatly decreases the time to stabilisation for the atmosphere. Although the mean concentration of CO_2 in the atmosphere is lower with VC weathering (than for F weathering) the range of uncertainty is larger, possibly due to the shorter time that this system takes to stabilise.
	VS & VCS	CO_2 continues to decrease Mean CO_2 for both VS and VCS are similar at this time – effect of variable carbonate weathering has ended and their range in uncertainty is also similar. The percentage of runs which have reached between 350 and 370ppmv is 44.6% (VS) and 47.3% (VCS). At this point in time 82% of the runs (VCS) have returned to concentrations similar to the present day.
Year 1 million (VS, VCS)		Range and mean similar for both VS and VCS, system has stabilised Concentration of CO_2 has not returned to that which was set for each run during the pre-industrial – due to the permanent destruction of the biosphere, as discussed in Chapter Three. Although due to the range of final values, some runs have reached values which are within the distribution that was set for the pre-industrial Uncertainty in final range is smaller than that set at calibration, but the distribution is less peaked A high positive correlation (Figure 5-4) can be seen between the concentration of CO_2 at pre-industrial at that at the end of the runs (year 2 million). This offset in values is directly related to the level of permanent destruction in the biosphere

CO_2 concentration in the atmosphere at selected times																
Time / Case	Year 3,000				Year 10,000				Year 100,000				Year 1 million			
	Min	Max	Mean	Range	Min	Max	Mean	Range	Min	Max	Mean	Range	Min	Max	Mean	Range
F	551	932	686	381	430	655	523	225	401	492	441	91	---	---	---	---
VC	504	911	665	407	403	651	480	248	383	490	423	107	382	490	423	108
VS	509	868	659	359	395	600	473	205	327	443	369	116	283	339	310	56
VCS	499	809	640	310	378	579	445	201	319	424	367	105	280	339	311	59

Table 5-5: *Data on CO_2 behaviour with time, for all three variable weathering cases and the fixed weathering case detailed in Chapter Four.*

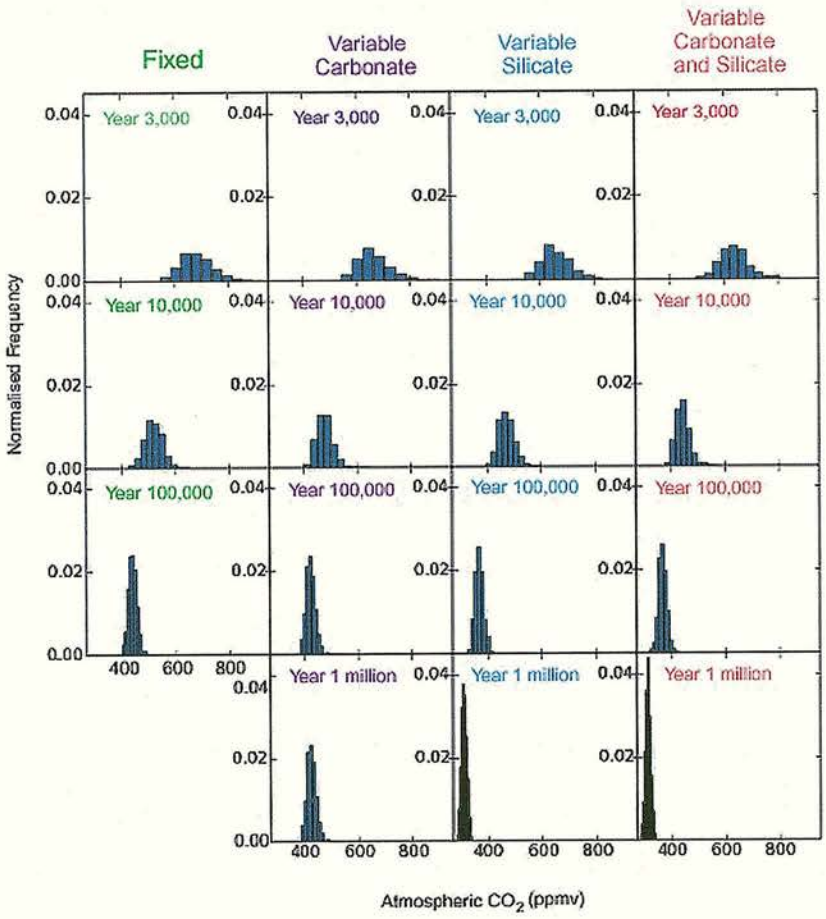

Figure 5-2: *Posterior distribution of CO_2 at year 3,000, 10,000, 100,000 and 1 million, for all 4 model variants*

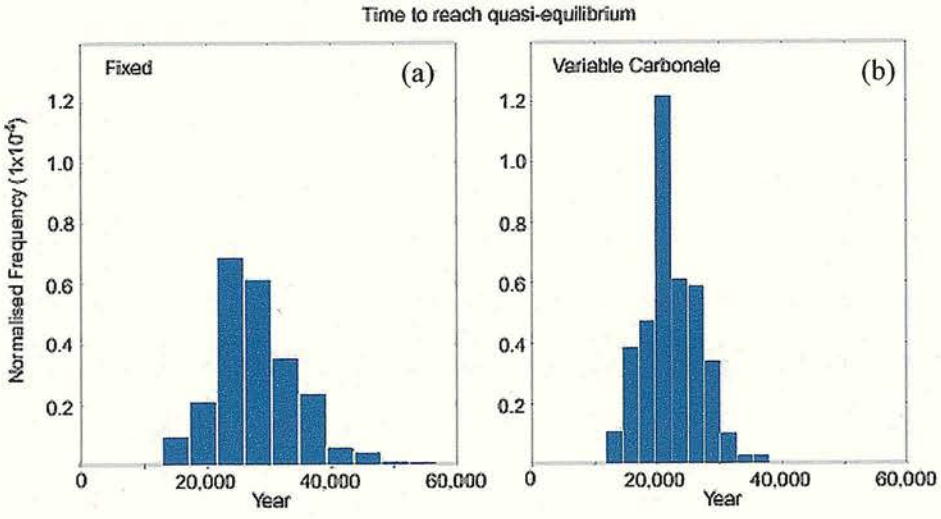

Figure 5-3: *Histogram showing time to stabilisation of CO_2 in the atmosphere, a) fixed weathering system, b) variable carbonate weathering system.*

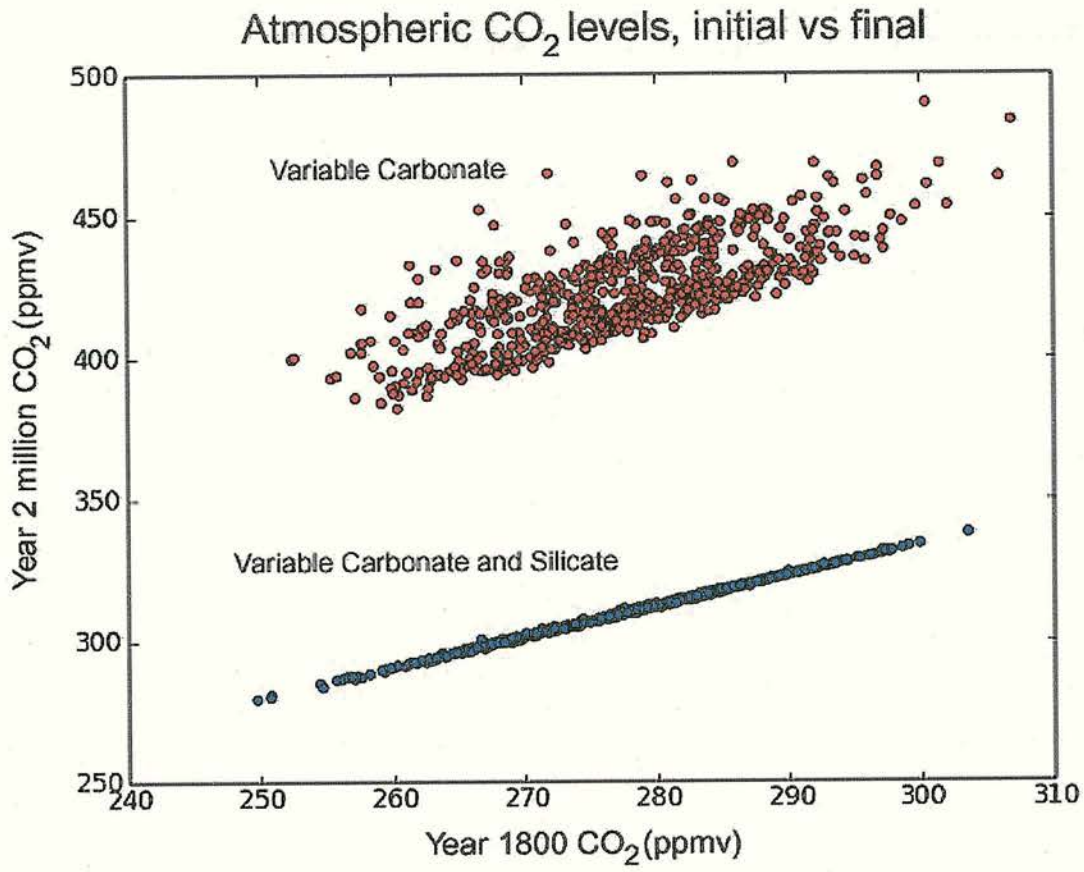

Figure 5-4:*CO_2 concentrations at year 2 million against year 1800 for the variable carbonate (red) and the variable carbonate and silicate (blue) weathering systems.*

5.5 *Discussion*

5.5.1 Comparison to other studies

5.5.1.1 Non-ensemble results for variable weathering model versions (Chapter Three)

As with the fixed weathering case discussed in Chapter Four, the trend of the CO_2 response from each of the variable weathering variants, remains the same in the ensemble study as for the non-ensemble study in Chapter Three. However the mean values are in general much lower (Table 5-4), by between 233 and 237ppmv in each case for peak CO_2 and this difference remains to the year 2 million, although it is much reduced by this time, to

~15ppmv. This indicates that our calibration has been very effective in constraining our model output, and that our previous results are highly unlikely with respect to the data we have subsequently used for calibration.

Study		**Non-Ensemble Study (Chapter Three)**				**Ensemble Study (Chapters Four & Five)**			
Model Variant / Data		F	VC	VS	VCS	F	VC	VS	VCS
Peak CO_2	**Mean**	1596	1585	1583	1572	1363	1349	1348	1335
	Min	---	---	---	---	1156	1131	1141	1047
	Max	---	---	---	---	1609	1580	1579	1547

Table 5-6: *Peak CO_2 concentrations in the atmosphere for the non-ensemble study (Chapter Three), the fixed weathering ensemble results from Chapter Four and the results from the three variable weathering cases detailed in this chapter.*

This study focussed on one emissions scenario only (L4 as defined in Chapter Three), however in comparing the range of possible values from the ensemble with this scenario, there are various overlaps with the results from other scenarios used (without an ensemble) in Chapter Three. However, until these emissions scenarios have been used in the same ensemble method as used here, it is difficult to make any direct comparisons.

The original estimate for stabilisation time for the variable carbonate weathering system (Chapter Three) was by year 57,000, this is around 20,000 years longer than the maximum time suggested from this study. Therefore in this study the time to stabilisation is highly dependent on the parameters in the ocean and sediment system

5.5.1.2 Previous results on long-term fate of fossil fuel CO_2 in the atmosphere (Archer 2005)

Archer (2005) has derived airborne fractions for CO_2 in the atmosphere for 1,000, 10,000 and 100,000 years into the future, with a range of emissions scenarios, using an ocean-sediment carbon cycle model. His output years approximate to our year 3,000, 10,000 and

100,000 timeslices, and his highest emissions scenario (5000GtC, including historical) is roughly comparable to the scenario used in this study.

Our most likely airborne fractions for each timeslice are well below that suggested in Archer's study. Archer's model does not however have variable carbonate weathering, and our sediment dissolution is more aggressive (see Chapter Two, also Lenton & Britton (2006)).

Study and model variant		**Year 3000**	**Year 10,000**	**Year 100,000**	**Year 1,000,000**
This study	F	*14.1-30.6%*	*8.6-18.1%*	*7.0-9.6%*	---
	VC	*11.9-29.3%*	*7.1%-16.8%*	*5.9-9.3%*	*5.9-9.3%*
	VS	*12.3-27.5%*	*6.9-15.3%*	*3.3-7.7%*	*1.4-2.8%*
	VCS	*11.7-25.3%*	*6.0-14.1%*	*3.2-7.1%*	*1.4-2.4%*
Archer (2005)	Carbonate weathering only, fixed	*33.9%*	*17.5%*	*17.5%**	---
	Carbonate and silicate weathering, fixed	*32.9%*	*15.1%*	*6.7%*	---

Table 5-7: *Range of airborne fraction of CO_2 for 4 model variants. Year 3000, 10,000, 100,000 and 1 million. (* We believe that this value is a typo in the paper)*

Overlap of our results with that of Archer's can be seen by year 100,000 when we include variable silicate weathering in some form, and Archer has included fixed carbonate and silicate weathering. Archer's value in this case is at the higher end of results. Again the lower values in comparison to Archer will be partly due to the more aggressive dissolution of our sediments on the 10^3-10^4 year timescale, and also the fact that neither Archer's carbonate nor silicate weathering systems are dynamically linked to the climate. Also Archer's value of

6.7% is reached as early as year 10,000 with our ensemble results, which demonstrates the large dependence of some of our model results on parameter choice.

5.5.2 Other Considerations

Due to the set-up of this study the initial size of the ensemble was 14400, a size which was investigated to be adequate for the fixed weathering system in Chapter Four. It could be argued however that as the inclusion of variable weathering may change the parameter calibration and will most definitely change the response of the CO_2 in the atmosphere, that the process of assessing a suitable sample size for the experiment should be undertaken again. However, the results show that the increase in alkalinity due to weathering had vary little (if any) effect on the calibration of the parameters, therefore a sample size of 14400 is still valid based on the initial work in Chapter Four.

This study allowed variable weathering only after year 1800, which again allows the direct comparison of results from Chapter Four and this chapter. There are two caveats to this, firstly it would be more comprehensive if the weathering feedback were to be allowed to interact to generate a steady-state, and secondly that our results suggest that the weathering feedback does not have a major impact over the 190 years of the transient calibration. This second point indicates that perhaps a better way of calibrating the response of the weathering system should be sought.

If the experimental system remains roughly similar to that used here it would be relatively easy to include the effects of varying the vegetation parameters that interact with the net primary productivity levels (see Chapter Three), that affect the weathering response. This would be useful in giving a more comprehensive analysis of uncertainty for this model, as currently only the ocean and sediment parameters are varied, and is a possibility for future studies.

This uncertainty study (and Chapter Four), has concentrated on one emissions scenario only, one that has does not completely dissolve the carbonate sediments in the ocean (Chapter Three). The effect of variable weathering is greater if all the sediments are dissolved (Chapter Three), therefore in future repeating the experiment with a higher emissions scenario would be beneficial. Comparisons to non-ensemble results from other scenarios used with this model (Chapter Three) have also been made. However, this study (and

Chapter Four) has shown that the results from Chapter Three are highly unlikely with respect to the calibration data chosen. Therefore such comparison should be made with care. Possible future studies would then involve repeating the experiment with a range of emissions scenarios, to quantitatively assess the overlap in response of CO_2 in the atmosphere, between emissions scenarios. If a probability can be assigned to the choice of emissions scenario, it may be possible to make a more comprehensive quantitative assessment of the response to anthropogenic perturbation, which also takes into account the uncertainty in future emissions.

This study looks into the future of the atmosphere and climate system on geological timescales however some climate effects have long periodicities, and therefore affect the earth system on geological timescales, such as glaciations (see Chapter One). A discussion about the future of the glacial cycles, and how this may interact with the enhanced weathering feedback system is included in Chapter Three.

5.6 *Conclusions*

A calibration has been performed on the parameters in this study, but there were no large differences between the posterior parameter results from this calibration, and from that in a previous study (Chapter Four). This suggests that the weathering feedback (through its effect on the alkalinity flux), is not affecting the CO_2 response in the atmosphere on the decadal timescale (as would be expected).

Mean concentrations of CO_2 and peak CO_2 concentrations are lower that that from a previous non-ensemble study with this model, indicating that the calibration has been very effective (with respect to the data we used here), however this difference does decrease with time.

Although the concentration of peak CO_2 is similar for the variable carbonate and the variable silicate weathering systems, the uncertainty in the posterior is different. The combined effect of variable carbonate and silicate weathering appears to increase the uncertainty in the prediction. However, the chance of peak CO_2 being within 1300-1400ppmv is around 45% in all three variable weathering cases.

The time to stabilisation of CO_2 in the atmosphere with variable carbonate weathering is highly dependent on uncertainty in ocean and sediment parameters (as it is for fixed weathering also, see Chapter Four). Inclusion of variable carbonate weathering improves the range of times to stabilisation. The possibility that the atmosphere stabilises between years 16,000-26,000 has improved from 43% in the fixed weathering case, to 79% by the addition of variable carbonate weathering.

If known conventional fossil fuel reserves are emitted the uncertainty in ocean and sediment parameters alone suggests that a return to approximately current concentrations of CO_2 with our model will occur by the year 10,000 in less than 1 % of cases, that in 57% of cases it will take greater than 50,000 years, but that there is still an 18% chance of recovery being delayed until beyond the year 100,000.

All of these conclusions suggest that looking at the uncertainties within the ocean and sediment system related to this and other models, as well as other parameters used within models is vital if we are to gain a greater understanding of the effect we are having on this planet.

If our model is assumed to be correct then it suggests for the emissions scenario chosen, that even with the feedback effects of enhanced variable carbonate and silicate weathering that there is a 45% chance that peak CO_2 will reach between 1300 and 1400ppmv and that there is an 18% chance that it will take until beyond the year 100,000 for the atmosphere to recover to even the current concentration of CO_2 in the atmosphere.

5.7 References

Archer, D. Fate of fossil fuel CO2 in geologic time, *Journal of Geophysical Research (Oceans)*, doi:10.1029/2004JC002625, 2005.

Lenton, T. M. Land and ocean carbon cycle feedback effects on global warming in a simple Earth system model, *Tellus, 52B*, 1159-1188, 2000.

Lenton, T.M., & C. Britton, Enhanced carbonate and silicate weathering accelerates recovery from fossil fuel CO_2 perturbations, *Glob. Biogeochem. Cycl., 20 (3),* 2006.

6 Summary and Conclusions

6.1 *Introduction*

This final chapter outlines key findings from this thesis and the results in the context of other studies. The limitations of the work, avenues of research not discussed elsewhere, possible future work and the wider implications of this research are presented. Conclusions to the thesis are given as answers to the three key questions posed in the introduction.

6.2 *Key Findings*

6.2.1 Variable weathering feedback on atmospheric CO_2

This work has demonstrated that the enhancement of weathering due to the increased CO_2 and temperatures that can be expected from anthropogenic perturbation will greatly increase the drawdown of CO_2 on the timescale of 10^4-10^6 years. It is the increase in levels of river alkalinity due to the enhanced weathering of carbonate and silicate minerals, which allows the ocean and sediment system to buffer more CO_2 from the atmosphere, ultimately increasing the ocean uptake of CO_2 with time, in comparison to fixed weathering studies.

Separating and comparing the effects of variable carbonate weathering from that of variable silicate weathering, and then combined variable carbonate and silicate weathering allowed the investigation of the timescales of improved ocean CO_2 uptake to be investigated. Variable carbonate weathering has an impact on atmospheric CO_2 on the 10^3-10^4 year timescale, but no effect on the 10^5 year timescale. Variable silicate weathering has similar effects to the carbonate system on 10^3-10^4 year timescales, but then continues to influence atmospheric CO_2 on timescales of 10^5-10^6 years. The effect of variable carbonate and silicate weathering is therefore effective on the entire range of timescales from 10^3-10^6 years. The greatest effect was found on the timescale of 10^4-10^5 years, in comparison to a fixed weathering system, and the variable carbonate and silicate weathering system takes millions of years to stabilise CO_2 in the atmosphere. Without the inclusion of variable silicate weathering in the model, the atmosphere will not return to pre-industrial concentrations of CO_2.

Although the inclusion of variable weathering was seen to affect the atmospheric CO_2 concentration in the results for a whole range of emissions scenarios, it was found that the effect of enhanced weathering was greatest when all the sediments were dissolved. In the model used in the study the total dissolution of sediments occurred when >7350GtC was emitted into the atmosphere after year 1990.

In the most pessimistic emissions scenarios, the sediment system overcompensates, and the lysocline returns to much shallower levels than initially. The system continues to be fed by alkalinity from enhanced weathering, and slowly recovers to a lysocline position similar to that at the start of the experiment. However, when the variable silicate weathering system is included a return to equilibrium takes millions of years, and the final concentration of CO_2 is higher than for the pre-industrial, if permanent changes to the biosphere are allowed by the model setup.

6.2.2 Quantifying uncertainty in model response

This study has shown that large improvements in the mean response and an indication of the uncertainty in overall response of a model system can be made by adopting a Bayesian ensemble modelling approach. In this study 11 parameters were allowed to vary, and data is used to calibrate the model response. The work in this case was based specifically on the uncertainty in the parameters concerned with the ocean and sediment system, and the uncertainty in the response of the CO_2 in the atmosphere to these changes. The data used to calibrate the model response were concerned with the CO_2 concentration and response of the atmosphere.

The efficiency of the model being used allowed a thorough investigation into a suitable sample size for an initial study and the accept-reject technique which makes few approximations of Bayes theorem. The study benefited from the investigation into sample size and the choice of initial size was not chosen due to computing limitation. However, if more parameters were included in the investigation then a larger sample size would be required.

Parameter probability distributions were updated by the Bayesian calibration, and the most likely parameter value found from this method was in one case an order of magnitude higher than that in the initial prior distribution, and used in previous studies with the same model.

Although in many cases the posterior parameter distributions were similar to that of their prior, the effect of them on the response of CO_2 in the atmosphere could easily be seen. Concentrations of peak CO_2 from earlier studies using this model were often outside the range of uncertainty found in this study, and the mean peak CO_2 concentration was ~235ppmv lower than in this earlier study.

The uncertainty in the response of CO_2 with time reached a peak at ~year 2450 (which is after the peak CO_2 concentration in the atmosphere had been reached), and declined from this point onwards. The way in which the uncertainty decreases with time is related to the weathering systems that are included/allowed to vary. Fixed weathering and variable carbonate weathering have similar responses, as do the variable silicate and variable carbonate and silicate systems. The uncertainty in long term response of the atmosphere is much better constrained than during the period of greatest CO_2 forcing as might be expected.

There is a large amount of overlap in the uncertainty in the response of CO_2 from the various weathering systems, on millennial and geological timescales. There is also overlap with some single run studies using this model with other emissions scenarios. The uncertainty in atmospheric fractions at some points in time are greater than suggested from a range of scenarios, in comparison to another model study.

The time which the atmosphere takes to stabilise when only fixed weathering is allowed varies by 44,000 years, and the mean value is ~year 28,000. The addition of variable carbonate weathering to the model system greatly decreases this stabilisation time, with a very high likelihood that it will occur in the years 20,000 to 22,500. The final range in uncertainty in CO_2 in the atmosphere with either system is still higher than that estimated for pre-industrial, although it is similar. The final range in uncertainty is lower for the fixed weathering system, than for the variable carbonate weathering system and is related to the stabilisation timescale.

The highest and least likely atmospheric fraction is lower than the value from an earlier non-ensemble study for many thousands of years, but the two systems have caught up by year 100,000. The range of uncertainty in CO_2 response does however suggest an 18% chance that it will take the atmosphere to beyond the year 100,000 to recover to even current concentrations of CO_2.

Return to stabilisation of the system when variable silicate weathering is included takes millions of years. However the range of uncertainty in final value is lower than that estimated for the pre-industrial, although the distribution is less tightly distributed. Final values of CO_2 were found to be higher than for the pre-industrial, due to the permanent changes to the biosphere that are allowed by the model setup. Final concentration of CO_2 for the variable carbonate weathering system is highly correlated to the initial pre-industrial concentration, but in the case of the systems that include variable silicate weathering, the final offset in CO_2 is completely determined by the permanent change in the biosphere from the model.

6.3 *Limitations*

6.3.1 Sediment Dissolution

The sediment model in this study represented the CO_2 response on 10^4-10^6 year timescales well in comparison to other studies. However, the dissolution of the sediment model was more aggressive than that of previous studies, this meant that the peak CO_2 response in the atmosphere, and the CO_2 concentration for the first few thousand years after the peak was lower than is likely. What does this mean in terms of the model results and response? The peak CO_2 concentration and that for the following few thousand years is likely to be lower than that in the real world, and should be treated with caution. However, the general response of the system is as expected, as the rate of dissolution has no effect once the dissolution is complete.

The benefit of the type of global biogeochemical model used here is to gauge the effects of the interacting feedbacks, i.e. a relative response to the default state, rather than predicting specific concentrations. The level of sediment dissolution in this model will have an effect on the atmospheric fraction figures that have been reported in this study. Again, our results in this area were lower than that from other studies, however, the results which demonstrate the uncertainties in atmospheric fraction with time, are still applicable. The technique that was used to calibrate the model with atmospheric CO_2 could possibly be used to investigate the level of dissolution in the model, and calibrate it, if appropriate data was available.

6.3.2 Over-riding effects of the climate system

The study looked at the effects of enhanced weathering and their effect on the atmospheric CO_2 concentration, up to 2 million years into the future, however on these timescales other systems could be coming into play. The inclusion of permanent land-use change for example suggests that humans will still be here to affect the biosphere in 2 million years. This may not necessarily be the case. There are some studies which suggest bi-stability in certain ecosystems (Betts 1999), which would permanently change the nature of the biosphere, and therefore the equilibrium level of weathering. At this point in time it is difficult to incorporate either of these effects mechanistically.

The glacial cycles also interact with the climate system on timescales of less than a million years. Our results represent the possibility that the next glaciation could be greatly delayed, due to the action of humans, in agreement with Archer & Ganopolski (2005). Again at this point, the mechanisms surrounding glacial inceptions are not completely resolved, and are therefore difficult to incorporate mechanistically.

6.3.3 Parameter Choice

The parameters that were involved in the uncertainty study were connected to the sediment and ocean system, there was no inclusion of the land parameters. This limits the effects of the weathering system on the uncertainty study, but the study still provides information on the effect of the weathering feedback on the system when a large amount of uncertainty has been taken into consideration. It also provides a first step in looking at uncertainty in the model, against which more complicated versions can be compared.

6.4 *The results of the thesis in the context of other modelling studies*

The work of Archer et al. (1998) and Archer (2005) suggests timescales and phases for the removal of fossil fuel CO_2 from the atmosphere, due to the dissolution of sediments, and the replenishment of alkalinity from a constant weathering flux. This study upholds this view, with a few amendments. The first is that on the 10^4-10^6 year timescale, the effect of variable weathering on the concentration of CO_2 in the atmosphere is important, and that this has the most effect when all the sediments in the ocean are dissolved. The second is that when the

lysocline first begins to recover from total dissolution (in more pessimistic scenarios) the sediment system may overshoot, storing more $CaCO_3$ in the deeper sediment levels than initially. This is then slowly corrected by the dissolution of the excess sediments. The third is a realisation that the uncertainties within the ocean and sediment system may well have an important effect on the time that the atmosphere will take to recover from anthropogenic perturbation. Work so far tends to suggest that these uncertainties are important in comparison to the uncertainty associated with the level of future CO_2 emission.

Walker & Kasting (1992) had previously included some of the effects of variable weathering in their assessment of the future response of the atmosphere to anthropogenic change. This study maintains their conclusion that weathering will have an effect on the concentration of CO_2 on timescales of 10^4 years and beyond. This study incorporated new components of this feedback, and a more realistic representation of the weathering feedback itself.

6.5 *The results of this thesis in the context of data based studies*

Although this study has been concentrating on the future of the global carbon cycle, there are some similarities between the results presented here and that seen in data based studies for the Palaeocene-Eocene Thermal Maximum (PETM). The PETM was a transient global warming event which occurred about 55 million years ago (Ma). It is marked by a negative carbon isotope excursion (CIE) in both terrestrial materials and marine carbonates as well as pervasive carbonate dissolution in the oceans with a benthic foraminferal extinction horizon and drop in diversity after recovery (Kelly et al. 2005 & Zachos et al. 2005, and references therein). It is believed that the rapid release of large quantities of (isotopically depleted) carbon into the ocean-atmosphere system triggered the dissolution event and caused the CIE. Sources of such carbon are likely to be either from methane hydrates or biogenic methane, however the extent and nature of the release is not yet well known.

Recent studies (Zachos et al. 2005 & Kelly et al. 2005) have been extracting records of the dissolution event from sediment cores (Figure 6-1a). These studies have reported several features of the dissolution events as represented in the cores. These include rapid shoaling of the CCD (carbonate compensation depth), gradual recovery of the CCD and then the lysocline, 'overshooting' of the lysocline during the recovery period (i.e. greater $CaCO_3$ percentages in sediments than previous to the event). These are similar to the responses seen

in the sediment layers with the model used in this study (Figure 5-1b, see also Chapter Three) – however at this stage I have included the figure only to highlight the similarity, not to pose a theory. Also Kelly et al. (2005) reported kaolinite increases during the CIE recovery stage, which could indicate an increase in silicate weathering fluxes on land – this also links well with the model variations which have been investigated in this thesis. Therefore it is possible that the model in this study could be used to investigate the large scale response of the carbon cycle at other times, such as the PETM.

Kelly et al. (2005) also discusses the possibility that enhanced chemical weathering may have fuelled prolific coccolithophorid blooms, which in turn would suppress the local lysocline (as seen in the recovery stage).This type of feedback has not been included in this study, but links between weathering and ocean productivity could be included (although care must be taken about local versus global phenomena, due to the type of model used here).

(a)

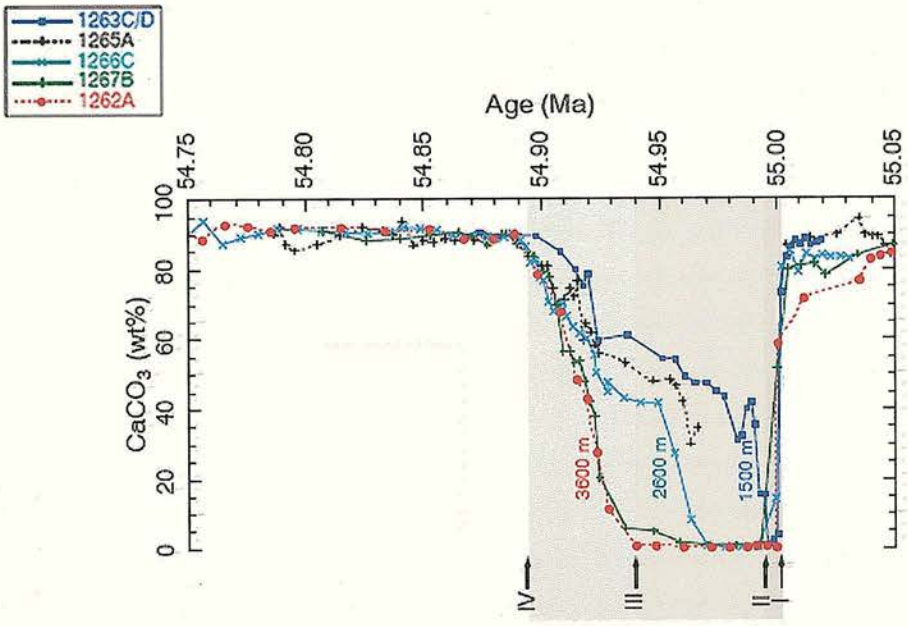

(b)

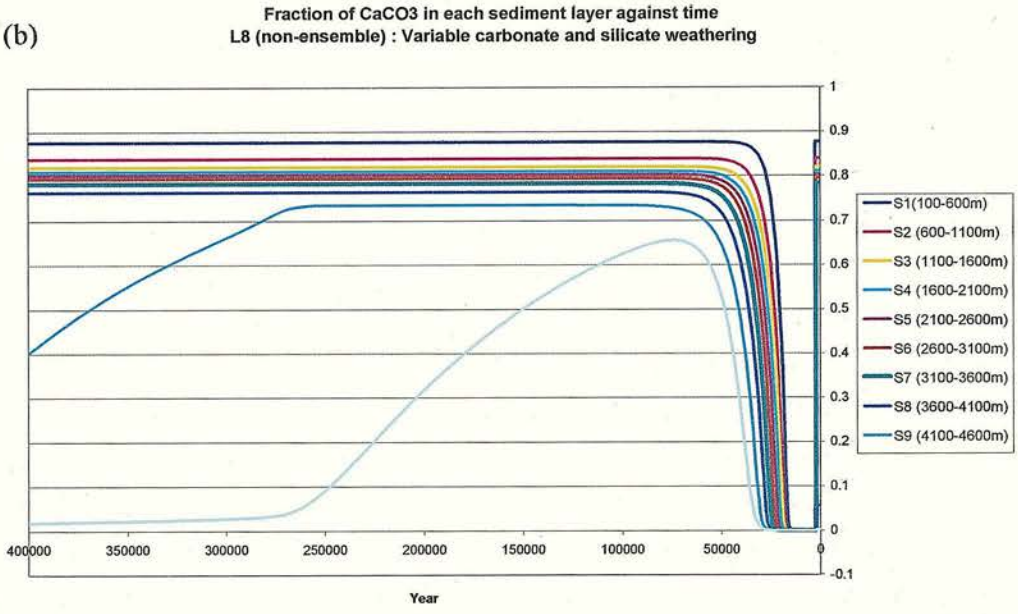

Figure 6-1: *a) Sediment core data from the PETM, showing the fraction of $CaCO_3$ over time for several palaeo-ocean depths (Zachos et al. 2005), b) Model output from this study (Chapter Three)Scenario L8, with variable carbonate and silicate weathering, non-ensemble system. The x-axis has been reversed to show similarity to a). Notice the fast dissolution and gradual recovery of the sediment level. Also levels S9 and S10 'overshoot' for a time, depositing more $CaCO_3$ than they did at the start of the run and eventually collapsing to their original levels as the CCD shoals again (this also happens to S8, but beyond year 400,000).*

6.6 *Other avenues of research and future work*

This section outlines areas of research connected to this study which were briefly investigated, but not with enough depth to be included in the thesis, due to time or technological constraints.

6.6.1 Deep Sea Injection

It has been suggested that to avoid the accumulation of fossil fuel CO_2 in the atmosphere, emissions could be injected into the deep ocean (Marchetti 1977). What effect would this have on the atmosphere? The model described in Chapter Two is suitable for investigating such a question and preliminary results are presented here, time constraints prevented a more comprehensive investigation.

The model which contained sediments and a constant weathering flux (Chapter Two) was run into the future with emissions scenario L8 (Lenton 2000), 25% of the emissions scenario was directly inserted into either the intermediate or deep ocean box from year 2010 onwards.

A 20 % decrease in peak atmospheric CO_2 was seen with deep sea injection of CO_2 and a 16% decrease with injection into the intermediate ocean (Figure 6-1). The CO_2 concentration in the atmosphere converges for all three systems beyond year 5,000 and by year 200,000 there is less than 1ppm difference between all three systems.

Figure 6-2: *The CO_2 response in the atmosphere when all emissions are allowed to enter the atmosphere (blue line), 25% are injected into the deep ocean after 2010 (red line), 25% are injected into the intermediate ocean (green line). The x-axis has been logged.*

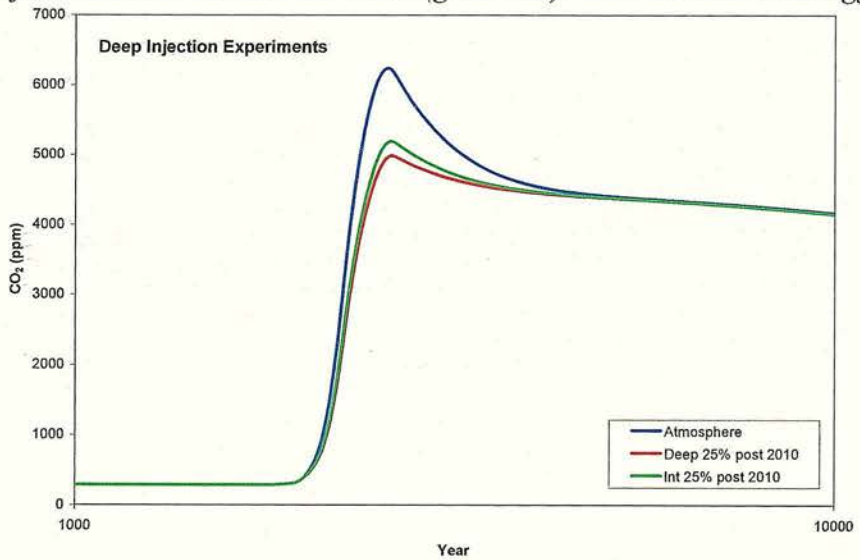

The injection of CO_2 into the intermediate or deep ocean allows the buffering of the CO_2 by the ocean and sediment neutralisation to begin earlier which decreases the peak CO_2 concentration reached in the atmosphere. Final concentrations of CO_2 in the atmosphere are the same in all three systems as the buffering capacity of the ocean and also the sediment reservoir available for neutralisation is the same across the experiments. Archer et al. (1998) also investigated deep injection of fossil fuel CO_2, they too found that the peak CO_2 was decreased dramatically with deep injection. However, a more direct comparison of the results from this study and that of Archer et al. (1998) is not possible as Archer et al. (1998) do not have a comparable emissions scenario to the one used here.

This work suggests that the injection of CO_2 into the intermediate or deep ocean could have a large impact on the peak CO_2 concentration reached in the atmosphere in the coming millennia. Further work would include a more thorough investigation of the effect on the sediment levels, repeat experiments with a range of emissions scenarios and further comparison to results presented by Archer et al. (1998). The impact of enhanced weathering could also be explored and an uncertainty study could also be attempted.

6.6.2 Investigating the effect of specific parameters on atmospheric CO_2 response

Although the uncertainty in the response of the atmosphere to the parameters in the ocean and sediment system has been assessed there has been little discussion of which parameters may be affecting aspects of the response such as the peak CO_2 value or time to stabilisation. Scatter plots of parameter values against various atmospheric CO_2 responses were created during the study and in some cases definite correlations could be seen between parameter and response (Figure 6-2). However, as the model response is due to changes in all 11 parameters at the same time, looking at one parameter in isolation must be attempted very carefully.

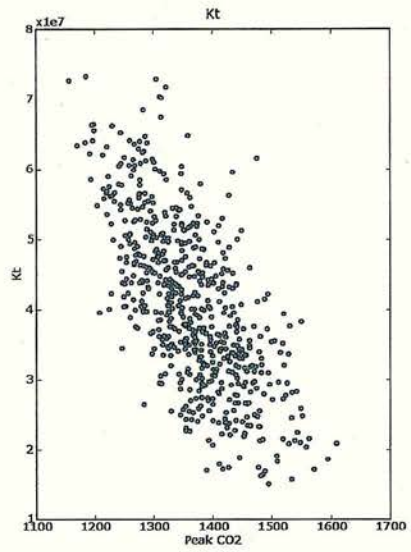

Figure 6-3: *Scatter plot of parameter Kt (thermohaline circulation m^3/s^{-1}) against peak CO_2 (ppmv).*

Stepwise linear regression can be used to look at the effects of combinations of parameters on model response, including ranking the importance of including certain parameters in a model system. However, a satisfactory method of applying a stepwise linear regression to the dataset in this study was not found in the time available. Future work would concentrate on applying this technique to the data already gathered to gain insights into the effects of various parameters on the system.

6.6.3 Future work

Results in Chapters Four and Five show only the future responses of the accepted runs (those that provided reasonable responses for steady-state and perturbation). Future work could involve running all of the initial ensemble (i.e. 14400 runs) into the future and then comparing the CO_2 response to that from the 'calibrated ensemble'. This has not been attempted so far, due to time constraints.

The experiments in Chapters Four and Five could be repeated with other emissions scenarios, a more comprehensive study could perhaps include the level of emissions as a new parameter, subject to probability.

More of the parameters in the model, specifically those associated with the land, and therefore the weathering enhancement could also be varied, to gauge the uncertainty connected with the weathering feedback itself. This however, raises several issues with the steady-state of the model system including the current treatment of the weathering system as a multiplier of a base level taken from the pre-industrial, and the uncertainties which will inevitably be associated with the land system, such as the reservoir size.

6.7 *Relevance to wider questions*

Learning more about the way in which the Earth system will respond to anthropogenic change, even on timescales well beyond that of the next few generations, is a useful exercise. As well as finding ways to save energy therefore reducing CO_2 emissions, research has begun on ways to manipulate the carbon cycle, to reduce the concentration of CO_2 in the atmosphere. The research presented here has wider implications in such fields as accelerated weathering of carbonate and silicate minerals (by man), CO_2 storage in empty oilfields, and deep injection of CO_2 into the ocean (as discussed above). All of these proposed mitigation strategies would have an impact on the global carbon cycle for many thousands of years to come, mostly on the ocean carbon cycle, which is the focus of this study. Future changes in land-use are also relevant to this study.

6.8 *Conclusions*

What effect will enhanced carbonate and or silicate weathering have on the concentration of CO_2 in the atmosphere on timescales of 10^3-10^6 years?

The effect of enhanced silicate and carbonate weathering will be to greatly reduce the concentration of CO_2 on timescales of 10^4-10^6 years. The magnitude of the effect is dependent on the type of weathering included, and also on the rate and level of emissions involved. Enhanced weathering will decrease the concentration of peak CO_2 in the atmosphere, but the specific values from this study must be taken with caution. The greatest effect is seen when both carbonate and silicate weathering enhancement is taken into consideration. Carbonate weathering feedback alone only affects CO_2 on the 10^3-10^4 year timescale. Only when the effects of silicate weathering are taken into consideration will the atmosphere return to concentrations of CO_2 similar to that of the pre-industrial. However, if humans affect a permanent change in the biosphere, atmospheric CO_2 may never return to pre-industrial concentrations.

What effect does parameter uncertainty have on the CO_2 response of the atmosphere and how does this change with time?

This study has shown that uncertainties of > 450ppmv in CO_2 response are possible with the model used here, when parameter uncertainty is taken into consideration (fixed weathering only). Uncertainty in CO_2 concentration appears to vary with time, peaking at around year 2450 (after peak CO_2 in the atmosphere), and declining after that. There is large uncertainty in the concentration of peak CO_2 in the atmosphere (1047 to 1609ppmv) and concentrations of CO_2 predicted on timescales of 10^4 years and above carry far less uncertainty. This suggests that there may be large uncertainties in the response time of the atmosphere to fossil fuel perturbation, when using Earth system models. The specific results from an uncertainty study are likely to be model dependent, however this study has shown that parameter uncertainty is an important consideration in model response and prediction.

What effect does parameter uncertainty have on the CO_2 response of the atmosphere when a weathering feedback is included, especially on timescales of one hundred thousand years or more?

When variable weathering systems are included, the time dependent response of CO_2 in the atmosphere is similar to that of fixed weathering. The magnitude of uncertainty seen does however vary with the model setup chosen. Similarities in response can be seen between the fixed weathering system and that of the variable carbonate system and also between the variable silicate and variable carbonate and silicate systems. The uncertainty in CO_2 response continues to decrease on timescales of one hundred thousand years or more, returning to a level similar to the initial range. When the most realistic setup is used (i.e. variable carbonate and silicate weathering) the uncertainty in peak CO_2 is 500ppmv with a mean concentration of 1335ppmv and a return to concentrations of ~380ppmv in the atmosphere (present concentration of CO_2) will most likely take 100,000 years.

6.9 *References*

Archer, D. Fate of fossil fuel CO2 in geologic time, *Journal of Geophysical Research (Oceans)*, doi:10.1029/2004JC002625, 2005.

Archer, D. and A. Ganopolski, A movable trigger: Fossil fuel CO_2 and the onset of the next glaciation, *Geochemistry Geophysics Geosystems*, *6*, doi:10.1029/2004GC000891, 2005.

Archer, D., H. Kheshgi, & E. Maier-Reimer, Dynamics of fossil fuel CO_2 neutralization by marine CaCO3, *Glob. Biogeochem. Cycl. 12*, 259-276, 1998.

Betts, R. A. Self-beneficial effects of vegetation on climate in an Ocean- Atmosphere General Circulation Model, *Geophys. Res. Lett. 26*, 1457-1460, 1999.

Kelly, D. C., et al., Enhanced terrestrial weathering/runoff and surface ocean carbonate production during the recovery stages of the Paleocene-Eocene thermal maximum, *Paleoceanography, Vol.20,* 2005.

Lenton, T. M. Land and ocean carbon cycle feedback effects on global warming in a simple Earth system model, *Tellus*, *52B*, 1159-1188, 2000.

Marchetti, C., On Geoengineering and the CO_2 Problem, *Climatic Change, 1,* 59-68, 1977.

Walker, J. C. G. and J. F. Kasting, Effects of fuel and forest conservation on future levels of atmospheric carbon dioxide, *Palaeogeography, Palaeoclimatology, Palaeoecology (Global and Planetary Change Section)*, *97*, 151-189, 1992.

Zachos, J.C., et al., Rapid acidification of the ocean during the Paleocene-Eocene Thermal Maximum, *Science, Vol.308,* 1611-1615, 2005.

Appendix A: Lenton & Britton 2006

Reprint of published paper: Lenton T.M., & C. Britton, Enhanced carbonate and silicate weathering accelerates recovery from fossil fuel CO_2 perturbations, *Glob. Biogeochem. Cycl., 20 (3),* 2006.

N.B. Page numbering remains as in original document.

GLOBAL BIOGEOCHEMICAL CYCLES, VOL. 20, GB3009, doi:10.1029/2005GB002678, 2006

Click Here for Full Article

Enhanced carbonate and silicate weathering accelerates recovery from fossil fuel CO_2 perturbations

Timothy M. Lenton[1] and Clare Britton[2,3]

Received 19 December 2005; revised 17 March 2006; accepted 26 April 2006; published 4 August 2006.

[1] Increasing atmospheric CO_2 and surface temperatures should increase carbonate and silicate weathering rates, directly via warming, and indirectly via the CO_2 fertilization effect enhancing plant productivity. Enhanced weathering should in turn increase alkalinity input to the ocean and accelerate long-term CO_2 uptake. We added silicate and carbonate weathering and carbonate sediments to an existing global carbon cycle and surface temperature model and subjected it to a range of long-term fossil fuel emissions scenarios, spanning 1100–15,000 GtC in total. Emissions of $\geq$7350 GtC dissolve all carbonate sediments, and enhanced carbonate and silicate weathering accelerate subsequent CO_2 removal from the atmosphere by up to a factor of 4. For 1100–4000 GtC emissions, enhanced weathering accelerates CO_2 removal by a factor of 1.5–2.5. However, it takes >1 Myr for silicate weathering to stabilize atmospheric CO_2. If land use tends to suppress vegetation and weathering rates on this timescale, then CO_2 will stabilize above preindustrial levels.

Citation: Lenton, T. M., and C. Britton (2006), Enhanced carbonate and silicate weathering accelerates recovery from fossil fuel CO_2 perturbations, *Global Biogeochem. Cycles*, *20*, GB3009, doi:10.1029/2005GB002678.

1. Introduction

[2] Humans are adding CO_2 to the atmosphere through fossil fuel burning and land-use change. Fossil fuel burning dominates current annual CO_2 emissions and is likely to dominate total future CO_2 emissions. The global carbon cycle will respond to the added CO_2 over a range of timescales [*Archer et al.*, 1998, 1997; *Walker and Kasting*, 1992]. At present the land and ocean are both acting as carbon sinks and buffering the rate of CO_2 rise. Over the coming centuries the land may become a carbon source [*Cox et al.*, 2000; *Lenton*, 2000] while the ocean is likely to remain a robust carbon sink [*Bala et al.*, 2005; *Joos et al.*, 1999; *Lenton et al.*, 2006]. On the millennial timescale, emissions are likely to have ceased owing to reserves running out, if not to a conscious policy. The added carbon will have been initially apportioned between the ocean, land and atmosphere, with the ocean being the main sink [*Lenton and Cannell*, 2002]. The fraction of added CO_2 that enters the ocean on this timescale depends inversely and non-linearly on the amount of CO_2 emitted [*Lenton*, 2006; *Lenton and Cannell*, 2002]. Model estimates of ocean uptake range from ~80–90% [*Archer et al.*, 1997; *Kasting and Schultz*, 1996] for minimal emissions of ~1000 GtC to as little as ~30% if ~15,000 GtC of exotic plus conventional fossil fuel are emitted [*Lenton*, 2006; *Lenton et al.*, 2006].

[3] In the coming centuries, the acidification of ocean waters by CO_2 will begin to dissolve marine carbonate sediments, causing the carbonate compensation depth (CCD) to shoal toward the ocean surface. Over an estimated ~5–6 kyr, this process of dissolution will add alkalinity to the ocean and thus increase its capacity to store CO_2, removing a further 9–15% of added CO_2 from the atmosphere [*Archer et al.*, 1998, 1997]. Carbonate weathering on land will replenish ocean alkalinity thus allowing carbonate sediments to be redeposited and removing an estimated further 3–8% of added CO_2 on a timescale of ~8 kyr [*Archer et al.*, 1998]. This will still leave ~10% of the added CO_2 in the atmosphere, to be removed by the weathering of silicate rocks and subsequent deposition of carbonates in the ocean, over hundreds of thousands of years [*Archer et al.*, 1998; *Walker and Kasting*, 1992]. Thus what was rock-bound organic carbon (fossil fuel) will gradually return to the Earth's crust as carbonates, lowering atmospheric O_2 very slightly.

[4] With one notable exception [*Walker and Kasting*, 1992], existing studies of the long-term response to fossil fuel burning have assumed fixed weathering fluxes [*Archer et al.*, 1998, 1997; *Ridgwell and Edwards*, 2006]. However, it is well known that the rate of weathering reactions increase with temperature, precipitation and with CO_2 concentration in soil [*Berner et al.*, 1983; *Walker et al.*, 1981; *White and Blum*, 1995]. Furthermore, the process of weathering is actively amplified by plants and their associated fungal mycorrhizae, as well as by lichens, and various free living soil organisms [*Berner*, 1997; *Berner and Cochran*, 1998; *Lovelock and Watson*, 1982; *Schwartzman*

[1]School of Environmental Sciences, University of East Anglia, Norwich, UK.
[2]School of GeoSciences, University of Edinburgh, Edinburgh, UK.
[3]Also at Centre for Ecology and Hydrology, Edinburgh, UK.

Copyright 2006 by the American Geophysical Union.
0886-6236/06/2005GB002678$12.00

and Volk, 1989]. These factors have been included in models of the long-term carbon cycle and CO_2 on geologic timescales [*Bergman et al.*, 2004; *Berner*, 1997; *Berner and Kothavala*, 2001]. In a pioneering study, *Walker and Kasting* [1992] included the rock cycle and carbonate and silicate weathering in long-term projections of future global change. They assumed an abiotic CO_2 dependence of both types of weathering, which encapsulates the effects of temperature and associated changes in precipitation and runoff [*Walker et al.*, 1981]. On multimillennial timescales, enhanced carbonate weathering was found to have a greater drawdown effect on atmospheric CO_2 than the dissolution of carbonate sediments [*Walker and Kasting*, 1992].

[5] We postulate a further biologically amplified increase in the rate of weathering of carbonate and silicate minerals, induced by CO_2 fertilization of plant growth and global warming increasing rates of soil respiration and producing higher soil pCO_2. In support of this, tree growth experiments under elevated CO_2 suggest that in nutrient replete conditions, carbonate weathering is increased [*Williams et al.*, 2003]. Biological amplification of weathering will increase the flux of alkalinity to the oceans and thus accelerate the replenishment of the ocean with alkalinity and removal of residual added CO_2 from the atmosphere. Enhanced carbonate weathering should be important on a 10^3–10^4 year timescale, while enhanced silicate weathering should be important over 10^3–10^6 year timescales.

[6] To examine the potential effect of these mechanisms we extended a simple box model of the global carbon cycle and surface temperature to include carbonate sediments, carbonate weathering and silicate weathering. The resulting model is distinguished from that of *Walker and Kasting* [1992] in that it includes one deep ocean box instead of three, but has more sophisticated representations of carbonate sediments and land biota, and a direct dependence of carbonate and silicate weathering on plant productivity. We place more emphasis on longer timescales than *Walker and Kasting* [1992], separating out the impacts of carbonate and silicate weathering, considering a wider range of total CO_2 emissions, and quantifying the size of CO_2 release required to dissolve all carbonate sediments.

[7] The rest of the paper is organized as follows. Section 2 describes the extensions to the model, section 3 describes the methods, section 4 gives the results, section 5 is the discussion and section 6 gives the conclusions.

2. Model Description

[8] We started with a seven-box global carbon cycle model, coupled to an energy-balance approximation of global temperature [*Lenton*, 2000]. The carbon cycle model comprises reservoirs in the atmosphere, vegetation, soil, high-latitude surface water, low-latitude surface water, intermediate waters, and the deep ocean. Processes captured are photosynthesis, plant respiration, litter fall/mortality, soil respiration, CO_2 exchange between the atmosphere and surface ocean, circulation and mixing between various ocean boxes, and the sinking of biogenic material in the ocean. The ocean model is based on that of *Knox and McElroy* [1984], and here we use their circulation fluxes. To this we added marine carbonate sediments at 10 different depth intervals. Alkalinity and a generic nutrient (nitrate) were made variables (rather than fixed concentrations) within each ocean box. The processes of export production and remineralization in the water column were elaborated. Carbonate and silicate weathering processes and their controls were added, together with net input fluxes of alkalinity and carbon. Figure 1 shows a schematic of the extended model. Values for new parameters and alterations to existing parameters from the values used by *Lenton* [2000] are given in Table 1. The energy-balance model has an equilibrium climate sensitivity of 2.8°C for doubling CO_2, while quadrupling CO_2 gives 6.3°C warming at equilibrium.

2.1. Sediments, Remineralization, Deposition, and Dissolution

[9] The sediment layers are described in Table 2. Each sediment interval covers 500 m in depth, starting beneath the surface layer, which is 100 m thick. Thus the intermediate water box (depth 100–1100 m) contains the first two sediment intervals and the deep water box (depth 1100–5100 m) contains the remaining eight. The fraction of total seafloor (below 100 m depth) represented by each sediment interval (A_i) was calculated using bathymetry data. Thus the ocean depth and distribution of volume with depth are changed from *Lenton* [2000]. The deepest 500-m interval is assumed to cover all remaining area to the bottom of the ocean. The real ocean is deeper than 5100 m in places, but we are able to capture the range of carbonate compensation depths and their possible movement. Each sediment interval has a thickness reflecting the depth within the sediment that ocean chemistry can penetrate to. This is taken as 2.5 cm, corresponding to a 10 cm depth with the average porosity removed. The volume of each sediment reservoir also depends on the area of seafloor that it underlies. The resulting sediment reservoirs contain $CaCO_3$ and other detritus (dust, silica, etc.), which are treated as well mixed in this model.

[10] The ocean box model is adapted from *Knox and McElroy* [1984], and here we use their circulation fluxes (k_U and k_T) rather than the larger values adopted by *Lenton* [2000]. Low-latitude new production is assumed to be limited by the upwelling flux of a generic nutrient (nitrate) from intermediate waters. In the high latitudes, surface uptake of nitrate is assumed incomplete to account for iron and/or light limitation (hence the upwelling flux of nitrogen is multiplied by a parameter, $\alpha < 1$). The two sinking fluxes are combined to give a total flux (F_N) of nitrogen in new production. The corresponding organic carbon (F_{OrgC}) and inorganic carbon (F_{CaCO3}) export fluxes use Redfield ratios of $R_{C/N} = 7$ and $R_{CaCO3/OrgC} = 0.25$. After leaving the surface box, these sinking fluxes are prone to remineralization, and here we alter the model of *Knox and McElroy* [1984].

[11] The sinking flux of organic matter as a function of depth (z) is given by [*Ridgwell*, 2001]

$$F_{OrgC}(z) = F_{OrgC}\left(0.05 + 0.95\left(\frac{100 + (z - z_0)}{100}\right)^{-0.950}\right). \quad (1)$$

[12] Ninety-five percent is prone to consumption by organisms, returning dissolved inorganic carbon and nitrate

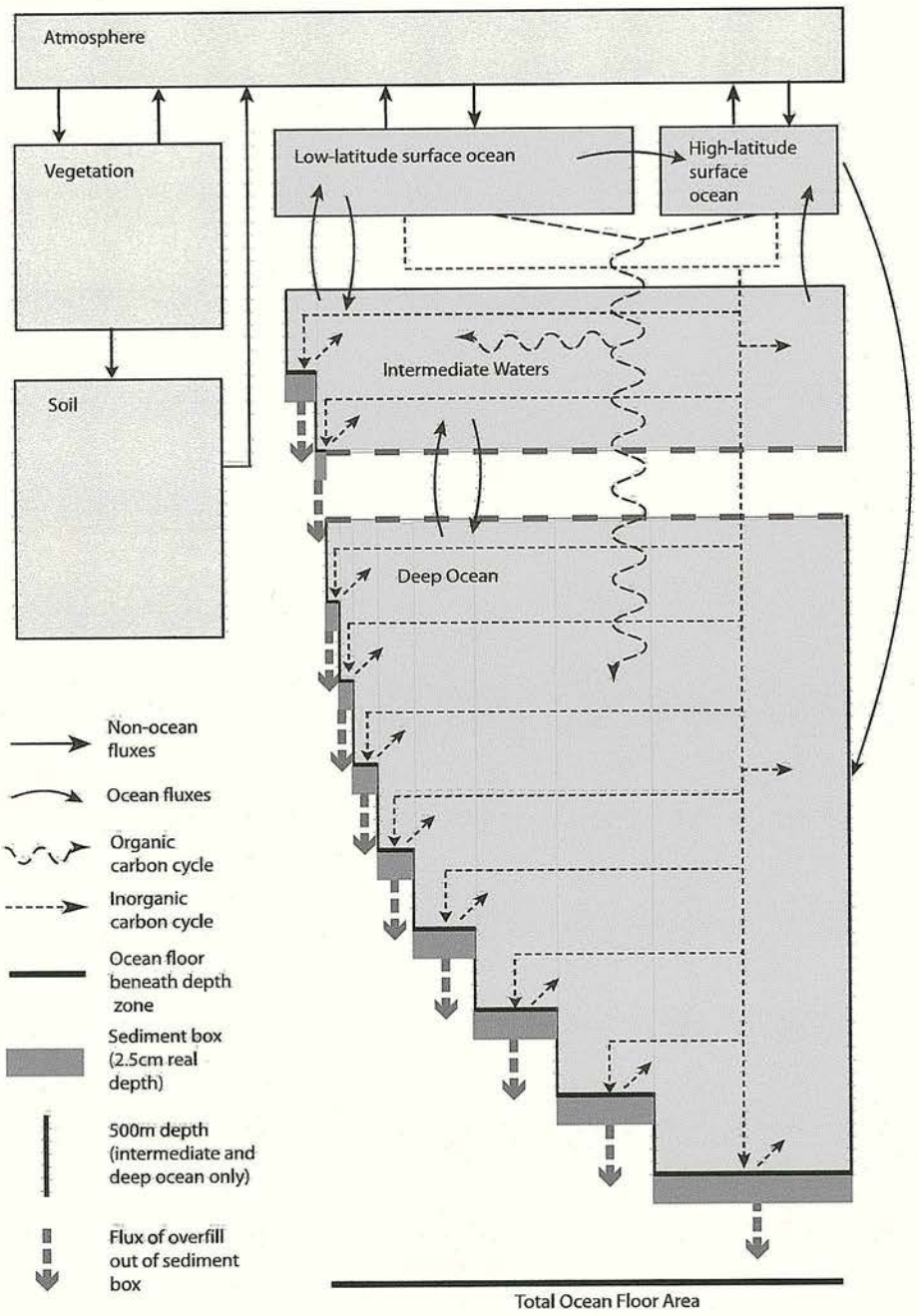

Figure 1. Schematic of the global carbon cycle model used herein, based on work by *Lenton* [2000] but with the addition of ocean sediments, ocean bathymetry, and weathering fluxes.

to the ocean water (in-transit remineralization). Some of the nonresistant fraction hits the seafloor and is remineralized in situ, returning dissolved inorganic carbon and nitrate to the ocean water above the sediment layer they have landed on. The remaining fraction (5%) of the sinking flux is assumed resistant to consumption in transit, and is only remineralized in situ when it lands on the seafloor. Thus all organic carbon is remineralized in the model, and none of it alters the chemistry of the sediments.

[13] The sinking flux of $CaCO_3$ (in the form of carbonate "tests" of organisms) as a function of depth (z) is given by [*Ridgwell*, 2001]

$$F_{CaCO_3}(z) = F_{CaCO_3}\left(0.4 + 0.6e^{\left(\frac{-(z-z_0)}{500}\right)}\right). \quad (2)$$

[14] Sixty percent is prone to in-transit dissolution, which returns dissolved inorganic carbon to the ocean. Forty

Table 1. Parameters Altered From *Lenton* [2000] and New Parameters

Parameter	Description	Value	Reference/Notes
k_T	thermohaline overturning	25 Sv	*Knox and McElroy* [1984]
k_U	high-latitude overturning	27 Sv	*Knox and McElroy* [1984]
K_M	half-saturation point for CO_2 fertilization	180 ppmv	tuned to give 1800–1990 CO_2 change
k_{MM}	photosynthesis normalizing constant	1.717	normalizes for preindustrial conditions
ε	dissolution exponent	4.5	*Berelson et al.* [1994]
χ	dissolution constant	20% d^{-1}	*Berelson et al.* [1994]
F_D	detrital flux	6×10^{12} mol/yr	*Treguer et al.* [1995]
$F^w_{Alk,0}$	preindustrial alkalinity input flux[a]	2×10^{13} mol Alk/yr	*Amiotte-Suchet et al.* [2003], *Milliman* [1993]
$F^w_{DIC,0}$	preindustrial carbon input flux[a]	1×10^{13} mol C/yr	*Amiotte-Suchet et al.* [2003], *Milliman* [1993]

[a]Net input to the open ocean is the river flux minus the coral reef removal flux.

percent is resistant to dissolution in transit and is guaranteed to reach the seafloor. The fate of the sinking $CaCO_3$ that reaches the sediments on the ocean floor depends on several factors. Deposition occurs if there is calcite oversaturation and in situ dissolution if there is undersaturation. The saturation state at any point within the ocean is described by

$$\Omega = \frac{[Ca^{2+}][CO_3^{2-}]}{k_{sp}}, \quad (3)$$

where $[Ca^{2+}]$ is the calcium ion concentration, $[CO_3^{2-}]$ the carbonate ion concentration and k_{sp} the stoichiometric solubility product. $[Ca^{2+}]$ is assumed constant throughout the ocean and proportional to total salinity [*Millero*, 1979]. Here k_{sp} depends on temperature and pressure [*Ingle*, 1975]. $[CO_3^{2-}]$ is calculated explicitly for each depth with the same chemistry scheme used in the surface ocean [*Lewis and Wallace*, 1998]. In situ dissolution from the ith sediment layer (F^i_{DIC}) is a function of the saturation state, Ω, and the volume of $CaCO_3$ in that sediment layer (V^i_{CaCO3}),

$$F^i_{DIC} = K_{VC} V^i_{CaCO_3} \chi (1 - \Omega)^{\varepsilon}, \quad (4)$$

where χ = 20% d^{-1} is the dissolution constant and ε = 4.5 is the dissolution exponent [*Berelson et al.*, 1994]. K_{VC} = 3.6525 converts from percent to fraction and from d^{-1} to yr^{-1}. There is also a constant detritus flux of silica deposited on the sediments, $F_D = 6 \times 10^{12}$ mol yr^{-1} [*Treguer et al.*, 1995]. The volume of each sediment layer (V_i) is held constant. After the balance of deposition and dissolution, there is in most cases net overfill, and in some cases net underfill, of the sediment layer, and to counteract this, the corresponding volume of sediment is removed from or added to the sediment layer (to/from outside the system). Detritus and $CaCO_3$ are removed or added in the same proportions that they are present in the sediment layer at that time step.

2.2. Weathering

[15] The net deposition of $CaCO_3$ in sediments and removal out of the system is balanced by a flux of alkalinity (F^w_{Alk}) and dissolved inorganic carbon (F^w_{DIC}) from weathering of carbonate and silicate rocks on land. These weathering fluxes were fixed initially, as a baseline from which to examine the effects of variable weathering. Our model input flux of alkalinity is the river flux from weathering minus the removal of alkalinity in coral reef formation, estimated at $\sim 1 \times 10^{13}$ mol yr^{-1} [*Milliman*, 1993] and assumed to be fixed. Using a recent estimate for the river alkalinity flux of $\sim 3.0 \times 10^{13}$ mol yr^{-1} [*Amiotte-Suchet et al.*, 2003], our initial input flux of alkalinity is $F^w_{Alk,0} = 2 \times 10^{13}$ mol yr^{-1}. This is found to give a model CCD somewhat below 3600 m as indicated by a drop to a low weight fraction of $CaCO_3$ in sediment layer 8 (3600–4100 m). In the real ocean the CCD varies with ocean basin, being at ~5 km in the Atlantic and at ~3.5 km in the Pacific, meaning there is no single "global" value but the model mean state is closer to the Pacific (the largest ocean basin). The fraction of the input flux of alkalinity due to carbonate weathering is f_{Ca} = 0.75 (1.5×10^{13} mol yr^{-1}) and the remainder due to silicate weathering is f_{Si} = 0.25 (5×10^{12} mol yr^{-1}) [*Bergman et al.*, 2004; *Walker and Kasting*, 1992].

[16] The carbon input flux is set at half the alkalinity flux, $F^w_{DIC,0} = 1 \times 10^{13}$ mol yr^{-1}, in order to balance the proportions in which carbon and alkalinity are removed from the system (under marine sediments). In effect this means that the input flux of volcanic/metamorphic CO_2 which is removed by silicate weathering and subsequent carbonate deposition, is added directly to rivers, rather than going via the atmosphere. This represents the smaller fraction (25%) of the river carbon flux, the remainder (75%) coming from carbonate weathering.

[17] Three formulations were used to separate the effects of variable carbonate and silicate weathering. In the first, the greater fraction (75%) of the river fluxes of alkalinity and carbon derived from carbonate weathering become a function of environmental variables, but silicate weathering

Table 2. Sediment Layer Depth Intervals, Areas, and Volumes

Layer i	Depth Interval, m	Fraction of Seabed A_i, %	Area of Seafloor, 10^{12} m^2	Volume of Layer V_i, 10^{12} m^3
1	100–600	5.056	17.39	0.4347
2	600–1100	2.095	7.20	0.1801
3	1100–1600	2.294	7.89	0.1972
4	1600–2100	2.662	9.15	0.2288
5	2100–2600	3.584	12.33	0.3081
6	2600–3100	6.488	22.31	0.5578
7	3100–3600	10.630	36.56	0.9139
8	3600–4100	14.832	51.01	1.2752
9	4100–4600	17.345	59.65	1.4913
10	4600–5100	35.014	120.41	3.0103

Table 3. Long-Term CO_2 Emissions Scenarios Used in This Study and Descriptions of the Fossil Fuel Emissions Trajectories

Label	Total LUC Emission,[a] GtC	Total Fossil Emission GtC	1990–2100	Beyond 2100	Reference, Label Therein
L1	212	2660	IS92a	linear decline to zero in 2200	*Lenton* [2000], 1
L2	212	1134	IS92c	linear decline to zero in 2200	*Lenton* [2000], 2
L3	212	4107	IS92e	linear decline to zero in 2200	*Lenton* [2000], 3
L4	212	4000	IS92a	linear decline to zero in 2332	*Lenton* [2000], 4
L5	212	4000	1990 level	linear decline to zero in 2926	*Lenton* [2000], 5
L6	212	4000	IS92e	linear decline to zero in 2194	*Lenton* [2000], 6
L7	212	9213	IS92a	+0.16 GtC/yr/yr to 2150 then linear decline to zero in 2599	*Lenton* [2006]
L8	212	15000	IS92a	+0.16 GtC/yr/yr to 2250 then linear decline to zero in 2634	*Lenton* [2006]
A23	0	4546	BAU A	constant 22.5 GtC/yr until 2300 and zero thereafter	*Archer et al.* [1998], A23

[a]In scenarios L1 to L8 the land-use change (LUC) scenario is identical and based on IS92a [*Lenton*, 2000].

remains fixed. We take the temperature response of carbonate weathering from the GEOCARB II model [*Berner*, 1994] and include plant productivity (P) in a manner similar to the COPSE model [*Bergman et al.*, 2004],

$$F^w_{\mathrm{Alk}} = F^w_{\mathrm{Alk},0}(f_{Si} + f_{Ca}(P/P_0)(1 + 0.087(T - T_0))) \quad (5)$$

$$F^w_{\mathrm{DIC}} = F^w_{\mathrm{DIC},0}(f_{Si} + f_{Ca}(P/P_0)(1 + 0.087(T - T_0))), \quad (6)$$

where T_0 is the initial (preindustrial) temperature (288.15K) and P_0 is the initial gross primary productivity, already calculated in the model as a function of CO_2 and T [*Lenton*, 2000]. It is assumed that carbonates saturate the soil or groundwater in contact with them so rapidly that changes in runoff do not result in appreciable dilution [*Berner*, 1994]. Hence the temperature term does not include the effect of changes in runoff. Changes in CO_2 have their dominant impact via their effect on plant productivity, represented by Michaelis-Menten kinetics (a hyperbolic response) and plant productivity responds to temperature following a cubic function [*Lenton*, 2000].

[18] In the second formulation, carbonate weathering is fixed and the smaller fraction (25%) of the river flux of alkalinity due to silicate weathering becomes a function of environmental variables. The whole river carbon flux must remain fixed because the fraction (25%) that counterbalances silicate weathering is derived from volcanic and metamorphic processes that are assumed constant on the timescales considered here. Once again the temperature response is taken from GEOCARB II and plant productivity introduced as a simple multiplier,

$$F^w_{Alk} = F^w_{Alk,0}(f_{Si}(P/P_0)(1 + 0.038(T - T_0))^{0.65} e^{0.09(T-T_0)} + f_{Ca}) \quad (7)$$

$$F^w_{\mathrm{DIC}} = F^w_{\mathrm{DIC},0}. \quad (8)$$

Changes in temperature have a direct effect on silicate weathering (the exponential term) and an indirect effect via changes in runoff [*Berner*, 1994].

[19] In the third formulation, both carbonate and silicate weathering are a function of environmental variables, making the river flux of alkalinity,

$$F^w_{Alk} = F^w_{Alk,0}(P/P_0)\Big(f_{Si}(1 + 0.038(T - T_0))^{0.65} e^{0.09(T-T_0)} + f_{Ca}(1 + 0.087(T - T_0))\Big). \quad (9)$$

In this case, the river flux of carbon is given by equation (6).

3. Methods

[20] The sediments were initialized without any $CaCO_3$ and spun up with the preindustrial river fluxes, giving the initial fractions of $CaCO_3$ shown in Figure 5b and an atmospheric CO_2 level of 287 ppmv. This is 9 ppmv higher than the preindustrial level of 278 ppmv and 7 ppmv higher than the 280 ppmv prescribed in the original model [*Lenton*, 2000]. The proximity to the actual preindustrial CO_2 level is good when compared with other coupled carbon cycle-sediment models [*Archer et al.*, 1998]. The model was then subjected to historical CO_2 emissions from fossil fuel burning and land-use change. The use of smaller fluxes for ocean thermohaline circulation (k_T) and mixing between the high-latitude surface ocean and the deep ocean (k_U) tend to weaken the ocean carbon sink. To achieve an improved fit to the historical change in atmospheric CO_2 from 1800 to 1990, the half-saturation constant for the CO_2 fertilization effect on photosynthesis was increased to K_M = 180 ppmv, which amounts to increasing the strength of the current land carbon sink.

[21] We subjected different model versions to a range of long-term CO_2 emissions scenarios (Table 3). These were chosen for comparison with earlier studies and to explore the effect of a wide range of plausible total CO_2 emissions. For each scenario the model was run with fixed weathering fluxes, with variable carbonate weathering, with variable silicate weathering, and with variable carbonate and silicate weathering. For the "L" scenarios in which there are land-use change (LUC) emissions, the default set-up is for the LUC carbon to be removed from vegetation and for a fraction (k_t = 0.27) of it to tend to permanently reduce steady state vegetation carbon ($C_{v(s)}$) [*Lenton*, 2000]. This represents the reduction in biomass associated with replacing forest with cropland or pasture. This permanent LUC

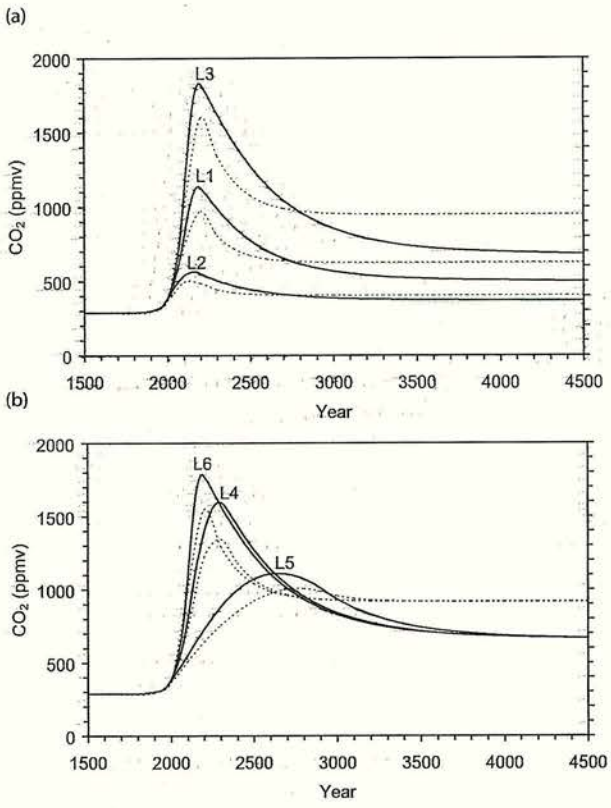

Figure 2. Comparing the millennial timescale CO_2 response of the extended model with carbonate sediments and fixed weathering fluxes (solid lines) with the original model (dashed lines) [*Lenton*, 2000] under different emissions scenarios (Table 3). (a) Burning different amounts of fossil fuel in the same time period (scenarios L1–L3). (b) Burning the same amount of fossil fuel (4000 GtC) in different time periods (scenarios L4–L6). For a given emissions scenario, peak atmospheric CO_2 is always higher and final atmospheric CO_2 is always lower in the extended model.

can be removed from the model without affecting total emissions, by treating LUC emissions as fossil fuel emissions and assuming no permanent reduction in vegetation carbon.

4. Results

[22] First we contrast the extended model with fixed weathering fluxes and the original [*Lenton*, 2000] (Figure 2). In 1990, atmospheric CO_2 is 364 ppmv, 11 ppmv higher than in the original model and observations. However, as CO_2 started 9 ppmv above observations, the CO_2 change is well captured. During the 1990s the ocean carbon sink is ~1.2 GtC yr^{-1}, somewhat below the observationally constrained estimate of 2.1 ± 0.7 GtC yr^{-1} [*Le Quéré et al.*, 2003]. This is largely compensated for by a strong land carbon sink of ~2.7 GtC yr^{-1} compared to estimates of 1.6–4.8 GtC yr^{-1} [*House et al.*, 2003]. Heading into the future, for a given emissions scenario, CO_2 typically peaks at a 10–20% higher concentration in the new model, due largely to the weaker ocean carbon sink. Toward the end of the millennium, however, CO_2 in the new model drops below that in the old model, as a consequence of dissolution of ocean carbonate sediments. By year 3000, CO_2 has fallen below that in the original model. By year 4500, CO_2 is still falling gradually and is significantly below that in the original model, in which it has stabilized.

[23] Next we compare our model with fixed weathering fluxes with that of *Archer et al.* [1998] (Figure 3). When driven with the same total emissions, atmospheric CO_2 peaks 130 ppmv lower in our model, having started ~30 ppmv lower. However, by year 10,000 the two models have reached similar atmospheric CO_2, sediment dissolution being close to complete and the total amount of dissolution being set by the total amount of fossil fuel emitted. Carbonate sediments dissolve much faster in our model than in that of *Archer et al.* [1998], thus maintaining a significant ocean carbon sink on the millennial timescale

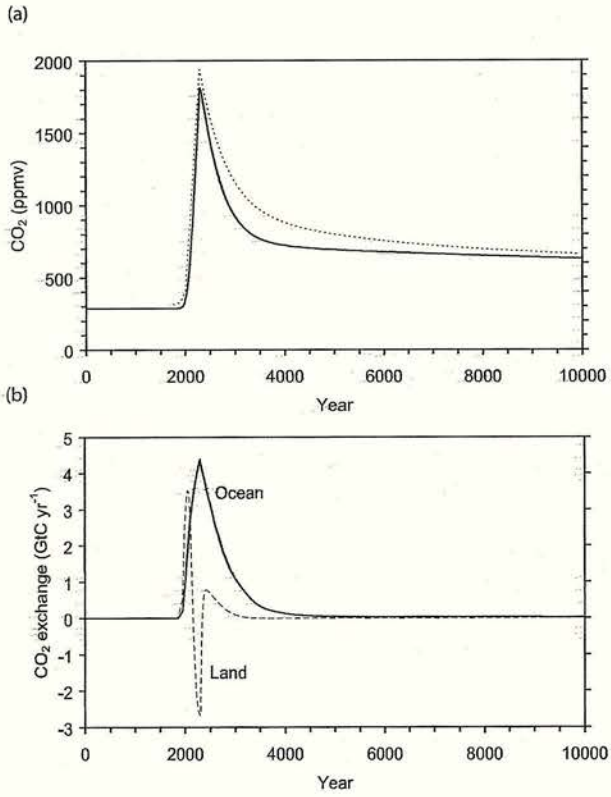

Figure 3. (a) Atmospheric CO_2 responses to year 10,000 for emissions scenario A23 (Table 3) of the extended model with fixed weathering fluxes (solid line) and the model of *Archer et al.* [1998] also with fixed weathering fluxes (dotted line). (b) CO_2 exchange in the extended model with fixed weathering fluxes from atmosphere to ocean (solid line) and from atmosphere to land (dashed line). Positive values indicate a carbon sink, and negative values indicate a carbon source.

Table 4. Effects of Variable Carbonate (Ca) and Silicate (Si) Weathering Fluxes and Permanent Land-Use Change (LUC) on Long-Term Atmospheric CO_2 for Different Emissions Scenarios[a]

			Atmospheric CO_2 in Year, ppmv				
Scenario	Permanent LUC	Variable Weathering	Peak	3000	10,000	100,000	1,000,000
L1	yes	fixed	1136	567	465	400	396
	yes	Ca	1131	556	442	384	384
	yes	Si	1131	555	441	361	323
	yes	Ca and Si	1125	545	423	361	324
	no	Ca and Si	1100	534	409	345	291
L2	yes	fixed	562	386	355	338	335
	yes	Ca	561	384	351	332	331
	yes	Si	561	384	351	328	321
	yes	Ca and Si	559	381	347	327	322
	no	Ca and Si	545	378	339	312	289
L3	yes	fixed	1830	855	615	466	461
	yes	Ca	1822	829	560	442	442
	yes	Si	1822	824	557	397	325
	yes	Ca and Si	1814	799	516	396	326
	no	Ca and Si	1796	776	494	369	292
L4	yes	fixed	1596	839	602	461	455
	yes	Ca	1585	814	548	437	437
	yes	Si	1583	810	545	394	325
	yes	Ca and Si	1572	787	508	394	325
	no	Ca and Si	1552	765	488	367	292
L5	yes	fixed	1110	933	602	460	455
	yes	Ca	1093	909	549	437	437
	yes	Si	1092	907	546	394	325
	yes	Ca and Si	1075	883	510	393	325
	no	Ca and Si	1054	862	490	367	292
L6	yes	fixed	1785	829	603	461	456
	yes	Ca	1777	804	549	438	438
	yes	Si	1777	800	546	395	325
	yes	Ca and Si	1769	776	509	394	325
	no	Ca and Si	1751	754	488	367	292
L7	yes	fixed	3619	2753	1892	764	750
	yes	Ca	3590	2695	1521	665	665
	yes	Si	3575	2658	1413	528	329
	yes	Ca and Si	3547	2600	1154	512	331
	no	Ca and Si	3559	2578	1057	476	297
L8	yes	fixed	6235	5303	4160	1342	1208
	yes	Ca	6209	5257	3730	1004	1002
	yes	Si	6182	5195	3284	670	334
	yes	Ca and Si	6155	5149	2869	665	338
	no	Ca and Si	6201	5166	2676	627	302
A23	no	fixed	1810	923	630	474	469
	no	Ca	1797	889	563	437	434
	no	Si	1796	884	560	385	292
	no	Ca and Si	1783	852	508	373	292

[a]LUC switch does not alter total CO_2 emissions for a given scenario.

(Figure 3b) and drawing down atmospheric CO_2 more rapidly. Although at the time of peak CO_2 (year 2300) the land has become a significant carbon source, uptake of carbon by the land surface since preindustrial time exceeds loss giving a net gain of 250 GtC, while 970 GtC have entered the ocean. Net land uptake can thus account for the reduction in peak atmospheric CO_2 relative to Archer's model of ~210 GtC, suggesting that the ocean sinks are of similar strength in the two models. In both Archer's model and our own, carbonate sediments are not totally dissolved under this emissions scenario. Complete stabilization of the system takes over 100 kyr, but the system is close to steady state after 60 kyr, with atmospheric CO_2 at about 475 ppmv, which is ~200 ppmv above the preindustrial. This corresponds to a remaining airborne fraction (of added CO_2) of 9.3% in close agreement with *Archer et al.* [1998]. The fate of this remaining anthropogenic CO_2 depends on the response of carbonate and silicate weathering processes.

[24] Now we contrast the effects of fixed weathering, variable carbonate weathering, variable silicate weathering, or variable carbonate and silicate weathering with or without land-use change, on the long-term response of atmospheric CO_2. Results for all the different emissions scenarios are summarized in Table 4. The effect of variable weathering on the future trajectory of atmospheric CO_2 is felt on 10^3–10^6 year timescales, there being only a minor effect on the atmospheric CO_2 peak that occurs on centennial timescales. Allowing carbonate weathering alone to vary accelerates the drawdown of CO_2 on 10^3–10^4 year timescales, lowers the final steady state modestly, but still leaves it well above the preindustrial level and does not alter

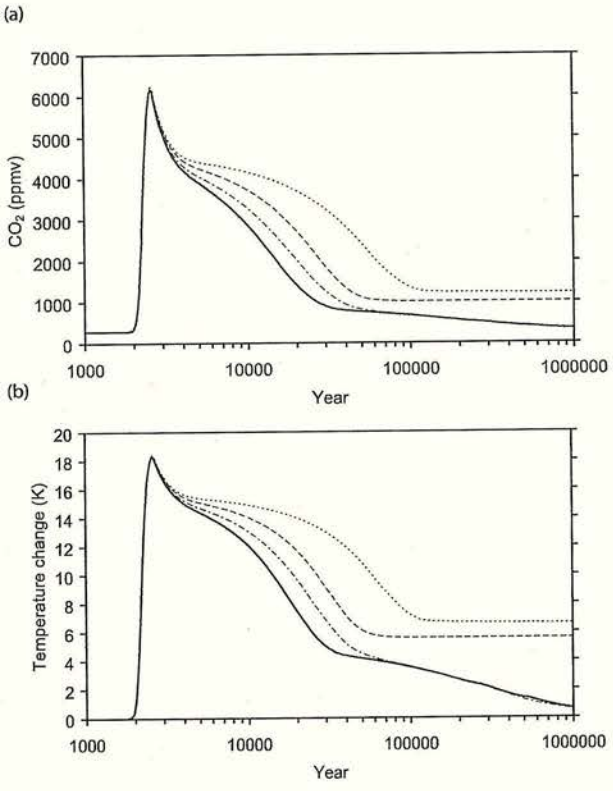

Figure 4. Long-term response of (a) atmospheric CO_2 and (b) global temperature to scenario L8, 15,000 GtC emissions of "exotic" and conventional fossil fuel reserves, for different model variants: fixed weathering (dotted line), variable carbonate weathering (dashed line), variable silicate weathering (dash-dotted line), and variable carbonate and silicate weathering (solid line).

the $\sim 10^5$ year timescale of response. Allowing only silicate weathering to vary has a similar effect to carbonate weathering on 10^3–10^4 year timescales, but on 10^5–10^6 year timescales it causes ongoing drawdown of CO_2, which, in the absence of permanent land-use change (e.g., scenario A23), is eventually returned to preindustrial level. Allowing carbonate and silicate weathering to vary together further accelerates CO_2 drawdown on 10^3–10^4 year timescales, but gives similar results to silicate weathering alone on 10^5–10^6 year timescales.

[25] The acceleration of CO_2 drawdown due to variable weathering is greatest in scenarios where sufficient fossil fuel is emitted to dissolve all carbonate sediments in the ocean, which corresponds to $\geq$7350 GtC. In such cases, the buffering effect of the sediments is removed, and the further drawdown of atmospheric CO_2 relies on weathering and the consequent increase in ocean alkalinity, until the sediments start to recover. To illustrate this, Figure 4 shows the results of emitting a total of 15,000 GtC from "exotic" and "conventional" fossil fuel reserves. Allowing carbonate weathering alone to vary accelerates the recovery of atmospheric CO_2 by more than a factor of 2 over much of the range of CO_2 drawdown. For example, instead of reaching 2000 ppmv after 61,000 years it is reached in 28,000 years. Allowing silicate weathering alone to vary accelerates the drawdown of CO_2 by a factor of 3 over much of the range, for example, 2000 ppmv is reached in 20,000 years. Allowing both carbonate and silicate weathering to vary accelerates the recovery by roughly a factor of 4 over much of the range, 2000 ppmv being reached in 15,000 years. Variable silicate weathering also allows an ongoing drawdown of CO_2 over the 10^5–10^6 year timescale. The temperature changes seen under this emission scenario are huge (Figure 4b). Without variable silicate weathering, temperature remains indefinitely 5.6°C (variable carbonate weathering) or 6.6°C (fixed weathering) above preindustrial.

[26] With variable carbonate and silicate weathering, the input flux of alkalinity is more than tripled for thousands of years (Figure 5a). An initial spike in weathering flux is followed by a decline, due to excessive warming suppressing productivity, and then a recovery as the planet cools and productivity recovers. The long, slow decline of CO_2 and temperature forces a corresponding decline in weathering

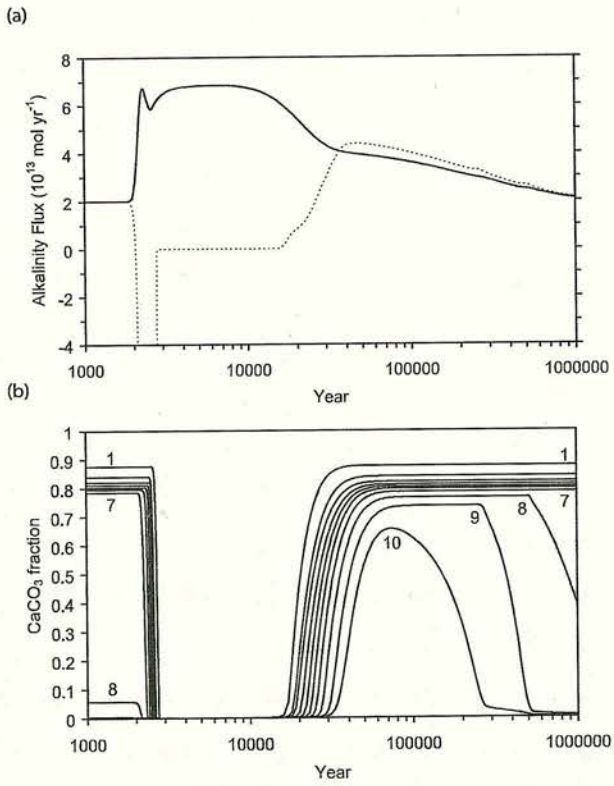

Figure 5. Long-term responses of weathering and sediments to scenario L8, 15,000 GtC emissions, in the model with variable carbonate and silicate weathering. (a) Alkalinity fluxes from weathering (solid line) and net sediment deposition or dissolution (dotted line). (b) Calcium carbonate fraction in the 10 sediment layers (number labels increase with depth). A negative value for the dotted line in Figure 5a indicates net sediment dissolution (i.e., addition of alkalinity to the ocean). When the weathering and sedimentation fluxes are equal, the system is in steady state.

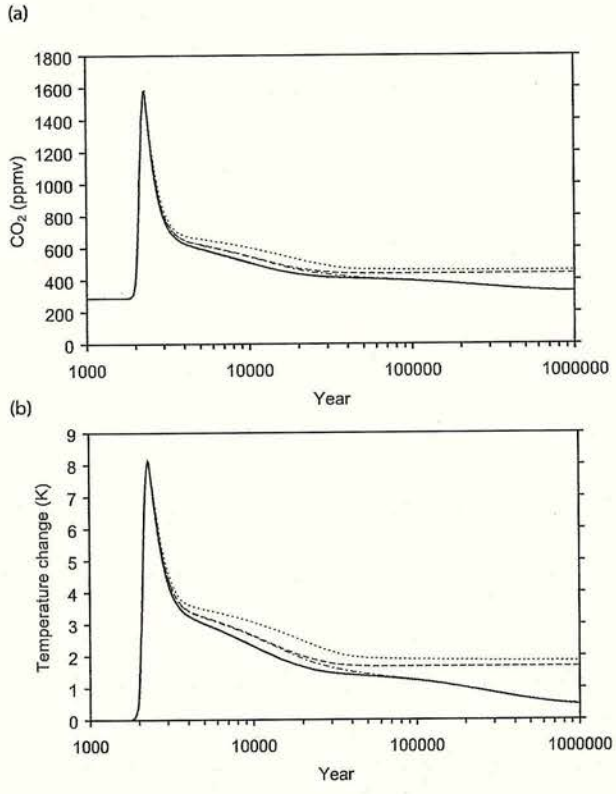

Figure 6. Long-term response of (a) atmospheric CO_2 and (b) global temperature to scenario L4, 4000 GtC emissions of all conventional fossil fuel reserves, for different model variants: fixed weathering (dotted line), variable carbonate weathering (dashed line), variable silicate weathering (dash-dotted line), and variable carbonate and silicate weathering (solid line).

rates. All carbonate sediments dissolve within the millennium by year 2800 (Figure 5b). The top layer of sediments begins to recover 14,000 years later and takes a further 11,000 years for its $CaCO_3$ content to exceed 80%. Each subsequent sediment layer with depth recovers in turn and takes progressively longer to do so. As the sediments recover they remove alkalinity from the ocean and thus buffer and slow the fall of CO_2. The bottom sediment layer starts to recover 28,000 years after the fossil fuel perturbation is complete and reaches a peak carbonate content of 65% after 75,000 years. This represents an overcompensation by the system and over the following hundreds of thousands of years, as the ocean continues to receive an enhanced alkalinity input from weathering, the CCD shoals. After 1 Myr, the CCD has yet to return to its original depth and CO_2 is still at 338 ppmv, 52 ppmv above its preindustrial concentration, and falling at $\sim 5 \times 10^{-5}$ ppmv yr^{-1}.

[27] Atmospheric CO_2 eventually stabilizes after ~8 Myr at 320 ppmv, still 34 ppmv above preindustrial. CO_2 fails to return to the preindustrial level because it is assumed that a fraction ($k_t = 0.27$ [*Lenton*, 2000]) of land-use change tends to permanently reduce vegetation carbon. This in turn tends to reduce the global terrestrial gross primary productivity (P), which is assumed to affect weathering. In order to compensate for this and return P and hence silicate weathering flux to its original value, to match the fixed volcanic CO_2 flux, CO_2 and temperature must stabilize above preindustrial levels.

[28] In response to emitting 4000 GtC of conventional fossil fuel reserves to the atmosphere initially following business-as-usual (scenario L4), although the CO_2 perturbation is much smaller and not all carbonate sediments are dissolved, weathering still greatly accelerates the recovery to a given CO_2 level and temperature (Figure 6). To return to a global temperature of 2.0°C above preindustrial, corresponding to 475 ppmv, takes until year 37,000 with fixed weathering, year 19,000 with variable carbonate weathering, year 18,000 with variable silicate weathering, and year 13,000 with variable carbonate and silicate weathering. Silicate weathering has a similar impact to carbonate weathering on 10^3–10^4 year timescales (Figure 6), despite supplying only 25% of the initial alkalinity input flux, because it is the excess input flux of alkalinity relative to carbon that contributes to CO_2 drawdown. This is very similar in both cases because when silicate weathering is amplified there is no change in the corresponding carbon flux, whereas when carbonate weathering is amplified, both carbon and alkalinity fluxes are increased, the latter more than the former.

[29] With variable carbonate and silicate weathering, the input flux of alkalinity nearly triples on the centennial timescale and is double preindustrial in year 3000 (Figure 7a). Carbonate sediments below 1600 m are completely dissolved by year 3000 (Figure 7b) and those in the range 600–1600 m experience ongoing dissolution, losing around half their carbonate by year 4000. The sediment system then begins to recover. At around 30,000 years after fossil fuel perturbation, alkalinity input from weathering and alkalinity removal in carbonate dissolution are temporarily in balance (Figure 7a) and hence CO_2 is stabilized. However, deposition continues to increase, with a maximum depth for the CCD being reached after 70,000 years. The system overshoots in that carbonate deposition and corresponding alkalinity removal exceeds alkalinity input, causing ongoing dissolution. This process is incomplete after 1 Myr when CO_2 is at 325 ppmv, 39 ppmv above its initial preindustrial level and falling at $\sim 10^{-5}$ ppmv yr^{-1}. CO_2 eventually stabilizes at 320 ppmv, as before, because this is determined by the land-use change scenario which is the same for the different fossil fuel scenarios.

[30] In response to a minimum emissions scenario (L2) totaling ~1100 GtC, weathering still markedly accelerates the recovery to a given CO_2 level (Table 4) and temperature; 350 ppmv is reached around year 14,000 with fixed weathering, year 11,000 with variable carbonate or silicate weathering, and year 9000 with variable carbonate and silicate weathering. The effect of variable carbonate weathering on final CO_2 after 1 Myr is small, lowering it from 335 ppmv to 331 ppmv, while variable silicate weathering reduces it further to 321 ppmv, only 1 ppmv above its final steady state, with a rate of decline of $\sim 10^{-6}$ ppmv yr^{-1}. When land-use change is assumed not to cause a permanent

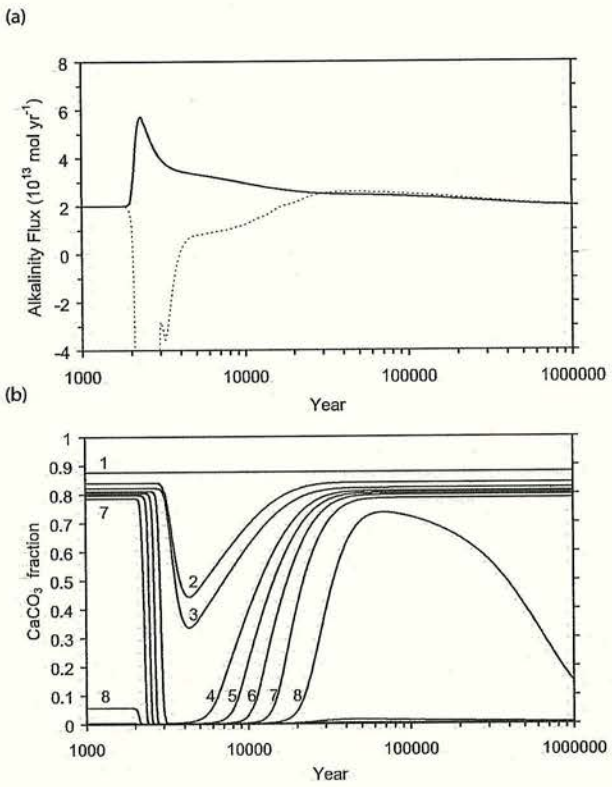

Figure 7. Long-term responses of weathering and sediments to scenario L4, 4000 GtC emissions, in the model with variable carbonate and silicate weathering. (a) Alkalinity fluxes from weathering (solid line) and net sediment deposition or dissolution (dotted line). (b) Calcium carbonate fraction in the 10 sediment layers (number labels increase with depth).

reduction in vegetation carbon, atmospheric CO_2 does eventually return to its preindustrial level, being 25 ppmv above it after 100 kyr and only 2 ppmv above it after 1 Myr.

[31] The fraction of cumulative CO_2 emissions remaining in the atmosphere on different timescales is summarized in Table 5 for all the emissions scenarios in the model with variable carbonate and silicate weathering and no permanent land use. This emphasizes that the lifetime of the remaining added CO_2 increases with time [*Kasting and Schultz*, 1996], and it will take more than a million years for all of it to be removed [*Walker and Kasting*, 1992].

5. Discussion

[32] Carbonate sediments dissolve more rapidly in our model than in previous studies [*Archer et al.*, 1998; *Walker and Kasting*, 1992]. This leads to a significant drawdown of CO_2 on the millennial timescale, relative to a version of the model without sediments. In the transient response, dissolution can exceed weathering as a source of alkalinity by a factor of ~20. This response should be treated with caution given the simplicity of our model. In reality, calcium carbonate below the sediment surface will be better protected from the corrosive effects of CO_2-rich ocean water than in our treatment with well mixed sediment layers. Despite this caveat, after ~10 kyr the responses of our model and that of *Archer et al.* [1998] are almost identical for the same total amount of CO_2 released, because a simple titration has occurred.

[33] We have not used the same emissions scenarios as *Walker and Kasting* [1992]. However, comparing their "profligate" scenario [*Walker and Kasting*, 1992, Figures 27 and 29], which emits 4200 GtC in a peaked fashion, to similar scenarios (L3, L4, L6, A23) in our model, it is clear that for the same emissions, peak CO_2 would be lower in our model, suggesting a stronger ocean sink. CO_2 recovers faster in our model over the first few thousand years for all formulations of weathering, indicating a much greater impact of sediment dissolution. *Walker and Kasting* [1992] find that carbonate weathering significantly enhances CO_2 drawdown on the millennial timescale, because it depends linearly on CO_2 in their standard model, and hence peaks at ~8 times the present rate. In contrast, variable carbonate and silicate weathering become more important for CO_2 drawdown after year 3000 in our model. However, beyond year 20,000 the two models converge, and both take over a million years for atmospheric CO_2 to recover to preindustrial levels.

Table 5. Fraction of Cumulative CO_2 Emissions Remaining in the Atmosphere at Different Times for All Emissions Scenarios[a]

	Airborne Fraction in Year, %											
Scenario	2000	2100	2300	2500	3000	5000	10,000	30,000	100,000	300,000	500,000	1,000,000
L1	46.3	55.8	48.9	32.8	18.3	12.4	8.99	5.66	4.30	2.10	1.06	0.25
L2	45.9	44.3	31.6	22.8	14.2	10.5	8.22	5.31	3.87	1.97	1.07	0.32
L3	46.6	63.5	63.4	44.8	24.0	14.9	10.2	5.70	4.01	2.25	1.10	0.24
L4	46.3	55.8	64.5	46.3	24.1	14. 9	10.2	5.71	4.02	2.23	1.10	0.24
L5	46.0	45.7	48.6	46.1	29.1	15.1	10.3	5.72	4.03	2.24	1.10	0.24
L6	46.6	63.5	62.3	43.8	23.5	14.9	10.1	5.70	4.02	2.24	1.10	0.24
L7	46.3	55.8	80.3	76.3	51.7	30.7	17.4	6.22	4.26	2.08	1.18	0.21
L8	46.3	55.8	87.4	86.3	68.3	49.9	33.4	7.33	4.76	2.10	1.04	0.20
A23	47.6	52.1	70.2	51.9	26.5	15.4	10.4	5.71	4.02	2.27	1.11	0.23

[a]The model used is with variable Ca and Si weathering and no permanent land-use change; hence the airborne fraction eventually reaches zero.

[34] We find that the contribution of enhanced weathering to carbon cycle recovery is somewhat dependent on whether all sediments dissolve and corresponding buffering capacity is lost in the ocean. The amount of fossil fuel CO_2 required to dissolve all carbonate sediments in our model is 7350 GtC, whereas *Archer* [2005] calculates ~5000 GtC. The difference is due to the calculated initial inventory of $CaCO_3$, which is in turn a function of assumed sediment depth, detrital flux and calculated CCD. Emitted CO_2 in excess of that required to dissolve all carbonate sediments tends to remain in the atmosphere until weathering can provide the alkalinity to neutralize it. Enhancement of weathering can accelerate the recovery of CO_2 in this regime by a factor of 4. However, even when all sediments are not dissolved, recovery can be accelerated by more than a factor of 2.

[35] *Archer* [2005] calculates that ~7% of added CO_2 remains in the atmosphere longer than 100 kyr. With variable carbonate and silicate weathering and no permanent land use, we estimate ~4–5% (Table 5) depending on the total emissions. This lower value is to be expected given the modeled enhancement of weathering. The lingering fossil CO_2 has potentially important consequences for the glacial-interglacial cycles that characterized the Quaternary. *Archer and Ganopolski* [2005] have recently calculated that a fossil fuel perturbation of 5000 GtC is sufficient to prevent glacial inception for at least the next 500,000 years.

[36] Our results support the suggestion that artificially accelerating carbonate weathering by reacting CO_2-rich power plant gases with seawater and then reacting the resulting carbonic acid solution with carbonate rocks would be an effective way of sequestering CO_2 [*Caldeira and Rao*, 2000]. The results also show interesting interactions between the negative feedbacks in the carbon cycle involving carbonate compensation and silicate weathering. The interaction is antagonistic and slows the recovery of atmospheric CO_2 when, after 20–50 kyr, sediments are reestablishing. Indeed, CO_2 is temporarily stabilized when alkalinity removal from the ocean due to carbonate deposition temporarily matches alkalinity input. The system then overshoots, and over 10^5–10^6 years, the interaction between carbonate dissolution and silicate weathering is synergistic, with a slight, gradual dissolution of sediments contributing to CO_2 uptake.

[37] This complicates the traditional interpretation of the response time of the silicate weathering feedback. Other studies [*Archer*, 2005; *Archer and Ganopolski*, 2005] have assumed a ~400-kyr response time based on the work of *Sundquist* [1991]. We find that after ~100 kyr, once sediments begin their final adjustment phase, the half-life for the decay of added CO_2 is ~200 kyr regardless of the amount of CO_2 added (Table 5), or whether land-use change is assumed to permanently reduce vegetation carbon or not. Ongoing sediment dissolution must be contributing to reducing this response time.

[38] It is notable that in the presence of land-use change, CO_2 never recovers to preindustrial level in our simulations even when they are run out to equilibrium. This is because it is assumed that a fraction ($k_t = 0.27$ [*Lenton*, 2000]) of land-use change tends to permanently reduce vegetation carbon, which in turn tends to reduce the global terrestrial gross primary productivity (P), which in turn affects weathering. To achieve a long-term steady state, the silicate weathering flux must return to its initial value and match the fixed volcanic CO_2 flux. This can only be achieved by stabilizing CO_2 and temperature above their preindustrial levels. The assumption that there is a permanent element to land-use change may be flawed, as it presumes either that humans will still be around and using the land a million years hence or that if we are not, natural ecosystems will have failed to recover to their preindustrial and preagricultural state. However, some vegetation-climate systems such as the Amazon rain forest are thought to be bi-stable [*Betts*, 1999] and if the forest either dies back [*Cox et al.*, 2004] or is deforested, they may remain in an alternative steady state with lower carbon storage. If that state tends to have smaller weathering fluxes, then the long-term steady state for CO_2 will accordingly be shifted upward.

[39] Natural mechanisms that have caused glacial drawdown of CO_2 by ~80–100 ppmv could in principle override the longer-term control by silicate weathering. However, drawdown of CO_2 appears to follow glacial inception, and *Archer and Ganopolski* [2005] have pointed out that a ~5000 GtC fossil fuel perturbation could prevent glaciation for at least the next 500,000 years. Our results agree with this and suggest that if humans choose to exploit "exotic" fossil fuel reserves and emit ~15,000 GtC, then glaciation could be prevented for over a million years. Furthermore, if there is a permanent change in vegetation cover that tends to reduce silicate weathering rates, then it may cause atmospheric CO_2 to remain at levels that prevent glaciation indefinitely.

[40] Future work will examine the weathering and carbonate sediment response to fossil fuel perturbation in "GENIE-1" [*Lenton et al.*, 2006] an Earth system model of intermediate complexity (EMIC) with a closed carbon cycle, to which ocean sediments have now been added.

6. Conclusions

[41] Increasing atmospheric CO_2 and global temperatures are expected to increase carbonate and silicate weathering rates, via the direct effects of warming, and indirectly, via the CO_2 fertilization effect on plants and warming enhancing soil respiration. This enhanced weathering should in turn increase alkalinity input to the ocean and long-term CO_2 uptake. Our model experiments suggest that amplified carbonate and silicate weathering will greatly accelerate CO_2 removal from the atmosphere 10^4–10^5 years after the fossil fuel perturbation. The acceleration of CO_2 drawdown is greatest for emissions of $\geq$7350 GtC, which cause the dissolution of all carbonate sediments. However, it still takes $>10^6$ years for silicate weathering to stabilize CO_2. The final steady state CO_2 could be above the preindustrial ~280 ppmv if the effects of land-use change persist on a million-year timescale and tend to reduce global productivity and weathering rates relative to preindustrial and preagricultural conditions (e.g., by having transformed areas of forest to pasture or cropland). This in turn could prevent glaciation indefinitely.

[42] **Acknowledgments.** We thank Andy Ridgwell for advice on modeling carbonate sediments, David Archer for providing model output and emissions scenarios, and Andrew Yool for assistance with calculating global bathymetry. Jim Kasting and Ken Caldeira provided helpful review comments. T. M. L.'s work is an output of the GENIE*fy* project (NE/C515904/1) of the UK Natural Environment Research Council (NERC). C. B.'s Ph.D. studentship is funded by NERC with CASE support from the Centre for Ecology and Hydrology, Edinburgh.

References

Amiotte-Suchet, P., J.-L. Probst, and W. Ludwig (2003), Worldwide distribution of continental rock lithology: Implications for the atmospheric/soil CO_2 uptake by continental weathering and alkalinity river transport to the oceans, *Global Biogeochem. Cycles*, *17*(2), 1038, doi:10.1029/2002GB001891.

Archer, D. (2005), fossil fuel CO_2 in geologic time, *J. Geophys. Res.*, *110*, C09S05, doi:10.1029/2004JC002625.

Archer, D., and A. Ganopolski (2005), A movable trigger: Fossil fuel CO_2 and the onset of the next glaciation, *Geochem. Geophys. Geosyst.*, *6*, Q05003, doi:10.1029/2004GC000891.

Archer, D., H. S. Kheshgi, and E. Maier-Reimer (1997), Multiple timescales for neutralization of fossil fuel CO_2, *Geophys. Res. Lett.*, *24*, 405–408.

Archer, D., H. Kheshgi, and E. Maier-Reimer (1998), Dynamics of fossil fuel CO_2 neutralization by marine $CaCO_3$, *Global Biogeochem. Cycles*, *12*, 259–276.

Bala, G., K. Caldeira, A. Mirin, M. Wickett, and C. Delire (2005), Multicentury changes to the global climate and carbon cycle: Results from a coupled climate and carbon cycle model, *J. Clim.*, *18*, 4531–4544.

Berelson, W. M., D. E. Hammond, J. McManus, and T. E. Kilgore (1994), Dissolution kinetics of calcium carbonate in equatorial Pacific sediments, *Global Biogeochem. Cycles*, *8*, 219–235.

Bergman, N. M., T. M. Lenton, and A. J. Watson (2004), COPSE: A new model of biogeochemical cycling over Phanerozoic time, *Am. J. Sci.*, *304*, 397–437.

Berner, R. A. (1994), Geocarb II: A revised model of atmospheric CO_2 over Phanerozoic time, *Am. J. Sci.*, *294*, 56–91.

Berner, R. A. (1997), The rise of plants and their effect on weathering and atmospheric CO_2, *Science*, *276*, 544–546.

Berner, R. A., and M. F. Cochran (1998), Plant-induced weathering of Hawaiian basalts, *J. Sed. Res.*, *68*, 723–726.

Berner, R. A., and Z. Kothavala (2001), Geocarb III: A revised model of atmospheric CO_2 over Phanerozoic time, *Am. J. Sci.*, *301*, 182–204.

Berner, R. A., A. C. Lasaga, and R. M. Garrels (1983), The carbonate-silicate geochemical cycle and its effect on atmospheric carbon dioxide over the past 100 million years, *Am. J. Sci.*, *283*, 641–683.

Betts, R. A. (1999), Self-beneficial effects of vegetation on climate in an ocean-atmosphere general circulation model, *Geophys. Res. Lett.*, *26*, 1457–1460.

Caldeira, K., and G. H. Rao (2000), Accelerating carbonate dissolution to sequester carbon dioxide in the ocean: Geochemical implications, *Geophys. Res. Lett.*, *27*, 225–228.

Cox, P. M., R. A. Betts, C. D. Jones, S. A. Spall, and I. J. Totterdell (2000), Acceleration of global warming due to carbon-cycle feedbacks in a coupled climate model, *Nature*, *408*, 184–187.

Cox, P. M., R. A. Betts, M. Collins, P. P. Harris, C. Huntingford, and C. D. Jones (2004), Amazonian forest dieback under climate-carbon cycle projections for the 21st century, *Theor. Appl. Climatol.*, *78*, 137–156.

House, J. I., I. C. Prentice, N. Ramankutty, R. A. Houghton, and M. Heimann (2003), Reconciling apparent inconsistencies in estimates of terrestrial CO_2 sources and sinks, *Tellus, Ser. B*, *53*, 345–363.

Ingle, S. E. (1975), Solubility of calcite in the ocean, *Mar. Chem.*, *3*, 301–309.

Joos, F., G.-K. Plattner, T. F. Stocker, O. Marchal, and A. Schmittner (1999), Global warming and marine carbon cycle feedbacks on future atmospheric CO_2, *Science*, *284*, 464–467.

Kasting, J. F., and P. A. Schultz (1996), Reservoir time-scales for anthropogenic CO_2 in the atmosphere: Commentary, *Tellus, Ser. B*, *48*, 703–706.

Knox, F., and M. B. McElroy (1984), Changes in atmospheric CO_2: Influence of the marine biota at high latitude, *J. Geophys. Res.*, *89*, 4629–4637.

Lenton, T. M. (2000), Land and ocean carbon cycle feedback effects on global warming in a simple Earth system model, *Tellus, Ser. B*, *52*, 1159–1188.

Lenton, T. M. (2006), Climate change to the end of the millennium, *Clim. Change*, *76*, 7–29.

Lenton, T. M., and M. G. R. Cannell (2002), Mitigating the rate and extent of global warming, *Clim. Change*, *52*, 255–262.

Lenton, T. M., M. S. Williamson, N. R. Edwards, R. Marsh, A. R. Price, A. J. Ridgwell, J. G. Shepherd, S. J. Cox, and the GENIE team (2006), Millennial timescale carbon cycle and climate change in an efficient Earth system model, *Clim. Dyn.*, *76*, 687–711, doi:10.1007/s00382-006-0109-9.

Le Quéré, C., et al. (2003), Two decades of ocean CO_2 sink and variability, *Tellus, Ser. B*, *55*, 649–656.

Lewis, E., and D. Wallace (1998), Program developed for CO_2 system calculations, report, Carbon Dioxide Inf. Anal. Cent., Oak Ridge, Tenn.

Lovelock, J. E., and A. J. Watson (1982), The regulation of carbon dioxide and climate: Gaia or geochemistry?, *Planet. Space Sci.*, *30*, 795–802.

Millero, F. J. (1979), The thermodynamics of the carbonate system in seawater, *Geochim. Cosmochim. Acta*, *43*, 1651–1661.

Milliman, J. D. (1993), Production and accumulation of calcium carbonate in the ocean: Budget of a nonsteady state, *Global Biogeochem. Cycles*, *7*, 927–957.

Ridgwell, A. J. (2001), Glacial-interglacial perturbations in the global carbon cycle, Ph.D. thesis, 134 pp., Univ. of East Anglia, Norwich, U. K.

Ridgwell, A. J., and U. Edwards (2006), Geological carbon sinks, in *Greenhouse Gas Sinks*, edited by D. Reay et al., CAB Int., Cambridge, Mass., in press.

Schwartzman, D. W., and T. Volk (1989), Biotic enhancement of weathering and the habitability of Earth, *Nature*, *340*, 457–460.

Sundquist, E. T. (1991), Steady- and non-steady-state carbonate-silicate controls on atmospheric CO_2, *Q. Sci. Rev.*, *10*, 283–296.

Treguer, P., D. M. Nelson, A. J. Van Bennekom, D. J. DeMaster, A. Leynaert, and B. Queguiner (1995), The silica balance in the world ocean: A reestimate, *Science*, *268*, 375–379.

Walker, J. C. G., and J. F. Kasting (1992), Effects of fuel and forest conservation on future levels of atmospheric carbon dioxide, *Palaeogeogr. Palaeoclimatol. Palaeoecol.*, *97*, 151–189.

Walker, J. C. G., P. B. Hays, and J. F. Kasting (1981), A negative feedback mechanism for the long-term stabilisation of Earth's surface temperature, *J. Geophys. Res.*, *86*, 9776–9782.

White, A. F., and A. E. Blum (1995), Effects of climate on chemical weathering in watersheds, *Geochim. Cosmochim. Acta*, *59*, 1729–1747.

Williams, E. L., L. M. Walter, T. C. W. Ku, G. W. Kling, and D. R. Zak (2003), Effects of CO_2 and nutrient availability on mineral weathering in controlled tree growth experiments, *Global Biogeochem. Cycles*, *17*(2), 1041, doi:10.1029/2002GB001925.

C. Britton, School of GeoSciences, University of Edinburgh, Grant Institute, Kings Buildings, West Mains Road, Edinburgh EH9 3JW, UK.

T. M. Lenton, School of Environmental Sciences, University of East Anglia, Norwich NR4 7TJ, UK. (t.lenton@uea.ac.uk)

Appendix B: Equations of State

Equations of state for dissolved inorganic carbon (DIC), nutrients (N) and alkalinity (ALK) in each of the ocean boxes.

$$\frac{dDIC(W)}{dt} = F_{iw} \times DIC(I) - (F_{wi} + F_{wc}) \times DIC(I) - R_{(C/N)} \times (1 + R_{(CaCO_3/OrgC)} \times F_{iw} \times N(I) + F_{aw} \times (C_a - pCO_{2_w}) + F^{W}{}_{DIC} \quad \textit{Equation A-1}$$

$$\frac{dDIC(C)}{dt} = F_{wc} \times DIC(w) + F_{ic} \times DIC(I) - F_{cd} \times DIC(C) - R_{(C/N)} \times (1 + R_{(CaCO_3/OrgC)}) \times \alpha \times F_{ic} \times NIT(I) + F_{ac} \times (C_a - pCO_{2_c}) \quad \textit{Equation A-2}$$

$$\frac{dDIC(I)}{dt} = F_{wi} \times DIC(w) + F_{di} \times DIC(D) - (F_{iw} + F_{id} + F_{ic}) \times DIC(I) + F_{diss(DIC)}(I) \quad \textit{Equation A-3}$$

$$\frac{dDIC(D)}{dt} = F_{id} \times DIC(I) + F_{cd} \times DIC(C) - F_{di} \times DIC(D) + F_{rem(DIC)}(D) + F_{diss(DIC)}(D) \quad \textit{Equation A-4}$$

$$\frac{dN(W)}{dt} = F_{iw} \times N(I) - (F_{wi} + F_{wc}) \times N(W) - F_{iw} \times N(I) \quad \textit{Equation A-5}$$

$$\frac{dN(C)}{dt} = F_{wc} \times N(W) + F_{ic} \times N(I) - F_{cd} \times N(C) - \alpha \times F_{ic} \times N(I) \quad \textit{Equation A-6}$$

$$\frac{dN(I)}{dt} = F_{wi} \times N(W) + F_{di} \times N(D) - (F_{iw} + F_{id} + F_{ic}) \times N(I) + F_{rem(N)}(I) \quad \textit{Equation A-7}$$

$$\frac{dN(D)}{dt} = F_{id} \times N(I) + F_{cd} \times N(C) - F_{di} \times N(D) + F_{rem(N)}(D) \qquad \textit{Equation A-8}$$

$$\frac{dALK(W)}{dt} = F_{iw} \times ALK(I) - (F_{wi} + F_{wc}) \times ALK(W) - R_{(C/N)} \left(R_{(CaCO_3/OrgC)} \times R_{(A/CaCO_3)} + \frac{1}{R_{(ALK/NIT)}} \right) \times F_{iw} \times N(I) + F^{W}{}_{ALK} \qquad \textit{Equation A-9}$$

$$\frac{dALK(C)}{dt} = F_{wc} \times ALK(W) + F_{ic} \times ALK(I) - F_{cd} \times ALK(C) - R_{(C/N)} \times \left(R_{(CaCO_3)} \times R_{(A/CaCO_3)} + \frac{1}{R_{(ALK/NIT)}} \right) \times \alpha \times N(I) \qquad \textit{Equation A-10}$$

$$\frac{dALK(I)}{dt} = F_{wi} \times ALK(W) + F_{di} \times ALK(D) - (F_{iw} + F_{id} + F_{ic}) \times ALK(I) + F_{diss(ALK)}(I) - F_{rem(ALK)}(I) \qquad \textit{Equation A-11}$$

$$\frac{dALK(D)}{dt} = F_{id} \times ALK(I) + F_{cd} \times ALK(C) - F_{di} \times ALK(D) + F_{diss(ALK)}(D) - F_{rem(ALK)}(D) \qquad \textit{Equation A-12}$$

Where the ocean boxes are warm surface ocean (W), cold surface ocean (C), intermediate ocean (I), deep ocean (D), see Figure 1.7 for a diagram of the ocean box system. Variables which are not listed and described below will have been described in Chapter Two.

F_x Flux of water between ocean boxes. Where x indicates two of the ocean boxes, water passes from the first named ocean box to the second.

$F_{diss(x)}(Y)$ Flux of constituent *(x)* (N, ALK or DIC) into box *(Y)*, due to dissolution of $CaCO_3$.

$F_{rem(x)}(Y)$ Flux of constituent *(x)* (N, ALK or DIC) into box *(Y)*, due to re-mineralization of organic carbon.

$F^{W}{}_{x}$ Flux of constituent *(x)* (ALK or DIC) from weathering of carbonate and silicate minerals on land.

Appendix C: Thesis Declaration

Thesis Declaration

I Clare Britton declare that this thesis has been composed by me, the work is my own and that the work has not been submitted for any other degree or professional qualification except as specified.

signed 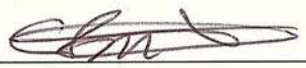

date 14/5/2007